The degradation of atrazine by soil minerals: effects of drying mineral surfaces

by
Adrian Richard Adams

Thesis presented in fulfilment of the requirements for the degree of Master of Science in the Faculty of AgriSciences at Stellenbosch University

Supervisor: Dr Catherine Elaine Clarke
Co-supervisor: Prof. Alakendra Narayan Roychoudhury

April 2014

The financial assistance of the National Research Foundation (NRF) towards this research is hereby acknowledged. Opinions expressed and conclusions arrived at, are those of the author and are not necessarily to be attributed to the NRF.

Declaration

By submitting this thesis electronically, I declare that the entirety of the work contained therein is my own, original work, that I am the sole author thereof (save to the extent explicitly otherwise stated), that reproduction and publication thereof by Stellenbosch University will not infringe any third party rights and that I have not previously in its entirety or in part submitted it for obtaining any qualification.

April 2014

Abstract

The herbicide atrazine (ATZ, 2-chloro-4-ethylamino-6-isopropylamino-1,3,5-triazine) has been identified as an environmental endocrine disruptor and possible human carcinogen. The presence of atrazine, along with its degradation products, in soils and water supplies therefore raises concern. Atrazine biodegradation in soils is well-covered to date, however, atrazine degradation by abiotic mineral surfaces, and the chemical mechanism by which it occurs, is not fully understood. Furthermore, with a changing global climate, the effects of wetting and drying cycles on soil processes (e.g. atrazine degradation) is largely unknown, but increasing in importance. This study therefore investigated atrazine degradation on six common soil mineral surfaces, namely birnessite, goethite, ferrihydrite, gibbsite, Al^{3+}-saturated smectite and quartz, as well as the effects that drying these surfaces has on atrazine degradation.

In the first part, a comparison was conducted between the reactivity of fully hydrated and drying mineral surfaces toward atrazine, by reacting atrazine-mineral mixtures under both moist and ambient drying conditions, in parallel, for 14 days. Under moist conditions, none of the mineral surfaces degraded atrazine, but under drying, birnessite and goethite degraded atrazine to non-phytotoxic hydroxyatrazine (ATZ-OH, 2-hydroxy-4-ethylamino-6-isopropylamino-1,3,5-triazine) as major product and phytotoxic deethylatrazine (DEA, 2-chloro-4-amino-6-isopropylamino-1,3,5-triazine) as minor product. The mineral surface reactivity was birnessite (66% degradation) > goethite (18% degradation) >> other mineral surfaces (negligible degradation), indicating possible atrazine oxidation. In the second part, the effects of drying rate were investigated on birnessite only (the most reactive surface), by conducting the drying (1) gradually at ambient rates, (2) rapidly under an air stream, and (3) gradually in the absence of water using only organic solvent. After 30 days of ambient drying, 90% of the atrazine was degraded to ATZ-OH and DEA, but the same extent of degradation was achieved after only 4 days of rapid drying with an air stream. Thirty days of gradual drying using only organic solvent did not increase atrazine degradation compared to the water-moist drying surface. In each case, degradation initiated at a critical moisture content of 10% of the original moisture content. In the third part, the degradation mechanism was further investigated. To test for the possible oxidation of atrazine by the birnessite surface, moist atrazine-birnessite mixtures were dried under a nitrogen (N_2) stream to eliminate possible oxidation by atmospheric oxygen (O_2). Dissolved Mn^{2+} was extracted at the end of the experiment to observe any reduction of birnessite. Under N_2, the same products were formed as before, with no appreciable Mn^{2+} production, indicating non-oxidative atrazine degradation

by birnessite. The final part investigated the effects ultraviolet (UV) radiation has on the degradation of atrazine by drying mineral surfaces. The UV-radiation enhanced the degradation of atrazine, but no other degradation products were formed.

It was therefore concluded that atrazine degradation on redox-active soil mineral surfaces is enhanced by drying, via a net non-oxidative mechanism. Furthermore, this drying-induced degradation is an atrazine detoxification mechanism which could be easily applied through agricultural practices such as windrowing, ploughing and any other practice that (rapidly) dries a Mn- or Fe-oxide rich agricultural soil.

Opsomming

Die onkruiddoder atrasien (ATS, 2-chloro-4-etielamino-6-isopropielamino-1,3,5-triasien) is as ‘n omgewings endokriene versteurder en moontlike menslike karsinogeen geidentifiseer. Die teenwoordigheid van atrasien, tesame met sy afbreekprodukte, in grond en water toevoere wek dus kommer. Die bio-afbreking van atrasien in gronde is tot dusver goed gedek, maar die afbreking van atrasien deur abiotiese mineraaloppervlaktes, en die chemiese meganisme waarmee dit plaasvind, word nie heeltemal verstaan nie. Verder, met ‘n veranderende globale klimaat, is die effekte van benatting- en drooging-siklusse op grondprosesse (bv. atrasien afbreking) grootliks onbekend, maar toenemend belangrik. Daarom het hierdie studie atrasien afbreek op ses algemene mineraaloppervlaktes, naamlik birnessiet, goethiet, ferrihidriet, gibbsiet, Al^{3+}-versadigde smektiet en kwarts, ondersoek, asook die effekte wat drooging van hierdie oppervlaktes op atrasien afbreking het.

In die eerste deel, was ‘n vergelyking gedoen tussen die reaktiwiteit van volgehidreerde en droëende mineraaloppervlaktes teenoor atrasien, deur atrasien-mineraal mengsels, in parallel, onder albei nat en omliggende droogings toestande te reageer vir 14 dae. Onder nat toestande, het geeneen van die mineraaloppervlaktes atrasien afgebreek nie, maar onder drooging het birnessiet en goethiet atrasien afgebreek na nie-fitotoksiese hidroksieatrasien (ATS-OH, 2-hidroksie-4-etielamino-6-isopropielamino-1,3,5-triasien) as hoofproduk en fitotoksiese deetielatrasien (DEA, 2-chloro-4-amino-6-isopropielamino-1,3,5-triasien) as minder-produk. Die mineraaloppervlakte-reaktiwiteit was birnessiet (66% afbreking) > goethiet (18% afbreking) >> ander mineraaloppervlaktes (geringe afbreking), wat moontlike atrasien oksidasie aandui. In die tweede deel, is die effekte van droogingstempo ondersoek, op birnessiet alleenlik (die mees reaktiewe oppervlak) deur drooging by (1) ‘n omliggende geleidelike tempo, (2) ‘n versnelde tempo onder ‘n lugstroom, en (3) ‘n geleidelike tempo in die afwesigheid van water, deur slegs gebruik te maak van ‘n organiese oplosmiddel. Na 30 dae se geleidelike drooging, is 90% van die atrasien afgebreek na ATS-OH en DEA, maar dieselfe hoeveelheid afbreking is bereik na slegs 4 dae onder versnelde drooging met die lugstroom. Dertig dae van geleidelike drooging met slegs organiese oplosmiddel het nie atrasien afbreking vermeerder in vergelyking met die water-nat droëende oppervlak nie. In elke geval, is afbreking geïnisieer by ‘n kritiese water inhoud van 10% van die oorspronklike water inhoud. In die derde deel is die afbrekingsmeganisme verder ondersoek. Om te toets vir die moontlike oksidasie van atrasien deur die birnessiet oppervlak, is nat atrasien-birnessiet mengsels onder stikstof (N_2) gedroog, om die moontlike oksidasie deur atmosferiese suurstof

(O_2) te verhoed. Opgeloste Mn^{2+} was teen die einde van die eksperiment geekstraëer om enige reduksie van birnessiet waar te neem. Onder N_2 is dieselfde produkte as voorheen gevorm, met geen aansienlike Mn^{2+} produksie nie, aanduidend van ‘n nie-oksideerende afbreek van atrasien deur birnessiet. Die laaste deel het die effekte van ultraviolet (UV) straling op die afbreek van atrasien op droëende mineraaloppervlaktes ondersoek. Die UV-straling het atrasien afbreek vermeerder, maar geen ander afbreek-produkte is gevorm nie.

Die gevolgtrekking is dus dat atrasien afbreking op redoks-aktiewe mineraal-oppervlaktes verhoog word met drooging, deur ‘n netto nie-oksidasie meganisme. Verder is hierdie drooging-geinduseerde afbreking ‘n atrasien ontgiftingsmeganisme wat eenvoudig toegepas kan word deur landboupraktyke soos windrying, ploeg en ander praktyke wat (vinnig) ‘n Mn- of Fe-oksied ryke landbou grond verdroog.

Acknowledgements

First and foremost, I wish to thank my supervisor Dr Cathy Clarke for her tireless assistance, enthusiasm, patience and endless help and support. Without her, I don't think this project would have ever been completed. I would also like to thank my co-supervisor Prof. Alakendra Roychoudhury for his generosity to make full use of his entire laboratory, any time of the day or night, even though I was not even under his department anymore.

I wish to thank the entire staff of the Soil Science department, for making me feel so welcome when I was the new guy, and especially the laboratory and cleaning staff, including Mr Nigel Robertson, for always making sure the laboratories were organized, clean and in working order.

I also wish to thank all the staff of the Central Analytical Facilities (CAF) laboratories, especially the staff of the Environmental Analysis CAF laboratory, Mr Matt Gordon, Mr Herschel Achilles and Dr Cynthia Sanchez-Garrido, for all their help and for allowing full access to their laboratory equipment. I also wish to thank everyone at the LC/MS division of CAF, Dr Marietjie Stander, Mr Fletcher Hiten and Mrs Meryl Adonis for their friendly assistance and generous attitude, in assisting me with getting to grips with the vast field of LC/MS and HPLC, and for assistance with all the analyses.

I would also like to thank Dr André de Villiers of the Chemistry department for all his useful tips on HPLC, as well as Dr Maritha le Roux for the generous usage of the Chemistry department's UV-lamp, as well as her always friendly assistance with the ChemWindow software. I also wish to thank Prof. Paul Papka (Department of Physics) and Dr Ailsa Hardie (Department of Soil Science) for all their assistance and advice with the ESR spectro-photometer and ESR in general. I also wish to thank Dr Remy Butcher from iThemba LABS for all the XRD work, and at such as reasonable price!

For all their financial support, and fantastic opportunity to visit Germany, I wish to thank Inkaba yeAfrica wholeheartedly for all their support throughout. Without your financial support in the first year of this study, there would have been no Masters study to start off with.

I also wish to thank the National Research Foundation (NRF) for their generous financial support for the year 2013 (Grant UID: 84078). Without your financial support this project would not have been completed, and without your continued financial support to so

many young South African scientists and to so many scientific projects, our entire research scene in South Africa would probably cease to exist.

To my parents, I want to say thank you for all your unending support and love in all my missions in life, for always being there when I needed it most, and for always being on call and available, 24 hours a day, 7 days a week. There will never be anybody else like you.

Lastly, but by no means the least (in fact it is the opposite), I would like to thank the LORD God almighty who tirelessly takes care of me day in and day out, and has saved me from countless encounters with my own demise, without ever ceasing. I wish to thank You, LORD, with my whole heart for all the gifts and abilities that you have blessed me with, because without these, I would not be able to do the things I do here right now.

Table of contents

List of figures

List of tables

Symbols and abbreviations used

a	Linear coefficient, for the linear regression $y = a + bx$
APCI	Atmospheric pressure chemical ionization
ATR-FTIR	Attenuated total reflectance – Fourier transform infrared
ATZ	Atrazine (2-chloro-4-ethylamino-6-isopropylamino-1,3,5-triazine, CEIT)
ATZ-imine	Atrazine-imine
ATZ-OH	Hydroxyatrazine (2-hydroxy-4- ethylamino-6-isopropylamino-1,3,5-triazine, OEIT), equivalent to HAT, HYAT, HYA, HA (Hydroxyatrazine)
b	Angular coefficient, for the linear regression $y = a + bx$
bar	Unit of pressure, equal to 100,000 Pascal (Pa)
BPI	Base peak intensity
c (prefix)	Centi-
CDAT	2-chloro-4-acetamido-6-amino-1,3,5-triazine
CDET	2-chloro-4-acetamido-6-ethylamino-1,3,5-triazine
CDIT	2-chloro-4-acetamido-6-isopropylamino-1,3,5-triazine
CE	Capillary electrophoresis
CI	Chemical ionization
CL	Chemiluminescence
©	Copyright
CZE	Capillary zone electrophoresis
d	Day(s)
Da	Dalton
DAD	Diode array detector
DDA	Didealkylatrazine (2-chloro-4,6-diamino-1,3,5-triazine, CAAT), equivalent to DACT (Diaminochlorotriazine), DEDIA (Deethyldeisopropylatrazine)
DDA-OH	Didealkylhydroxyatrazine (2-hydroxy-4,6-diamino-1,3,5-triazine, OAAT), equivalent to AMML (ammeline), DEDIHA (Deethyldeisopropylhydroxy-atrazine)
DEA	Deethylatrazine (2-chloro-4-amino-6-isopropylamino-1,3,5-triazine, CAIT)
DEA-OH	Deethylhydroxyatrazine (2-hydroxy-4-amino-6-isopropylamino-1,3,5-triazine, OAIT), equivalent to *N*-isopropylammeline
DIA	Deisopropylatrazine (2-chloro-4-ethylamino-6-amino-1,3,5-triazine, CEAT)
DIA-imine	Deisopropylatrazine-imine
DIA-OH	Deisopropylhydroxyatrazine (2-hydroxy-4-ethylamino-6-amino-1,3,5-triazine,

	OEAT), equivalent to *N*-ethylammeline
e.g.	Exempli gratia, Latin for "*for example*"
EIA	Enzyme immuno assay
ELISA	Enzyme-linked immunosorbent assay
EI	Electron impact
ESI	Electrospray ionization
ESR	Electron-spin resonance, equivalent to electron paramagnetic resonance (EPR)
et al.	Et alia, Latin for "*and others*"
γ_b	Reductance degree
g	Gram
g	Gravitational acceleration
GC/MS	Gas chromatography – mass spectrometry
Gt	Gigatons
GUS	Groundwater ubiquity score
h	Hour(s)
ha	Hectare(s)
HPLC	High performance liquid chromatography
i.e.	Id est, Latin for "*that is*"
ICP-AES	Inductively coupled plasma – atomic emission spectroscopy
k (prefix)	Kilo-
K_{oc}	Organic carbon partitioning coefficient
K_{ow}	Octanol-water partitioning coefficient
L	Litre
LC/MS	Liquid chromatography – mass spectrometry
LOD	Limit of detection
LOQ	Limit of quantification
m	Metre
MEKC	Micellar electrokinetic chromatography
m (prefix)	Milli-
MS/MS	Tandem mass spectrometry
m/*z*	Mass-to-charge ratio
mol	Mole(s)
M	Molecular mass
μ	Specific growth rate (h^{-1})
µ (prefix)	Micro-

n (prefix)	Nano-
N_2	Dinitrogen
NPD	Nitrogen-phosphorous detection
ODAT	2-hydroxy-4-acetamido-6-amino-1,3,5-triazine
ODIT	2-hydroxy-4-acetamido-6-isopropylamino-1,3,5-triazine
p	Probability
PDA	Photo-diode array
%	Percent
pK_a	Negative logarithm of an acid ionization constant
PP	Polypropylene
PTFE	Polytetrafluoroethylene, known by trade name Teflon®
®	Registered trademark, also TM
R^2	Coefficient of determination
$\sum$	Summation
$t_{1/2}$	Half-life, equivalent to DT_{50} (Degradation time for 50% degradation)
TIC	Total ion current
TOF	Time-of-flight
UV	Ultraviolet

1 Introduction

The growing global demand for food has placed a great amount of pressure on the agricultural sector to supply this demand, and the greatest challenge to agriculture today is *how to produce more food with fewer resources*. The degree of success with which the agricultural sector adapts to these modern requirements depends greatly on technological and scientific advancements that attempt to safeguard against losses in production or reduced yields.

1.1 The role of herbicides in agriculture – focus on atrazine

An important component of the advancements mentioned previously is herbicides, of which approximately 260,000 tons are applied annually to crops (FAO 2010). One of the most popular herbicides currently in use is atrazine (2-chloro-4-ethylamino-6-isopropyl-amino-1,3,5-triazine), a Photosystem II disrupting herbicide (Mullet and Arntzen 1981). Atrazine has been classified by the Herbicide Resistance Action Committee (HRAC) as a group C1 herbicide, a designation that is equivalent to the group 5 classification of the Weed Science Society of America (WSSA) (Menne and Köcher 2007). It is a member of the symmetrical (*s*)-triazine family, and was originally discovered in the 1950's by J. R. Geigy Ltd in Basel, Switzerland (Esser et al. 1975), the same company that is known as Novartis AG today (Ceccatti 2004). Atrazine finds its use mostly as a pre- and post-emergent herbicide to control broadleaf and grassy weeds in important food or cash crops such as maize, sorghum and sugarcane, as well as pineapple (Cavas 2011). Along with its closest *s*-triazine relatives, simazine (2-chloro-4,6-bis(ethylamino)-1,3,5-triazine) and propazine (2-chloro-4,6-bis(isopropylamino)-1,3,5-triazine), it has also become useful in maintaining roadside verges, young plantations, rights of way at railway crossings, turf lawns and golf courses (Abián et al. 1993).

1.2 The environmental and health effects of herbicides

The post application effects of herbicides include the movement of these toxic compounds over and through the soil into surface and ground water systems, their persistence in the environment and the disruption of soil and aquatic ecosystems. These effects are highly varied, because herbicides take on many different chemical forms. Some are hydrophobic (non-polar), moderately polar or polar, with some even being ionic. This means that the fate of these compounds in the environment can vary greatly, and are significantly affected by interactions with soil components, be they biotic or abiotic. Their recalcitrance (or

persistence) in the environment is largely affected by interactions with soil components. Generally, the more susceptible a herbicide is to interactions and transformations (reactions) with or by soil components, the less persistent it will be. The most persistent herbicides in the environment tend to be the non-polar, uncharged species, a characteristic attributable to their relatively low solubility in water (where many microbial reactions take place) and poor interaction with soil mineral components, especially permanently charged clay minerals and variably charged sesquioxides. As such, these recalcitrant organic herbicides have been included in a group of contaminants known as xenobiotic, persistent organic pollutants (POPs).

The presence of herbicides in soil and water systems can be of concern if these compounds have detrimental toxic and mutagenic effects to the organisms found within them, which could lead to a decrease in biodiversity in these ecosystems. Most notable are carcinogenic and endocrine disruptive effects associated with exposure to these compounds, in various species of fauna. Furthermore, these effects can manifest at relatively low concentrations, often at a few parts per billion (ppb) (or $\mu g\ L^{-1}$).

1.3 Atrazine as a model herbicide

Atrazine is quite possibly the most popular herbicide in use today, especially in the production of maize. Maize yield advantages of 1–6% (Ackerman 2007) and even 8% (Swanton et al. 2007) have been reported when using atrazine. Atrazine is most commonly applied as a pre-emergent herbicide, usually in the form of a water spray or wettable powder, at a rate of 2.2–4.5 kg ha^{-1} (Mudhoo and Garg 2011). As a result, its extensive application on maize has resulted in its detection in surface and ground waters associated with agricultural regions.

Maximum contaminant levels (MCLs) for pesticides and other contaminants in water supplies have been set by authorities and organizations such as the United States Environmental Protection Agency (USEPA), World Health Organization (WHO) and European Union (EU). For example, the MCLs for atrazine set by the USEPA and WHO are 3 $\mu g\ L^{-1}$ (USEPA 2009) and 100 $\mu g\ L^{-1}$ (WHO 2011), respectively. The levels set by the EU are more stringent, yet arbitrary, with maximum levels being set at 0.1 $\mu g\ L^{-1}$ for any individual pesticide (not atrazine specifically) and 0.5 $\mu g\ L^{-1}$ for the total amount of pesticides present (Dolan et al. 2013). In many regions, however, atrazine levels exceed these set limits, especially in regions associated with maize production. Data from numerous studies

conducted (e.g. Jayachandran et al. 1994; Gerecke et al. 2002; Benotti et al. 2009; Loos et al. 2010; Byer et al. 2011) indicate that the average concentration of atrazine in the waters of North America and Europe is in the range of 0.03–250 µg L^{-1}.

Studies on the carcinogenicity and endocrine disruptive effects of atrazine have been conducted over the last few decades. Results are varied, with both definitive correlations in some cases and no trends in others, especially when trying to find a causal link between atrazine exposure and occurrences of cancer and endocrine-related disruptions (such as hermaphroditism in certain species of animals). For example, tumour formation in female Sprague-Dawley (SD) rats was correlated with exposure to atrazine (Jowa and Howd 2011), but data from a long-term cohort known as the Agricultural Health Survey (AHS) (Waggoner et al. 2011) conducted among farm workers regularly exposed to atrazine found no link between atrazine exposure and incidences of cancer (Rusiecki et al. 2004; Weichenthal et al. 2010; Jowa and Howd 2011; Boffetta et al. 2013). However, the possibly more definitive effects are mutagenic in nature. Incidences of hermaphroditism and feminization of male African clawed frogs (*Xenopus laevis*) (Hayes et al. 2002) have been reported at concentrations as low as 0.1 and 1.0 µg L^{-1}, respectively. A ten-fold decrease in testosterone levels in *X. laevis* was also observed at atrazine concentrations of 25 µg L^{-1} (Hayes et al. 2002). Generally, the most severe reproductive abnormalities are noted in amphibians, fish and rats (de la Casa-Resino et al. 2012), and at relatively low exposure ranges (Ackerman 2007; Suzawa and Ingraham 2008), sometimes as low as 2–25 µg L^{-1} (Suzawa and Ingraham 2008).

Studies on atrazine's carcinogenicity and endocrine disruptive effects have sparked vast interest in the herbicide, but have also spurred on the banning of atrazine in some countries. In 1991, atrazine was banned in both Germany and Italy, and by 2004 it had been banned across the entire EU region (Ackerman 2007). The USEPA also reviewed atrazine's carcinogen status in 1999, promoting atrazine from group 1 (unlikely to be a human carcinogen) to group 2B of the WHO's International Agency for Research on Cancer (IARC) classification, thereby classifying it as a possible human carcinogen (Jowa and Howd 2011). However, these actions have been met with criticism and have been called premature and non-scientific by some parties (e.g. Pastoor 2007; Ross 2007), especially with regards to the arbitrary and indiscriminatory limit of 0.1 µg L^{-1} set by the EU for all pesticides. Several subsequent studies have been undertaken by the Australian Pesticides and Veterinary Medicines Authority (APVMA) as well as the USEPA and these studies have found no causal relationship between incidences of cancer and atrazine exposure when the herbicide is used in

accordance with the guidelines set out by the manufacturer (LeBaron et al. 2008). The result was a demoting of atrazine by the USEPA from the IARC's group 2B back to group 1, classifying it as unlikely to be a human carcinogen (LeBaron et al. 2008). Despite the damming evidence of atrazine's effects on animals, the effects on humans are still inconclusive, partly due to the fact that data collected on animals cannot be directly extrapolated to humans (Stewart 2012).

The use of atrazine is greatly relevant to South Africa, since South Africa ranks as the tenth largest producer of maize globally, producing 10,360 Gt in 2011 (FAO 2011). The major maize producing area is situated in the northern half of the country, in a quadrangle from the North-West Province to the western Free State, then over to the eastern Free State and northward into the Mpumalanga province, encompassing the area known as the Highveld. A study by Du Preez et al. (2005) investigated the atrazine concentrations in surface waters of a maize-growing region of the North-West Province. In areas where maize was grown (and hence atrazine was applied), atrazine concentrations were in the range of 1.2–9.3 µg L^{-1}, whilst in areas where maize was not grown, atrazine concentrations were in the range of 0.39–0.84 µg L^{-1}. This presence of atrazine in waters where the herbicide was not initially applied, indicates the degree to which atrazine can be transported in water systems, as well as its persistence in the environment. Even in areas where the use of atrazine has been banned (in Germany for example), significant atrazine concentrations have still been detected years later (Tauber and von Sonntag 2000), in both agricultural and pristine water systems. This is one of the major reasons why atrazine has been extensively studied in the past, and will probably be extensively studied in the future as well.

1.4 Research rationale

1.4.1 The degradation of atrazine in soils

In the environment, atrazine can be transformed or degraded into new compounds, known as *metabolites*, or simply *degradation products*. These metabolites are themselves *s*-triazine compounds, often closely resembling their atrazine parent or precursor. The transformation of atrazine into its metabolites can be mediated by a variety of soil components, both biotic (soil microorganisms for example) and abiotic (the minerals present in the soil). The degradation of atrazine in soils is an important factor controlling the overall behaviour of atrazine in soils, because atrazine metabolites can differ greatly from the parent atrazine molecule in a number of properties, including their toxicity to plants (phytotoxicity), water solubility (polarity) and

affinity for various soil materials. The mobility and fate of atrazine in a soil-water system can therefore be greatly influenced by the degree to which atrazine is degraded within that system.

1.4.1.1 Atrazine degradation by abiotic catalysis

The degradation of atrazine by biotic soil components, a process known as biodegradation, has been well documented in the literature, and often the full spectrum of species, enzymes, strains and genes responsible for atrazine degradation have been well elucidated and fully characterized (Mudhoo and Garg 2011). In contrast, the degradation of atrazine by abiotic soil components, especially soil minerals, has been researched far less (Shin and Cheney 2005), despite the crucial role that soil minerals, and more specifically the surfaces of soil minerals, play in the catalysis (enhancement or acceleration of the reaction rate) of abiotic transformations of a wide variety of organic pollutants (Huang and Hardie 2011). The abiotic degradation of organic pollutants is also sometimes several orders of magnitude faster than the corresponding biodegradation reaction. Furthermore, in cases where the survival of bacterial communities for example is not well supported by the environment, the abiotic components of a soil will play the dominant role in the degradation of organic pollutants.

The degradation of organic compounds by soil mineral surfaces occurs most effectively on two major types of soil mineral surfaces, namely the clay minerals and the sesquioxides. A variety of clay mineral surfaces have the capacity to both retain and degrade organic compounds. Studies by Russell et al. (1968) and White (1975/1976) have demonstrated the degradation of a variety of *s*-triazine compounds, including atrazine, by clay mineral surfaces. In each of these studies, the clay mineral's surface acidity provided by cations in its interlayer is the driving force behind the degradation of the *s*-triazine compounds.

The most notable sesquioxide mineral surfaces involved in organic pollutant degradation are the manganese (Mn)-oxides. Manganese oxides possess a very high oxidation-reduction (redox) potential relative to other sesquioxide minerals, and are often a key component in the oxidation (and degradation) of organic compounds in the soil environment. They are also fairly common components in a variety of soil types, after iron (Fe)- and aluminium (Al)-oxides, which are the most common sesquioxide minerals. The degradation of atrazine on Mn-oxide mineral surfaces has been studied by several authors (e.g. Wang et al. 1999; Shin et al. 2000; Shin and Cheney 2004, 2005). These authors have proposed step-wise reaction mechanisms for the degradation of atrazine on these Mn-oxide surfaces, and although the proposed mechanisms account for the formation of atrazine metabolites relatively well,

the exact mechanism of the reaction still remains elusive. This is partly due to both the lack of direct spectroscopic evidence for the reaction mechanism steps, as well as the overall lack of studies that currently exists in this field. However, despite the lack of direct spectroscopic evidence, these authors have proposed the degradation mechanism by investigation through indirect methods, one of which involves eliminating atmospheric oxygen (O_2) as a possible oxidant by conducting the experiments under a nitrogen (N_2)-only atmosphere, whilst the other methods involve the measurement of so-called *surrogate parameters* which include measuring the production of carbon dioxide (CO_2) and water soluble divalent manganese (Mn^{2+}), both species which are considered possible reaction by-products of the abiotic atrazine degradation on Mn-oxide surfaces.

1.4.2 Drying and wetting cycles in soils

Drying and wetting cycles are important processes in soils. These cycles are prevalent in the unsaturated horizons of the soil profile, most notably the vadose zone and rhizosphere (the area adjacent to roots). The rhizosphere is one of the zones in the soil where the greatest amount of microbial activity takes place, whilst the vadose zone is dominated by soil minerals. Since it is known that moisture content is central to the survival and activity of soil microbial communities, the effects of drying and wetting on their activity will, in turn, affect their ability to degrade atrazine, and these effects on atrazine biodegradation have been investigated in numerous studies (e.g. Stearman 1993; Issa and Wood 2005; Ngigi et al. 2011). However, the effects of drying and wetting on the properties of mineral surfaces are possibly of equal importance, since it has been demonstrated that mineral surfaces such as those of the Mn-oxides and clay minerals are able to catalyze the abiotic degradation of atrazine. Despite the apparent importance that these drying and wetting cycles might have on abiotic atrazine degradation, the effects of such cycles have not been investigated thus far. However, a few studies have investigated the effects of drying and wetting on the properties of some soil mineral surfaces themselves. For example, Ross et al. (2001) investigated the effects of drying and rewetting on Mn-oxides and found that drying induced the reduction of the central tetravalent manganese cation (Mn^{4+}) to divalent manganese (Mn^{2+}), which could have an impact on the reactivity of the Mn-oxide mineral surface. Other studies have found that drying on its own increases the acidity of a soil mineral surface (McBride 1994; Dowding et al. 2005; Clarke et al. 2011), and this is true for both clay mineral and Mn-oxide surfaces. Although the effects of drying on the abiotic degradation of atrazine by mineral surfaces has not been investigated thusfar, some studies on the effects of drying on the degradation of other organic pollutants by mineral surfaces have been conducted. Clarke et al. (2012) found

that the drying of a Mn-oxide surface increased its ability to degrade the POP anthracene, a common polyaromatic hydrocarbon (PAH). The authors partly attributed the enhanced degradation to the increased acidity of the drying Mn-oxide surface. It is also proposed that drying causes extreme acidity on clay mineral surfaces (McBride 1994), especially those intercalated with cations such as Al^{3+} and Fe^{3+}. Therefore, drying of a soil mineral surface could possibly have a marked effect on the abiotic degradation of atrazine by soil mineral surfaces and it is therefore important to know how the degradation of atrazine on a mineral surface will be affected when moisture on the mineral surface is allowed to evaporate.

It is envisaged that drying and wetting cycles will become more important in the near future, as they are controlled by climatic factors. Given the current global changes in climate being observed, the occurrence, severity and periodicity of these cycles could change drastically over the years and decades to come, of which the effects on various soil processes are still largely unknown. Given the timeframe of the current project, the effects of rewetting (adding moisture back onto the mineral surface) on mineral surface properties will not be investigated, only the drying half of the drying-wetting cycle will be investigated.

The drying of natural soils, however, is a process usually restricted only to a very thin layer at the soil surface, with the immediate subsurface remaining relatively moist, even in very dry regions. The soil is also usually covered by vegetation, protecting the soil from direct sunlight (and hence drying out). In contrast, agricultural soils often have this vegetative cover removed, especially during practices such as tilling. Tilling, and other practices such as windrowing, also exposes the subsurface soil to sunlight and wind. For this reason, agricultural soils can become much drier than natural soils, at a much faster rate as well. Direct sunlight also contains ultraviolet (UV)-radiation. Organic pollutants are highly sensitive to UV-exposure and often degrade rapidly in UV-light. The added effect of this phenomenon, coupled with the effects of drying, could have a marked effect on the degradation of atrazine by soil minerals and is worth investigating.

1.4.2.1 The effect of drying on the degradation mechanism

The majority of studies involving the reaction of minerals such as birnessite with atrazine, have been conducted either in fully hydrated systems (e.g. Shin and Cheney 2005) or in completely dry systems (e.g. Shin et al. 2000). It is not known what the effects of a drying mineral surface are on both the degree and mechanism of atrazine degradation. This information would add to our overall understanding of abiotic atrazine degradation pathways.

The possible effects of direct sunlight and wind on the drying of mineral surfaces also have to be considered. Exposure of moist mineral surfaces to direct sunlight and wind means that they could possibly dry at a faster rate than unexposed mineral surfaces. Since it is not known what the effects of drying time or drying rate are on the degradation of atrazine, this aspect is also worth investigating.

1.4.3 The lack of soil organic carbon (SOC)

The soil organic carbon (SOC) content in soils has been highlighted previously as an important component in the interaction of atrazine with soils, since atrazine is a hydrophobic (or organophillic) compound and thus interacts most effectively with organic carbon (OC). Furthermore, SOC is a primary energy source for microbial communities in soils, which means the SOC content of a soil ultimately exercises the greatest control on the rate of atrazine biodegradation in soils. In many of the soils of South Africa, however, SOC content is relatively low, with over 58% of the soils containing less than 0.5% OC (Du Preez et al. 2011). At these levels and lower levels of SOC, the interactions between atrazine and soil minerals become more important than the interactions with SOC (Mudhoo and Garg 2011), and these atrazine-mineral surface interactions become the only substantial controlling factor of atrazine degradation. It is therefore important to understand these mineral-atrazine interactions more clearly, by investigating the degradation of atrazine on various soil mineral surfaces.

1.4.4 Final rationale

Considering the uncertainties surrounding atrazine's effects on human health, and since it is widely used in South Africa (one of the largest producers of maize globally), this forms part of the reason why atrazine was chosen as a model herbicide for this study. The other reasons include that it is generally recalcitrant in the environment and fairly non-polar, making it a typical POP. Also, its frequent detection in water systems is of concern, and is directly related to atrazine's interactions with soil components, en route to these systems. Atrazine is also one of the most studied herbicides in the literature, and the wealth of information available on its behaviour in the environment broadens the scope for applications regarding its behaviour in soils. These various points mentioned, lead to the aims and objectives of this study, as outlined in the next section.

1.4.5 Aims and objectives

The primary goal of this research is to investigate the transformation of atrazine on the drying surfaces of soil minerals. The first aim is to:

1. Investigate the effect of drying on the capacity of selected soil mineral surfaces to transform atrazine, by fulfilling the following objectives:
    - React atrazine with birnessite (δ-MnO_2), goethite (Fe_2O_3·H_2O), ferrihydrite (Fe_2O_3·*n*H_2O), gibbsite ($Al(OH)_3$), Al^{3+}-saturated smectite, and quartz (α-SiO_2) in one set of experiments that are kept fully hydrated conditions, and in another set that are left unsealed and allowed to dry;
    - Identify the reaction products in each experiment after allowing each mixture to react for a set period of time;
    - Quantify the amount of atrazine degraded, and product(s) formed, after that period of time in both the fully moist and drying experiments; and

Using the most reactive mineral from aim 1 (birnessite), the second aim is to:

2. Determine if atrazine transformation on a drying mineral surface is either a function of moisture content or contact-time with the mineral surface. This is achieved by:
    - Allowing a moist mixture of birnessite and atrazine to dry gradually for a set period of time; then
    - Repeating the experiment, but whilst accelerating the drying rate signifi-cantly; and finally
    - Removing moisture content as a variable by drying an atrazine-birnessite mixture using organic solvent only and no water.

The third aim is to:

3. Elucidate the atrazine transformation mechanism on birnessite surfaces as far as possible, by:
    - Drying a birnessite-atrazine mixture under nitrogen (N_2) to eliminate the possible effects of oxygen (O_2) on the transformation of atrazine;
    - Measuring a surrogate parameter, such as dissolved Mn^{2+} formation in the nitrogen drying experiment, to detect possible oxidation; and
    - React the transformation products of atrazine with birnessite to gain more

information about where the transformation reaction terminates, and which surface processes occur during the transformation reaction.

Finally, the fourth aim is to:

4. Simulate the possible effects of solar radiation on the transformation of atrazine under conditions of drying, by:
    - Conducting a drying experiment with an atrazine-birnessite mixture whilst irradiating the mixture with UV-radiation of different wavelengths; and
    - Comparing the results with a non-radiation reference drying experiment using the same drying mixture, but without the UV-radiation.

This research aims to deepen the understanding of the interactions of atrazine soil mineral surfaces, as well as possibly revealing a useful, yet simple, application of a drying process that could be applied to environmental remediation strategies that deal with atrazine contamination.

1.5 Document layout

This thesis is divided into six chapters. The first chapter (this one, the introduction) is a basic introduction providing background information as to (1) why atrazine was chosen as the herbicide to be studied, (2) to highlight all the current areas in the knowledge of atrazine behaviour in soils that require further investigation (such as the abiotic degradation mechanisms of atrazine for example, and the effects of drying on such mechanisms), and (3) providing the reader with an understanding of how this thesis aims to address some of these "knowledge gaps".

The second chapter is a review of the current literature on the degradation and sorption of atrazine in the soil environment, with the focus shifted more to the interactions of atrazine with the abiotic components of the soil, since comprehensive reviews on the interactions of atrazine with the biotic components of soils already exist. This review also delves, but only slightly, into some of the engineered chemical systems that are used to treat atrazine in industry (for example, the advanced oxidation processes (AOPs)). However, since these processes do not directly relate to soil systems, they are only highlighted for comparative purposes. The chapter ends with the sorption of atrazine to various soil components, and the factors affecting the retention and mobility of atrazine in soils.

The third chapter is a miniature review chapter that briefly outlines all the current analytical methods available to monitor atrazine in both the environment and during laboratory experiments. Special focus is given to the chromatographic methods of liquid chromatography (LC) and gas chromatography (GC) (the most sensitive methods for atrazine), but the non-chromatographic methods are also listed.

The fourth chapter (materials and methods) is a detailed account of all the materials and methods used in this study, providing information about the various compounds themselves, the experimental designs aimed to answer the aims and objectives of section 1.4.5, and detailed information on all the analytical procedures that were conducted.

The fifth chapter (results and discussion) presents all the most important data gathered which provides the best information relating to the key questions that have to be answered in this study (from section 1.4.5) and at each point, the data is presented and then interpreted. This chapter not only presents the data, in a detached form, but also investigates exactly what this data means in terms of the desired research outcomes.

The sixth and final chapter (conclusions and future work) concludes whether the data that was presented and interpreted in the fifth chapter answers the questions that were asked in chapter one, and also concludes on what the significance of the findings are in an environmental sense for example, since the research being conducted ultimately has a an environmental bearing. There are some cases where either the data did not provide a clear answer to the research questions, or the data has provided more than the desired answer, leading to more research questions to be investigated. In these cases, the issues that were raised were suggested as future work to be conducted. This suggested future work also contains questions that were out of the scope of the current study, or where the resources did not exist for those questions to be answered.

Finally, the addenda give all the data that was not included in the fifth chapter, and is provided as a reference database. The first addendum (A), contains raw data for the graphs provided in chapter five, among other items as well. The second addendum (B) provides data from preliminary studies that were done, but did not provide key information to answer the main research aims and objectives. They are simply provided as a reference.

2 Review: the degradation and sorption of atrazine in the environment

This review aims to provide an overview of all the current literature available on the degradation of atrazine in the environment, as well as its sorption (or retention on) various soil components.

2.1 Introduction

Atrazine (2-chloro-4-ethylamino-6-isopropylamino-1,3,5-*s*-triazine) forms part of the group of compounds known as symmetrical (or *s*) triazines. Together with the asymmetrical (or *as*) triazines, they comprise the entire family of triazines, a group of compounds with the heterocyclic triazine ring in its structure, as shown in Figure 2.1 below:

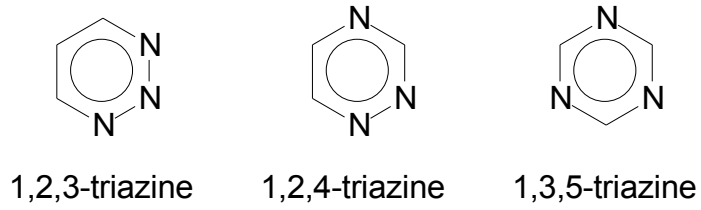

Figure 2.1 The basic chemical structures of the triazines (from Gilchrist 1992).

This heterocyclic ring is not unlike the benzene ring, with three of the carbon (C) atoms substituted by nitrogen (N) atoms, thus giving the formula $C_3H_3N_3$ as oppose to C_6H_6 of benzene. Furthermore, properties such as stability that is synonymous with some aromatic compounds, is also true for these triazine compounds. However, there are some differences between triazine compounds and aromatic compounds. The presence of the more electronegative N atoms in the ring redistributes the uniform delocalized electron density observed in benzene, with a higher electron density localized around the N atoms and less around the C atoms. This causes a slight polarization within the ring (Esser et al. 1975; Pacáková et al. 1996), with the slightly more negative (δ−) regions found on the N atoms and the slightly more positive (δ+) regions found on the C atoms. The result is a ring structure that is more prone to nucleophilic attack on the C atoms. For example, in *s*-triazines, the N atoms are found in ring positions 1, 3 and 5, allowing nucleophilic substitution to occur in the alternative positions 2, 4 and 6 (C-atoms). Generally, species such as Cl^- (-azine suffix),

H_3CO^- (-ton suffix), H_3CS^- (-tryn suffix) (Pacáková et al. 1996) and HO^- (hydroxy- prefix) substitute in position 2, with alkylamino substituents (RHN^-, where R represents H or alkyl group) occupying positions 4 and 6. It is these substituent combinations that yield the various *s*-triazine compounds, of which the 2-chloro-*s*-triazines (including atrazine) form a major component.

2.2 Atrazine transformation products

There are a variety of degradation products (metabolites) that are derived from atrazine, and many are common to atrazine and its closest relatives, such as simazine and propazine (not dealt with in this study). This is attributable to transformation occurring by attack on the moieties (functional groups) in the 2, 4 and 6 substituent positions, and since the three closely related 2-chloro-*s*-triazines mentioned share so many similar moieties, they necessarily share common metabolites.

In almost all transformation reactions, there exist two mechanisms by which the atrazine (and other substituted *s*-triazines) molecule is altered, namely *dealkylation* and *hydroxylation*. Dealkylation occurs by transforming the alkylamino (mostly secondary amines, —NHR, where R is an alkyl chain) moieties in positions 4 and 6 into simpler structures, usually a primary amine (—NH_2). Hydroxylation usually occurs by replacing the species in position 2 (for example —Cl, —OCH_3, —SCH_3) with the hydroxyl group (—OH). The mechanism of degradation dictates the nomenclature of these metabolite compounds as well, in the form of appropriate prefixes added to the base name *atrazine*. For example, when dealkylation occurs and depending on which moiety was altered, either the prefix *deethyl-* or *deisopropyl-* is added to the name *atrazine*. Similarly, if hydroxylation has occurred, the prefix *hydroxy-* is added to the name *atrazine*. Transformation can continue to occur on these metabolites as well, meaning atrazine metabolites can undergo dealkylation and hydroxylation too. These further transformations are all indicated by the nomenclature system, with multiple prefixes being added in combination to the base name *atrazine*. For the sake of brevity, some of the metabolites occurring further down in the degradation hierarchy (further degraded) have their names shortened, for example if two dealkylations have occurred, the prefix *didealkyl-* is preferred over the *deethyldeisopropyl-* prefix. In some cases other names exist for some of the highly degraded metabolites, where overlap occurs with other disciplines of biochemistry or medicine for example, and these include compounds such as *ammeline*, *ammelide* and *cyanuric acid*. Generally, shorter names are preferentially used. In some cases the chemical name is also written differently, using the rules that emphasize the position of a moiety

relative to an N atom or with preference to the fact that it contains an amino group. Atrazine is often written as 6-chloro-*N*-ethyl-*N*′-isopropyl-*s*-triazine-2,4-diamine or 6-chloro-N^2-ethyl-N^4-isopropyl-*s*-triazine-2,4-diamine (e.g. Cheney et al. 1998; García-González et al. 2003) and some of the hydroxy-metabolites such as deethylhydroxyatrazine (2-hydroxy-4-amino-6-isopropylamino-*s*-triazine) and deiso-propylhydroxyatrazine (2-hydroxy-4-ethylamino-6-amino-*s*-triazine) are called *N*-isopropyl-ammeline and *N*-ethylammeline, respectively (e.g. Erickson et al. 1989) (note now the emphasis is on the *presence* of a specific alkyl chain, and not the absence (i.e. de- prefix) as before). The chemical structures, names and abbreviations of these various compounds are given in Table 2.1.

2.3 Overall atrazine transformation pathways

The overall pathway for atrazine degradation, both in the environment and various other settings, is shown in Figure 2.2. However, it should be realized at this point that each step can proceed via drastically different mechanisms, both biotic and abiotic. In some cases, the end products are the only commonality shared by two mechanisms, whilst in others, there exists considerable overlap.

Biotic transformation reactions are termed *biodegradation* or *biotransformation* reactions and are mediated by various microorganisms, higher plants and fauna, either using atrazine as a N or C source in the case of microorganisms (e.g. Yanze-Kontchou and Gschwind 1994; Ralebitso-Senior et al. 2002; García-González et al. 2003; Zhang et al. 2009), or metabolizing atrazine in the case of higher plants and fauna (e.g. Bakke et al. 1972; Adams et al. 1990; Egaas et al. 1993; Burken and Schnoor 1997; Raveton et al. 1997). Biodegradation is influenced by (and to a certain degree is a reflection of) the various factors that influence microorganisms and biota in the soil environment, which include energy or nutrient supply, especially N and C (Sims and Cupples 1999; Dehghani et al. 2013), water content as well as wetting and drying cycles (Shelton et al. 1995), pH (Kells et al. 1980; Mueller et al. 2010), redox potential (E_h) (e.g. Cook et al. 1985; Crawford et al. 2000), conditioning of the microbial community toward atrazine (application history) (e.g. Yassir et al. 1999; Mueller et al. 2010) and the consortia of various species present (Assaf and Turco 1994). Abiotic transformation reactions result from the interaction of atrazine with abiotic soil components such as clay minerals, sesquioxides and humic substances. Generally, less research has been conducted on abiotic reactions, and they are often ignored in remediation programmes (Shin and Cheney 2005). These reactions are also affected by pH and redox potential (E_h), as well as dissolved substances present in the soil solution.

Table 2.1 The chemical structure, names and abbreviations used for atrazine and its metabolites. Modified after Erickson et al. (1989).

Structural formula	Common name (abbreviation) Code [a]	Chemical name based on IUPAC [c] rules (abbreviated chemical name [d])
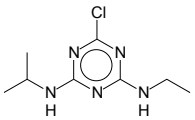	Atrazine (ATZ) G-30027 [b]	2-chloro-4-ethylamino-6-isopropylamino-1,3,5-triazine (CEIT)
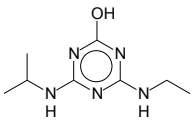	Hydroxyatrazine (ATZ-OH) G-34048	2-hydroxy-4-ethylamino-6-isopropylamino-1,3,5-triazine (OEIT)*
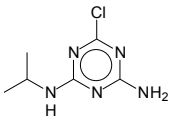	Deethylatrazine (DEA) G-30033	2-chloro-4-amino-6-isopropylamino-1,3,5-triazine (CAIT)*
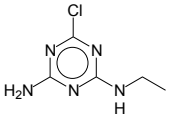	Deisopropylatrazine (DIA) G-28279	2-chloro-4-ethylamino-6-amino-1,3,5-triazine (CEAT)*
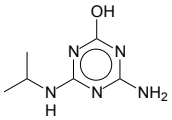	Deethylhydroxyatrazine (DEA-OH)/ *N*-isopropylammeline GS-17794	2-hydroxy-4-amino-6-isopropylamino-1,3,5-triazine (OAIT)*
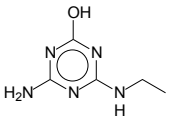	Deisopropylhydroxyatrazine (DIA-OH)/ *N*-ethylammeline	2-hydroxy-4-ethylamino-6-amino-1,3,5-triazine (OEAT)*
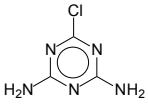	Didealkylatrazine (DDA)/ Diaminochlorotriazine (DACT) G-28273	2-chloro-4,6-diamino-1,3,5-triazine (CAAT)*
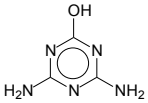	Ammeline (AMML)/ Didealkylhydroxyatrazine (DDA-OH)	2-hydroxy-4,6-diamino-1,3,5-triazine (OAAT)*
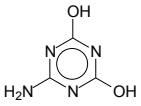	Ammelide (AMMD)	2,4-dihydroxy-6-amino-1,3,5-triazine (OOAT)*
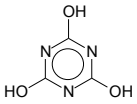	Cyanuric acid (CYA)	2,4,6-trihydroxy-1,3,5-triazine (OOOT) / 1,3,5-triazine-2,4,6-triol

a. Ciba-Geigy experimental code, after Rustum et al. (1990).
b. From White (1975/1976).
c. The chemical names are based on the International Union of Pure and Applied Chemistry (IUPAC) nomenclature, but the alphabetical rules are ignored in this case to emphasize the specific moieties that have undergone changes. Where the rule has been ignored, the name is succeeded by an asterisk (*).
d. Abbreviations are: A = amino, C = chloro, E = ethylamino, I = isopropylamino, O = oxo (hydroxy, enol-tautomers are shown in the above cases, see equation 2.13 in section 2.4.4.1 for interconversion reactions), T = triazine.

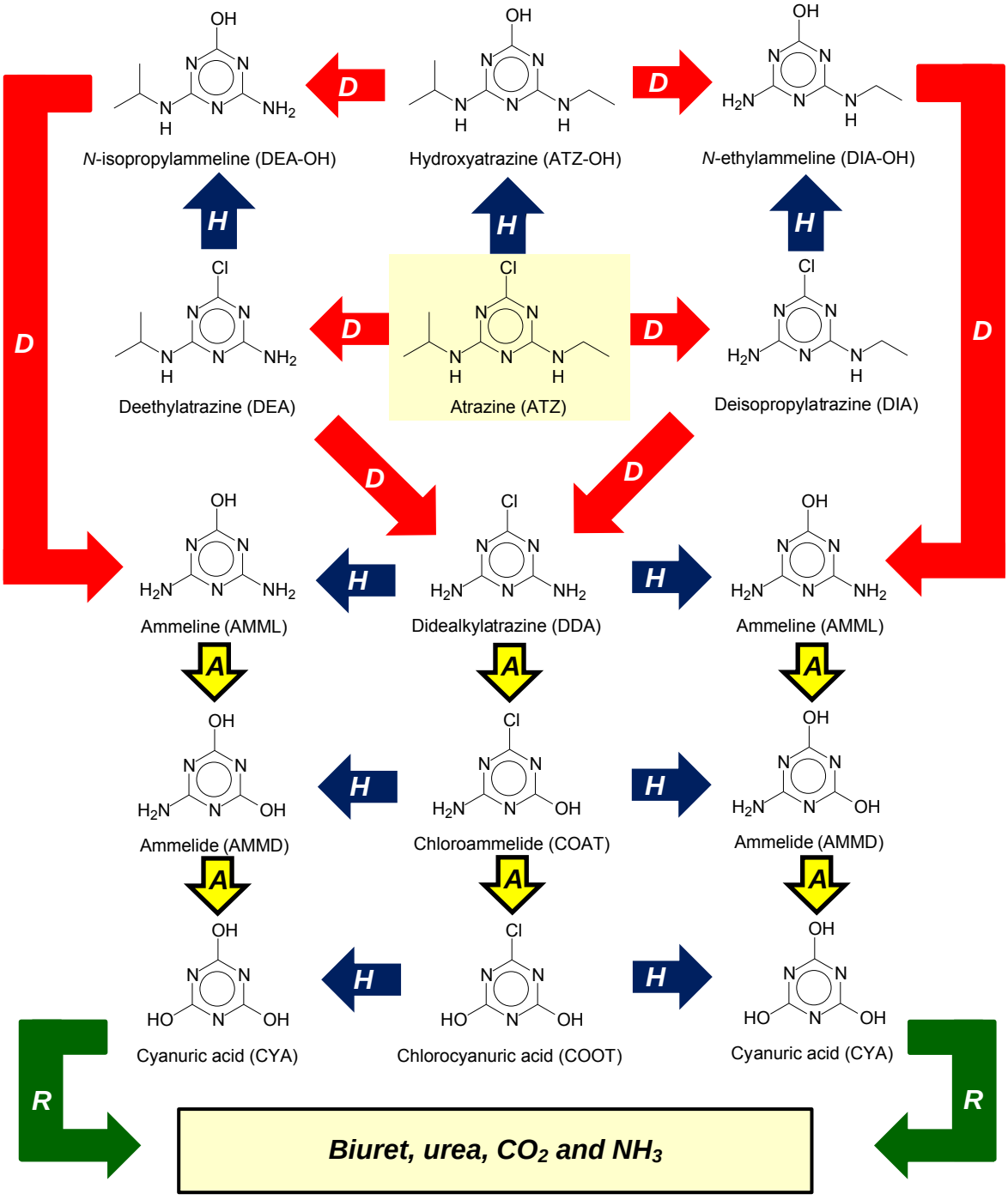

Figure 2.2 The degradation of atrazine to cyanuric acid, and then onward to biuret, urea, carbon dioxide (CO_2) and ammonia (NH_3). Red arrows labelled "D" are dealkylation reactions, blue arrows labelled "H" are hydroxylation reactions, yellow arrows labelled "A" are deamination reactions and green arrows labelled "R" are ring-cleavage reactions. The reaction pathways shown are combined from the various reaction pathways provided in Cook et al. (1985), Clay and Koskinen (1990), Sorenson et al. (1993), Arnold et al. (1995a) and Shin and Cheney (2004).

Both biodegradation and abiotic degradation can occur by dealkylation and hydroxylation (or hydrolysis) reactions. However, dealkylation is generally regarded as mostly a biodegradation mechanism, whilst hydrolysis is considered abiotic (Shin and Cheney 2004, 2005). Despite this however, there is always overlap and both reaction types can be important for both biodegradation and abiotic degradation.

The formation of hydroxy-metabolites is often associated with the reduction of the herbicidal activity of atrazine, since the phytotoxic Cl atom is removed and is replaced by the non-phytotoxic OH group. However, since the Cl atom remains intact during the dealkylation of atrazine, it is expected that dealkylated metabolites of atrazine (for example DEA, DIA and DDA) will have a similar phytotoxicity as atrazine.

2.4 General physico-chemical properties of atrazine and its metabolites

Several physico-chemical properties for atrazine and its metabolites are listed in Table 2.2. These properties include their water solubility, octanol-water partitioning coefficient (K_{ow}), organic carbon partitioning coefficient (K_{oc}), acid ionization constants (pK_a), degradation half-life ($t_{1/2}$), reductance degree (γ_b) and groundwater ubiquity score (GUS). Water solubility, the partitioning coefficients and the acid ionization constants of these compounds all play a role in their degradation and retention (immobilization), and thus ultimately their fate, in soils. These properties interact with various soil parameters such as soil pH, water content, porosity, permeability as well as clay and organic carbon content (total and dissolved).

2.4.1 Water solubility

The water solubility of atrazine is typically 33 mg L^{-1} at 22–27 °C (Weed Science Society of America 1994; Mudhoo and Garg 2011) with its chloro-metabolites (DEA, DIA, DDA) having much greater solubility values than its hydroxy-metabolites (ATZ-OH, DEA-OH, DIA-OH, DDA-OH) (see Table 2.2). On the whole, however, they can all be considered essentially hydrophobic. The water solubility is influenced by the soil or solution pH to a great degree, since this determines whether the compounds are ionized or not. Atrazine and its metabolites are weak organic bases and are protonated and cationic below their pK_a values, meaning that if the solution or soil pH is below the pK_a values, these compounds will have greatly enhanced water solubility. In the case of chloro-metabolites, pK_a values are approximately 2 (Vermeulen et al. 1982), so at significantly acidic pH values (pH < 2) the

water solubility of atrazine and its chloro-metabolites will be greatly enhanced. The pK_a values of the hydroxy-metabolites are higher, approximately 5 (Vermeulen et al. 1982), and these metabolites thus become more soluble at fairly less acid conditions (pH < 5) than their chloro-metabolite counterparts. The solubility of these compounds is the key to their mobility in soils. The generally hydrophobic nature of these compounds mean they are often more soluble in several organic solvents, relative to water, and this is especially true for atrazine and its chloro-metabolites. Atrazine solubility increases from 33 mg L^{-1} in water to 18,000 mg L^{-1} in methanol (CH_3OH), 52,000 mg L^{-1} in chloroform ($CHCl_3$) and up to 183,000 mg L^{-1} in dimethyl sulfoxide (DMSO) ($(CH_3)_2SO$) (Weed Science Society of America 1994). The hydroxy-metabolites require the addition of acid to aid dissolution in organic solvents (Lerch and Donald, 1994). In a more natural sense, aqueous soil solutions containing endogenous (derived from the soil itself) dissolved organic carbon (DOC) may enhance or reduce the retention (or sorption) of atrazine and its metabolites to soil materials (Barriuso et al. 1992; Celis et al. 1998; Mudhoo and Garg 2011) through various organic complexation reactions and competition for sorption sites on soil materials. Atrazine solubility can also be enhanced anthropogenically by the addition of various exogenous organic compounds and solvents. Irrigation of agricultural land with pre-used water such as wine-effluent can add ethanol to the soil solution which will increase the solubility of atrazine. Surface active agents (surfactants) and emulsifiers are also compounds that are sometimes added to agricultural land to enhance properties such as wettability. These are typically in anionic (e.g. sodium dodecyl sulfate, SDS), cationic (cetyltrimethylammonium bromide, CTAB) or non-ionic (e.g. Brij® 35 and Triton®-X 100) form and can have variable effects on atrazine behaviour in soils (e.g. Sanchez-Camazano et al. 2000; Chappell et al. 2005; Tao et al. 2006; Zhang et al. 2011). Most commercial formulations of hydrophobic pesticides contain, or are packaged with, surfactants to allow the applicator to dissolve the pesticide in water, which is more practical for various reasons. The effect of organic compounds and surfactants on the mobility of atrazine and its metabolites in soils are variable, with many factors influencing their mobility. These factors are discussed in more detail in the section on atrazine sorption in soils (section 2.7).

Table 2.2 The physico-chemical properties of atrazine and selected metabolites.

Abbreviated name (and Hill formula†)	Molecular mass, M (g mol^{-1})	Solubility in water		pK_a at 25 °C	log(K_{ow})	$t_{1/2}$ (d)	K_{oc} (L kg^{-1})	Reductance degree, γ_b [o]	GUS [p]
		mg L^{-1}	mmol L^{-1}						
ATZ ($C_8H_{14}ClN_5$)	215.59	33 [a], 30 [b]	0.15	1.71 [d]	2.56 [h], 2.60 [i], 2.2–2.8 [b]	60 [k], 41–231 [b]	140 [m], 155 [n], 129 [b]	3.75	2.92–4.47
ATZ-OH ($C_8H_{15}N_5O$)	197.15	16 [a], 5.9 [c]	0.081, 0.030	5.15 [d]	1.94 [h], 1.4 [b]	60 [k], 32–188 [b]	609 [m], 583 [n], 793 [b]	3.75	1.66–2.76
DEA ($C_6H_{10}ClN_5$)	187.55	2700 [a], 3200 [b]	14.40, 17.06	1.65 [d]	1.24 [h], 1.5 [b]	52 [k], 19–186 [b]	80 [m], 31.8 [n], 56 [b]	3.00	2.68–5.67
DIA ($C_5H_8ClN_5$)	173.53	980 [a], 670 [b]	5.65, 3.86	1.58 [d]	0.60 [h], 1.1–1.2 [b]	36 [k], 32–173 [b]	128 [m], 45 [n], 61 [b]	2.40	2.85–5.25
DDA ($C_3H_4ClN_5$)	145.49	94 [a], 600 [b]	0.65, 4.12	1.5 [e]	−0.60 [h], 0.32 [b], 0 [e]	19 [l], 14–68 [b]	1 [m], 54 [b]	0	2.60–7.33
DEA-OH ($C_6H_{11}N_5O$)	169.11	26.7 [c]	0.158	4.57 [d]	0.56 [h], −0.2 [b]	0.05–7 [b]	927 [b]	3.00	(−1.34)–0.87
DIA-OH ($C_5H_9N_5O$)	155.09	22 [c]	0.14	4.65 [d]	−0.1 [b]	0.05–7 [b]	600 [b]	2.40	(−1.59)–1.03
AMML ($C_3H_5N_5O$)	127.05	21 [c]	0.17	4.5 and 9.4 [f]	−1.20 [h]	–	–	0	–
CYA ($C_3H_3N_3O_3$)	129.03	5000 [b]	38.75	6.5 [g]	−0.2 [j]	6–51 [b]	124 [b]	0	1.48–3.25

a. Bayless (2001), b. Hu et al. (2009), c. Stutz et al. (1998), d. Vermeulen et al. (1982), e. Jin and Ke (2002), f. Kokotou and Thomaidis (2012), g. Ma and Bong (2011), h. Burken and Schnoor (1997), i. Ongley et al. (1992), j. Pichon et al. (1995), k. Krutz et al. (2010), l. Webb et al. (2008), m. Panshin et al. (2000), n. Solomon et al. (1996), o. Calculated using equations 2.8, 2.9 and 2.10 in text, p. Minimum GUS values are calculated from the shortest half-life and greatest K_{oc} value (lowest possible value, best case scenario in terms of leaching) whilst maximum GUS values are calculated from the longest half-life and lowest K_{oc} value (greatest possible value, worst case scenario in terms of leaching) for each compound where applicable. † Formulae adapted from the system proposed in Hill (1900).

2.4.2 Properties governing atrazine retention in soils

Given the hydrophobic nature of atrazine and its metabolites, the retention of these compounds by inorganic soil components such as variably charged sesquioxide surfaces and clay mineral surfaces is not as prevalent as it is for many other polar or ionic contaminants (e.g. polar organics, inorganic anions and metal cations). These neutral, hydrophobic compounds lack the affinity for these inorganic mineral surfaces and rather interact with organic carbon in the soil. They are thus also called organophillic ("organic loving"). However, organic soil carbon contains many organic functional groups and even though these compounds show greater affinity for these organic soil components than for the inorganic mineral surfaces, the interaction is still fairly weak, as is the nature of hydrophobic interactions in general. The hydrophobicity of a general organic compound, C, can be estimated by the degree to which it partitions between an organic solvent and water when shaken in a mixture of the two solvents which is then allowed to separate into two layers (it is important that the organic solvent is not miscible in water). The general equation (equation 2.1) representing such an experiment defines a partitioning coefficient (P) as a ratio of the measured concentration in the organic layer, $[C]_o$, over the measured concentration in the water layer, $[C]_w$:

$$P = \frac{[C]_o}{[C]_w} \tag{2.1}$$

Addition of the two concentrations yields the initial analytical concentration (c_C):

$$c_C = [C]_w + [C]_o \tag{2.2}$$

Commonly, octanol ($CH_3(CH_2)_7OH$) is used as the organic solvent, and the parameter P is then called the octanol-water partitioning coefficient (K_{ow}):

$$K_{ow} = \frac{[C]_o}{[C]_w} \tag{2.3}$$

The octanol-water partitioning coefficient is a useful way of determining the organophil-licity of a compound. The octanol-water partitioning coefficient is a typical distribution constant between two phases, namely aqueous and organic. However, a distribution co-efficient, K_d, can also be defined for the partitioning of a compound between a soil solid phase, such as soil organic carbon, and the soil solution. However, since soils contain different amounts of organic carbon, and since many organic compounds, including atrazine, preferentially

partition into this organic-rich material, the distribution coefficient of an organophillic compound is often normalized to the organic mass fraction of a soil (f_{oc}) (Loague and Green 1991; Oliveira et al. 2001):

$$K_{oc} = \frac{K_d}{f_{oc}} \tag{2.4}$$

where f_{oc} is the fraction of the soil that is organic carbon (%) and K_{oc} is the new parameter defined as the organic carbon partitioning coefficient, with units L kg^{-1} (Sprague et al. 2000).

2.4.3 Half-life, reductance degree and groundwater ubiquity score (GUS)

The remaining physico-chemical parameters, namely half-life, reductance degree and groundwater ubiquity score (GUS), are all numerical parameters designed to give an indication of the kinetics of a compound's degradation, how oxidized a compound is and its mobility from soils to groundwater, respectively.

2.4.3.1 Half-life

The half-lives of atrazine and its metabolites in soils vary considerably depending on how efficient all types of degradation are, collectively. The values quoted in Table 2.2 are more often than not only generally accepted pooled (or field) values, and give no indication of the degradative ability of a specific soil to atrazine. The typical half-life of atrazine has been accepted to be approximately 60 days (Krutz et al. 2010), but this value can vary considerably as a result of many factors. For atrazine, a first order kinetic model of degradation is often assumed. In such a model the concentration (c) of a compound of interest at a particular time t is power-dependent on the initial concentration (c_0) of that compound. These variables of interest are stated in the exponential equation of the form:

$$c = c_0 e^{-kt} \tag{2.5}$$

where c is the concentration of the compound of interest (e.g. atrazine) at time t, k is a constant and c_0 is the initial concentration of the compound. The half-life is defined as the time ($t_{1/2}$) at which 50% of the compound has degraded, therefore Equation 2.5 is solved for the particular case where c is exactly half of c_0:

$$\tfrac{1}{2}c_0 = c_0 e^{-kt_{1/2}} \tag{2.6}$$

Restating the equation in the natural logarithm form leads to the solution for $t_{1/2}$:

$$t_{1/2} = \frac{\ln 2}{k} = \frac{0.693}{k} \tag{2.7}$$

The constant k is a rate constant that is usually determined experimentally.

2.4.3.2 Reductance degree

The reductance degree (γ_b) of a compound, as defined by Erickson et al. (1989) and Erickson et al. (1978), provides a numerical value of how oxidized or reduced a compound is. The parameter is derived from the biomass degradation equation, relative to one C atom. Using oxygen as oxidant, it gives the equivalent amount of O_2 required per quantity of biomass containing 1g of C to oxidize that biomass completely to carbon dioxide (CO_2), water (H_2O) and ammonia (NH_3), as per equation 2.8 for the oxidation of some general compound containing C, H, N and O:

$$CH_pO_nN_q + 0.25\gamma_bO_2 = CO_2 + 0.5(p - 3q)H_2O + qNH_3 \tag{2.8}$$

Considering the case of atrazine, the chlorine atom in position 2 of the ring is also factored into equation 2.8, modifying it accordingly:

$$CH_pO_nN_qCl_r + 0.25\gamma_bO_2 = CO_2 + 0.5(p - 3q)H_2O + qNH_3 + rCl^- \tag{2.9}$$

Here, the end-product for Cl^- is assumed to be hydrochloric acid (HCl). The reductance degree is then calculated by using the valences C = 4, H = 1, O = −2, N = −3 and Cl = −1 as follows:

$$\gamma_b = 4 + p - 2n - 3q - r \tag{2.10}$$

Conducting the calculation for atrazine ($C_8H_{14}N_5Cl$) in terms of one C atom ($CH_{1.75}N_{0.625}Cl_{0.125}$) a value of 3.75 is obtained for γ_b. This, to a certain degree, indicates quite well the oxidized state of C in the atrazine molecule, rendering it fairly resistant to further oxidation. However, this value does not take into account the actual properties of the atrazine molecule. From the structural formula of atrazine, it is clear that it has an oxidized core (the triazine ring), but more reduced alkyl chains as moieties. These chains are susceptible to

oxidation, and oxidation reactions are well known to occur on them (see abiotic degradation section 2.6).

2.4.3.3 Groundwater ubiquity score (GUS)

The groundwater ubiquity score (GUS), as defined by Gustafson (1989) and applied to atrazine by Oliveira et al. (2001) provides an approximate prediction in the form of a numerical value as to how mobile (or leachable) a compound is, according to its half-life and organic carbon partitioning coefficient:

$$GUS = (\log t_{1/2})(4 - \log K_{oc}) \qquad (2.11)$$

The values produced by this equation have been arranged into three categories or ranges. The first category include all compounds that are *non-leachers* (immobile in soils) and these have a GUS value of lower than 1.8. Compounds with values greater than 2.8 are considered *leachers* (highly mobile in soils) and those with values between 1.8 and 2.8 are *transitional*. The GUS value ranges have been calculated for atrazine and its metabolites in Table 2.2. According to the calculated values, the triazines studied are borderline transitional cases to leachers, and atrazine and its chloro-metabolites are fairly mobile in soils (GUS ~ 2.8 or greater). The hydroxy-metabolites have much smaller values and are thus less mobile than their chloro-metabolite counterparts. The relatively low GUS value is confirmed by the observation that hydroxyatrazine and the hydroxy-metabolites have a greater affinity for soil organic carbon than atrazine and related chloro-metabolites (Bosch and Truman 2002), an observation supported by their greater K_{oc} values.

2.4.4 Atrazine properties affected by soil properties

2.4.4.1 Protonation

The physico-chemical parameters of the soil also play an important role in the general behaviour of atrazine and its metabolites. The soil or soil solution pH, as mentioned previously, controls the protonation of these compounds. Below their pK_a values, they become cationic (Russell et al. 1968):

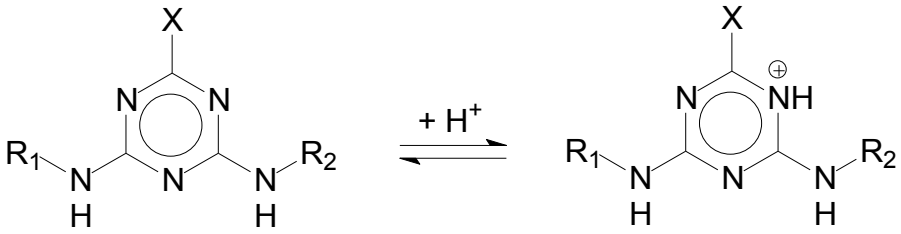

(2.12)

where X = Cl or OH, R_1 = H or $CH(CH_3)_2$, and R_2 = H or C_2H_5. Further reactions are possible for the protonated forms of the hydroxy-metabolites. Tautomerization of these metabolites occurs, yielding the 2-oxo form (Russell et al. 1968):

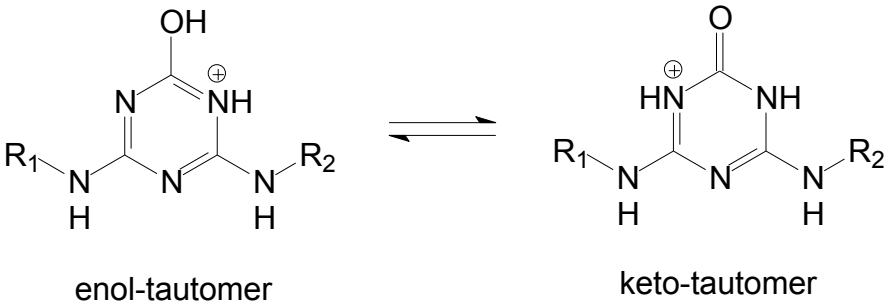

enol-tautomer keto-tautomer

(2.13)

Groups R_1 and R_2 are designated as in equation 2.12. With reference to Table 2.1, the O in the abbreviated chemical name (e.g. OEIT for hydroxyatrazine) refers to the oxo-group in position 2 on the triazine ring, as depicted by the keto-tautomer in equation 2.13.

2.4.4.2 Degradation, fate and mobility

The soil water content may affect degradation as a lack of soil water is detrimental to soil microorganisms that degrade atrazine. Soil water content is intrinsically linked to soil porosity, as a greater porosity would provide greater capacity for the soil to hold water. However, the degree to which these pores are linked, termed the soil permeability, determines how efficiently water will move through the soil. These properties relating to movement of water through the soil have a direct impact on the mobility of atrazine and its metabolites in soils. The size of soil pores is also important. Finer pores are generally associated with slower water movement in soils (Mudhoo and Garg 2011) and are ideal microsites for retaining or degrading atrazine, since these small sites can either store organic material (with atrazine possibly bound to it) and protect atrazine from degradation or they conversely provide ideal sites for small colonies of atrazine degrading microorganisms to degrade atrazine in a microenvironment different from the bulk soil. The net result is an immobilization of atrazine and its metabolites. Larger pores on the other hand promote the flow of water through the soil

(Mudhoo and Garg 2011), hence enhancing the mobility of atrazine and its metabolites. The presence of clay minerals has the general tendency to retard atrazine movement in the soil. The high surface area (or small particle size) can act as a weak sorption (or retention) surface for atrazine, but clay minerals also have the capability of modifying soil porosity and permeability, either clogging pores or reducing the general size of the soil pores. Both scenarios will have a retarding effect on the movement of atrazine. The role of soil organic carbon as an atrazine retention or binding medium has already been covered. However, soil organic carbon also acts as a C source for many microorganisms, including those that degrade atrazine. Therefore, soil organic carbon has two major roles in the control of the fate of atrazine in soils, by both enhancing the degradation of atrazine as well as immobilizing atrazine and its metabolites.

2.5 Biodegradation of atrazine

As the name suggests, this type of degradation is driven by the biotic component of soils. Atrazine is known to degrade by the action of various bacterial species, through uptake by resistant plants, crops and trees, metabolism within soil fauna and mammals, as well as metabolism by fungi. Despite the several biodegradation pathways elucidated, atrazine biodegradability is still fairly low in the environment (Sene et al. 2010) and this is mainly attributable to its low water solubility of 33 mg L^{-1}. Although many metabolites have been discovered (see Figure 2.2), only two metabolites dominate in bulk soils, namely hydroxy-atrazine (ATZ-OH) and deethylatrazine (DEA) (Mudhoo and Garg 2011). However, there are many factors that determine both the amount and which metabolites are produced, which are either general or specific to the involved organisms.

2.5.1 Bacteria

A few microorganisms have the ability to mineralize atrazine completely to carbon dioxide (CO_2) and ammonia (NH_3) (Sene et al. 2010) but many only partially degrade atrazine to one or more of the metabolites shown in Figure 2.2. In the case of bacteria, atrazine can be degraded by either individual strains or several consortia of species. The metabolites produced are dependent on the strain of bacterial species, or the identity of the consortium, and the environmental factors that affect them.

Sene et al. (2010) have summarized the individual strains and consortia that are known to degrade atrazine. These include various strains of species belonging to the genera *Pseudomonas*, *Acinetobacter*, *Aerobacterium*, *Microbacterium*, *Bacillus*, *Micrococcus*,

Deinococcus Rodococcus, *Delftia*, *Agrobacterium*, *Caulobacter*, *Sphingomonas*, *Nocardia*, *Rhizobium*, *Flavobacterium* and *Variovorax*. The bacterial degradation of *s*-triazines is a catabolic process, and the two major factors controlling the rate of *s*-triazine biodegradation by bacteria are the availability of a carbon substrate (energy) as well as a nitrogen (N) source. The triazines have the capacity to act as both a C and N source, under conditions of C or N limitation, respectively (Erickson et al. 1989). The addition of external C sources, however, has a marked enhancing effect on the degradation rate under C limiting conditions, and common substrates often added include lactate (Jutzi et al. 1982), glucose (Giardina et al. 1982; Jutzi et al. 1982; Hogrefe et al. 1985) and glycerol (Cook and Hütter 1984). Under conditions of N limitation, the degradation follows a different degradation path than the one observed in Figure 2.2, with hydroxylation occurring as a first step, followed by direct deamination of hydroxyatrazine to alkyl-ammelide metabolites, instead of the usual dealkylated metabolites. This purpose of this mechanism is to release N-containing compounds (such as simple amines) as soon as possible in the degradation process, so that they can be mineralized to NH_3 and used as an N source. This mechanism has been fully elucidated for the bacterium *Pseudomonas* sp. strain ADP (Mudhoo and Garg 2011) and is illustrated in Figure 2.3.

The degradation rate of atrazine can therefore be manipulated under various C and N limited conditions by adding (or not adding) external C and N sources. External N sources would include N-based fertilizers for example, whilst external C sources would be the substrates mentioned previously. The half-lives ($t_{1/2}$) thus obtained for atrazine could vary considerably from the average 60 days stated in Table 2.2.

The metabolites of atrazine can also act as an N source in N limited conditions (e.g. Cook and Hütter 1981, 1984; Cook et al. 1985), and the degradation rate can also be enhanced using substrates such as glucose (Cook and Hütter 1981; Cook et al. 1985; Behki and Khan 1986), lactate (Cook and Hütter 1981). A summary of the most prevalent studies conducted is presented in Table 2.3. Included are the species and strains of bacteria used, the starting triazine compounds, the products produced, the C and N sources present, as well as the specific growth rate (μ) of the bacterial culture during each experiment.

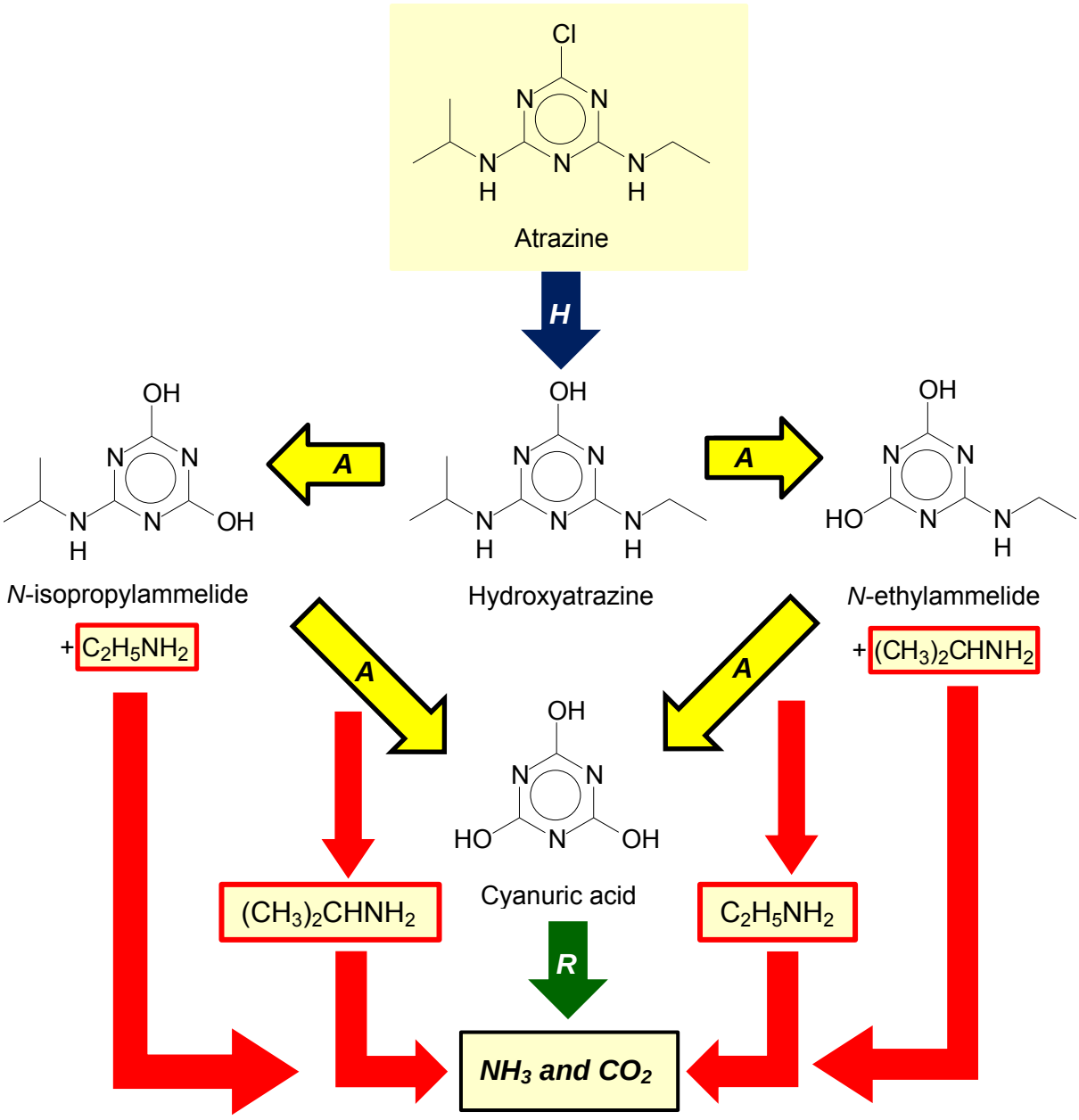

Figure 2.3 The degradation of atrazine under conditions of nitrogen (N) limitation. The blue arrow labelled "H" represents hydroxylation, yellow arrows labelled "A" represent deamination and the green arrow labelled "R" represents ring cleavage. The red arrows represent the mineralization of simple amines, originating from the atrazine molecule, to ammonia (NH_3) and carbon dioxide (CO_2). Modified from de Souza et al. (1998).

Table 2.3 Examples of the typical kinetics of bacterial atrazine and metabolite biodegradation using the viable cell count method. Summarized from Erickson et al. (1989) and references therein.

Bacterium	Triazine used	Initial triazine concentration	Triazine as N source	C (energy) source	Redox conditions	Product(s) formed	Incubation temperature (°C)	Average specific growth rate, μ (h^{-1})	Original reference
Pseudomonas spp.									
strains 192 and 194	atrazine; DEA, DIA, DDA	atrazine = 60 mg L^{-1}; DEA, DIA, DDA = 40 mg L^{-1}	–	atrazine; glucose, 3 g L^{-1}	aerobic	DIA > DEA; DEA-OH, DIA-OH, DDA-OH	–	–	Behki and Khan (1986)
strain S55	atrazine	60 mg L^{-1}	–	atrazine only	aerobic	DIA > DEA	29	0.005–0.008 [a]	Behki and Khan (1986)
strains A and D	NH_4^+, CYA, biuret, urea	2.5 mmol N L^{-1}	CYA (along with NH_4^+, biuret, urea)	lactate, 10 mmol L^{-1}	aerobic and anoxic	ring cleavage products, CO_2, NH_4^+	–	0.30–0.50 for NH_4^+, 0.28–0.33 for CYA, 0–0.26 for biuret, 0.30–0.50 for urea	Cook et al. (1985)
Klebsiella pneumoniae strain 99	NH_4^+, CYA, biuret, urea	2.5 mmol N L^{-1}	CYA (along with NH_4^+, biuret, urea)	glucose, 10 mmol L^{-1}	aerobic and anoxic	ring cleavage products, CO_2, NH_4^+	–	0.87 for NH_4^+, 0.46 for CYA, 0 for biuret, 0.39 for urea	Cook et al. (1985)
Gram positive *Nocardia* sp. strain	atrazine	30 mg L^{-1}	–	atrazine, atrazine and glucose	aerobic	DIA, DEA, CAHT*	30	0.014 [a]	Giardina et al. (1980)

Table 2.3 continued

Gram negative sulfate reducer, facultative anaerobe	CYA, atrazine	75 mg L^{-1}	–	industrial waste, cysteine, cyanuric acid	anaerobic	ring cleavage products, e.g. NH_3	30	0.15 [a]	Jessee et al. (1983)
Rhodococcus corallinus	DIA	2.5 mmol N L^{-1}	DIA	glycerol, 10 mmol L^{-1}	aerobic and anaerobic	DIA-OH	30	0.043	Cook & Hütter (1984)
Pseudomonas strains A, D and F	NH_4^+, DEA-OH, DIA-OH, AMML, AMMD and CYA	2.5 mmol N L^{-1}	DEA-OH, DIA-OH, AMML, AMMD and CYA (along with NH_4^+)	lactate, 10 mmol L^{-1}	aerobic 80:20 He:O_2 N_2-free atmosphere	NH_4^+ and CO_2	30	0.12–0.52	Cook & Hütter (1981)
Klebsiella pneumoniae strains 90 and 99	NH_4^+, AMMD and CYA	2.5 mmol N L^{-1}	AMMD and CYA (along with NH_4^+)	glucose, 10 mmol L^{-1}	aerobic 80:20 He:O_2 N_2-free atmosphere	NH_4^+ and CO_2	30	0.31–0.76	Cook & Hütter (1981)

*CAHT = 2-chloro-4-amino-1,3,5-triazine, a hydrogenated metabolite not discussed in the text.
a. Calculated by Erickson et al. (1989) using data from the original references.

As mentioned previously, atrazine, or its metabolites, can also act as a C source. However, since the ring C atoms in the triazine ring are oxidized (e.g. Erickson et al. 1989), it is concluded that the more likely source of C is the alkyl side chains of atrazine or its metabolites that still contain them. This preference for the side chain as C source is demonstrated by radiolabelling either the triazine ring or side chain with ^{14}C (i.e. [U-^{14}C-ring]-atrazine or [^{14}C -chain]-atrazine). The CO_2 evolved due to mineralization thus contains both unlabelled and labelled ^{14}C-CO_2, the proportions of which correspond to the source of ^{14}C on the atrazine molecule originally. In C limited conditions, it is often found that the alkyl side chains act more as a C source than the ring C atoms (Erickson et al. 1989; Mudhoo and Garg 2011). However, in many cases of N limitation, it is found that the ring C atoms are used as a C source, often via cyanuric acid (Cook 1987) or the amount of CO_2 produced does not correlate (it is usually less) than the amount of C obtained from the alkyl side chains because this C is assimilated into biomass (Radosevich et al. 1996). No assimilation of C from atrazine occurs when cultures use the ring C atoms as C source (Radosevich et al. 1995), since these C atoms are fully oxidized.

At the field scale, the degree of atrazine mineralization decreases with soil depth, from surface zones and the rhizosphere to the vadose zone (Topp et al. 1995; Blume et al. 2004). Atrazine degradation decrease with depth mirrors the decrease in total organic carbon (TOC), temperature (*T*), available N and phosphorous (P) as well as biomass size with depth (Radosevich et al. 1996; Blume et al. 2004). This demonstrates the important roles the availability of nutrients, C and energy sources as well as sufficient quantities of microbial colonies play in the microbial degradation of atrazine. The amount of degraders and the presence of various consortia at the surface far outnumber the microbial colonies of the vadose zone. Even when specific microbial activity is greater in the vadose zone relative to the surface environment, there exist more species at the surface and this is reflected in the rate of atrazine degradation (Blume et al. 2004).

Repeated exposure of a bacterial colony to atrazine has shown to increase the rate of degradation over time (Shaner et al. 2007; Sene et al. 2010). This is not necessarily as a result of increased microbial biomass, but a reduction of the acclimatisation period for a particular colony toward atrazine. Considering the usual 60 day half-life of atrazine under field conditions, a study by Mueller et al. (2010) demonstrated that the half-life of atrazine was reduced to under 8 days when applied to a field previously exposed to atrazine for a period of 4 years. Atrazine exposure history was also provided as an explanation to the observed enhanced atrazine degradation in studies by Krutz et al. (2009) and Shaner et al. (2011). However, Shaner et al. (2011) also

identified TOC and pH as two important factors that also control degradation, along with repeat exposure. Reduced TOC and pH (< 5.5) decreased the rate of degradation, somewhat mitigating the degradation-enhancing effects of repeated exposure to atrazine.

Soil moisture content and temperature also affects the microbial biodegradation rate of atrazine. Roeth et al. (1969) demonstrated that an increase in temperature by 10 °C increased the atrazine biodegradation rate 2–3 times. In the same study, they found that a doubling of the soil moisture content increased the atrazine mineralization rate up to 6 times. This tends to support the notion that varying soil moisture content has a greater effect on degradation than temperature fluctuations (e.g. Ngigi et al. 2011). Similarly, another study by Issa and Wood (2005) found that reduced soil moisture by desiccation greatly reduced the rate of atrazine degradation, and so too did Stearman (1993) in a study using an aged air-dried soil and a fresh moist soil. Although drying appears to inhibit microbial atrazine biodegradation, Ngigi et al. (2011) found that periodic rewetting and then redrying over 7 day cycles increased the mineralization of atrazine relative to a soil with constant moisture contents. They attributed this to the bioavailability of atrazine to the microbial community for degradation, stating that drying had changed the structure of organic matter by shrinking the microsites within it and thus made it more difficult for atrazine to reach and bind with these sites. Upon rewetting, the atrazine is more available for microbial attack.

Other factors also affect the microbial degradation of atrazine. Antibiotics reduce the microbial activity of a soil, and would therefore decrease the rate of atrazine biodegra-dation. The effect of three antibiotics derived from poultry manures, namely monensin, narasin and salinomycin, on atrazine degradation was investigated by Kim et al. (2011). In all three cases, the antibiotics had an inhibitory effect on atrazine degradation. The effect of pH on biodegradation demonstrate mixed results, indicating the effect it has on many different soil parameters, which, in turn, again effect the atrazine degradation rate. Several studies have reported a slightly acidic (~5) to neutral pH (~6.5) as optimal for degradation (e.g. Kells et al. 1980; Mueller et al. 2010; Dehghani et al. 2013) whereas another study by Hance (1979) found atrazine biodegradation to be virtually independent of pH. Variations in pH are capable of affecting the microbial community itself as well as the bioavailability of atrazine for microbial breakdown. In more acidic conditions, atrazine can form bound residues (e.g. Kells et al. 1980) that would be unavailable to the microbial community for degradation. Soil pH also affects the functional groups of humic substances, which are typical binding sites for organic compounds such as

atrazine. Oxidation-reduction (or redox) conditions also affect atrazine microbial degradation by mostly affect the microbial community itself. The optimum redox conditions for degradation are highly dependent on the atrazine degrading microbes present, which survive under a variety of redox conditions. Several survive under aerobic conditions only, whilst others are strictly anaerobes. Some species are aerobic but become facultative anaerobes (e.g. Jessee et al. 1983) under conditions of low oxygenation in order to survive. Some microbes degrade atrazine under anaerobic conditions (e.g. Jessee et al. 1983; Issa and Wood 2005) whilst others do so under aerobic conditions (e.g. Behki and Khan 1986).

2.5.2 Fungi

Atrazine can be degraded by numerous species of fungi, including several species of the genera *Aspergillus*, *Fusarium*, *Penicillium*, *Rhizopus* and *Trichoderma* (Sene et al. 2010). Fungal degradation of atrazine commonly proceeds via dealkylation to form DEA and DIA as well as DDA in some cases. However, dechlorination can also occur (Sene et al. 2010; Mudhoo and Garg 2011). Khromonygina et al. (2004) studied a nonsporulating mycelial fungus, which could degrade atrazine at concentrations of up to 500 mg L^{-1}, using glucose as a sole C (energy) source.

White rot fungi are able to degrade a wide variety of organic pollutants, including dioxins, polychlorinated biphenyls (PCBs), pesticides, petroleum hydrocarbons (PHCs), trinitrotoluene (TNT) and dyes (Marco-Urrea and Reddy 2012). The degradation of atrazine by white rot fungi has also been documented (e.g. Mougin et al. 1994; Doruk and Kolankaya 2012). An oxidative dealkylation mechanism (e.g. Cook 1987) is proposed for the degradation of atrazine by white rot fungi, since they are able to degrade several organic pollutants by radical mechanisms which are, in turn, mediated by the peroxidase enzymes (Sene et al. 2010). The mechanism involves the oxidation of the alkyl chains, yielding the dealkylated metabolites, either DEA or DIA.

Some species of yeast can also degrade atrazine. Abigail et al. (2012) studied atrazine degradation by *Cryptococcus laurentii* which was able to degrade 150 mg L^{-1} atrazine completely within 9 days to form DEA, DIA, DDA and ATZ-OH. The rate of degradation was greatest when atrazine was used as a sole C and N source. The metabolites formed show that not only does dealkylation occur in yeast, but hydrolytic dechlorination occurs as well. Abigail et al. (2013) proposed a novel strain, *Pichia kudriavzevii* strain Atz-EN-01, that was able to degrade 500 mg L^{-1} atrazine completely within 7 days. The metabolites formed were hydroxyatrazine (ATZ-OH), *N*-isopropylammelide and cyanuric acid (CYA).

2.5.3 Uptake by plants and animals

The resistance of several plant species, such as corn and sorghum for example, to atrazine is a result of the plant's ability to take up and metabolise atrazine to compounds that are not actively toxic toward it. This metabolism occurs by hydroxylation to ATZ-OH, dealkylation to DEA or DIA, and by another mechanism known as *S*-glutathione and *S*/*N*-cysteine conjugation (Shimabukuro et al. 1970, 1971, 1973; Lin et al. 2008). Both hydroxy-lation and dealkylation occur to the same degree in maize, but dealkylation is the dominant mechanism of atrazine degradation in sorghum (Shimabukuro 1968; Lamoureux et al. 1973; Shimabukuro et al. 1973).

Atrazine was also found to be taken up by poplar tree cuttings, in studies conducted by Burken and Schnoor (1997) and Chang et al. (2005). In both studies, it was found that poplar trees can hydrolyze and dealkylate atrazine to its hydroxy- and dealkylated-meta-bolites, and the degree of metabolism was greater with increased residence time of atrazine in the tissue.

The abilities of these various plant species to take up and metabolise atrazine has been suggested as a possible remediation strategy to remove atrazine in the environment. This process has been termed phytoremediation (Chang et al. 2005) and has the capability of being used not only for atrazine clean up, but also for various other organic pollutants (Mudhoo and Garg 2011).

Animals can have either metabolise atrazine directly, or can affect the degradation of atrazine indirectly. In mammals, atrazine is metabolised directly, either by dealkylation (Panuwet et al. 2008; Panuwet et al. 2010) or by conjugation in a similar way to resistant plants (Shimabukuro et al. 1971; Panuwet et al. 2008; Panuwet et al. 2010). Conjugation can also occur on the dealkylated metabolites. Once in the metabolic system, the glutathione conjugates can transform into mercapturic acid conjugates (Panuwet et al. 2008; Panuwet et al. 2010) which are then excreted in the urine of the mammal.

Faunal activity can also indirectly affect the degradation of atrazine. The activity of several species of earthworms can have a significant, but highly varied, impact on the biodegradation of atrazine in soils (Farenhorst et al. 2000a, b; Alekseeva et al. 2006; Binet et al. 2006; Kersanté et al. 2006). Alekseeva et al. (2006) found that earthworm casts were enriched in organic matter (especially labile C such as proteins and sugars) and clay relative to the matrix soil. This stimulated the activity of *Pseudomonas* sp. strain ADP which in turn degraded more atrazine. In contrast, Farenhorst et al. (2000a) and Binet et al. (2006) found that earthworm activity, including soil ingestion and organic-rich worm cast formation, resulted in greater amounts of atrazine non-

extractable bound residues. This decreased the bioavailability of atrazine to the microbial community, thus decreasing atrazine minera-lization. A similar inhibitory effect on atrazine degradation was observed by Kersanté et al. (2006) who attributed the decrease in atrazine mineralization to the regulatory effect earthworm activity had on microbial community population size and structure. Further-more, earthworms have the ability to alter the physical structure of the soil. Earthworm burrows act as macropores and become preferential flow paths for atrazine movement, taking atrazine away from the surface and deeper into the soil profile (Farenhorst et al. 2000b), greatly increasing atrazine mobility. In addition, earthworm activity leads to a deeper and disseminated distribution of atrazine (Mudhoo and Garg 2011) from the surface into the subsoil, where there exists decreased microbial activity, leading to the enhanced formation of bound residues and increased atrazine persistence in soil.

2.6 Abiotic degradation of atrazine

The non-biological or chemical degradation of atrazine also gives the general hydroxylated and dealkylated products as the biodegradation mechanisms do. Abiotic atrazine degra-dation can proceed via hydrolysis, mineral surface catalysis, advanced oxidation processes and radiation.

2.6.1 Chemical hydrolysis

Atrazine is converted to hydroxyatrazine (ATZ-OH) by a reaction called hydrolytic dechlorination, or simply hydrolysis. The dealkylated chloro-metabolites, namely DEA, DIA and DDA, can also undergo hydrolysis. For abiotic or chemical hydrolysis of atrazine and its metabolites, the rate of hydrolysis is highly dependent on pH, with the highest rates occurring at very low or very high pH values (Erickson et al. 1989). In acidic conditions, protonation of one of the ring N atoms (below the pK_a) is the first step in the reaction. This step draws electron density away from the C atom in position 2 of the ring (where Cl is attached), rendering it more susceptible to nucleophilic attack. The second step now occurs, where a water molecule (the nucleophile) attaches to the C atom in position 2 and the C—Cl bond is cleaved (Russell et al. 1968; Erickson et al. 1989; McBride 1994). This is depicted in Figure 2.4a. In basic conditions, a simpler process ensues, with the $^{-}$OH anion substituting for the Cl^{-} anion (Figure 2.4b) in a nucleophilic substitution reaction (Erickson et al. 1989).

(a) Acidic conditions:

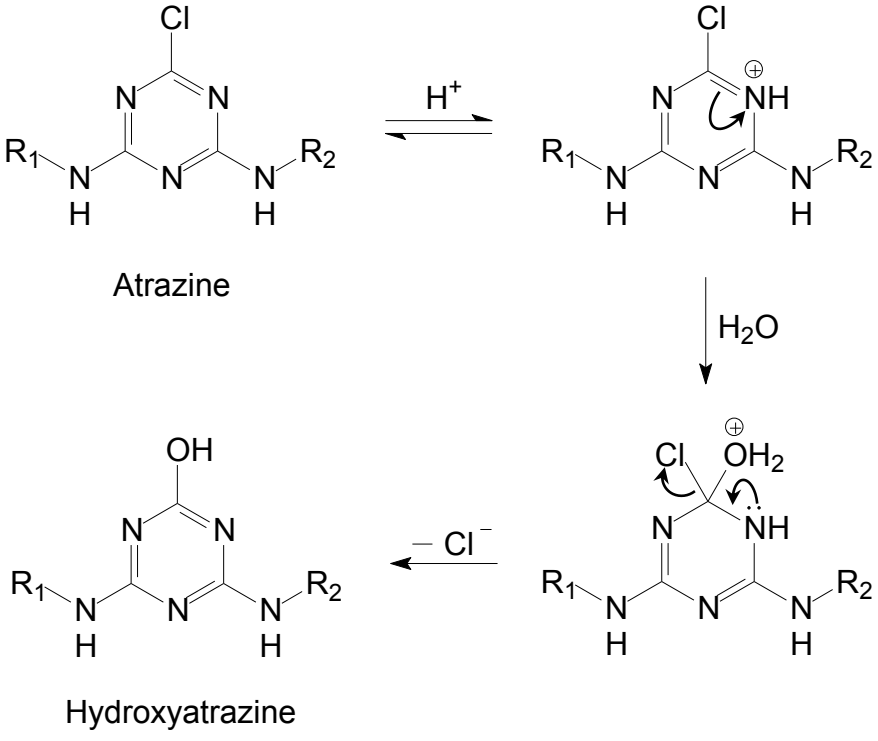

(b) Basic conditions:

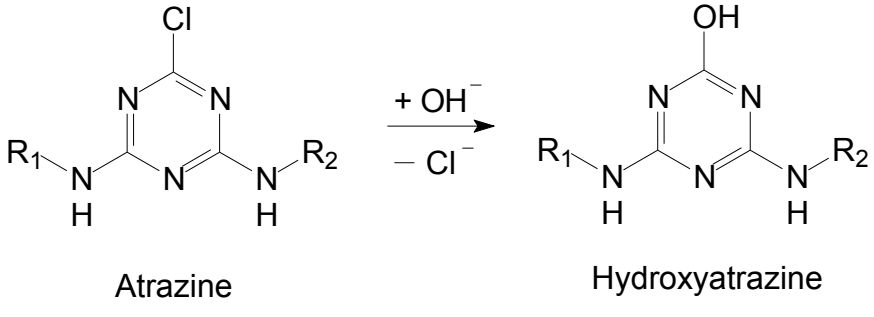

Figure 2.4 The hydrolysis of atrazine and its metabolites in (a) acidic and (b) basic conditions. Curved arrows indicate electron flow. R_1 = H or C_2H_5, R_2 = H or $(CH_3)_2CH$.

2.6.1.1 Mineral surface catalysis

In soils, mineral surfaces often play a key role in either the generation of acidity (in the case of clay minerals for example) or they possess the necessary hydroxyl groups for the hydrolysis reactions (in the case of the sesquioxides for example). Clay minerals, such as smectites, possess permanent negative charge that is satisfied by cations present in the interlayer between the clay mineral's sheets. In natural environments, these cations are coordinated to a shell of water molecules surrounding it, and these water molecules bridge the permanent negative charge and the cation's positive charge. The interlayer cations present can vary greatly, from larger and softer Lewis acids (low charge to radius ratio) such as K^+ and NH_4^+, to smaller and harder Lewis acids (high charge to radius ratio) such as Fe^{3+} and Al^{3+}. The greater the electronegativity of the cation present, the greater its polarizing effect will be on the water molecules surrounding it. This polarizing effect is typically in the order: $K^+ < Na^+ < Ca^{2+} < Mg^{2+} < Al^{3+} < Fe^{3+}$ (Laird and Koskinen 2008). In the case of highly polarizing cations, using Al^{3+} as an example, acidity can be generated by polarizing the water molecule to such an extent that a proton (H^+) is released (McBride 1994):

$$Al(H_2O)_6^{3+} = Al(OH)(H_2O)_5^{2+} + H^+ \qquad (2.14)$$

This leads to the protonation of one of the ring N atoms on the *s*-triazine, and subsequent hydroxylation occurs by the mechanism in Figure 2.4a. This hydroxylation can also be driven by the atrazine molecule itself. On clay minerals, the negative charge is not uniformly distributed. This leads to the formation of hydrophobic microsites where the alkyl chains of atrazine interact with the clay mineral surface (see sorption section 2.7.1) (Laird and Koskinen 2008). Also, significant hydrogen bond interactions exist between the atrazine N atoms and the H atoms of the water molecules situated in the interlayer. The combined polarizing effect of the metal cation on the one hand, and the hydrogen bond to the N atom on the other, is in many cases enough to remove H^+ from the water molecule and protonate the atrazine molecule via one of the ring N atoms. This once again reduces the electron density on the C atom in position 2 on the ring. Upon doing so, the hydroxyl group left behind on the hydrated cation can itself attack the C atom in position 2, thereby hydrolyzing the atrazine molecule. This mechanism is depicted in Figure 2.5:

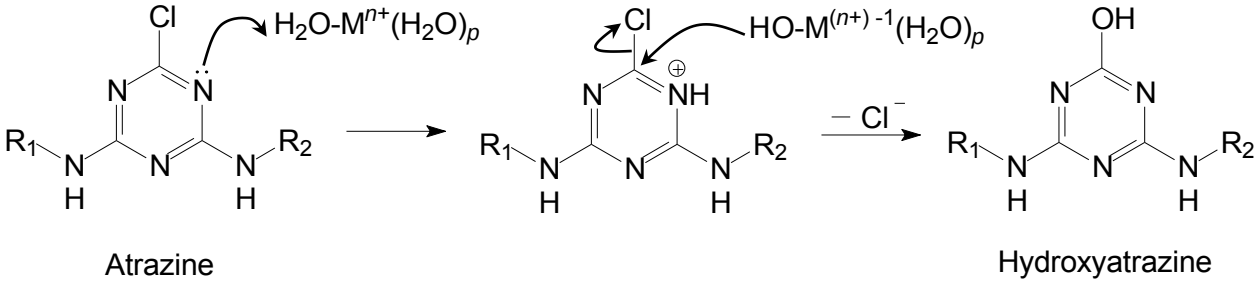

Figure 2.5 The hydrolysis of atrazine by a hydrolyzed cation. R_1 = H or C_2H_5, R_2 = H or $(CH_3)_2CH$, *n* = charge on metal cation, *p* = number of coordinated water molecules not part of hydrolysis reaction. Curved arrows indicate electron flow. From Laird and Koskinen (2008).

The sesquioxides of Fe, Mn and Al are another important component of soil minerals. Unlike the permanently charged clay minerals, the surfaces of these minerals are variably charged, and this charge is dependent on pH. The structure of these minerals usually contain either tetrahedra or octahedra which comprise a metal cation (e.g. Mn^{4+}, Si^{4+}, Fe^{3+} or Al^{3+}) in the centre surrounded by either 4 or 6 oxygen anions (O^{2-}), respectively. These structures fit together in various ways to yield the various oxide minerals, and the oxygen anions act as bridging O atoms to link the metal cations and thereby form the solid lattice. At the mineral edges, however, there is a break in this regular pattern and there exist O atoms that are not bridging, and these are called terminal or non-bridging oxygens (e.g. McBride 1994; Laird and Koskinen 2008). These terminal O atoms are usually in the form of hydroxyl groups (OH) and can be variably protonated or deprotonated depending on the pH and the type of oxide (the metal cation present). This leads to the variably charged nature of the oxide surface. Under basic conditions these hydroxyl groups are partially or wholly negatively charged, whereas under acidic conditions they are partially or wholly positively charged. The size of the charge is dependent on the coordination of the metal cation and the charge of that cation. For example, an octahedrally coordinated Fe^{3+} cation, surrounded by six O atoms, will yield an overall effective charge of −1.5 on each O atom. When in the form of an OH group, that charge will be −0.5. Upon protonation, this group becomes an OH_2 group, also known as surficial (e.g. Laird and Koskinen 2008) or bound water, and has a charge of +0.5. For octahedrally coordinated Mn^{4+}, the charge on the hydroxyl group will be −0.33 and on the surface water molecules +0.67. These are all examples of partial charge. For cations such as Mn^{4+} and Si^{4+} that are tetrahedrally coordinated, the charge on each O atom will

be −1. When in hydroxyl (OH) and protonated (OH_2) form, the charges will be 0 and +1, respectively. These are examples of whole charges. The protonation reactions for these oxide surfaces are illustrated by equations 2.15 through 2.19 (e.g. Stone and Morgan 1984a; Laird and Koskinen 2008):

$$>Fe—OH^{-1/2} + H^+ = >Fe—OH_2^{+1/2} \quad (2.15)$$

$$>Al—OH^{-1/2} + H^+ = >Al—OH_2^{+1/2} \quad (2.16)$$

$$>Mn(octahedral)—OH^{-1/3} + H^+ = >Mn—OH_2^{+2/3} \quad (2.17)$$

$$>Mn(tetrahedral)—OH + H^+ = >Mn—OH_2^+ \quad (2.18)$$

$$>Si—OH + H^+ = >Si—OH_2^+ \quad (2.19)$$

The '>' symbol indicates the bonds of the metal cation to the rest of the oxide lattice (Ulrich and Stone 1989). These protonation reactions of course occur at different pH values for the different oxides, and these values have been defined as the point where all negative charge on the surface is balanced by the same amount of positive charge, yielding an overall charge of zero. This is known as the point of zero net charge (pH_{PZNC}). Given the heterogeneous nature of these oxides, and the variability that can occur within each type, the pH_{PZNC} is more a narrow range than a single value. For Si and Mn oxides, the pH_{PZNC} is often lower than or approximately equal to 3, but for Al and Fe oxides, it is significantly higher at approximately 6–8 and 7–9, respectively (Laird and Koskinen 2008).

These terminal hydroxyl groups have the capacity to hydrolyze atrazine. In a mechanism similar to the one shown in Figure 2.5, the combined polarization effect of the metal cation and one of the ring N atoms on atrazine has the ability to protonate that N atom, setting up atrazine for hydrolysis. Hydrogen bonding between the H atom on the surficial water and the N atom on the ring of atrazine, plays a crucial first step in this reaction. The mechanism is depicted in Figure 2.6.

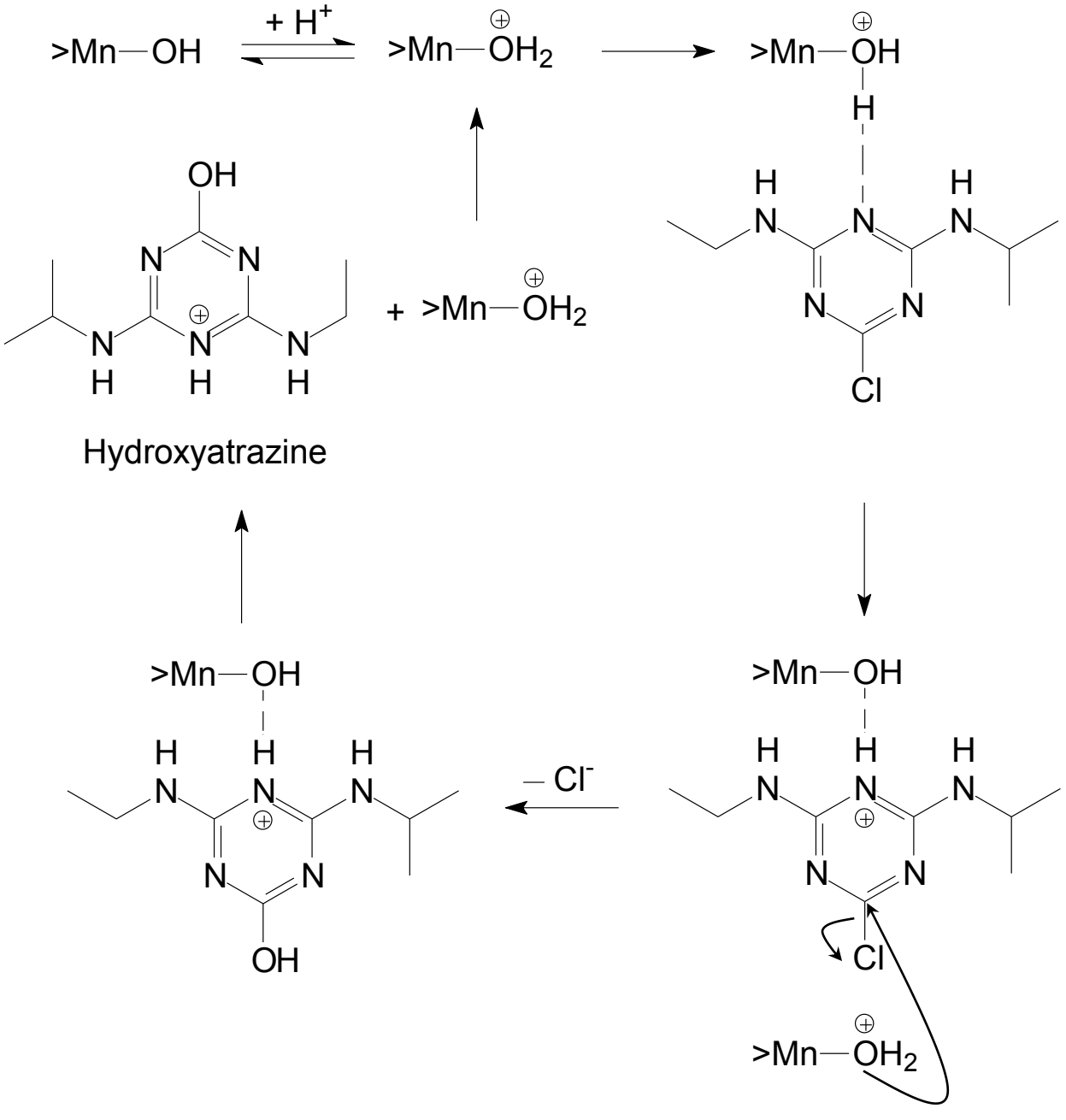

Figure 2.6 The proposed hydrolysis of atrazine on an oxide mineral surface. Hydrogen bonding is a key initial step in this reaction. The formula >Mn—OH represents the Mn-oxide (birnessite) surface and the dashed lines indicate hydrogen bonds. Curved arrows indicate electron flow. Modified from Laird and Koskinen (2008).

Shin and Cheney (2005) have also proposed a hydrolysis mechanism for atrazine on tetravalent Mn-oxide (e.g. $Mn(IV)O_2$) surfaces. They have highlighted the importance of delocalization of electrons from the triazine ring onto the substituted side-chains (see Figure 2.7) as a precursor step to protonation. Once atrazine is protonated, the hydroxyl groups on the Mn-oxide surface act as the nucleophile, attacking the C atom in position 2 of the ring and cleaving its bond with the Cl atom:

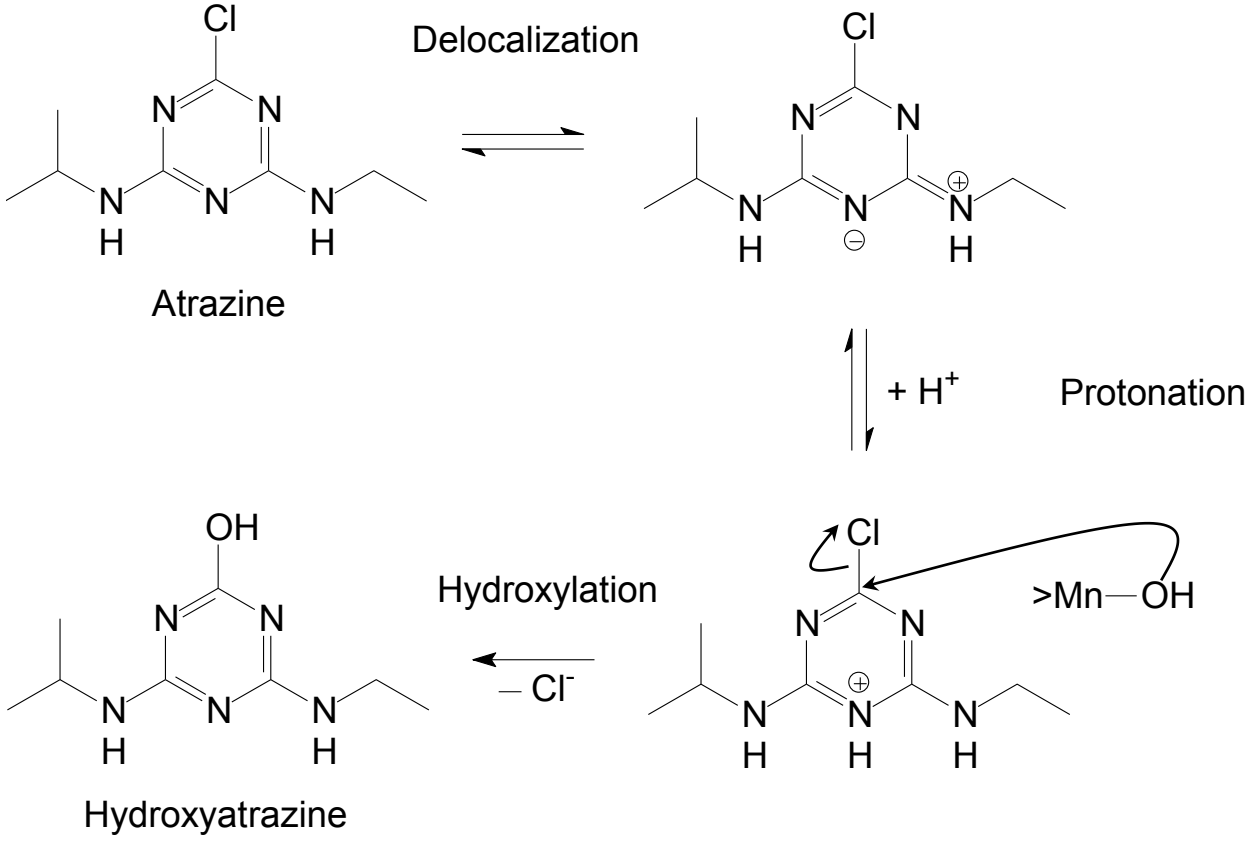

Figure 2.7 The hydrolysis of atrazine by a birnessite surface (>Mn—OH). Curved arrows indicate electron flow. Modified from Shin and Cheney (2005).

In the same study, the authors also investigated the effects of pH on the reaction rate between birnessite (δ-MnO_2) and atrazine. They found that the reaction rate increases with decreasing pH, and they have proposed that at lower pH values, below the pH_{PZNC} of birnessite (~ 2.7) and close to the pK_a of atrazine (pH ~ 2), there exists competition between protons and protonated atrazine for the hydroxyl surface sites (surface waters at low pH) and underlying metal cation, Mn^{4+}. They postulated the possible formation of a "precursor complex" which displaces the surface waters on the oxide surface. These water molecules could then act as the nucleophile, causing the hydroxylation of atrazine. The formation of the precursor complex is an exchange reaction, with the protonated N atom coordinating to the Mn^{4+} cation:

$$>Mn—OH_2^+ + H^+N—R = >Mn—HN—R + H_2O \qquad (2.20)$$

where H^+N represents a protonated ring N atom and R represents the rest of the atrazine molecule (Shin and Cheney 2005).

2.6.2 Oxidation

The dealkylation of atrazine is also possible abiotically, and yields the same products such as DEA, DIA and DDA that biotic degradation reactions do. These dealkylation reactions are typically catalyzed by sesquioxides of Fe and Mn, the redox active sesquioxides. The sesquioxide minerals of Fe, and especially Mn, are strong oxidants and they are common in soils such as oxisols. The oxides of Mn have greater redox potential (denoted *E*, or *E*° under standard conditions: pH = 0, temperature = 25 °C and pressure = 1 bar) than do Fe-oxides, as is illustrated by the following electron-transfer reactions (Stone 1987):

$$Mn(III)OOH + 3H^+ + e^- = Mn^{2+} + 2H_2O \qquad E° = +1.50\ V \qquad (2.21)$$

$$½Mn(IV)O_2 + 2H^+ + e^- = ½Mn^{2+} + H_2O \qquad E° = +1.23\ V \qquad (2.22)$$

$$Fe(III)OOH + 3H^+ + e^- = Fe^{2+} + 2H_2O \qquad E° = +0.67\ V \qquad (2.23)$$

The strongest oxidants, not mentioned in the previous discussions up until now, are the trivalent Mn (or Mn^{3+}) oxides. These are closely followed by the tetravalent Mn (or Mn^{4+}) oxides and then, at a relatively lower level are the trivalent Fe (or Fe^{3+}) oxides.

The oxidative degradation of various organic molecules by Mn-oxides have been investigated extensively (e.g. Stone and Morgan, 1984b; Ulrich and Stone 1989; Matocha et al. 2001; Zhang and Huang 2003, 2005; Barrett and McBride 2005; Shin et al. 2009; Clarke et al. 2012). However, the reported oxidation of atrazine by Mn-oxides is very scant in the literature. Shin et al. (2000) report the oxidation of atrazine to CO_2 and dealkylated metabolites by cryptomelane (α-Mn(IV)O_2), but the mechanism of this reaction still remains elusive. Concomitant release of Mn^{2+} was also observed, indicating reduction of the Mn^{4+} cation within the oxide. The authors have postulated possible oxidation of the alkyl side chains to give CO_2, as well as ring cleavage. However, ring cleavage seems unlikely due to the already oxidized nature of the ring C atoms (Erickson et al. 1989).

Shin et al. (2000) also demonstrate a technique called mechanochemical grinding, which involves the grinding of a solid to 'activate' it, or increase its reactivity, by breaking intramolecular bonds (Kaupp 2009). This can lead to the formation of highly reactive dangling bonds, for example an unbounded or unbridged terminal Mn^{4+} cation, altering the reactivity of the mineral surface. The net effect of mechanochemical treatment of a solid is to increase internal and surface energy, surface area for reactivity, and decrease the degree of cohesion of the solid (Beyer and Clausen-Schaumann 2005). The purpose is to initiate a reaction under non-equilibrium processes and conditions (Baláž et al. 2013). Mechano-chemical degradation of atrazine was achieved using this technique by Shin et al. (2000). Mechanochemical degradation of other organic compounds such as catechol on Mn-oxides has also been investigated previously (e.g. Leo et al. 2012).

The rates of abiotic atrazine oxidation reactions appear to be much faster than the corresponding biodegradation rates. The studies by Cheney et al. (1998) and Shin et al. (2000) show atrazine half-lives of 4–48 hours, a 30–360 fold increase in degradation rate over the usual 60 day half-life for biodegradation.

2.6.2.1 Partial oxidation and surface catalysis

Some investigations have questioned the idea of atrazine oxidation by minerals such as Mn-oxides, particularly birnessite (δ-MnO_2) (Shin et al. 2000), since insufficient Mn^{2+} release is observed to justify the disappearance of atrazine. Furthermore, a time-lag exists between atrazine disappearance/metabolite formation and CO_2 production. Considering this, several authors have postulated a mechanism of dealkylation in which no net oxidation or reduction occurs (Wang et

al. 1999; Shin and Cheney 2004, 2005), although there may be steps in the reaction that are redox reactions. The mechanism was also suggested to be independent of atmospheric oxygen (O_2) by Wang et al. (1999), after these authors conducted a parallel experiment under nitrogen (N_2) only and found equivalent rates of atrazine disappearance and metabolite formation compared to the same reaction under atmospheric conditions. Oxygen appeared to be solely involved in the oxidation of the detached alkyl side-chains to byproducts such as acetone, acetaldehyde and CO_2, and the formation of these products occurred at a time-lag after atrazine metabolite formation. A schematic representation of the mechanism is depicted in Figure 2.8. A further justification for such a mechanism was proposed by Shin and Cheney (2005) who noted that due to the electron withdrawing Cl atom on the triazine ring as well as the oxidized nature of the ring, the side-chains were somewhat deactivated to oxidation. Instead, they propose an initial bridge formation between the side-chain N atom and the Mn^{4+} cation in the oxide lattice, through an initial oxidation step. This step involves a π-electron pair transfer from the N atom to the empty *d*-orbitals of the Mn^{4+} cation. This electron addition to form a temporary Mn^{2+} cation reduces the cation's electronegativity momentarily and a shift of electron density occurs onto terminal hydroxyl groups on the oxide surface. A reduction of electron density at the N atom occurs, due to its temporary oxidation and loss of an electron pair. This yields a generally weaker bonding of the hydrogen (H) atoms on the alkyl chain. The hydroxyl groups of the oxide can now more readily abstract a loosely bound H atom from the alkyl chain, forming an alkene which ultimately breaks away from the N atom as either ethylene or propylene. The N atom is now electron poor and an electron pair is returned from the Mn^{2+} cation to the N atom, reoxidizing the Mn^{2+} cation to Mn^{4+}. The N atom now abstracts the H atom from the terminal hydroxyl group via the regained lone pair of electrons, and this step resets the metal oxide surface and produces the dealkylated NH_2 group on the atrazine molecule. This mechanism is thus truly catalytic and no net oxidation or reduction occurs (Shin and Cheney 2004, 2005).

The proposed mechanisms for both hydrolysis (section 2.6.1.1) and dealkylation (this section) by non-oxidative mineral surface catalysis has also been extended to Fe(III)-oxides by Waria et al. (2009).

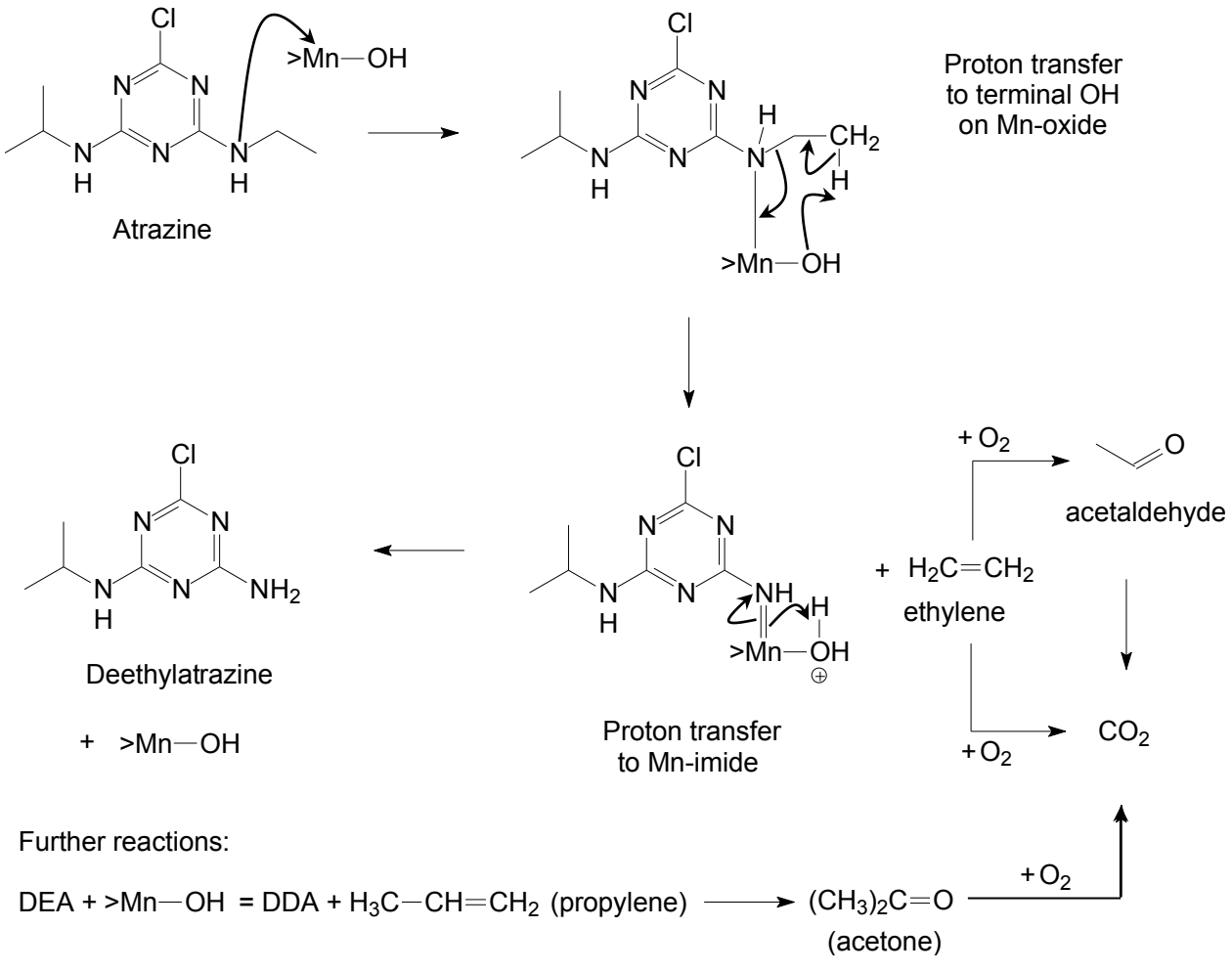

Figure 2.8 The net non-oxidative dealkylation of atrazine by a birnessite surface (>Mn—OH). Curved arrows indicate electron flow. Modified after Wang et al. (1999).

2.6.2.2 Advanced oxidation processes (AOPs)

These processes are often used in the removal of organic pollutants in drinking water, and include treatments such as ozone (O_3) and ultraviolet (UV) photolysis. However, atrazine is ozone refractory (Tauber and von Sonntag 2000) and is only oxidized in systems where hydroxyl radicals ($^{\bullet}OH$) are generated, usually by the addition of hydrogen peroxide (H_2O_2) or some form of radiation (UV and γ-radiation are common) to the system. The most popular hydroxyl radical generating systems used for atrazine degradation are O_3 with H_2O_2 or UV photolysis, titanium dioxide (TiO_2) with UV photolysis and Fenton's reagent (the reaction of ferrous iron (Fe^{2+}) with H_2O_2 to form $^{\bullet}OH$) (Tauber and von Sonntag 2000). Using a γ-radiation and nitrous oxide (N_2O) system, water is split into various highly reactive species, among which are hydroxyl radicals

($^{\bullet}OH$), single hydrogen atoms ($H^{\bullet}$), solvated electrons (e^{-}_{aq}) and superoxide radicals ($O_2^{\bullet -}$) (Tauber and von Sonntag 2000):

$$H_2O \xrightarrow{\gamma-\text{radiation}} {}^{\bullet}OH,\ e^{-}_{aq},\ H^{\bullet},\ H^{+},\ OH^{-},\ H_2,\ H_2O_2 \tag{2.24}$$

$$e^{-}_{aq} + N_2O \rightarrow {}^{\bullet}OH + N_2 + OH^{-} \tag{2.25}$$

$$H^{\bullet} + O_2 \rightarrow HO_2^{\bullet} \tag{2.26}$$

$$HO_2^{\bullet} = H^{+} + O_2^{\bullet -} \tag{2.27}$$

Hydroxyl radicals are also produced by Fenton's reagent, a combination of ferrous iron (Fe^{2+}) and hydrogen peroxide (H_2O_2), as illustrated by the reaction equation below (Arnold et al. 1995a):

$$Fe^{2+} + H_2O_2 = Fe^{3+} + {}^{\bullet}OH + OH^{-} \tag{2.28}$$

The mechanism of atrazine oxidation by hydroxyl and other radicals is depicted in Figure 2.9. These reactions proceed via radical reactions, producing intermediates and end products that are not seen in other systems. Molecular oxygen (O_2) also plays a role, producing the peroxyl radical intermediate as one of the steps during dealkylation. Furthermore, many unique products are observed, such as atrazine-imine (ATZ-imine), deisopropylatrazine-imine (DIA-imine), 2-chloro-4-acetamido-6-isopropylamino-1,3,5-triazine (CDIT), 2-chloro-4-acetamido-6-amino-1,3,5-triazine (CDAT) and 2-hydroxy-4-acetamido-6-amino-1,3,5-triazine (ODAT) (Acero et al. 2000; see Figure 2.9 for structures).

Although these reactions are viable in a laboratory setting, hydroxyl radicals are easily scavenged and rendered into another unreactive form in soils. Both humic substances (Ma and Graham 1999) and bicarbonate (Ma and Graham 2000) are known OH-radical scavengers. In addition, hydroxyl radicals can be consumed by ferrous iron (Fe^{2+}) to produce ferric iron (Fe^{3+}) and hydroxyl anions (OH^{-}) (Arnold et al. 1995a):

$$Fe^{2+} + {}^{\bullet}OH = Fe^{3+} + OH^{-} \tag{2.29}$$

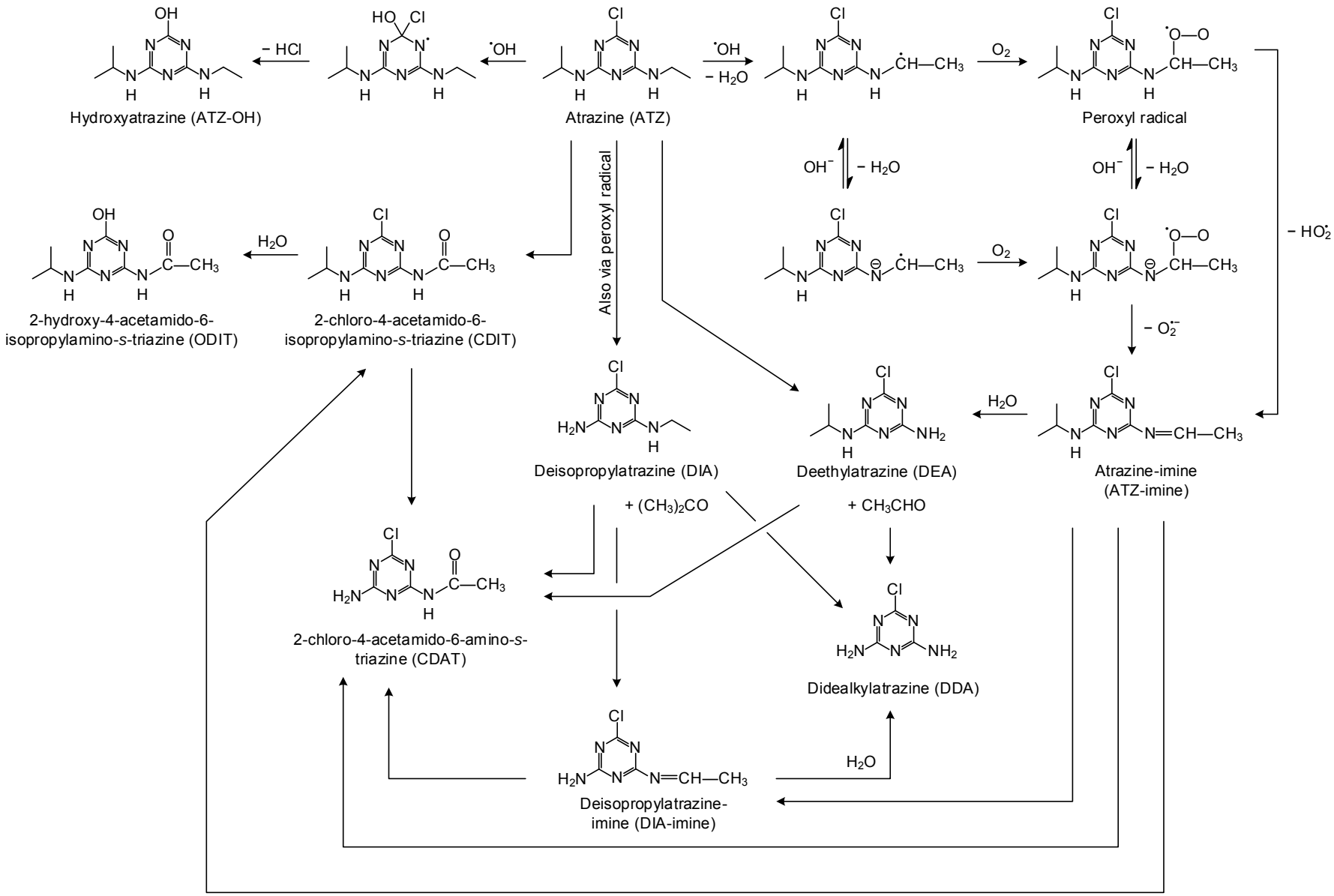

Figure 2.9 (previous page). The oxidation of atrazine by radical generating systems. Modified from Acero et al. (2000) and Tauber and von Sonntag (2000).

These reactions with atrazine are far less representative of natural systems when compared to biodegradation or mineral surface catalysis for example, but they tend to have much faster kinetics (hours vs. months) and are thus always considered as possible remediation strategies. However, there are some disadvantages to AOPs, which include the high capital input and running costs involved in applying these processes to remediation scenarios.

2.6.3 Zero-valent iron (ZVI) and reduction reactions

Zero-valent iron (ZVI or Fe^0) (e.g. Satapanajaru et al. 2008) has the potential to degrade atrazine. A study by Singh et al. (1998) found that 10% (on a weight per volume basis) of finely ground Fe^0 powder was able to degrade approximately 50% of the atrazine in a 20 µg L^{-1} solution of radiolabeled ^{14}C-atrazine. The metabolites formed were hydroxyatrazine (ATZ-OH), DEA, DIA and DDA. The authors have not proposed a mechanism for the reaction, but have postulated the following reaction equation for the formation of ATZ-OH:

$$Fe^0 + 2H_2O + 2\text{Atrazine-Cl} \rightarrow 2\text{Atrazine-OH} + Fe^{2+} + 2Cl^- + H_2 \quad (2.30)$$

From the equation, the reaction appears to be a single electron transfer reaction, given the 1:2 stoichiometry of Fe^0 vs. atrazine. In the same study, a certain degree of sorption was also observed, with 11% of the ^{14}C measured being unextractable residues. The authors have suggested that the readily oxidizable Fe^{2+} initiates the formation of ferric hydroxides by molecular oxygen (O_2):

$$4Fe^{2+} + 4H^+ + O_2 = 4Fe^{3+} + 2H_2O \quad (2.31)$$

$$Fe^{3+} + 3H_2O = Fe(OH)_3 + 3H^+ \quad (2.32)$$

This provides a sorbent for protonated hydroxyatrazine to adsorb onto, either by hydrogen bonding or cation exchange at lower pH values.

Apart from oxidation, atrazine can also be degraded by reductive dechlorination, replacing the Cl atom in position 2 with an H atom (Figure 2.10).

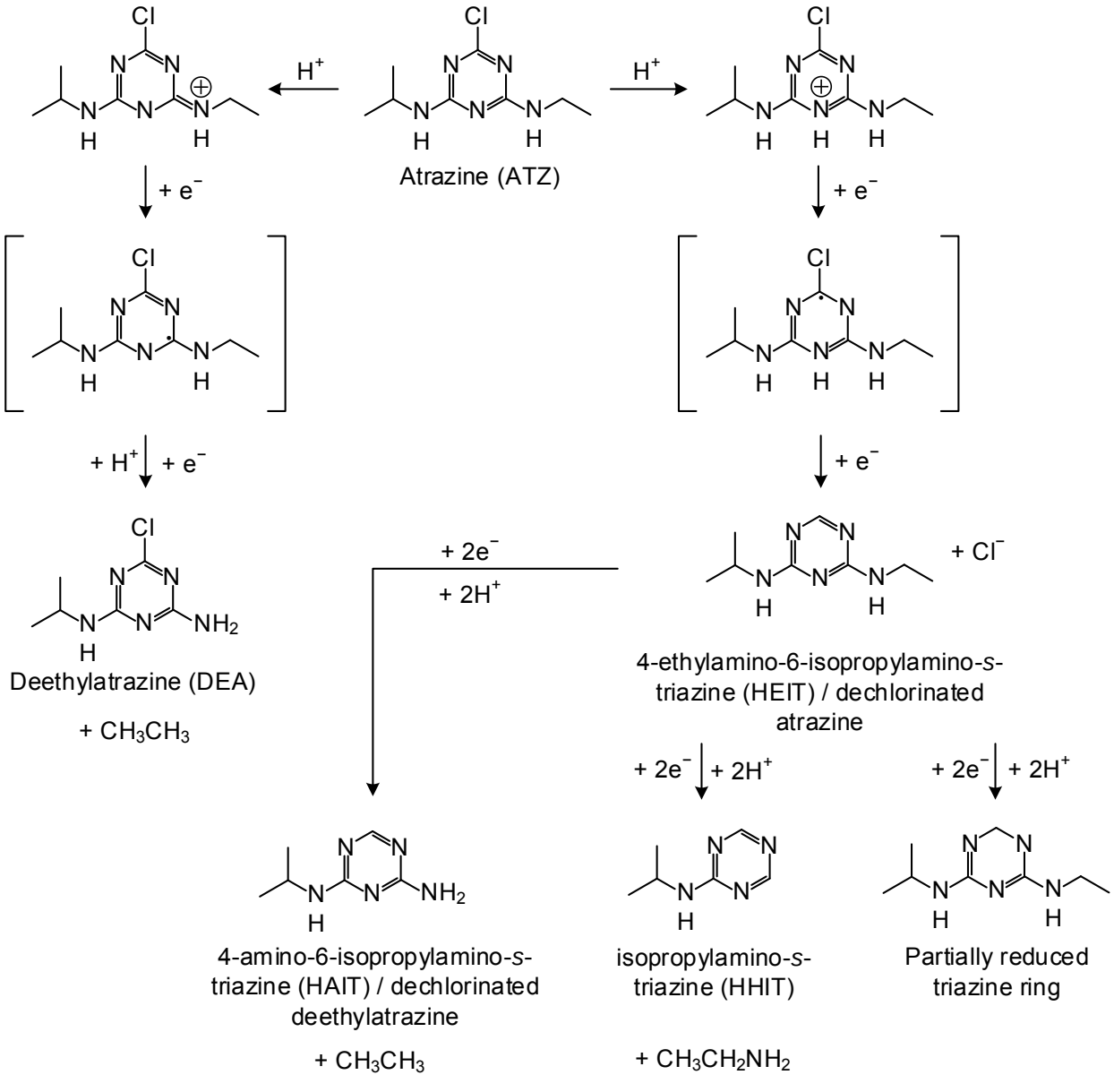

Figure 2.10 The reduction of atrazine. Modified from Pospíšil et al. (1995) and Guse et al. (2009).

This reaction has been achieved by using Fe^0 as well, but under low oxygen and pH conditions (Dombek et al. 2001; Satapanajaru et al. 2008; Bezbaruah et al. 2009). This is because the first step in reductive dechlorination is protonation of the triazine ring (Dombek et al. 2001). These reactions are also conducted using nano zero-valent iron (nZVI or nano ZVI) (e.g. Satapanajaru et al. 2008; Bezbaruah et al. 2009). The reductive dechlorination of atrazine is a two-step reaction. Following protonation, a two-electron transfer occurs to replace the Cl atom with H (see Figure 2.10). Some studies have found that the product (4-ethylamino-6-isopropylamino-1,3,5-

triazine) can be further degraded by the addition of two further electrons (Guse et al. 2009). These products are mostly dealkylated or deaminated forms of the dechlorinated atrazine or contain a partially reduced triazine ring (Figure 2.10). Pospíšil et al. (1995) also proposed a two-electron formation of DEA, with the release of ethane (C_2H_6) rather than ethylene (C_2H_4) as before. In both of the studies, by Pospíšil et al. (1995) and Guse et al. (2009), the reduction reactions were conducted electrochemically, using a standard mercury drop electrode (SMDE) and a platinum (Pt) wire or net electrode.

2.7 Sorption

The umbrella term sorption refers to the partitioning of matter between one phase and another and includes different forms of partitioning, such as penetration, the adsorption of a substance onto the surface of a phase and the accumulation of a substance at the interface between two phases (Mudhoo and Garg 2011). In terms of atrazine and its metabolites, the term sorption generally refers to the behaviour of these compounds between the aqueous phase (the soil solution) and the solid phase (solid soil materials). In simple terms, sorption can be viewed as a process that scavenges atrazine and its metabolites from the soil solution and then facilitates their retention on the surfaces of various soil materials. Sorption is thus one of the most important controls on the ultimate fate and mobility of atrazine and its metabolites in the soil system (Clay and Koskinen 1990; Sorenson et al. 1993). Furthermore, the adsorption of atrazine, as well as many other organic contaminants, to the surfaces of oxide minerals, is considered a crucial first step in the reaction of organic pollutants with oxides (e.g. Ulrich and Stone 1989; Shin and Cheney 2005). In reference to the properties in Table 2.2 for atrazine and its metabolites, especially GUS and K_{oc}, a general pattern of mobility emerges. The sequence of decreasing mobility for atrazine and its metabolites is: DDA > DEA > DIA > atrazine > hydroxyatrazine. Along with the properties of the compounds, soil components, both organic and inorganic, also play a role in the amount of sorption that occurs. These components affect sorption because atrazine and its metabolites sorbs onto these various components via different mechanisms.

2.7.1 Sorption mechanisms

In most soils, which fall in the natural pH range of approximately 4–10, atrazine and its metabolites are usually uncharged, which means they have an affinity for organic matter. Atrazine mostly interacts with the functional groups and aliphatic (alkyl) groups located on humic substances. The alkyl groups on atrazine interact with the alkyl groups on the humic

substances through weak hydrophobic van der Waals bonding. Atrazine can also act as either a hydrogen bond acceptor or donor (Welhouse and Bleam 1993a, b) via its ring N atoms or H atoms on the amine group, respectively (see Figure 2.11a). These interactions occur between the phenolic, ketone and carboxylic acid functional groups on the humic substances and the electronegative groups of atrazine. Sposito et al. (1996) have provided infrared spectroscopic evidence of actual proton transfer between the carboxylic acid groups and the amino group on atrazine. This renders a protonated amino group and negative carboxyl group with then interact via cation exchange. Interactions also include π-π interactions between the triazine ring and aromatic structures. In cases, this interaction can lead to electron transfer between the triazine ring and quinone-like structures within the humic substances. This process was observed in the same study by Sposito et al. (1996), using electron-paramagnetic resonance (EPR) spectroscopy. The authors concluded that proton transfer mechanisms were favoured upon interactions between humic substances containing a high amount of carboxylic acid functional groups and triazines with low basicity (low pK_a values, such as atrazine), whilst electron transfer was favoured in cases where the humic substances had a low amount of carboxylic acid functional groups and the triazines were of greater basicity.

These interactions with organic matter are most effective for immobilizing atrazine and its metabolites in soils, but in soils with relatively low total organic carbon (TOC < 0.1%), these mechanisms become unimportant and the interactions of triazines with soil mineral surfaces become more important (Mudhoo and Garg 2011). These interactions include electrostatic, ion-exchange and surface complexation processes. One of the most important minerals involved are clay minerals, especially the hydrated smectites (Figure 2.11b). Atrazine interacts with the hydration sphere surrounding the interlayer cation through hydrogen bonding between its amino groups and the O atoms of water as well as the ring N atoms and the H atoms of water. There are also ion-dipole interactions between atrazine, the interlayer cations and the negative charges on the smectite surface, using water as a bridge. The strength of hydrogen bonding also depends on the Lewis acidity of the interlayer cation. A study by Sawhney and Singh (1997) found that Al-saturated smectite sorbed more atrazine than Ca-saturated smectite. This is due to the greater polarizing effect of Al^{3+} than Ca^{2+} on the water molecules, leading to a weaker bound H atom on water and creating a stronger hydrogen bond between this H atom and one of the ring N atoms on atrazine. The negative charge on smectite surfaces is not uniformly distributed, leading to the formation of hydrophobic microsites (Laird 1996) that then allow the alkyl groups on atrazine to interact with the smectite surface.

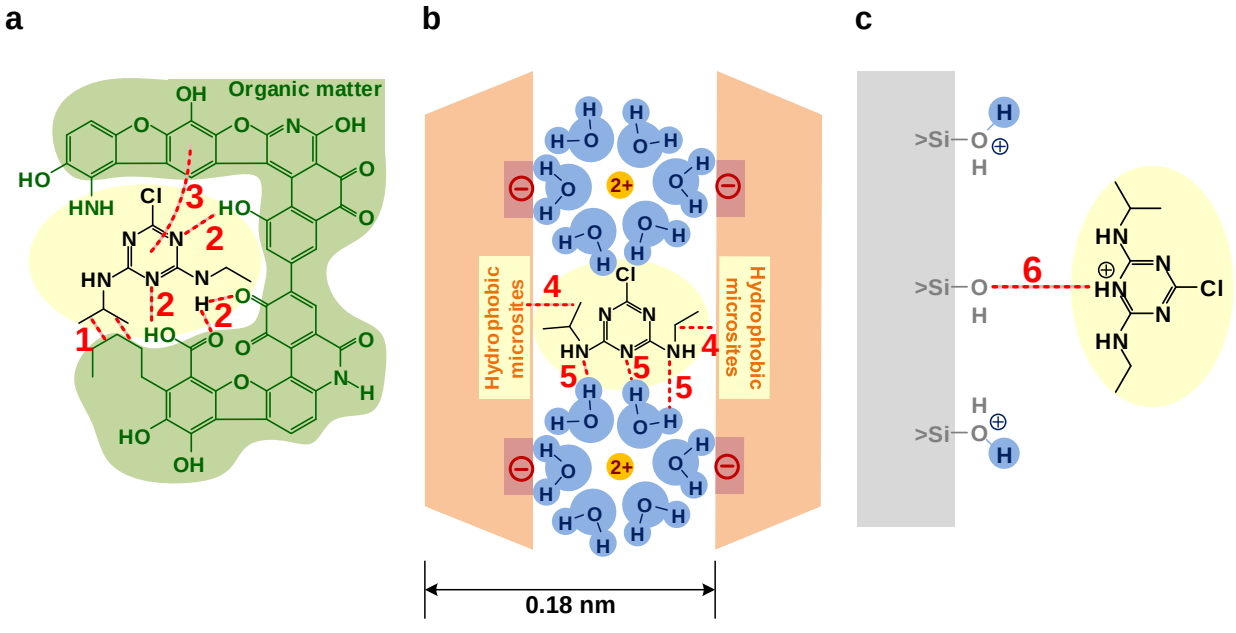

Figure 2.11 The mechanisms of atrazine sorption to various soil components. Atrazine can interact with organic matter (a) and humic substances by hydrophobic interactions or van der Waals bonding with alkyl groups on organic matter (1), hydrogen bonding with polar phenolic, carboxylic and ketone functional groups (2) and π-π interactions with aromatic structures (3). Atrazine can also interact with hydrated smectites (b) through hydrophobic interactions/van der Waals bonding with hydrophobic microsites (4) and hydrogen boding with interlayer water including ion-dipole interactions via water bridging (5). In this case, the hydration of a divalent (2+) cation is shown. At low pH conditions, protonated atrazine or its metabolites can interact with oxide surfaces with a low point of zero net charge (pH_{PZNC}) initiating competition for cation exchange sites between protons and cationic triazines and leading to the formation of surface complexes (6). Modified from Laird and Koskinen (2008).

Laird et al. (1992) concluded that in general, clay surfaces show greater affinity for atrazine with decreased cation-exchange capacity (CEC) and surface charge density. At low pH conditions, the possibility of surface complexation also exists, especially when atrazine is protonated. Oxide surfaces such as Mn-oxides and silica or quartz (SiO_2) have a low point of zero net charge (pH_{PZNC}) in the order of 2–3, and when the pH reaches these low levels, the degree of protonation of atrazine increases, as well as the degree of protonation of surface hydroxyl groups to surface water. Competition exists between these protonated atrazine molecules and protons for the hydroxyl groups, and this allows atrazine to complex with the surface of the oxide (Figure 2.11c). These electrostatic interactions are pH-dependent, and the degree of sorption increases with decreasing pH (Shin and Cheney 2005; Kovaios et al. 2006).

The degree of sorption onto mineral surfaces is affected by several factors. Surface area is important in determining the number of sites available for adsorption, with an increase in surface area leading to an increase in sorption (Mudhoo and Garg 2011). Surface charge density is another important factor, and is usually negatively correlated with the affinity of atrazine for that specific surface.

2.7.2 Modified sorbents for atrazine

Natural potential sorbent materials, such as soil minerals for which atrazine and its metabolites would not normally have a natural affinity, are often modified in order to increase that affinity. Abate and Masini (2005a) intercalated the clay minerals vermiculite and montmorillonite (smectite) with Fe(III)-OH polymers of different Fe:OH ratios. Their study found that the degree of sorption did not depend on the Fe:OH ratio, but that the intercalated clay minerals sorbed more atrazine, hydroxyatrazine, DEA and DIA than the clay minerals alone. In a similar study by the same authors (Abate and Masini 2005b), the intercalation of vermiculite with the organic cation hexadecyltrimethyl-ammonium ($CH_3(CH_2)_{15}(CH_3)_3N^+$) greatly enhanced sorption of atrazine, its metabolites DEA, DIA and hydroxyatrazine, as well as propazine, a similar triazine to atrazine. The sorption was independent of pH.

2.7.3 Sorption isotherms

The sorption of atrazine to soil components comprises fairly weak, mixed-mode interactions. The sorption of atrazine in soils is best described as physical sorption, rather than specific adsorption. This is attributable to the low affinity atrazine and its metabolites have for various soil components. This low affinity is reflected in the type of isotherms that most commonly describe atrazine sorption. The isotherms are generally near-linear in nature and are usually best described by the Freundlich equation (e.g. Clay and Koskinen 1990; Ma et al. 1993; DeSutter et al. 2003):

$$\frac{x}{m} = K_f c_e^n \tag{2.33}$$

In the equation, (x/m) is the amount of sorbate (e.g. atrazine) sorbed (x) as a fraction of the mass of sorbent (e.g. soil, clay, organic matter) (m), K_f is the partitioning coefficient between the solution and sorbent, c_e is the equilibrium concentration of the sorbate in solution and n is the index or degree of sorptivity. For the sorption of atrazine in soils, Blume et al. (2004) found K_f values ranging from 8.17–3.31 for the surface to the vadose zones of a silty clay loam. The values

for *n* were near unity, in the range 0.72–0.81. This illustrates the near-linearity (Francioso et al. 1992; Blume et al. 2004) of these isotherms, since an *n* value of 1 would yield a completely linear isotherm. This corroborates well with the general non-specific physical sorption processes that typically characterize atrazine sorption in soils. Hydroxyatrazine (ATZ-OH) is known to show greater sorption in soils than atrazine, an observation supported by the greater K_f values (22–60) and smaller *n* values (0.63–0.76) found for ATZ-OH in a study by Clay and Koskinen (1990). The greater K_f values and lower *n* values indicate the greater affinity ATZ-OH has for soil components compared to atrazine.

In general, the K_f value for atrazine and its metabolites correlates positively with soil organic matter (SOM) content (DeSutter et al. 2003; Blume et al. 2004) but shows less correlation with the clay content of soils, indicating the greater general affinity for SOM over other soil components. Apart from smectites, other clay minerals (e.g. kaolinite, vermiculite and illite) do not show high affinity for atrazine. Laird et al. (1994) have proposed that triazine sorption onto clay minerals occurs by weak physical sorption processes, whereas sorption to SOM can include chemisorption over and above physical sorption.

2.7.4 Bound residues

Bound residues are sorbed amounts of the sorbate that are not extractable (desorbable) after sorption has occurred. Bound residue formation increases with the SOM content of a soil (Hang et al. 2003) and pesticide-soil contact time (a term called aging) (Blume et al. 2004), but decreases with depth (Blume et al. 2004). This depth-discrimination is important because it means that any leached atrazine (or metabolites) is available for further leaching. Bound residue formation positively correlates with soil SOM content (Francioso et al. 1992; DeSutter et al. 2003; Dorado et al. 2003) and clay content (Hang et al. 2003), but negatively correlates with pH (Ma et al. 1993; Jenks et al. 1998; Hang et al. 2003) – a lower pH is more favourable for bound residue formation.

The formation of bound residues are an important factor in the general recalcitrance (resistance to degradation or removal) of atrazine, because they protect atrazine from microbial breakdown, plant uptake and transport (Mudhoo and Garg 2011) by rendering it less available for these processes. Bound residue formation thus increases the recalcitrance of atrazine. The effect of bound residue formation and aging on the bioavailability of atrazine for biodegradation can be determined by incubation with common atrazine degrading bacteria such as *Pseudomonas* sp.

ADP for example. After incubation, the amount of bound atrazine is often determined by measuring the total radioactivity of the sample due to ^{14}C-atrazine and subtracting the amounts of atrazine extractable by $CaCl_2$ (aqueous) and organic solvent (physically sorbed) (e.g. Barriuso et al. 2004). However, no consensus has been reached as to which parts of which fractions are truly bioavailable.

2.7.4.1 Desorption hysteresis

As is the case for many compounds, including atrazine and its metabolites, desorption of a compound from soil components cannot be predicted from its sorption isotherm, because a lesser amount of the compound is desorbed than was originally sorbed (Barriuso et al. 2004). This phenomenon is known as desorption hysteresis. Bound residues are possibly partly responsible as well as the presence of stronger forms of sorption, such as chemisorption or specific adsorption, especially in the presence of humic substances.

Since hydroxyatrazine sorbs more strongly to soils than atrazine or the dealkylated metabolites, it is not surprising that ATZ-OH shows the greatest desorption hysteresis. The typical desorption isotherms of all these compounds show a lot less linearity than the original sorption isotherms, with *n* values falling in the range 0.4–0.5 (Hang et al. 2003).

2.7.5 Effects of exogenous compounds

The sorption of atrazine and its metabolites can be greatly affected by the presence of other compounds or substances in the soil solution. These substances can be natural such as natural dissolved organic matter (NDOM) but are more often than not introduced anthropogenically. Soil amendment with organic matter can increase both solid and dissolved organic matter (DOM), and the addition of surface active agents (surfactants) to increase the wetting ability of pesticides for example, can all have an effect on atrazine and metabolite sorption, and ultimately the fate and mobility of these compounds in soils.

The affinity of triazines for organic matter has been highlighted before. Solid organic matter particles can have a dual effect on triazine mobility. Their hydrophobic surfaces increase sorption and decrease mobility of the triazines, but if they are present in colloidal form (suspended particles), they can facilitate transport by carrying the sorbed triazines along with them, wherever they may be transported (Mudhoo and Garg 2011). Liquid dissolved organic matter (LDOM) has the capability to both complex with herbicides and to compete with

herbicides for sorption sites on solids (Mudhoo and Garg 2011). Dissolved organic matter (DOM) moves in the absence of soil pores or preferential flow paths, and by complexing herbicides such as the triazines, it increases the mobility of triazines in soil. By competing for sorption sites, DOM also reduces the sorption of triazines, rendering them more mobile. However, the complexation of hydrophobic compounds by organic compounds that might be slightly more polar also has the capability of increasing sorption to sites that these hydrophobic compounds would otherwise not have affinity for. In this way, the mobility of the triazines can be greatly reduced.

Commercial formulations of most hydrophobic pesticides, including atrazine, are prepared with added surfactants to enhance spreading (or wetting ability) upon application as well as facilitating its preparation in an aqueous, easily manageable mixture, perhaps even in a "cocktail" with other water-soluble pesticides or compounds. All surfactants are characterized by having two ends, one polar or ionic, and the other hydrophobic. Atrazine prefers interacting with the hydrophobic end, but since that end is attached to the other polar end that prefers interacting with water, atrazine is able to become more dispersed (and essentially dissolved) within the aqueous mixture. Therefore, as expected, these surfactants can have significant effects on the sorption of atrazine and its metabolites in soils.

Surfactants are divided into two main groups, the ionic and non-ionic surfactants. Furthermore, all surfactants possess a critical micelle concentration (CMC), which is the point where several surfactant molecules aggregate to form micelles or aggregated structures. In water, these are regular micelles, with the polar ends oriented towards the water matrix and thereby forming a hydrophobic core, capable of "housing" various hydrophobic compounds.

It is therefore important to investigate the effects of these compounds on the sorption of atrazine, as these processes are all present and occur simultaneously with atrazine sorption. Furthermore, the processes of degradation are not separate from the processes of sorption, and vice versa. Instead, all these processes act in unison to control the fate and mobility of atrazine and its metabolites in soils.

2.8 Conclusions

Atrazine and its metabolites are important contaminants of groundwater, but the formation, mobility and fate of these compounds is largely controlled by processes in soils. The biodegradative processes controlling atrazine degradation dominate in the soil system, but work

on a timescale slow enough to allow these compounds to leach into the groundwater system, as they are often limited by carbon, energy and nitrogen availability, in a manner similar to many other biological processes in soils. Abiotic degradation of atrazine appears to be the next logical step in accelerating the degradation of these compounds in the environment. There are methods utilizing natural soil components, such as soil minerals, to degrade atrazine as well as discreet chemical laboratory-based methods that appear to be the fastest way of degrading atrazine. However, these laboratory methods are capital-intensive and not readily applicable to soils.

Apart from degradation, there are sorption processes that control the retention of atrazine and its metabolites in soils. These sorption mechanisms are mixed-mode and are highly dependent on soil organic matter (SOM) content as well as the soil mineral surfaces available. The various factors influencing sorption also include additional compounds present in the soil system, such as surfactants that are often included in herbicide formulations. These compounds have a vast potential effect on the mobility of atrazine and its metabolites in soils. As with the laboratory-based degradation mechanisms, there are engineered sorbents for atrazine as well, but would most likely also involve great development costs.

The most workable compromise appears to be the use of the soil mineral surfaces present in the soils already. They show both the capability to degrade and sorb atrazine and its metabolites, with slight modification of their conditions. Furthermore, little is yet known of the mechanisms involved in the interactions of soil minerals with these compounds, and even less is known about the effects of natural cycles such as wetting and drying on the degradation and sorption of atrazine and its metabolites.

2.9 Summary

This chapter reviews the environmental behaviour of atrazine (2-chloro-4-ethylamino-6-isopropylamino-1,3,5-triazine) and its metabolites in the environment. This common herbicide degrades to a number of metabolites, by both biodegradative and abiotic degradative processes. Biodegradation involves the action of soil bacteria, fungi, resistant plants and animals. Bacterial degradation is dependent on sources of external carbon (C), and nitrogen (N), with varying levels of these components in soils leading to very different degradation pathways and rates of degradation. Fungal, plant and animal degradation follows pathways different to those of bacteria. Biodegradation is the dominant process in soils, but is kinetically slower than the abiotic degradation processes. Soil minerals, such as the sesquioxides and clay minerals, are able to

catalyze the degradation of atrazine, at rates of days vs. months in the case of biodegradation. Several laboratory-based methods also exist, and produce very different metabolites from those found in soils. The kinetics of these processes are fastest of all (a few hours), but these methods are difficult to apply in a soil context, as they are generally discrete and highly engineered pure chemical systems. The retention of atrazine and its metabolites in soils through several sorption processes is also reviewed. The prevalent mechanisms are weak interactions with soil components such as soil organic matter (SOM), clay minerals and sesquioxide surfaces. These sorption processes are an important control on the mobility of atrazine into natural resources such as the global water systems.

3 Review: analytical methods for *s*-triazine analysis

3.1 Introduction

The presence of atrazine and its metabolites in soils and waters at usually very low to trace quantities (µg L^{-1} to ng L^{-1} levels) means that there have been numerous developments in analytical chemistry to extract, isolate, separate and quantify these compounds in a variety of matrices. At the forefront are the chromatographic methods, able to separate and quantify very low concentrations of triazine compounds accurately and efficiently, although it can be accompanied by arduous sample preparation, extraction and clean-up. Not far behind are various screening methods, which can handle low concentrations, but are not as good at separating the various triazines as the chromatographic techniques. Finally, there are spectroscopic techniques that allow insights into triazine interactions with the sample matrix material, as well as allowing the measurement of surrogate parameters (e.g. Mn^{2+} and CO_2 production), along with wet chemical methods, to determine product formation and rates of degradation.

3.2 Extraction methods

This is a crucial first step in analyzing a sample for triazines, especially for chromatography. Triazines in water samples are most easily extracted using liquid-liquid extraction. The water sample is shaken with an immiscible solvent such as dichloromethane (CH_2Cl_2) (e.g. Aslam et al. 2013), carbon tetrachloride (CCl_4) (e.g. Zhou et al. 2009) and chloroform ($CHCl_3$) (e.g. Blume et al. 2004). The triazines partition into the organic solvent which is then separated and usually evaporated to either a smaller volume for the purpose of concentrating the sample, or to dryness, upon which the sample is redissolved in another solvent such as methanol (CH_3OH) or acetonitrile (CH_3CN) for the purposes of high-performance liquid chromatography (HPLC) analysis (next section 3.3.1). However, for the purposes of analyzing trace quantities of triazines in a water sample, some form of solid-phase extraction (SPE) is usually used. Traditional SPE methods use C-18 cartridges (Nash 1990; Lucas et al. 1991), which is the most common phase used to extract most hydrophobic organic compounds and consists of silica particles with their surfaces functionalized by an octadecyl chain ($>Si(CH_3)_2—(CH_2)_{17}CH_3$). The cartridges are conditioned with a mixture of a buffer (e.g. acetate buffer, CH_3COOH/CH_3COONH_4) and an organic solvent such as methanol. The sample is thereafter passed through the cartridge, so that the triazines partition onto the solid C-18 phase. The cartridge is then eluted with a mixture of buffer and organic solvent as before, in order to retrieve the triazines. At this point, or during

elution, the sample volume is evaporated in order to concentrate the sample. A modification of SPE, called solid-phase microextraction (SPME) (e.g. Boyd-Boland and Pawliszyn 1995) uses micro-fibres to sorb analytes (e.g. triazines) which can then be desorbed directly into a gas-chromatography (GC) system, once the sample matrix has passed through, eliminating the need for solvents. Most SPE or SPME can now be performed on-line, meaning the cartridge is situated just before the chromatography column and the samples are extracted and cleaned-up as they are being run. Another approach uses a strong acid, such as 30% HCl (e.g. Blume et al. 2004) to protonate the triazines present, after which the acidified sample is passed through a strong cation exchange (SCX) column (e.g. Shin and Cheney 2005) which then binds the cationic protonated triazines. The cations are then displaced with another cation (e.g. NH_4^+) in an acidic solution, possibly with some organic solvent added. The advantages of SPE over liquid-liquid extraction for sample preparation are significant, with SPE yielding much greater recoveries, allowing trace analysis of triazines to be conducted more effectively and providing a much cleaner sample overall. However, the SPE cartridges can be costly, and each cartridge is for single use only. Furthermore, the user has to conduct the SPE skilfully, so as to not allow the cartridges to dry out at any point, since this renders both the cartridge and sample completely unusable.

For water samples, extraction and clean-up is practically done in one step. For soil samples, the triazines first have to be extracted from the soil matrix, and then the extract needs to be cleaned-up and concentrated. In single solid-phase systems, such as model studies with soil a single soil mineral (e.g. Shin et al. 2000; Shin and Cheney 2005) extractions are usually simple, using either a volume of organic solvent (e.g. methanol) or a mixture of acid-organic solvent (e.g. 90% acetonitrile and 10% 0.1 mol L^{-1} HCl) (Alvey and Crowley 1996) which is preferred when it is required to extract hydroxylated products as well, since they are not readily soluble in organic solvents and are more easily extracted when protonated (Lerch and Donald 1994). However, these extractions become much more complex with increasing complexity of the soil matrix. More complex soils are often extracted with a variety of aqueous and organic mixtures, in various proportions and at various pH values for the specific purpose of a specific soil. The steps also usually include shaking the samples or ultrasonication (Stipičević et al. 2003). Some techniques also include microwave-assisted solvent extraction (MASE) (Xiong et al. 1999; Eskilsson and Björklund 2000; Kovačić et al. 2004) and supercritical fluid extraction (SCFE) using supercritical CO_2 (Castelo-Grande et al. 2005). Clean-up almost always also includes centrifugation of the solid-solvent mix (Waria et al. 2009) and subsequent filtration with 0.1–0.2 µm PTFE (Teflon®) (Shin et al. 2000; Shin and Cheney 2005) or Nylon® membranes.

3.3 Analysis methods

3.3.1 Chromatography

The simplest and oldest form of chromatography in use for triazines is thin-layer chromatography (TLC) (Erickson et al. 1989) which has been adapted systematically to include specific methods for soils (e.g. Johnson and Sims 1998) and developments such as high-performance thin-layer chromatography (HPTLC) (e.g. Espinoza and Báez 2003) have also arisen. In TLC, the triazines can be developed on silica-gel plates, with mixtures of dichloromethane-methanol or dichloromethane-acetonitrile. These methods are cost effective and do not require the costly instrumentation that other chromatographic methods do.

A popular method for the analysis of triazines is gas chromatography (GC), coupled with nitrogen-phosphorous detection (GC-NPD) or flame-ionization detection (GC-FID). The variety of columns used are OV-1, OV-101, SE-30, DB-1, DB-5, polyethylene glycol (PEG) based phases and SPWax 10 (Pacáková et al. 1996), and these are usually capillary columns between 10 and 30 m in length, with a 0.2–0.3 mm internal diameter and 0.2–0.4 µm film thickness. The sample volume injected is relatively small, typically in the order of 1 µL, and is injected in splitless mode for optimum determination of trace levels. The carrier gas commonly used is helium (He) at flow rates of 1–2 mL min^{-1} and the separation is done using a temperature ramping program. The GC methods, especially GC-NPD are very sensitive to the chlroro-triazines, with detection limits usually around 50 ng L^{-1} (Pacáková et al. 1996). However, GC is not suitable for the hydroxy-triazines (e.g. hydroxyatrazine, DEA-OH, DIA-OH) due to their low volatility and the presence of the hydroxyl (OH) group, which are a group of compounds generally not suitable for analysis by GC. To circumvent this, a separate derivatization step of these compounds is required during sample preparation (Abián et al. 1993; Berg et al. 1995) and includes silylation, acylation and alkylation (e.g. methylation) (Pacáková et al. 1996). However, Berg et al. (1995) noted that silylation and alkylation are often not reproducible.

The most popular method for the determination of triazines is by means of reversed-phase high-performance liquid chromatography (RP-HPLC) with ultraviolet (UV) detection (e.g. Berg et al. 1995; Shin et al. 2000; Blume et al. 2004; Shin and Cheney 2004, 2005 and numerous others). This method can analyze both chloro- and hydroxy-triazines simultaneously without derivatization. The most widely used column is the octadecylsiloxane (ODS or C-18) (McMaster 2005; Shin and Cheney 2005) although some authors (e.g. Vermeulen et al. 1982; Waria et al.

2009) have shown preference for octylsiloxane (C-8) column. Other stationary phases, such as C6-Phenyl have also been used (Panuwet et al. 2010). Columns are much shorter than GC columns, usually 10–30 cm long, but are considerably larger in diameter, in the range of 2–5 mm. These columns are also packed with the stationary phase (vs. capillary columns for GC) and particle size can range from 2–10 µm (McCalley 2002; Waria et al. 2009). Elution of the analytes have to be conducted using solvents and buffers that are highly pure (> 98%) and do not absorb UV-radiation in the range 210–280 nm, as this is where the triazines are UV-active (see Table 3.1) and are detected, and an interfering mobile phase would mask the absorption by the triazines. The most common solvents used are methanol (absorbs UV-radiation below 205 nm) and acetonitrile (absorbs UV-radiation below 190 nm) and the most common buffers used are formic acid (HCO_2H), ammonium formate (HCO_2NH_4), acetic acid (CH_3CO_2H) ammonium acetate ($CH_3CO_2NH_4$) (McMaster 2005) and sometimes the dihydrogen phosphate/phosphoric acid system (H_3PO_4/KH_2PO_4) (e.g. Rustum et al. 1990). The organic solvents used are also completely miscible with water (and therefore the buffer). The buffer is chosen to ensure that the triazines remain neutral during analysis since ionic compounds do not readily sorb onto this stationary phase. The buffer concentration is usually greater than 5 mmol L^{-1} in order to buffer the compounds effectively, but do not exceed 100 mmol L^{-1} (McMaster 2005) since this would possibly lead to precipitation of the buffer salts in the column pore spaces. The triazines can be analyzed by an isocratic method (constant ratio of buffer to organic solvent), but in order to separate all analytes (or compounds) effectively, a gradient program (varying ratio of buffer to organic solvent over time) is often employed. The detection limits for HPLC is sometimes as low as those for GC, but slightly more variable, with typical limits around 0.05–50 µg L^{-1} (Steinheimer 1993; Pacáková et al. 1996). Lower concentrations are readily analyzed by pre-concentrating the sample before analysis, or by a larger injection volume into the column. Typical injection volumes are 10 µL (e.g. Shin and Cheney 2005) and can be increased as required, but should be limited to the pressure which the column can handle. Most UV detectors are diode-array detectors (DADs) that are able to run several UV-channels (wavelengths) at once, which is useful as the triazines tend to have multiple UV absorbance bands that do not all coincide (see Table 3.1). Photo-diode array (PDA) detectors (Jeannot et al. 2000) also exist which can scan a full range of wavelengths (e.g. 200–300 nm) every few milliseconds, giving a full UV-spectrum for each retention time (i.e. compound). Other detectors for HPLC analysis of atrazine include chemilumin-escence detection (HPLC-CL) (Beale et al. 2009), with similar detection limits.

Table 3.1 The UV absorption wavelengths and mass spectral mass-to-charge ratios (parent and daughter ions) for atrazine and its metabolites using ESI positive (ESI+) mass spectral mode. Data from Abián et al. (1993), Steinheimer (1993), Arnold et al. (1995b), Acero et al. (2000), Balduini et al. (2003) and Shin and Cheney (2005). Abbreviated names of compounds are the same as they appear in Chapter 2, where they are defined for each compound (Table 2.1 and Figure 2.9)

Compound	Peak UV absorption wavelengths, λ_{max} (nm)	Mass-to-charge (*m*/*z*) values with relative intensities during MS/MS mode (ESI+)	
	Primary, secondary*	Precursor ion, $[M + H]^+$	Secondary ions (relative intensity where reported)
Atrazine (ATZ)	218, 262	216	215(12), 174(100), 146(12), 138(7), 132(21), 104(17), 96(35), 79(15), 71(18)
Hydroxyatrazine (ATZ-OH)	204, 238	198	156(94), 128(6), 114(34), 97(36), 86(100), 71(17), 69(23)
Deethylatrazine (DEA)	224, 268	188	146(100), 110(10), 104(30), 79(24), 68(15)
Deisopropylatrazine (DIA)	224, 262	174	173(37), 172(10), 146(24), 138(16), 132(100), 104(40), 96(56), 79(34), 71(28), 68(17), 62(15), 43(35)
Didealkylatrazine (DDA)	202, 230	146	145(26), 144(14), 110(9), 104(25), 79(22), 68(30), 62(57), 43(100)
N-isopropylammeline (DEA-OH)	210, 235	170	155(–), 128(–)
N-ethylammeline (DIA-OH)	210, 235	156	141(–), 128(–)
Ammeline (DDA-OH)	218, 258	128	–
2-chloro-4-acetamido-6-isopropyl-amino-*s*-triazine (CDIT)	–	230	188(–), 146(–), 110(–), 104(–), 79(–), 68(–), 43(–)
2-chloro-4-acetamido-6-ethyl-amino-*s*-triazine (CDET)	–	216	174(–), 132(–), 104(–), 96(–), 79(–), 71(–), 43(–)
2-hydroxy-4-acetamido-6-isopropylamino-*s*-triazine (ODIT)	–	212	170(–), 128(–), 86(–), 43(–)
2-chloro-4-acetamido-6-amino-*s*-triazine (CDAT)	–	188	146(–), 43(–)
Atrazine-imine (ATZ-imine)	–	215	–
Deisopropylatrazine-imine (DIA-imine)	–	173	–

UV = ultraviolet,
*The primary wavelength is the largest *s*-triazine absorbance peak usually in the region of 220 nm, whilst the secondary wavelength is the smaller peak, usually between 230 and 270 nm.

Another, less popular chromatographic technique for triazines include capillary electrophoresis (CE) (Pacáková et al. 1996) which separates compounds by electroosmotic flow using buffers similar to those in HPLC. Capillary-zone electrophoresis (CZE) separates atrazine and its metabolites based on their basicity, whilst micellar electrokinetic chromatography (MEKC) separates them on the basis of polarity, by adding a surfactant at concentrations greater than its CMC to the buffer system (Pacáková et al. 1996). The limitations of this method is that the detection limits for triazines are not as low as those for HPLC and GC (Picó et al. 2003).

3.3.1.1 Chromatography with mass spectrometry

Mass spectrometry (MS) has become very popular as a method of detection for both GC and HPLC. The analysis of triazines is no different (Pacáková et al. 1996). Both gas chromatography – mass spectrometry (GC-MS) and liquid chromatography – mass spectro-metry (LC-MS) are popular methods for determining low levels of triazines in various samples (e.g. Jeannot et al. 2000; Pozzebon et al. 2003; Dagnac et al. 2005). The MS detectors provide detection limits comparable to the sensitive detectors mentioned previously for GC and LC, but allow the analyte to be fully identified as well, by a specific mass-to-charge (*m*/*z*) ratio. These values for the triazines have been listed in Table 3.1 as the "precursor ions" (see the reason for this terminology below). The triazines can be ionized by several methods. For LC-MS, electrospray ionization (ESI) and atmospheric pressure chemical ionization (ACPI) are commonly used (Dagnac et al. 2005), and are usually conducted in the positive ionization mode (denoted ESI+ for example). For GC-MS, electron impact (EI) and chemical ionization (CI) are often used (Pacáková et al. 1996) in either positive or negative mode. However, in some cases there are interfering compounds that can have the same *m*/*z* ratio as the triazine being analyzed, and in this case, structural information about the triazine molecule itself is more useful than the overall mass of the molecule (the parent or precursor ion), as the structure is unique and would set it apart from another compound. Structural information is gained by tandem mass spectrometry (GC-MS/MS and LC-MS/MS) where the original triazine ion with its *m*/*z* value (i.e. what is known as the precursor or parent ion) is further fragmented into smaller ions known as secondary or daughter ions, each with their own characteristic *m*/*z* values that would be diagnostic of the structures within the triazine molecule. These secondary ions can then be monitored instead, to both quantify and identify the compound(s) of interest. These ions can be monitored one at a time, a method known as single ion monitoring (SIM) mode, or several ions can be monitored at once.

However, SIM mode is more sensitive. This is analogous to setting a single UV wavelength in a DAD, which would be more sensitive than a full scan by a PDA detector.

The *m*/*z* values are related to the molecular masses of the compounds, but are slightly different, depending on the ionization mode. Positive ionization yields an *m*/*z* value for the precursor ion of one atomic mass unit (amu) higher than the molecular mass, and this is represented as $[M + H]^+$. Similarly, negative mode will yield m/z values one less than molecular mass $[M – H]^+$. However, this is not always the case, and several atomic mass units, representing different masses, can be added or subtracted (e.g. $[M + HCO_2H]^+$ or $[M + 2H]^{\bullet 2-}$; Abián et al. 1993). Another characteristic of the chloro-triazine mass spectra, is the ^{37}Cl isotope mass pattern, which manifests as an ion two atomic mass units (amu) above the precursor ion, at one-third (33%) of the intensity of the precursor ion (Acero et al. 2000).

3.3.2 Non-chromatographic methods

These methods include the immuno-assay, spectroscopic, and wet chemical methods. Atrazine and its metabolites have been analyzed by enzyme immuno-assay (EIA) (Pacáková et al. 1996) as well as enzyme-linked immunosorbent assay (ELISA) (e.g. Gascón et al. 1997). These methods involve a colour change upon reaction of the triazine with a specific antibody, which is then quantified using visible spectroscopy. The methods show very good to reasonable detection limits in the order of 4–160 ng L^{-1} (Koivunen et al. 2006). However, they cannot distinguish between the various metabolites and atrazine.

Several studies have used mid-infrared radiation to investigate the interactions of triazines with soil components and synthetic polymers. Usage is typically made of Fourier-transform infrared (FTIR) spectroscopy (e.g. Alekseeva et al. 2006; Cea et al. 2010). The areas of interest in the mid-IR range (400–4000 cm^{-1}) are the amine (N—H) and (C—H) stretches in the range 2900–3300 cm^{-1} and the C—Cl stretch at 805 cm^{-1}. Russell et al. (1968) were able to investigate the hydroxylation of atrazine on montmorillonite by observing the shift in absorbance from 805–795 cm^{-1} and were also able to conclude the conversion of hydroxyatrazine to its keto-tautomer by observing the formation of the carbonyl (C═O) band at 1740 cm^{-1}.

There are also methods which measure certain surrogate parameters, such as CO_2-production due to atrazine mineralization (e.g. Blume et al. 2004) or Mn^{2+} production due to atrazine oxidation by Mn-oxide (e.g. Shin et al. 2000; Shin and Cheney 2005). The production of CO_2 is usually measured by trapping the gas in a caustic soda solution (NaOH) followed by

titrimetry. Other methods for CO_2 include degrading radiolabelled ^{14}C-atrazine, which then produces ^{14}C-CO_2 which is once again trapped in NaOH, but measured by liquid scintillation counting (LSC) (Blume et al. 2004). Atrazine itself, in the form of ^{14}C-atrazine, can also be measured by extraction from soil and using LSC, but the result will be total ^{14}C, so it will include both the radioactivity from atrazine as well as that from its metabolites. However, Rustum et al. (1990) have combined the methods of HPLC with measuring ^{14}C to separate the different fractions contributing to the total ^{14}C, and in so doing, have been able to isolate and quantify these different fractions. Dissolved Mn^{2+} on the other hand is measured by methods such as atomic absorption spectroscopy (AAS) or inductively coupled plasma – atomic emission spectroscopy (ICP-AES) (Cheney et al. 1998; Shin et al. 2000). The dissolved Mn^{2+} is capable of adsorbing to the Mn-oxide surface, so extractions with $CaCl_2$ for example are usually performed to displace the Mn^{2+} cations from the surface (e.g. Shin et al. 2000). Dissolved Mn^{2+} can also be determined by electron spin resonance (ESR) (synonymous with electron paramagnetic resonance, EPR) spectroscopy. Spectra consist of a 6-band hyperfine spectrum centred on 3480 G (348 mT) (Díaz et al. 1990) when exposed to X-band microwave radiation at 9.75 GHz (Shin et al. 2000).

3.4 Conclusions and summary

The monitoring of atrazine and its metabolites in soils is conducted by many different methods. Chromatographic methods such as GC and HPLC, coupled with mass spectro-metry (MS) appear to be the most versatile and sensitive, but several other methods are also useful for screening certain aspects of atrazine behaviour in soils. However, the triazine herbicides remain one of the most challenging group of compounds to measure in the environment, and much scope still exists for the development of even more sensitive, cost-effective, faster and more versatile methods.

4 Materials and methods

4.1 Materials

4.1.1 Standards, solutions and solvents

Atrazine (2-chloro-4-ethylamino-6-isopropylamino-*s*-triazine), hydroxyatrazine (2-hydroxy-4-ethylamino-6-isopropylamino-*s*-triazine) and deethylatrazine (2-chloro-4-amino-6-isopropylamino-*s*-triazine) were purchased from Sigma-Aldrich® (Seelze, Germany) at PESTANAL® (> 98% purity) grade and were used without further purification. Acetonitrile (CH_3CN) and methanol (CH_3OH) (Romil, Cambridge, UK) as well as acetone ($(CH_3)_2CO$) (Sigma-Aldrich®) used were HPLC-grade. Organic-free milliQ® (18.2 MΩ cm) reverse-osmosis deionized water (RODW) was obtained from a MilliQ® RG system by Millipore™ (Millipore, Milford, MA, USA). Hydrochloric acid (HCl) and nitric acid (HNO_3) used was assayed at 37% and 55%, respectively, and were supplied, along with analytical reagent grade (> 98% purity) ammonium acetate ($CH_3CO_2NH_4$), ferric nitrate nonahydrate ($Fe(NO_3)_3{\cdot}9H_2O$) and aluminium chloride ($AlCl_3$), from Merck (Darmstadt, Germany).

Stock solutions at 1.0 mg mL^{-1} of atrazine and deethylatrazine were prepared in acetonitrile. Hydroxyatrazine was not directly soluble in acetonitrile, and was prepared at 0.10 mg mL^{-1} in an acidified solution comprising 90% acetonitrile and 10% 0.1 mol L^{-1} HCl (Alvey and Crowley 1996). All HPLC and LC/MS standards were made up in this acetonitrile-HCl solution as well, so as to avoid precipitation of any compounds and to reduce deterioration of the standards over time. Three separate atrazine, deethylatrazine and hydroxyatrazine standards of 25 µg mL^{-1} each were first made as a precursor for the other standards and as a single standard of each compound to define retention times on the HPLC system. Standard atrazine, deethylatrazine and hydroxyatrazine cocktails of 10, 5 and 1 µg mL^{-1} were made from serial additions and dilutions of the 25 µg mL^{-1} standards with the acetonitrile-HCl solution. From these cocktails, five low concentration standards were made by serial dilution to yield concentrations of 500, 100, 50, 10 and 5 ng mL^{-1}. These lower concentration standards were used for determination of the limits of detection (LOD) for each compound with the HPLC system.

4.1.2 Soil minerals

All representative soil minerals used were synthetic, except for quartz. Birnessite (δ-MnO_2) and gibbsite ($Al(OH)_3$) used were pre-synthesized as per the methods of McKenzie (1971) and Kyle et al. (1975). Goethite (α-Fe_2O_3·H_2O) and ferrihydrite (Fe_2O_3·nH_2O) were synthesized by the respective methods in Schwertmann and Cornell (2000) by adding 5 mol L^{-1} NaOH to a $Fe(NO_3)_3$ solution as described in their methods. Aluminium (Al^{3+})-saturated smectite was prepared by a method similar to the procedures in Russell et al. (1968), Whittig and Allardice (1986) and Sawhney and Singh (1997). Briefly, approximately 20 g of montmorillonite (STX-1B from Gonzalez County, TX provided by the Clay Minerals Society) was washed with a 0.3 mol L^{-1} $AlCl_3$ solution by placing 5 g portions of the clay into four 50 mL polypropylene centrifuge tubes (Eurotubo® by Deltalab, Barcelona) and filling to the 45 mL mark with the $AlCl_3$ solution. The tubes were then vortex-shaken to create a uniform suspension, before centrifuging the mixtures at 2,150 × *g* (MRC CN-6000) for 5 minutes and decanting the supernatant. This procedure was repeated twice to saturate the clay with the $AlCl_3$ solution. The pH of the suspension was checked at random intervals (Metrohm pH lab 827, calibrated at the start of each day) to confirm a value below approximately 4–5, so as to avoid precipitation of gibbsite. After saturation, excess Cl^- was removed by washing the clay with milliQ water, using a vortex shaker to resuspend the clay and then centrifuging the mixture at 2,150 × *g* for 5 minutes. The supernatant was decanted and tested for the presence of Cl^- by adding a few drops of 0.1 mol L^{-1} silver nitrate ($AgNO_3$) solution and checking for the formation of the white AgCl precipitate. The washing procedure was repeated until no white precipitate was formed in the supernatant. The final saturated clay was dried. Quartz powder (α-SiO_2) was obtained by milling a sample of milky quartz into a fine clay-like powder. The identities of all the mineral phases were confirmed with powder X-ray diffraction (XRD) analysis, using Cu Kα radiation (λ = 0.15418 nm). The major *d*-distances for each of the minerals were as follows: birnessite – 0.714, 0.356, 0.243 and 0.142 nm, goethite – 0.417, 0.245, 0.270 and 0.172 nm, ferrihydrite (2-line) – 0.686 and 0.249 nm, gibbsite – 0.487, 0.437, 0.316 and 0.237 nm, Al^{3+}-saturated smectite – 1.473, 0.446, 0.404 and 0.250 nm, quartz – 0.427, 0.335, 0.182 and 0.154 nm. The X-ray diffractograms of each mineral are shown in Figure A1 in Addendum A.

4.2 Methods

4.2.1 Experimental design – drying vs. non-drying experiments

The aims and objectives of this study all involve the effect of drying on the transformation of atrazine on mineral surfaces, which leads to two main experimental scenarios: (1) a comparison between samples that were allowed to evaporate (or dry) and samples that were not allowed to dry, or (2) manipulating the drying samples only to yield other information, such as the effect of changes in the drying rate, the reaction mechanism, or the effect of ultraviolet (UV) radiation. This lead to four basic sample types in every experiment (unless otherwise stated or not all of them were required), and these four different sample types were run in parallel to one another, all influenced by the same conditions at that time. The first sample type was termed a "treatment drying (TD) sample", which involved adding a pre-weighed amount of mineral solid to an aqueous solution of atrazine and mixing the components. This sample was then allowed to dry for a set period of time (*mineral* + *atrazine* + *drying*). The second type was termed a "treatment hydrated (TH) sample" which also comprised adding a mineral solid to an atrazine solution, but was followed by sealing the reaction vessel to prevent drying from taking place (*mineral* + *atrazine*, no drying). The third type was termed a "control drying (CD) sample" which involved the drying of an atrazine solution without the addition of a mineral solid, to obtain the background atrazine degradation without the mineral surface (*atrazine* + *drying*, no mineral). An equivalent also exists for the fully hydrated sample, termed the "control hydrated (CH) sample". The fourth and final type was a "blank (B) mineral" sample which was prepared in the same manner as the TD sample, only excluding the atrazine (*mineral* + *drying*, no atrazine). These blanks were used to identify artefacts during analyses.

For each sample type, several replicates were run as deemed necessary, and vary with each experiment (see the following sections). The basic setup of each replicate or individual sample was to add a total of 1 mL of either the atrazine or blank solution to a pre-cleaned 25 mL amber vial. The amber vials were soaked for 24 hours in a 5% HNO_3 solution and were then rinsed thoroughly thereafter with acetone and milliQ water before drying in an oven at 120 °C. The 1 mL of atrazine solution was composed of 900 µL of milliQ water mixed with 100 µL of the 10 µg μL^{-1} atrazine stock solution (measured out with an Eppendorf® pipette) in acetonitrile, to give a final aqueous solution of 100 µg mL^{-1} of atrazine (0.465 µmol in the vial). The blank solution contained both milliQ water and acetonitrile in the same ratio, but did not contain any atrazine. To these solution-containing vials, 500 mg of the predetermined mineral solid was added, and the

mixture was gently mixed into a moist, crumbly paste with a pre-cleaned (acetone and milliQ water wash) stainless steel spatula. Drying experiments were conducted by leaving the vials open to the atmosphere, whilst moist experiments were conducted by sealing the vial with a Teflon® (PTFE) liner and a screw-cap. All experiments were conducted in the dark so as to avoid the effect of daylight on the reaction.

All experiments were categorized into two major types, namely a *mineral series* or a *time series* experiment. In a mineral series, several atrazine-mineral mixtures were allowed to dry to complete dryness over a fixed two-week period. In a time series, a single mineral-atrazine mixture was sampled over predetermined periods of time, at varying degrees of (partial) dryness. This was achieved by setting up several replicates of the same mixture and then sacrificing either one, two or three replicates at a predetermined time, as the experiment required. A visual illustration of the experimental design is provided in Figure 4.1.

4.2.1.1 The effect of mineral type on atrazine degradation

To investigate the degradation of atrazine on different mineral surfaces relative to one another, 7 drying experiments were set up (500 mg mineral + 100 µg atrazine in water-acetonitrile solution) which included 6 mineral surfaces – namely birnessite, goethite, ferrihydrite, gibbsite, Al^{3+}-saturated smectite and quartz – as well as 1 non-mineral control (100 µg atrazine in water-acetonitrile solution) (Figure 4.1). The 7 vials were inspected after 7 days and were all visibly dry. These vials were left for another 7 days (a total of 14 days). In a parallel experiment, moist analogues were set up for the same 7 vials containing the minerals and the atrazine non-mineral control. These 7 vials were sealed with the Teflon®-lined screw caps and left for 14 days as well. Seven drying blanks were also set up, which mimicked the 7 drying vials but these blanks contained no atrazine. The blank control (CB, see Figure 4.1) was a drying solution of milliQ water and acetonitrile in the usual 9:1 ratio. After 14 days the samples were extracted by the procedure outlined in section 4.2.2 and analyzed by liquid chromatography – mass spectrometry (LC/MS) (section 4.2.3).

(a) The effect of mineral type on atrazine degradation

Sampling time	Samples sacrificed						
14 days	TD-br	TD-gt	TD-fh	TD-gb	TD-sm	TD-qz	CD
14 days	TH-br	TH-gt	TH-fh	TH-gb	TH-sm	TH-qz	CH
14 days	B-br	B-gt	B-fh	B-gb	B-sm	B-qz	CB

(b) The effect of drying time on atrazine degradation – 10 day experiment

Sampling time	Samples sacrificed				
1 day	TD-br-1		TD-qz-1		
2 days	TD-br-2	TH-br-2	TD-qz-2	TH-qz-2	CD-2
3 days	TD-br-3		TD-qz-3		
4 days	TD-br-4	TH-br-4	TD-qz-4	TH-qz-4	CD-4
5 days	TD-br-5		TD-qz-5		
6 days	TD-br-6	TH-br-6	TD-qz-6	TH-qz-6	CD-6
7 days	TD-br-7		TD-qz-7		
8 days	TD-br-8	TH-br-8	TD-qz-8	TH-qz-8	CD-8
9 days	TD-br-9		TD-qz-9		
10 days	TD-br-10	TH-br-10	TD-qz-10	TH-qz-10	CD-10

Figure 4.1 Visual layout of the sampling programme used in this study. Visual layouts with sample names are given for the experiments investigating (a) the effect of mineral type on atrazine degradation, (b and c, continued on next pages) the effect of drying time on atrazine degradation, (d) the effect of accelerated drying under compressed air and nitrogen on atrazine degradation, and (e) the effect of ultraviolet (UV) radiation on atrazine degradation. Codes are as follows: br = birnessite, gt = goethite, fh = ferrihydrite, gb = gibbsite, sm = Al^{3+}-saturated smectite, qz = quartz, TD = drying treatment, TH = moist treatment, B = blank, CD = drying control, CH = moist control, CB = blank control, N = nitrogen dried, Mn(II) = samples reserved for dissolved Mn^{2+} analysis, WR = without ultraviolet (UV) radiation, LW = long wave UV radiation treatment at 365 nm, SW = short wave UV radiation treatment at 254 nm. Numerical codes in name ends indicate number of the replicate. In the long-term experiment, A and B indicate a replicate pair.

(c) The effect of drying time on atrazine degradation – 30 day experiment

Sampling time	Samples sacrificed					
Initial, 0 days	TD-br-0A	TD-br-0B	TD-qz-0A	TD-qz-0B	CD-0A	CD-0B
5 days	TD-br-5A	TD-br-5B	TD-qz-5A	TD-qz-5B	CD-5A	CD-5B
7 days	TD-br-7A	TD-br-7B	TD-qz-7A	TD-qz-7B	CD-7A	CD-7B
9 days	TD-br-9A	TD-br-9B	TD-qz-9A	TD-qz-9B	CD-9A	CD-9B
11 days	TD-br-11A	TD-br-11B	TD-qz-11A	TD-qz-11B	CD-11A	CD-11B
13 days	TD-br-13A	TD-br-13B	TD-qz-13A	TD-qz-13B	CD-13A	CD-13B
16 days	TD-br-16A	TD-br-16B	TD-qz-16A	TD-qz-16B	CD-16A	CD-16B
20 days	TD-br-20A	TD-br-20B	TD-qz-20A	TD-qz-20B	CD-20A	CD-20B
25 days	TD-br-25A	TD-br-25B	TD-qz-25A	TD-qz-25B	CD-25A	CD-25B
30 days	TD-br-30A	TD-br-30B	TD-qz-30A	TD-qz-30B	CD-30A	CD-30B

(d) The effect of accelerated drying under compressed air and nitrogen on atrazine degradation – compressed air

Sampling time	Samples sacrificed			
1 day	TD-br-A1	TD-br-A2		
4 days	TD-br-A3	TD-br-A4		
35 days	TD-br-A5			
35 days	TD-br-A6-Mn(II)		TD-qz-A1	CD-A1
35 days	B-br-A1-Mn(II)			

Figure 4.1 continued.

(d) The effect of accelerated drying under compressed air and nitrogen on atrazine degradation – nitrogen

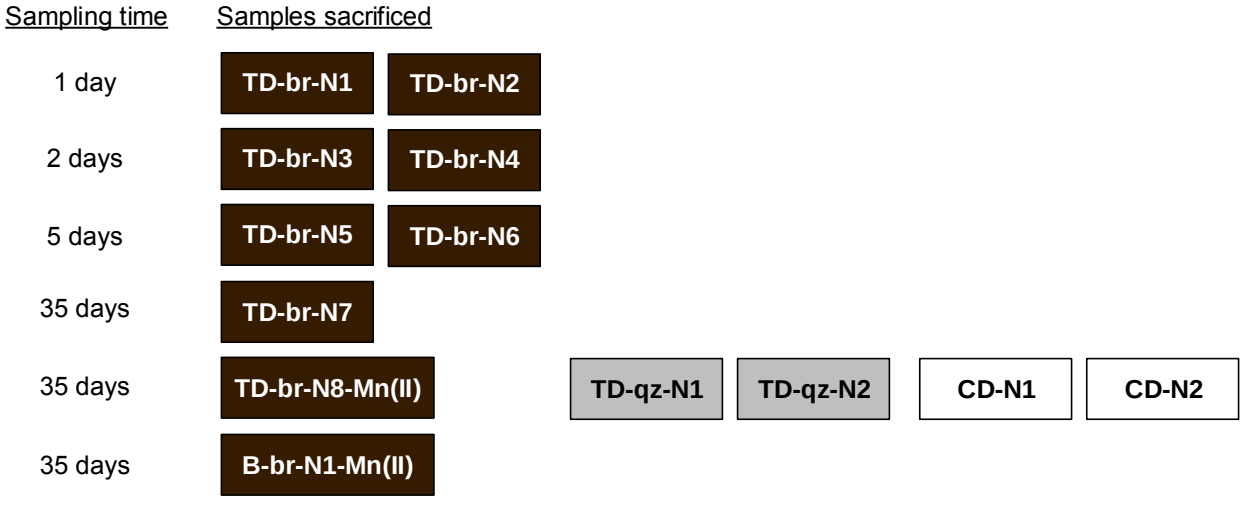

(e) The effect of ultraviolet (UV) radiation on atrazine degradation

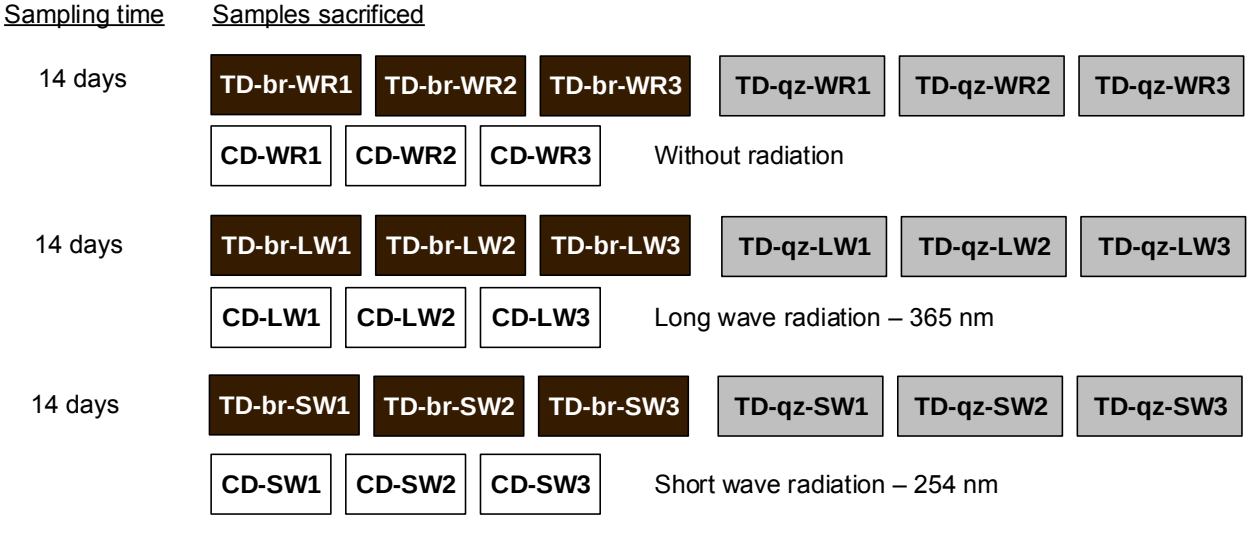

Figure 4.1 continued.

4.2.1.2 The effect of drying time on atrazine degradation

Birnessite was identified as the most reactive toward atrazine in the mineral series experiments (see results and discussion). Therefore, birnessite was chosen as a model mineral surface to study atrazine degradation over time. Two sets of experiments were conducted, the first a short-term experiment over 10 days to investigate the degradation of atrazine as the birnessite surface was drying. Ten replicates of birnessite-atrazine mixtures (100 µg atrazine in 1 mL milliQ water-acetonitrile + 500 mg birnessite) were set up and 1 replicate was sacrificed per day. Five moist analogues were set up and sacrificed every second day. Quartz was identified as the least reactive (virtually unreactive) toward atrazine in the mineral series experiments (see results and discussion) and was therefore chosen from that point on as a representative mineral-containing control in comparison to birnessite. Thus, a quartz analogue of both the drying and moist birnessite experiments was conducted and sacrificed in the same manner. Five non-mineral control (100 µg atrazine in 1 mL milliQ water-acetonitrile) replicates were also set up and allowed to dry. One of these control replicates was sacrificed every second day. The results (see chapter 5) indicate that atrazine degradation was incomplete over the 10 day period, so a second set of experiments were conducted, over a 30 day period. In a similar set up to the 10 day experiments, 20 replicates each of birnessite and atrazine, quartz and atrazine, and non-mineral atrazine controls (60 in total) were allowed to dry over the 30 day period. Two replicates (duplicates) of each of the three types of samples were sacrificed at 0 (initial), 5, 7, 9, 11, 13, 16, 20, 25 and 30 days (6 at a time). The samples were once again extracted as before and this time analyzed with high performance liquid chromatography (HPLC), since the retention times and peak identities were previously confirmed on LC/MS.

The mineral series experiments (section 4.2.1.1) were dried beyond (14 days) the required drying time for the atrazine-mineral mixtures and non-mineral controls (typically less than 7 days). However, for both the short- and long-term time series experiments, some sampling times in the first few days coincided with times at which the samples were only partially dried. This provided information about the degradation of atrazine in terms of moisture content. This moisture content was measured by pre-weighing all of the replicate mixtures in their vials at the start of the experiments, and then weighing each replicate vial as it was sacrificed. The samples were weighed to the nearest 0.1 ± 0.05 mg, just prior to extraction.

4.2.1.3 The effect of accelerated drying under compressed air and nitrogen on atrazine degradation

To investigate whether the degradation of atrazine was a result of the mineral-atrazine interaction time (more degradation was observed over a longer time period) or whether it was a result of the moisture content (the moist replicates showed no reaction), drying experiments were once again set up but were rapidly dried this time under a gentle stream of compressed air. To determine the effect of atmospheric oxygen (O_2) as a possible oxidant of atrazine during the experiment, the same experiment was conducted in parallel under a gentle stream of nitrogen (N_2) (e.g. Wang et al. 1999), in order to purge the vials of any O_2. Both the air and N_2 streams were adjusted to their most gentle setting (~ 14 mbar), so as to limit the amount of material becoming airborne and thus being lost from the experiment. Once again, birnessite, quartz (mineral control) and a non-mineral control were investigated. In both the air-dried and N_2-dried samples, once moisture had been rapidly removed, the samples were purged continually for a maximum of 35 days. At various time intervals replicates were sacrificed for analysis. On the 35th day of each experiment one replicate was sacrificed for atrazine and metabolite analysis, whilst another was extracted for dissolved Mn^{2+} (see section 4.2.2), to measure as a surrogate parameter for possible oxidation of atrazine and reduction of birnessite (e.g. Shin et al. 2000; Shin and Cheney 2004, 2005). Visual inspection of the air- and N_2-dried experiments showed that all the replicates had dried within a few hours of starting the air or N_2 stream, and the replicates were weighed simply to confirm that total drying had occurred.

4.2.1.4 The effect of ultraviolet (UV) radiation on atrazine degradation

The possible effects of sunlight on drying in a natural setting were contemplated as part of this study. To simulate these possible effects, three sets of parallel experiments were conducted, two at two different wavelengths of ultraviolet (UV) radiation, typically 254 and 365 nm, and another without UV light. Experiments were conducted in a black box to avoid any other light entering the experimental chamber. In order for the radiation to make direct contact with the mineral-atrazine mixtures, the amber vials were traded for open watch-glasses upon which the experiments were conducted. The normal drying experiment conducted on the watch glass thus acted as a non-UV control under these conditions. The shortwave radiation at 254 nm was provided by a mercury (Hg) vapour lamp, and the longwave radiation at 365 nm was provided by a black light phosphor lamp. To determine statistical differences between the three cases, samples of birnessite-atrazine, quartz mineral control and non-mineral control were run in triplicate (9 for

each experiment, 27 in total) for 14 days, after which they were extracted and analyzed by HPLC. A summary of the experiments described in sections 4.2.1.1 – 4.2.1.4 is provided in Figure 4.1.

4.2.1.5 The effect of drying under solvent-only conditions (no water) on atrazine transformation

To eliminate all the possible effects of water content on drying and atrazine transformation, drying experiments were set up in the total absence of water, using only organic solvent as the liquid medium. Atrazine-birnessite mixtures were set up and moistened by an acetone-atrazine solution, instead of the aqueous solution as before. This solvent was then allowed to evaporate. Samples were set up with 100 µg in 1 mL of acetone ($(CH_3)_2CO$) to which 500 mg of birnessite and quartz was added, separately. Also, a non-mineral control was conducted as before, but with acetone as solvent (100 µg atrazine in 1 mL acetone). Samples were extracted after 30 days. Analyses were conducted by LC/MS instead of HPLC to identify any additional possible transformation products not encountered in the moisture drying experiments.

4.2.1.6 The degradation of atrazine degradation products by drying mineral surfaces

To establish if the degradation products of atrazine detected in this study, namely hydroxyatrazine and deethylatrazine, would be transformed further on birnessite surfaces, these compounds were reacted with birnessite. Parallel controls were conducted with quartz and without a mineral surface (non-mineral control). However, given the solubility issues with hydroxyatrazine, these compounds were mixed with birnessite using the acidified 9:1 acetonitrile-HCl solution. Given that the effect of pH on the reactivity of the mineral surface toward these compounds are outside the experimental scope of this investigation, a parallel "control" (in terms of the transformation products) was run which included atrazine (same concentration, but now in 9:1 acetonitrile-HCl) mixed with birnessite and quartz, as well as a non-mineral control. The final permutation was thus atrazine, deethylatrazine and hydroxyatrazine (100 µg in 1 mL of 9:1 acetonitrile-HCl) were each mixed with birnessite and quartz (both 500 mg), and in the form of a non-mineral control (3 vials per compound – one for birnessite, another for quartz and another for the non-mineral control). These vials were then allowed to dry over a 14 day period. As with the solvent-only drying experiments, analyses were also conducted by LC/MS instead of HPLC, in order to identify any additional possible transformation products not encountered before.

4.2.2 Extraction and sample clean-up

Upon sacrificing (and weighing in some cases) a drying replicate from an experiment, the sample was immediately extracted by adding 5 mL of the same 9:1 acetonitrile: 0.1 mol L^{-1} HCl (Alvey and Crowley 1996) solution used to make up the standards, to the vial. For moist replicates, only 4 mL of the extraction solution was added, since the original 1 mL of moisture added in the experiment initially was assumed not to have evaporated in the sealed vial. The vial that was sacrificed was then capped with a screw cap containing a Teflon® (PTFE) liner and shaken on an orbital shaker at 250 revolutions per minute (rpm) for 1 hour. After shaking, the samples were filtered through a 0.2 µm Nylon® syringe filter. For the mineral series experiments, some of the mineral phases, such as goethite, were difficult to pass through the filter, so all of the mineral-liquid mixtures in these experiments were first decanted out of the vials into 50 mL polypropylene (PP) centrifuge tubes (Eurotubo® by Deltalab, Barcelona) and centrifuged at 2,150 × *g* (MRC CN-6000) for 5 min, and the supernatant was filtered. The filtered extracts were stored in HPLC vials and kept frozen until ready for analysis by HPLC or LC/MS. In a separate test (data not shown), to test for the possible sensitivity and sorptivity of these organic compounds to plastics, solutions of atrazine and its transformation products were allowed to equilibrate for 1 hour in plastic centrifuge tubes, and ultraviolet (UV) spectra of these solutions were compared with the UV spectra of fresh solutions from glass containers at the same concentration, using an ultraviolet-visible (UV-vis) spectrophotometer (Thermo Scientific). No discernable differ-ence between the spectra was observed.

Dissolved Mn^{2+} was extracted by adding 5 mL of 0.5 mol L^{-1} $CaCl_2$ (e.g. Shin et al. 2000) solution to the desired replicate prior to shaking at 250 rpm for 1 hour. The samples were filtered through a 0.2 µm Nylon® syringe filter. Two drops of 1 mol L^{-1} HCl was then added to the sample to acidify it to a pH below 2, so as to ensure Mn^{2+} remained in solution. Blank birnessite samples (no atrazine) were subjected to the same drying conditions and were also extracted in parallel using the same extraction procedure. This blank Mn^{2+} value was used as a reference to compare to the extracts from the atrazine-birnessite extractions. The samples were stored and kept refrigerated at just below 4 °C until they were analyzed by inductively coupled plasma – atomic emission spectroscopy (ICP-AES).

4.2.3 Analytical techniques

Atrazine and its transformation products in samples originating from the mineral series, solvent-only drying experiment and the transformation products plus birnessite experiments were analyzed by LC/MS on a Waters® Synapt™ G2 quadrupole time-of-flight (TOF) accurate mass spectrometer (Waters® Corporation, Milford, MA, USA) which was fitted with a Waters® Acquity™ UPLC system and a photo-diode array (PDA) UV detector. Separation of atrazine and its metabolites was achieved on an Agilent ZORBAX Eclipse XDB-C8 column (15 cm × 4.6 mm, 5 µm particle size) using a gradient programme with two solvents, namely 10 mmol L^{-1} ammonium acetate ($CH_3CO_2NH_4$) dissolved in milliQ water (solvent A) and acetonitrile (CH_3CN) (solvent B). The gradient programme was adapted from Waria et al. (2009) and was as follows: an initial isocratic run for 5 min at 95% solvent A and 5% solvent B, followed by a gradient (applying gradient curve type 6) for 10 min to 10% solvent A and 90% solvent B, these conditions are then held for 3 min before a 5 min gradient back to initial conditions (95% A and 5% B) and a final 7 min isocratic equilibration run at 95% A and 5% B. The flow rate was 1 mL min^{-1} and the injection volume was 10 µL. Mass spectra were collected in the electrospray ionization positive mode (ESI+) using a capillary voltage of 2.5 kV, a cone voltage of 15 V, a desolvation temperature of 250 °C and a N_2 (desolvation gas) flow rate of 650 L h^{-1}. The rest of the MS settings were optimized for best performance. Mass data were collected at a scan rate of 0.2 s and in the *m*/*z* range of 100–600. Real time accurate mass determination was performed using a lock mass flow rate of 0.002 mL min^{-1} and leucine enkephalin as lock mass, acquiring lock mass data in 20 s intervals. The instrument was calibrated using sodium formate (HCO_2Na) and the PDA detector was set to a scan range of 190–450 nm. Data collection and processing was performed using the Masslynx 4.1 software system. Standard cocktails (atrazine, deethylatrazine and hydroxyatrazine) of 25, 10, 1, 0.1 and 0.01 µg mL^{-1} were run for quantification purposes. The limit of quantitation (LOQ) for atrazine was 10 ng mL^{-1} and 100 ng mL^{-1} for the metabolites deethylatrazine and hydroxyatrazine. The calibration results for the LC/MS runs are shown in Addendum A at the end of this document. The retention times obtained for each compound was 10.0 min for hydroxyatrazine, 10.7 min for deethylatrazine and 13.0 min for atrazine.

The time series, air- and N_2-dried, as well as the UV sample extracts were run on a Waters® 1525 binary HPLC pump system, fitted with a Waters® 2487 dual wavelength diode-array detector (DAD) set to 228 and 239 nm for UV absorbance and a Waters® 717plus autosampler. The same separation conditions (gradient and column) were applied to this system, but the

injection volume was increased to 40 µL. Standards at 25, 10, 5, 1, 0.5, 0.1, 0.05, 0.01 and 0.005 µg mL^{-1} were run, and the greatest linearity was found for the range 25–0.05 µg mL^{-1} for all compounds. The limit of quantitation (LOQ) for atrazine and its metabolites was thus 50 ng mL^{-1} and the limit of detection was 5 ng mL^{-1} for atrazine and 10 ng mL^{-1} for deethylatrazine and hydroxyatrazine. Calibrations were performed with each new batch of eluent (solvent A and B) prepared, and the results are shown in Addendum A at the end of this document. A simple method validation was also performed, by measuring the injection error (triplicate injections of the same standards) and biological error (single injections of standards prepared in triplicate), the results of which are shown in Addendum B. For the HPLC analysis, it was found that the best chromatograms were collected at 239 nm, despite the greater UV absorbance of the triazines at the lower wavelengths (218–228 nm). The chromatograms collected at the lower 228 nm wavelength were found to have an unsatisfactory sloping baseline, and were eventually disregarded in the final data processing. The processed data is shown in Addendum A, along with each sample name.

Dissolved Mn^{2+} was measured on an iCAP 6300 ICP-AES (Thermo Scientific) using argon (Ar) as plasma gas, fixed at a flow rate of 12 L min^{-1}. Total dissolved manganese (Mn_{diss}) was measured, which was assumed to be present only in the divalent, Mn^{2+} state.

4.2.4 Inherent birnessite moisture content

The gravimetric moisture content inherent in the birnessite mineral structure was also quantified by oven drying 1 g of birnessite for 24 hours at 110 °C (e.g. Cheney et al. 1998). The moisture content (%) was determined by the equation:

$$\text{Moisture}\% = \left(\frac{\text{Original mass} - \text{Oven dried mass}}{\text{Oven dried mass}} \right) \times 100 \qquad (4.1)$$

From equation 4.1, the moisture content was determined to be 7%.

5 Results and discussion

5.1 The effect of mineral type on atrazine transformation on moist and drying surfaces

The LC/MS results shown in Figure 5.1 indicate that the birnessite drying experiment yielded the greatest number of metabolites (two, namely hydroxyatrazine and deethylatrazine) and the greatest degree of atrazine degradation than all the other mineral phases. An *m*/*z* search for all the atrazine metabolites listed in Table 3.1 was conducted, but these two metabolites were the only ones found. As a result only analytical data from the birnessite treatments, controls and blanks are shown. These chromatograms are intermittently compared with the non-mineral controls where warranted. The mass-extracted $[M + H]^+$ ion chromatograms and total ion current (TIC) chromatogram for the birnessite drying experiment extract is shown in Figure 5.1. The identities of atrazine, deethylatrazine and hydroxyatrazine in the birnessite drying experiment extract were confirmed with the mass spectra in Figure 5.2, from the exact masses of 216.1028, 188.0703 and 198.1363 Dalton (Da), respectively. The identities of atrazine and deethylatrazine was further confirmed by the ^{37}Cl isotopic mass pattern (Acero et al. 2000) with peaks at 218.0992 and 190.0671 Da, respectively, at one-third the intensity of the parent ion peak located approximately 2 Da lower.

The total ion current (TIC) chromatograms of both the atrazine-birnessite dried and moist samples, as well as the birnessite blank, the dry and moist non-mineral atrazine controls, and the non-mineral control blank were compared to one another in Figure 5.3. Several contaminant mass peaks such as *m*/*z* = 130.2, 453.3, 264.2, 149.0, 313.3 and 348.3 were observed, as they were present in the blank birnessite and non-mineral control blank TIC chroma-tograms (Figures 5.3c and f). In all of the chromatograms that contained the atrazine peak (*m*/*z* = 216.1), a relatively small peak at 13.5 min with *m*/*z* = 230.1 appears. Exact mass determination identified the compound as propazine (2-chloro-4,6-bis(isopropylamino)-1,3,5-triazine), a *s*-triazine very similar to atrazine, with an exact mass at 230.1132 Da and 232.1123 Da, representing the ^{37}Cl isotopic pattern. This was considered as a contaminant forming part of the original standard compound. A similar investigation into product formation and contaminant peaks/masses was conducted for the other mineral surfaces (TIC chromatograms shown in Addendum A).

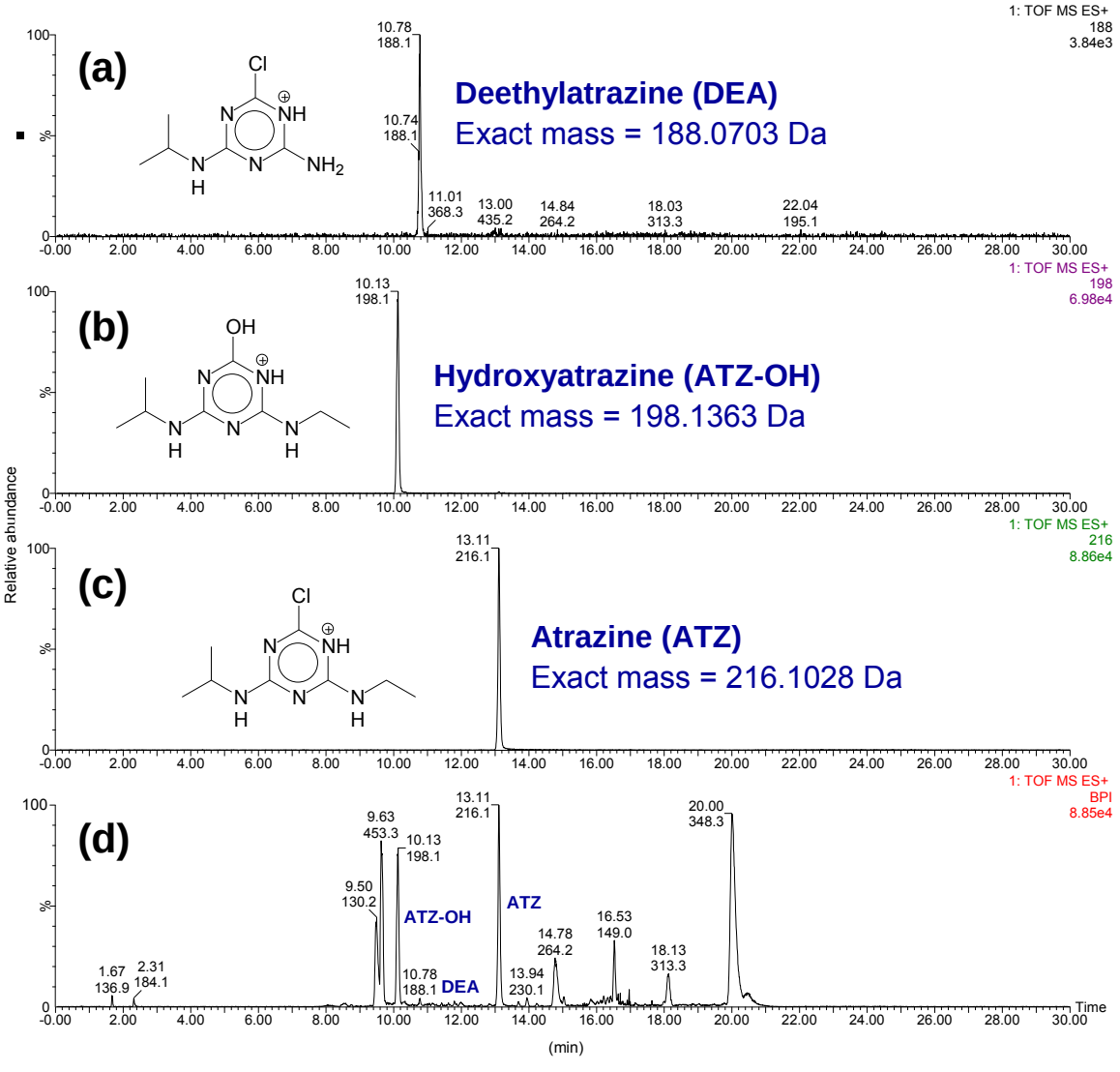

Figure 5.1 The mass-extracted $[M + H]^+$ ion chromatograms of (a) deethylatrazine (*m*/*z* = 188), (b) hydroxyatrazine (*m*/*z* = 198), (c) atrazine (*m*/*z* = 216) and (d) the total ion current, normalized to the base peak intensity (BPI) for the birnessite drying experiment extract.

The extent of atrazine transformation on each mineral surface, and the amount of hydroxyatrazine and deethylatrazine formed, over the 14-day period, was quantified by running the standard cocktails at 25, 10, 1, 0.1 and 0.01 µg mL^{-1} and calibrating the LC/MS system. The results obtained were tabulated, along with the calibration parameters in Table A1 in Addendum A. The results were plotted graphically in Figure 5.4 for each mineral surface, both under moist and drying conditions, along with non-mineral atrazine controls. The percentage recovery of each individual compound (atrazine, hydroxyatrazine or deethylatrazine) is plotted as bars in Figure 5.4, and was calculated using the amount of µmoles of each compound recovered as a fraction of the initial 0.465 µmoles atrazine used.

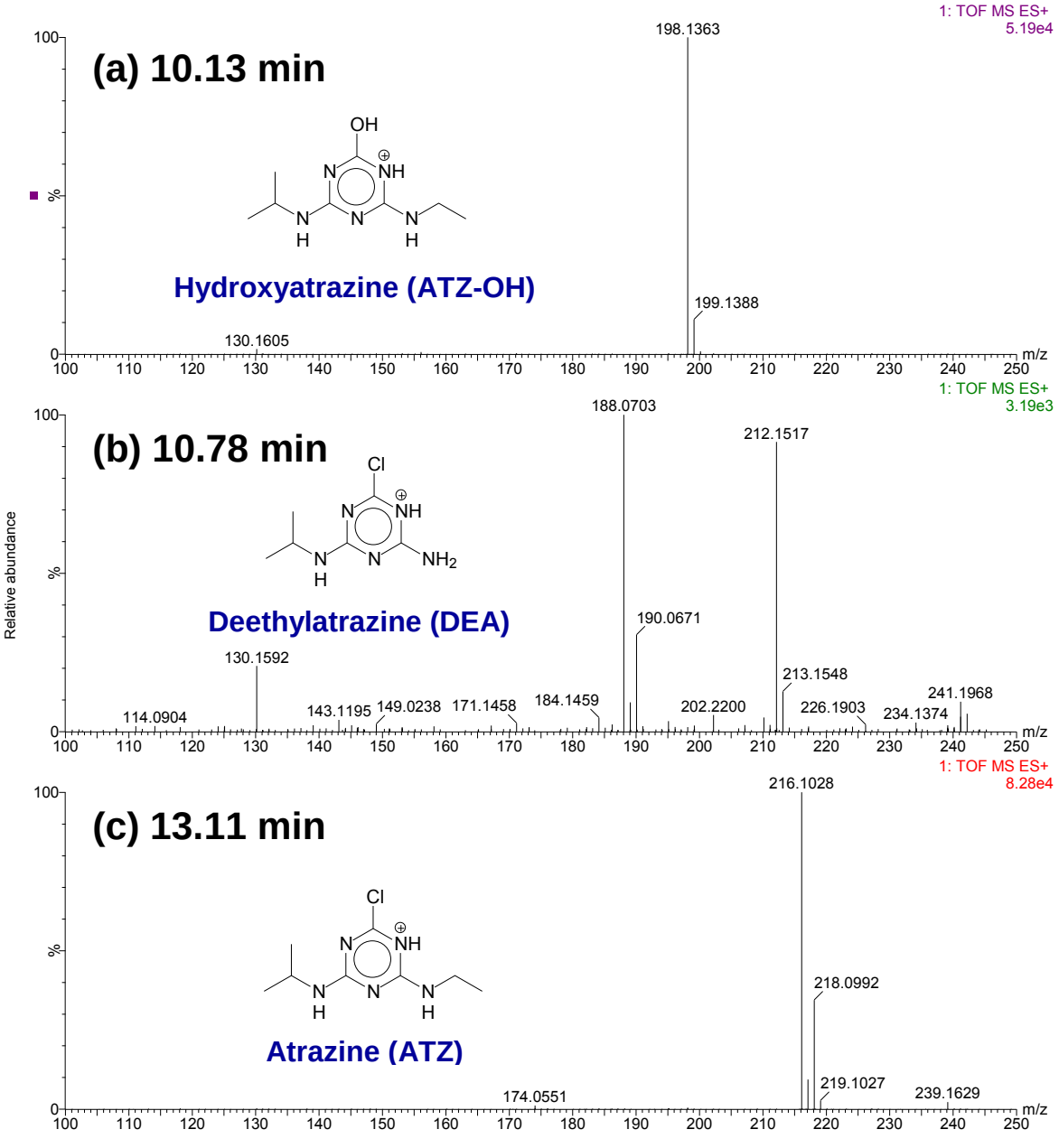

Figure 5.2 The mass spectra of (a) hydroxyatrazine (retention time = 10.13 min), (b) deethyl-atrazine (retention time = 10.78 min) and (c) atrazine (retention time = 13.11 min) in the birnessite drying experiment extract.

The percentage recovery calculation is shown in Equation 5.1:

$$\%\,\text{Recovery} = \left(\frac{\mu\text{moles of individual compound recovered}}{0.465\,\mu\text{moles atrazine intially}} \right) \times 100 \qquad (5.1)$$

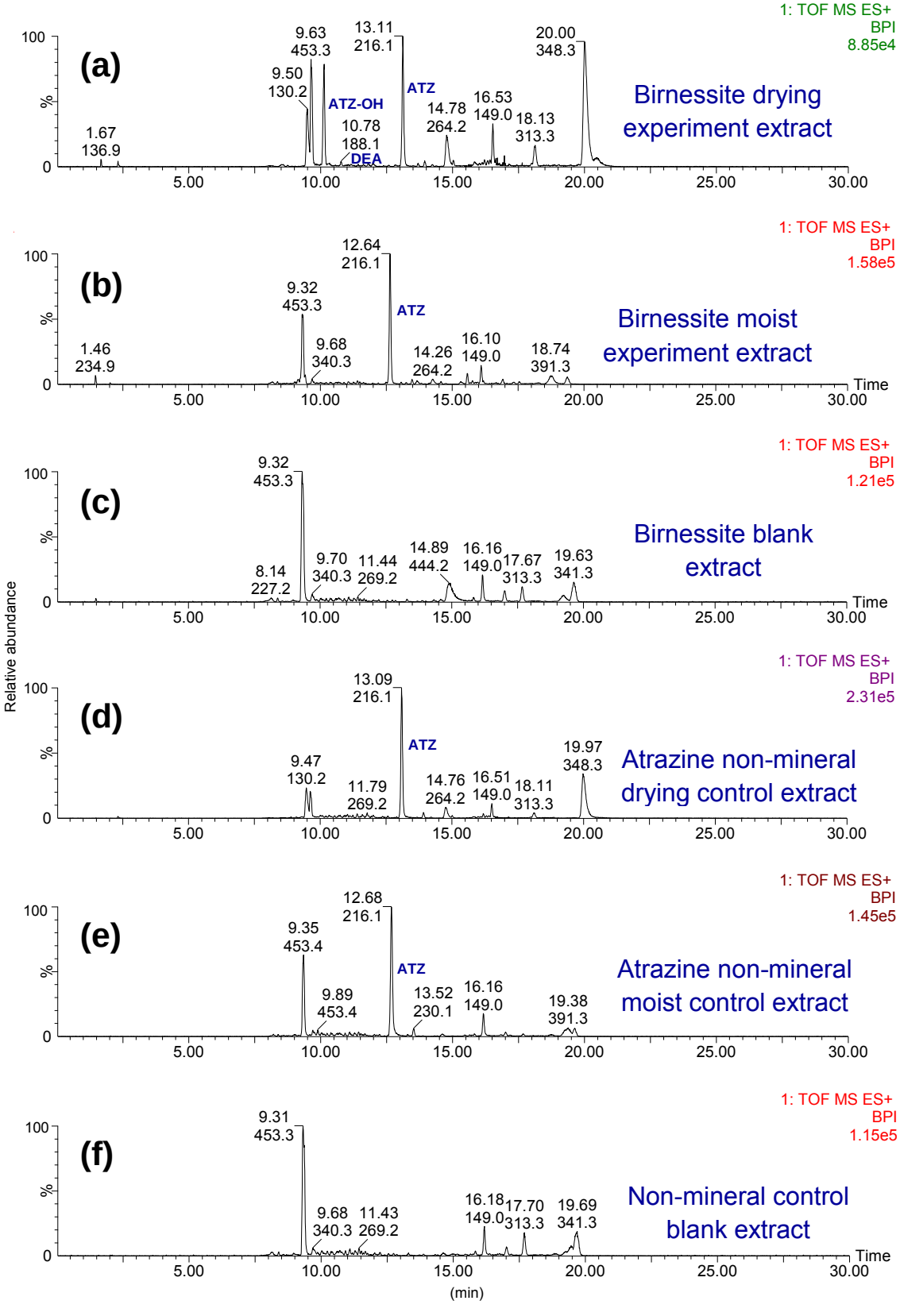

Figure 5.3 Total ion current (TIC) chromatograms of the extracts from the (a) birnessite drying experiment, (b) birnessite moist experiment, (c) birnessite blank, (d) atrazine non-mineral drying control, (e) atrazine non-mineral moist control, and (f) non-mineral control blank.

(a) Drying experiments

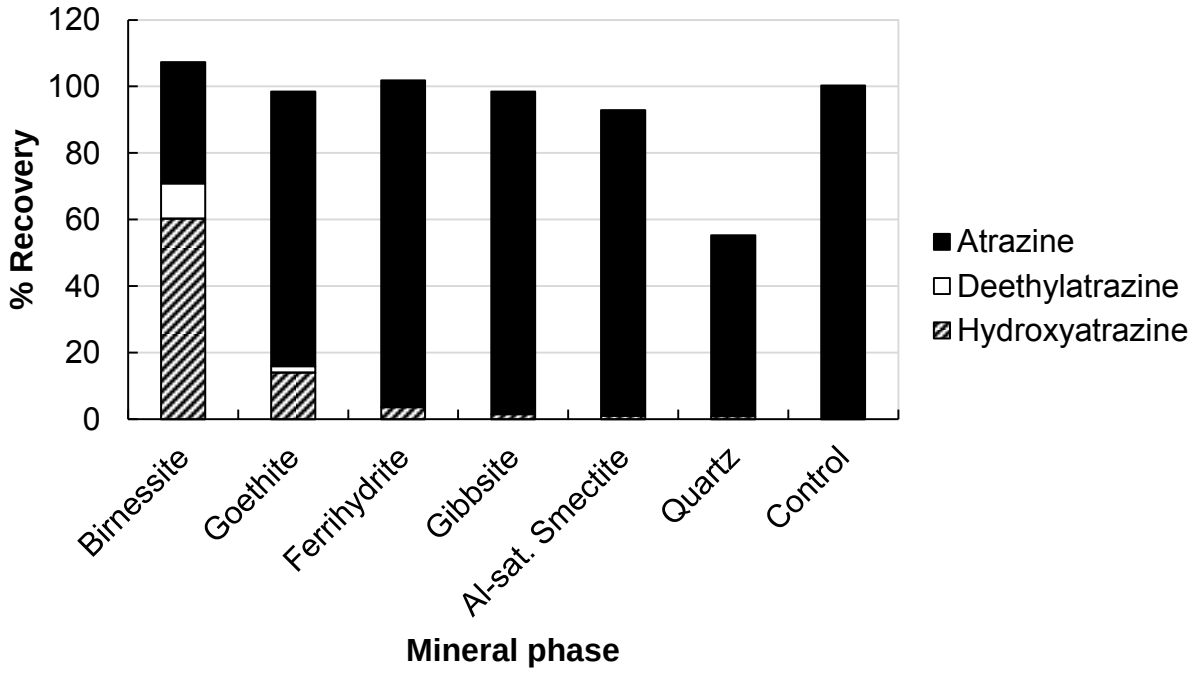

(b) Moist experiments

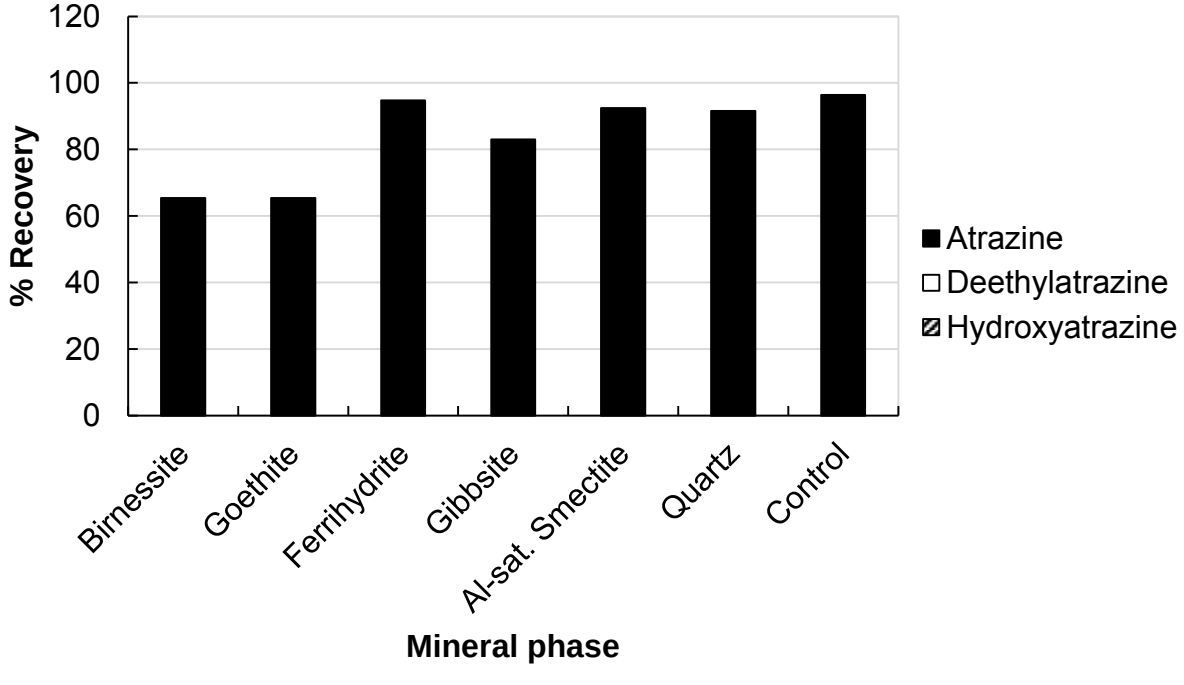

Figure 5.4 The results of the mineral series (a) drying and (b) moist experiments. The percentage recovery represents the recovered amount of µmoles of each compound as a fraction of the initial 0.465 µmoles atrazine added to the mineral surface or control. Al-sat Smectite = Al^{3+}-saturated smectite.

The total *s*-triazine recovery ranges from 107% to 55% for the drying experiments, but the range is less pronounced in the moist experiments, with values ranging from 96% to 65%. The recovery is a measure of the extraction efficiency of a particular extraction solvent or method, and is an indirect indication of the degree of sorption of a compound to a solid phase, in the case of simple monominerallic systems such as these. In the case of birnessite, goethite, ferrihydrite and gibbsite, the recovery from the drying experiments is greater than that from the moist experiments. Considering the acidifying effect of the drying mineral surface (McBride 1994; Dowding et al. 2005; Clarke et al. 2011, 2012), and the addition of the acidified acetonitrile-HCl solution used to extract the compounds, it is possible that in the case of the drying experiments, the pH reaches a low enough value in order to protonate the oxide surface. At very low pH values, the triazines are also protonated. This indicates that in all likelihood more repulsion was occurring by the mineral surface in the drying experiments upon extraction, than was occurring in the moist experiments. The recoveries from both the dry and moist Al^{3+}-saturated smectite experiments were similar, indicating that possibly more complex mixed-mode sorption (Mudhoo and Garg 2011) of the *s*-triazines is occurring. This is possible since the triazines can sorb onto clay surfaces by both hydrophobic interactions (via hydrophobic microsites) and hydrogen bonding to the hydration shells of the interlayer cations (Laird and Koskinen 2008). In the case of quartz, however, the recovery from the drying experiment is much lower than that from the moist experiment. It is not clear why quartz shows greater sorption of atrazine. It is possible that the surface pH of quartz after drying might be relatively low, and some authors have noted the increased sorption capacity of quartz at lower surface pH (e.g. Kovaios et al. 2006). The sorption of atrazine does increase with decreasing pH on Mn-oxide surfaces (Shin and Cheney 2005), but it is not clear why the same should hold true for the quartz surface. Another possibility is that the quartz surface is one of the most neutral mineral surfaces at natural pH ranges (it has one of the lowest points of zero net charge), which could increase its hydrophobicity somewhat, allowing physical sorption of atrazine onto the quartz surface. To normalize the effects of recovery, the percentage recovery of each compound can be scaled to the total recovery percentage for that mineral surface as follows:

$$\text{Normalized \% recovery} = \left(\frac{\text{\% recovery of specific } s\text{ - triazine}}{\sum \text{\% recoveries of all } s\text{ - triazines for that mineral}} \right) \qquad (5.2)$$

Using Equation 5.2, birnessite shows the greatest atrazine degradation, at 66%, of the original atrazine applied, forming hydroxyatrazine as a major product (56%) and deethylatrazine as a

minor product (10%). Following birnessite is goethite, with 18% degradation of atrazine, forming hydroxyatrazine as major product (14%) and deethyl-atrazine as minor product (2%). The rest of the mineral surfaces showed comparably lower degradation, between 1 and 4%, forming only a minor amount of hydroxyatrazine (1–4%) and no deethylatrazine. The drying non-mineral atrazine control (CD) showed no degradation, and so too did all the moist experiments.

The degradation appears to follow the order: Mn^{4+}-oxide > Fe^{3+}-oxide >> Al^{3+}-oxide, Al^{3+}-saturated smectite and Si^{4+}-oxide. This order correlates well with the redox potentials ($E°$) of the oxide phases, typically 1.23 V for MnO_2 and 0.67 V for FeOOH (Stone 1987). This trend supports the notion of Mn-oxides being the most reactive toward organics, and the oxidative (and often radical-mediated) mechanisms encountered (e.g. Ulrich and Stone 1989; Matocha et al. 2001; Zhang and Huang 2003, 2005; Barrett and McBride 2005; Shin et al. 2009; Leo et al. 2012). The oxidation mechanisms (e.g. Fenton's reagent, ozone and UV radiation) and products of atrazine are well known, and have been documented by several authors (e.g. Arnold et al. 1995b; Acero et al. 2000; Tauber and von Sonntag 2000). Apart from the radicals, these oxidation products are fairly stable once formed, and should be detectable once extracted (Acero et al. 2000). However, no recognised oxidation products could be identified in the ion current (using mass extraction values in Table 3.1) or total ion current (TIC) mass chromatograms obtained of the dried mineral treatments. Furthermore, the final total amounts of *s*-triazines, especially in the case of birnessite and goethite, are close to the original amount of atrazine (0.465 µmol) which suggests no other products were formed, only hydroxyatrazine and deethylatrazine.

5.2 The effect of reaction time and moisture content on atrazine transformations

5.2.1 Gradual evaporation under ambient conditions

In these experiments the most active mineral surface, namely birnessite, was chosen as a model surface to investigate the degradation of atrazine as the surface was drying (effect of moisture content). This was compared to the most inactive mineral surface, namely quartz (a mineral "control") and a non-mineral control (Figure 4.1b). The results of the short-term (10 day) experiments are depicted graphically in Figure 5.5 (tabulated data in Table A4 of Addendum A). On the drying birnessite surface, approximately 30% of the atrazine was degraded over the 10 day period, forming hydroxyatrazine (as major product) and deethylatrazine (as minor product). The plots in Figure 5.5 also depict a term called the residual gravimetric moisture percentage

(RGM%). It is determined from the mass data obtained for the vials, as described in section 4.2.1.2 of the methods and materials. The mass difference obtained between the mass of the vial initially and the mass at sampling time is subtracted from the original 1 mL (or 1 g) of moisture in the vial initially. This is then expressed as a percentage of the original 1 g of moisture:

$$\text{RGM}\% = \left(1 - \left[\text{mass}_{\text{vial}}(\text{initially}) - \text{mass}_{\text{vial}}(\text{sampling time})\right]\right) \times 100 \qquad (5.3)$$

On the moist birnessite surface, the drying and moist quartz surface, as well as the drying non-mineral control, virtually no atrazine degradation had occurred. A closer look at the birnessite drying experiment data reveals that degradation is not occurring during the first 6 days of drying, but then rapidly begins to take place after this. The point at which this degradation is initiated coincides with a moisture content of approximately 10% (see Figure 5.5a). This is evident in both the formation of hydroxyatrazine and deethylatrazine. It also appears that after the initial drying of the surface, the degradation continues on the dry surface and is then a function of time. The short-term experiments provide crucial insight into the initiation of degradation at what appears to be a critical residual gravimetric moisture content of 10%. However, these short-term experiments have proven insufficient in providing information about how atrazine degrades over a longer period of time, especially considering that the half-life (50% degradation) was not reached. Furthermore, in the 10 day period investigated, it also appears that the total molar amount of *s*-triazines was conserved ($\sum$ amount in Figure 5.5). With advanced degradation, several authors (e.g. Wang et al. 1999; Shin et al. 2000) have reported a loss of total *s*-triazines, attributing it to possible CO_2 formation from ring-cleavage. A loss in total *s*-triazines in this study would also have the further implication that products other than hydroxyatrazine and deethylatrazine were forming in appreciable amounts over time. It therefore became important in this study to conduct a long-term investigation in addition to the 10 day study. This long-term experiment was conducted over a 30 day period, and the results are shown in Figure 5.6 (tabulated in Table A6 in Addendum A).

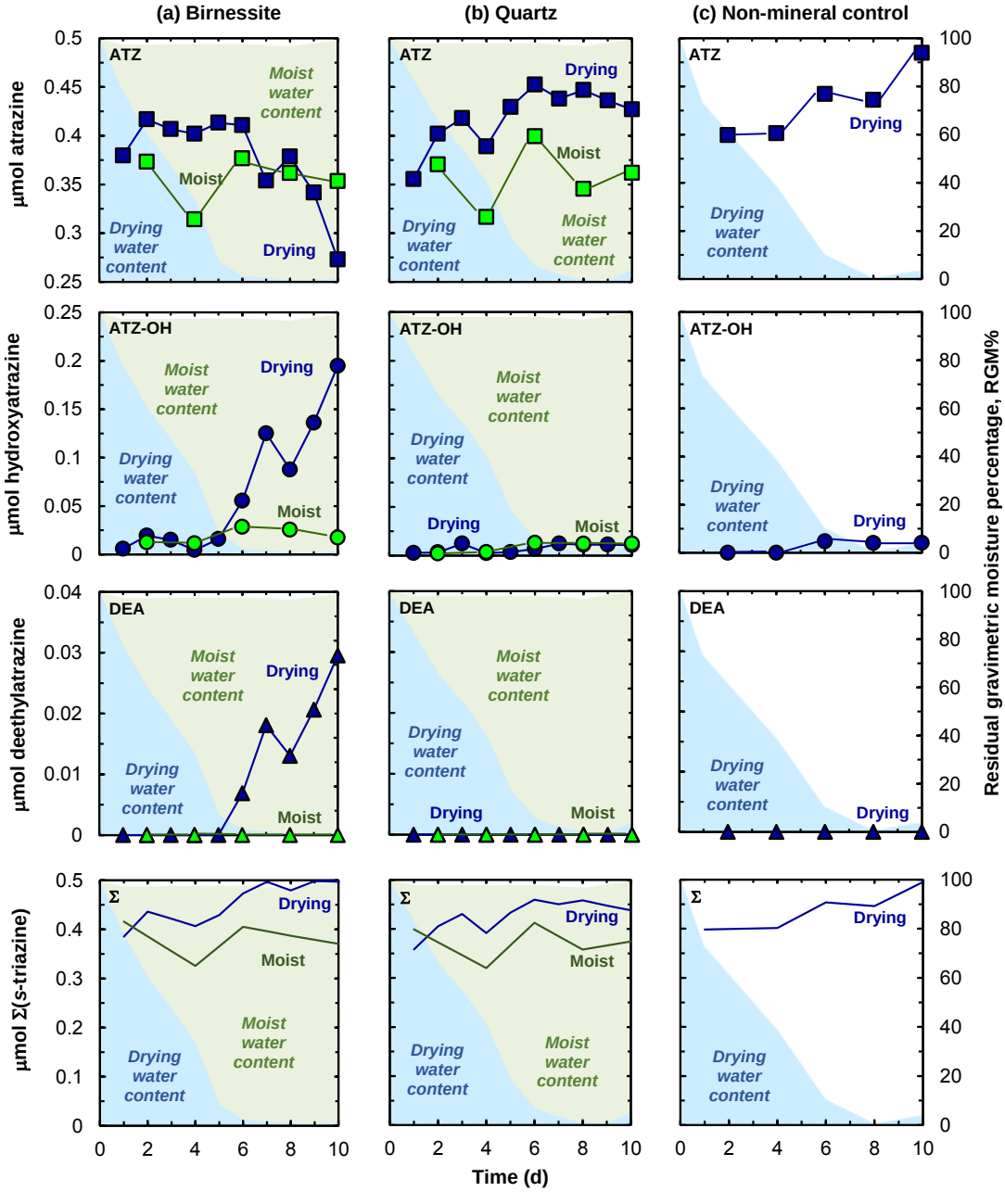

Figure 5.5 The results of the short-term drying (dark blue markers and lines) and moist experiments (light green markers and lines) for (a) birnessite, (b) quartz and (c) a non-mineral control. For each case (a, b or c), four panels showing the amounts of atrazine (squares), hydroxyatrazine (circles), deethylatrazine (triangles) and total *s*-triazine (no markers, only lines) are arranged in a *vertical* orientation. For the non-mineral control, there is no moist experiment data (hence no light green markers or lines). Also shown are the residual gravimetric moisture percentages (RGM%s) (shaded areas) for both the drying (light blue shade) and moist experiments (light green shade). Abbreviations are as follows: ATZ = atrazine, ATZ-OH = hydroxyatrazine, DEA = deethylatrazine and ∑ = sum of molar amounts of all three *s*-triazines.

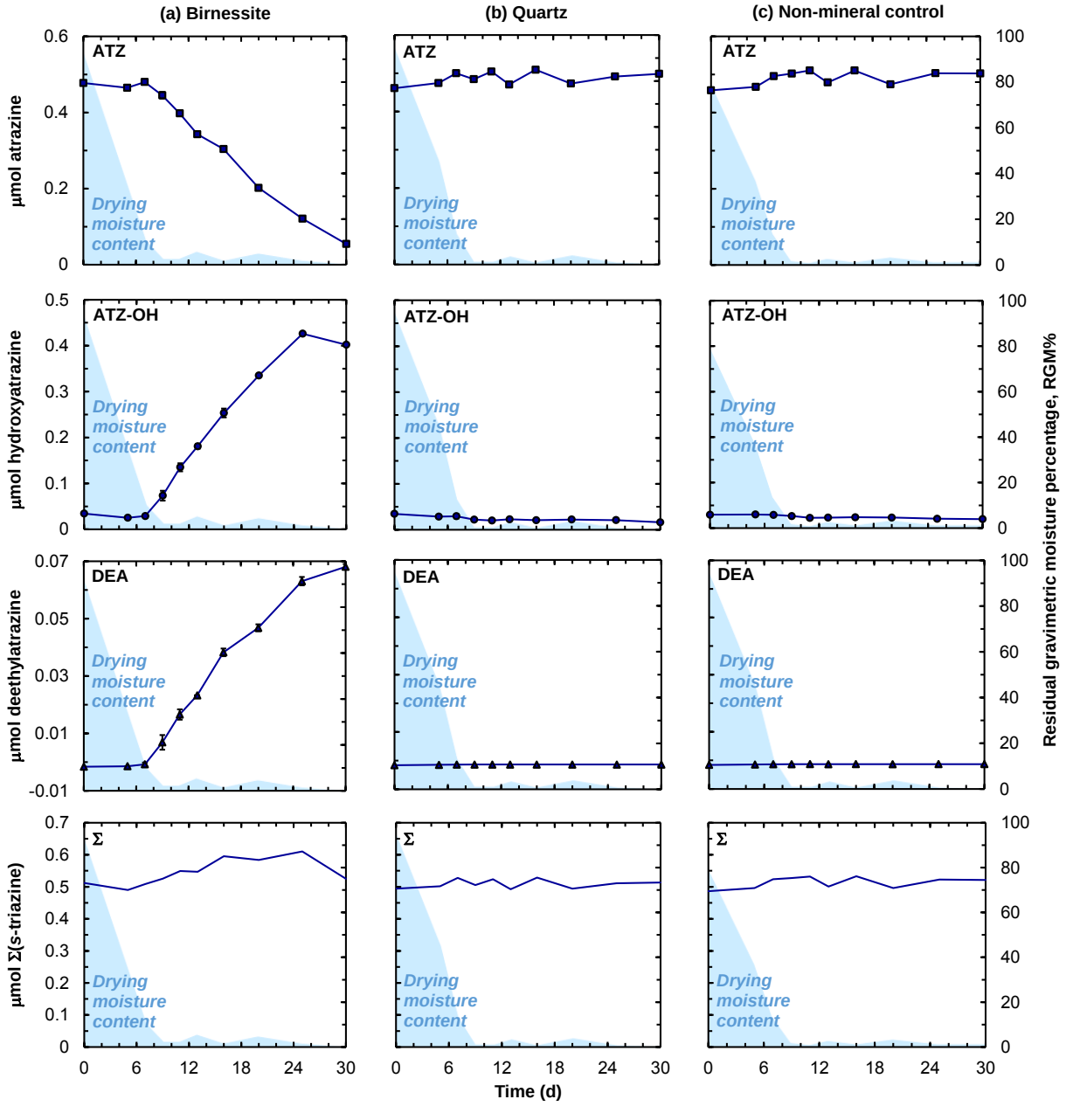

Figure 5.6 Results from the long-term (30 day) drying experiments (dark blue markers and lines) are shown for the (a) birnessite drying experiment, (b) quartz drying experiment and (c) the non-mineral control drying experiment. The amount of atrazine (squares), hydroxyatrazine (circles), deethylatrazine (triangles) and total *s*-triazines (no markers, only lines) are given for each case (a, b or c) in a *vertical* orientation. Each datum point is a mean value of two data. Bars on each of the points represent the extent of the data pair (i.e. 2 times the deviation from the mean). Where bars are absent they are obscured by the marker. The residual gravimetric moisture percentage (RGM%) versus time is shown shaded in blue. Abbreviations are as follows: ATZ = atrazine, ATZ-OH = hydroxyatrazine, DEA = deethylatrazine and ∑ = sum of molar amounts of all three *s*-triazines.

Figure 5.6 reveals appreciable atrazine degradation only occurs on the birnessite surface, with two metabolites forming, namely hydroxyatrazine (major) and deethylatrazine (minor). Furthermore, degradation once again only ensues once a critical residual moisture content (RGM%) of approximately 10% is reached (after 7 days). The quartz drying experiment, as well as the non-mineral control drying experiment showed no appreciable degradation over this extended time-period. As was the case with the 10 day experiments, no loss of total *s*-triazines was observed in any of the experiments. As a matter of fact, the recoveries of *s*-triazines appeared to be greater than the initial amount of atrazine added (0.465 µmol), which is generally attributable to analytical error. The lack of total *s*-triazine loss indicated no formation and loss of CO_2 to any processes of ring-mineralization, and also indicated that no other products other than hydroxyatrazine and deethylatrazine were formed.

From Figure 5.6a, the half-life for the degradation of atrazine on birnessite appears to be approximately 19 days. However, considering that degradation only ensues virtually after the first 7 days, the actual half-life is more in the order of 12 days, once degradation has been initiated. Shin and Cheney (2005) have calculated a half-life of 17 days for their fully hydrated system. However, their initial molar amount of atrazine relative to their birnessite mass (4.6 µmol g^{-1} birnessite) varied from the one in this study (0.93 µmol g^{-1} birnessite).

Applying Equation 5.2 to calculate the molar degradation percentage of the total triazine molar amount in the birnessite drying experiment shows that 90% of the initial atrazine was degraded over the 30 day period, forming 77% hydroxyatrazine and 13% deethylatrazine. The accumulation of metabolites (hydroxyatrazine and deethylatrazine) follows the same linear trend as atrazine degradation. However, it appears that hydroxyatrazine formation had reached a maximum (0.43 µmol) after 25 days (Figure 5.6a), where it remains for the rest of the experiment. Deethylatrazine, however, only began to taper-off slightly and was still following an upward trend. It has become apparent at this point that moisture content is an initial limiting factor until it reaches a minimum critical value (10%), and that once degradation has initiated on the drying to dry surface, degradation continues to increase with atrazine-mineral surface (only birnessite in this case) contact time, a process also known as aging (Mudhoo and Garg 2011). Therefore, hypothetically, it should be possible to accelerate the initiation of atrazine degradation by accelerating the rate of initial drying, from 7 days to a much shorter time, if possible. The reduction of drying time is considered in the next section.

5.2.2 Accelerated evaporation with compressed air

To accelerate the rate of drying, and hence the rate of atrazine degradation, air dried experiments were conducted. The results of the air-dried experiments are depicted in Figure 5.7 and tabulated in Table A6 of Addendum A. The data in Figure 5.7 shows the rapid increase in atrazine degradation that resulted from the reduction in drying time. The gravimetric water content of the samples confirmed that all moisture had been removed by day 1. The enhanced drying has resulted in a reduction of the atrazine half-life on the birnessite drying surface from 19 days to less than 1 day (approximately 14–16 hours). Within the 35 days of drying, approximately 97% of atrazine had been degraded on the birnessite surface, forming hydroxyatrazine as a major metabolite (86%) and deethylatrazine as a minor metabolite (11%). As was the case in the previous experiments, no degradation occurred in the quartz and non-mineral control drying experiments. At first inspection, it appears that there was a decrease in the total *s*-triazine molar amount. However, given the fact that no other metabolites were formed, and that there appeared to be more mass loss (negative moisture content, see also Figure 5.8) than the original 1 g added to the vial initially (see Table A6 for moisture content), it was concluded that a net loss of material had occurred. This loss occurred despite the greatest efforts to limit the amount of material that became airborne during the experiment. Therefore, the apparent loss in total *s*-triazines was most likely as a result of total material loss and not mineralization to CO_2.

5.2.3 The effect of moisture content

From the time series (gradual drying) and the air-dried experiments, it is clear that moisture content is a major control on the degradation of atrazine by drying mineral surfaces, especially birnessite. In order to observe this effect more clearly, both the drying and moist birnessite data from these experiments (since it is the only mineral surface showing sufficient degradation of atrazine) was plotted as a function of moisture content rather than time in Figure 5.8. The plot confirms that degradation (and metabolite formation) on birnessite only initiates below a critical residual gravimetric moisture percentage of 10%, and that the moisture content on the birnessite surface is a major limiting factor in the degradation of atrazine.

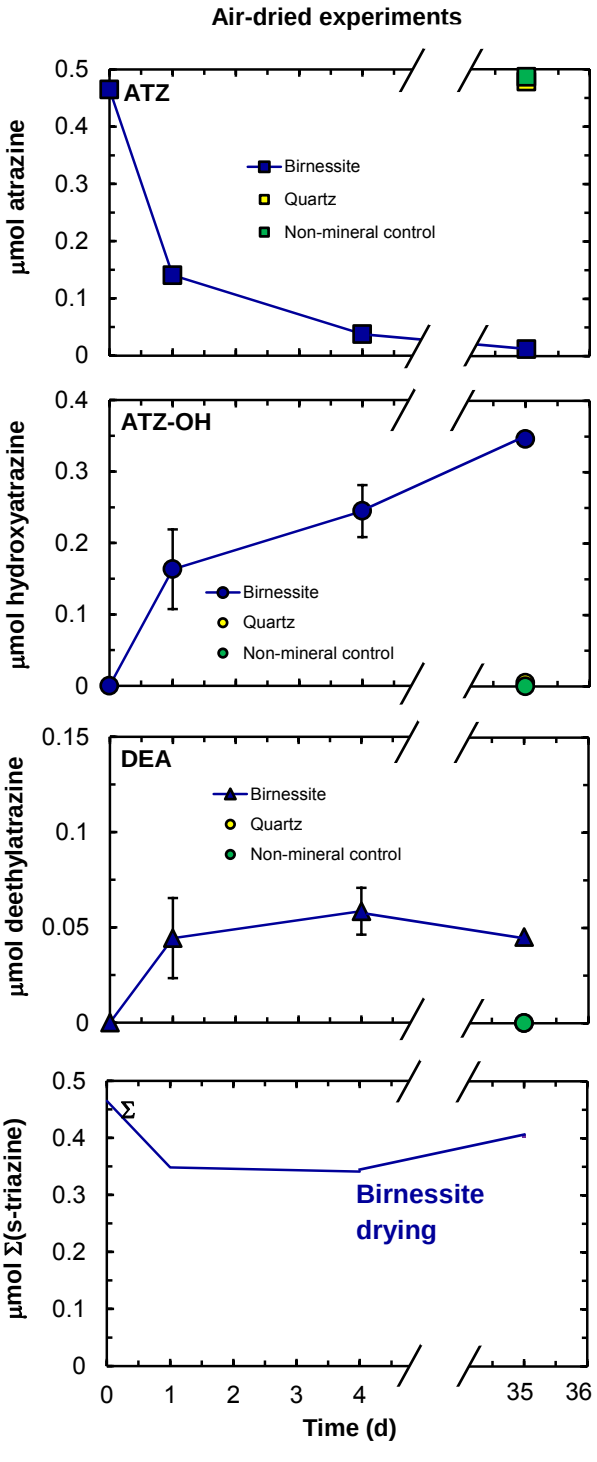

Figure 5.7 Results from the air dry experiments. Each of the three drying experiments, namely birnessite, quartz and the non-mineral control, are shown on each panel together. For quartz and the non-mineral control only one point was measured at 35 days as a comparable mineral and non-mineral control (the markers obscure each other somewhat). Data points are a mean value of a duplicate pair, except for 0 (hypothetical point) and 35 days. Bars indicate the extent of the duplicate pair sampled (2 times the deviation from the mean) and where missing they are obscured by the data points (of duplicate data only). Points at 0 and 35 days are not in duplicate (hence no bars). Moisture content was insignificant at sampling time and hence is not shown here, unlike the previous figures. Abbreviations are defined as follows: ATZ = atrazine, ATZ-OH = hydroxyatrazine, DEA = deethylatrazine and ∑ = sum of all the *s*-triazine molar amounts.

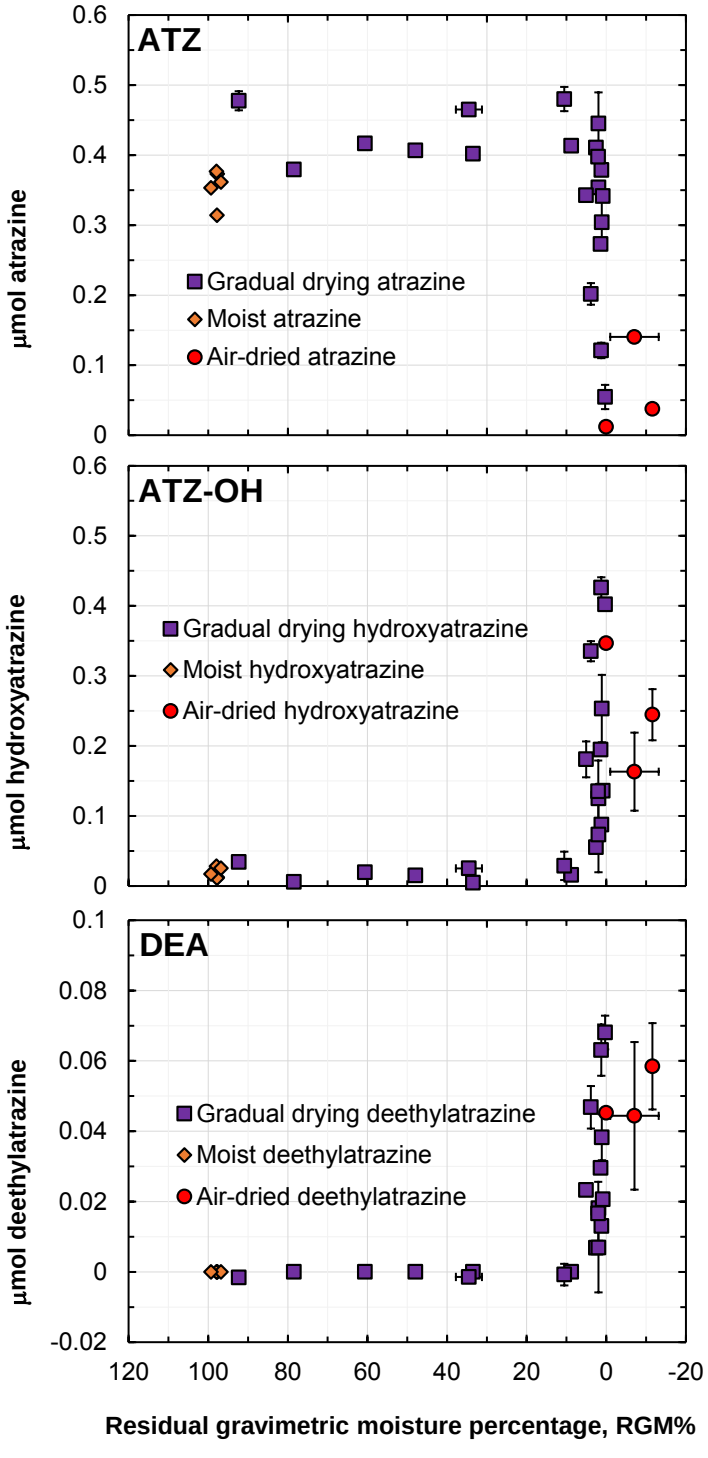

Figure 5.8 The degradation of atrazine on birnessite as a function of moisture content, for the gradual drying experiments (purple squares), their moist analogues (orange diamonds) and the air-dried experiments (red circles). For each case, the amount of atrazine, hydroxyatrazine and deethylatrazine is shown (in *vertical* order). Data points indicate a mean value of two data, except for the moist experiments. Vertical bars indicate the extent of the duplicate pair (2 times the deviation from the mean) and where they are absent they are obscured by the marker. Horizontal bars similarly indicate the deviation in moisture content from the mean moisture content of the data duplicate pair. Abbreviations are: ATZ = atrazine, ATZ-OH = hydroxyatrazine and DEA = deethylatrazine.

The results from Figure 5.8 show that atrazine degradation is indeed a function of moisture content. In order to eliminate the apparent effect of moisture content, a birnes-site-atrazine mixture was allowed to dry for 30 days, in the same manner as the gradual drying experiments. However, instead of the aqueous atrazine solution used in the gradual drying experiments, atrazine in pure acetone was used in this experiment. The results from the solvent drying experiment are shown in Figure 5.9, along with the data from the 30th day of sampling in the gradual drying birnessite experiment.

From the data in Figure 5.9, it appears that the solvent birnessite drying experiments showed a similar atrazine degradation trend as the gradual drying experiment, with the same metabolites forming, in approximately the same molar proportions. The formation of hydroxyatrazine as the major product in the solvent-only system is in contrast to the findings of Cheney et al. (1998) and Shin et al. (2000) who did not detect any hydroxy product under similar solvent conditions. In the aforementioned studies, the authors pre-dried their birnessite at 110°C to remove any moisture. Their resulting birnessite showed a mass loss of approximately 10% suggesting structural water was removed. In the current investigation, the birnessite was not oven-dried. However, the inherent moisture content was determined to be 7%. The general formula for birnessite, δ-MnO_2, does not take into account the structural water that is contained within birnessite (McKenzie 1989). The true formula of birnessite, $[(Na, K)_{0.7}Ca_{0.3}]Mn_7O_{14}{\cdot}4H_2O$ (McKenzie 1989), takes into account this structural water, and on a mass basis this structural water makes up 7.8% of the mass of birnessite. This provides 2.2 mmol of water (in 500 mg of birnessite), which far exceeds the µmole quantities of hydroxyatrazine formed. The birnessite mineral structure consists of sheets that contain interlayer cations, usually Na^+, K^+ and Ca^{2+} (Lopano et al. 2007). The water is present as hydration shells around these interlayer cations, and could, quite possibly be available for reaction. Furthermore, upon drying, these water molecules could undergo hydrolysis too, not as intensely as with Al^{3+} (e.g. McBride 1994) or Fe^{3+}, but still significant enough to perhaps generate some acidity. The interlayer cation depends on the synthesis method for the birnessite (Lopano et al. 2007). The method of McKenzie (1971) used to synthesize the birnessite in this study uses potassium permanganate ($KMnO_4$) as starting reagent, meaning K^+ is the interlayer cation. This means that the effect of hydrolysis should be almost negligible in this case, since K^+ is not known as a strong polarizer of water molecules in hydration shells.

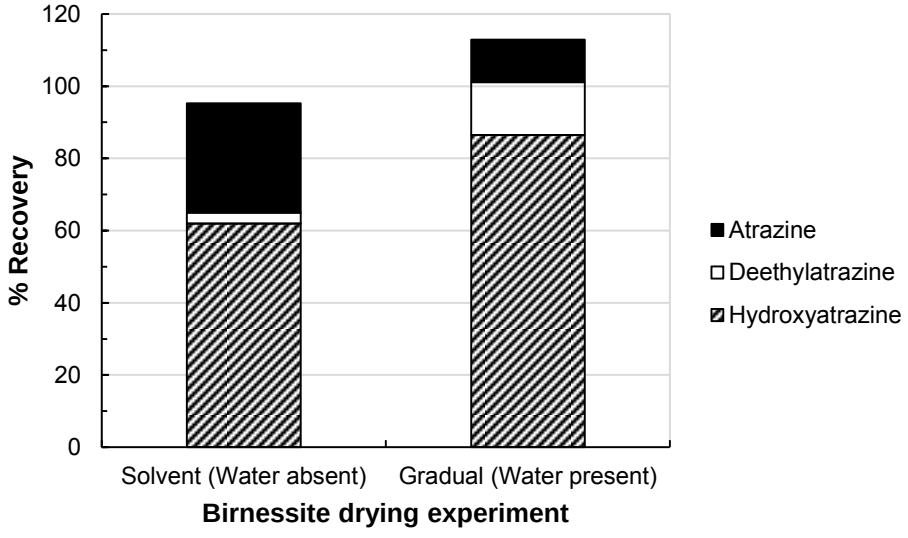

Figure 5.9 Results from the solvent (water absent) birnessite drying experiment, along with comparative data from the gradual drying (water present) experiment discussed previously.

The data in Figure 5.9 shows that the removal of water did not increase the degradation of atrazine, as a matter of fact, in comparison to the gradual drying experiments that did contain water, it showed less degradation. This could be indicative that atrazine degradation requires a certain amount of moisture (despite the hydrophobicity of atrazine) to be present on the birnessite surface, and that this amount of moisture is greater than the inherent 7% already present in the mineral structure. It is not completely clear why atrazine degradation requires this moisture, but this could be indicative of the importance of water molecules on the surface specifically, not within the birnessite structure, playing a crucial role in the initial formation of a surface atrazine-birnessite complex prior to degradation.

5.3 The possible role of oxygen (O_2) in atrazine degradation

5.3.1 Drying with nitrogen (N_2)

Numerous studies have used a nitrogen (N_2) atmosphere or the process of purging the sample with nitrogen to determine the role of atmospheric oxygen as a possible oxidant of organics during degradation studies (e.g. Wang et al. 1999; Shin and Cheney 2005; Clarke et al. 2012). The accelerated drying of the air-dried experiments was mimicked in a parallel experiment using N_2 as the purging gas. The purpose of the N_2-drying experiments was twofold. The first purpose was once again to accelerate drying and enhance degradation as was the purpose with the air-drying experiments, but the second purpose was to investigate whether the same metabolites were

formed and whether the same amount of degradation was observed, without oxygen as a possible interfering oxidant (only under the action of the oxide surface). The results of this experiment are shown in Figure 5.10 (see also Table A6 in Addendum A). From Figure 5.10, the data from the birnessite drying experiment indicate a similar atrazine degradation (and metabolite formation) rate as the air-dried experiments (Figure 5.7). No degradation was observed in the quartz and non-mineral control drying experiments. This is indicative of an oxygen-independent catalytic degradation mechanism for atrazine on birnessite, which confirms the mechanism originally proposed by Wang et al. (1999) and subsequently applied in the work of Shin et al. (2000), Shin and Cheney (2004, 2005) and Waria et al. (2009). The data for the total *s*-triazine molar amount shows a similar trend to the trend in the air-dried experiments, indicating an apparent loss on first inspection, but is most likely due to losses via airborne material, given the fact that no other metabolites were found in these experiments (as was the case with the air-dried experiments). This means that the ring-mineralization of atrazine to CO_2, as proposed by Wang et al. (1999) and Shin et al. (2000) to account for the loss in total *s*-triazines in their studies, was not a process occurring here.

5.3.2 Dissolved manganese (Mn^{2+})

In both the N_2-dried and air-dried experiments (previous section), one of the atrazine-birnessite replicates from each experiment was sacrificed and extracted for dissolved Mn^{2+} on the 35th day of the experiment. The air-dried experiment was chosen because the N_2-dried and air-dried experiments showed the same enhanced degree of atrazine degradation due to accelerated drying. The Mn^{2+} extracted from both of these samples was referenced against the Mn^{2+} contents of two blank birnessite samples (which contained no atrazine) run in parallel, also under compressed air and nitrogen. The purpose of measuring dissolved Mn^{2+} is to use it as a surrogate parameter for any possible oxidation of atrazine, which would appear as a reduction of the Mn-oxide to Mn^{2+} (Shin et al. 2000; Shin and Cheney 2005). The dissolved Mn^{2+} data is given in Table 5.1. The amount of Mn^{2+} measured in both the air-dried and N_2-dried atrazine-drying experiments were lower than the Mn^{2+} from the blank birnessite samples. This means that in all likelihood, no soluble Mn^{2+} was formed during the degradation of atrazine by birnessite, which suggests no net reduction of birnessite, and hence no net oxidation of atrazine, occurred in the reaction. This supports the observations of Shin et al. (2000) and Shin and Cheney (2005). However, this result does not infer that no redox steps occur within the mechanism, and it only accounts for dissolved

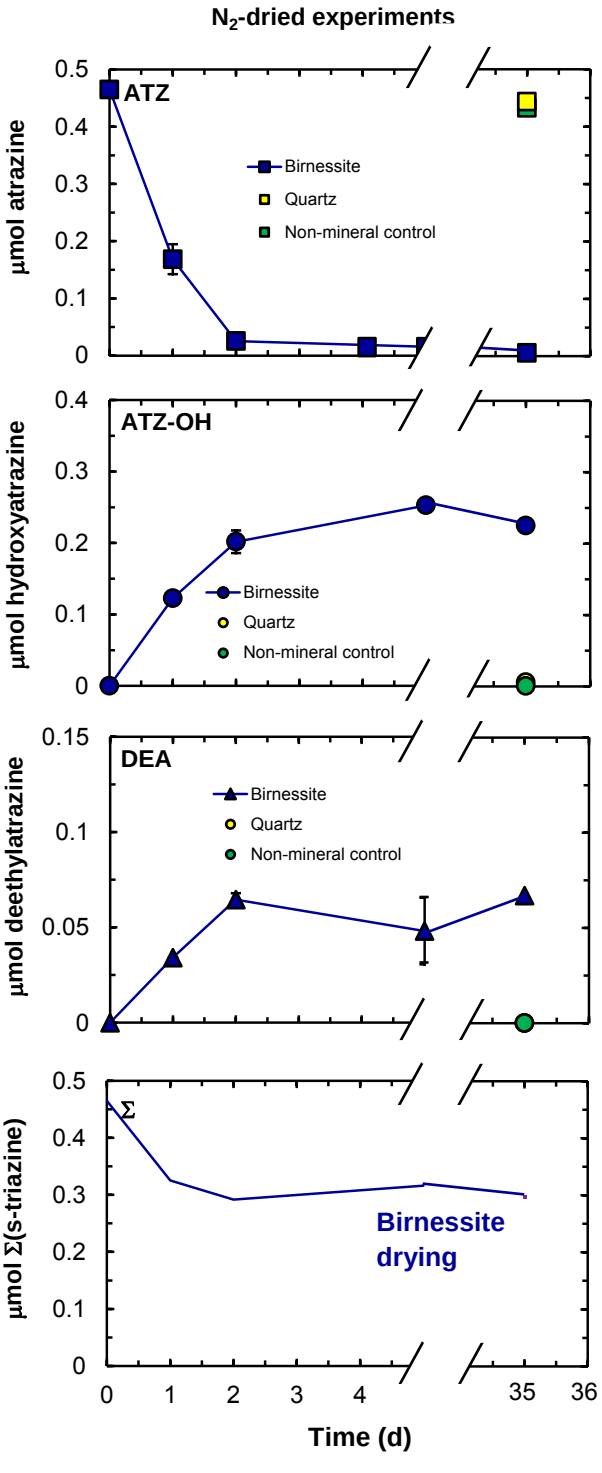

Figure 5.10 Results of the nitrogen (N_2)-dried experiments. Each of the three cases (birnessite, quartz and the non-mineral control) are shown on the same panel. Each datum for days 1, 2 and 5 are the mean value of a pair of duplicate data and the bars indicate the extent of each datum (2 times the deviation). The points at 0 and 35 days are a single datum for birnessite (no bars), but are a data pair for quartz and the non-mineral control (the markers obscure one other somewhat). Where no bars are present for the duplicate pairs, they are obstructed by the marker. Moisture content was insignificant at all points and is not shown here in the shade of blue found in some of the previous figures. Abbreviations are: ATZ = atrazine, ATZ-OH = hydroxyatrazine, DEA = deethylatrazine and ∑ = sum of all the *s*-triazine molar amounts.

Table 5.1 The dissolved manganese data for the air- and N_2-dried samples.

Sample	Dissolved Mn^{2+} (µmoles)
Birnessite-atrazine sample under air drying	0.030
Blank birnessite sample under air drying	0.037
Birnessite-atrazine sample under N_2 drying	0.008
Blank birnessite sample under N_2 drying	0.012

Mn^{2+} either already present in solution, or desorbed from the birnessite surface during extraction (displaced by Ca^{2+} in extraction solution). No indication of solid-state reduction can be inferred from the Mn^{2+} data, so whether solid-state reduction of the lattice-bound Mn^{4+} to Mn^{2+} (which then remains in the birnessite lattice) is occurring during the reaction is still unknown at present. Furthermore, as required by the mechanism proposed by Shin and Cheney (2005), initial reduction of Mn^{4+} by electron transfer from the alkylamino N atom on atrazine along the Mn-N bridge is a crucial first step in the degradation of atrazine. However, it is possible that the lattice-bound Mn^{2+} cation remains within the mineral surface long enough to be auto-oxidized back to Mn^{4+} during the final step of unbridging between Mn and N, and in so doing is never released from the lattice into solution.

5.4 The degradation mechanism

5.4.1 The hydroxylation mechanism

The lack of oxidation products from the different mineral surface experiments (section 5.1) appears to point to a catalytic non-oxidative mechanism, such as the chemical hydrolysis of atrazine in an acidic medium to form hydroxyatrazine. This would explain the greater degradation of atrazine in the drying experiments versus the moist experiments, since it is postulated that drying induces acidity (McBride 1994; Dowding et al. 2005; Clarke et al. 2011, 2012). However, this acidity generated is linked to the Lewis acidity of the cation involved, as the acidity is generated by the polarization of water on these mineral surfaces. This Lewis acidity is directly related to the electronegativity of the relevant cation, and thus one would expect greater reactivity and hydroxyatrazine formation with increased Lewis acidity of the cation. However, arranging the cations in order of electronegativity (Si^{4+}> Fe^{3+}> Al^{3+}> Mn^{4+}; Huang and Hardie 2011) does not reflect the pattern of reactivity observed. The lack of oxidation products and the reactivity trend correlating with redox potential supports the novel partial oxidation mechanism originally postulated by Wang et al. (1999) and again by Shin and Cheney (2004,

2005). The formation of an inner-sphere precursor complex (Shin and Cheney 2005) between the surface Mn^{4+} cation and one of the N atoms on atrazine is the first step of the reaction. This corroborates the notion that adsorption of the organic molecule to the Mn-oxide surface is the crucial first step in the reaction of many organic pollutants with Mn-oxide surfaces (Ulrich and Stone 1989). However, whilst the authors that have postulated the partial oxidation mechanism have highlighted the importance of the interaction between Mn^{4+} and the N-atom in the alkyl-amine group of atrazine (termed the formation of a Mn-N bridge), for the formation of dealkylated products such as deethylatrazine, they have not suggested that this is a crucial step for the formation of hydroxyatrazine. Electron transfer back and forth within this Mn-N bridge is an important part of the reaction, and it is highly likely that the ability of the cation to do this is directly related to its redox potential. These authors, along with others (see Shin et al. 2000), have compared the reactivity of birnessite (Mn-oxide) with a typically non-redox active Al-oxide, alumina (α-Al_2O_3), which was unreactive toward atrazine. This investigation is the first study comparing birnessite (Mn-oxide) and goethite (Fe-oxide) in the same experiment. By observing their comparative reactivity trend in the same study, the importance of redox potential as a control on the degradation of atrazine is reinforced, despite the reaction being deemed net non-oxidative (Shin and Cheney 2004, 2005). Waria et al. (2009) investigated the degradation of atrazine on Fe-oxides and applied the same net non-oxidative (or partial oxidative) mechanism to their degradation reaction. However, Mn-oxides were not included in their study. Considering the importance of the Mn-N (or Fe-N) bridge for the formation of deethylatrazine, it would appear this bridge is equally important for hydroxyatrazine formation, but it is more likely that such a bridge is forming between Mn^{4+} (or Fe^{3+}) and a *ring* N atom in the case of hydroxyatrazine formation, and not an N atom from the amino group. An interaction between a ring N atom and Mn^{4+} was briefly postulated by Shin and Cheney (2005), but it was not explicitly stated that a Mn-N bridge had formed, by which electron transfer was occurring. From the results of the current investigation, it appears that cation-N bridge formation as well as electron transfer (and hence the redox potential of the oxide surface) are two crucial elements for both the dealkylation *and hydroxylation* of atrazine. The formation of the cation-N bridge is a surface interaction, which implies that adsorption processes are an important part of the reaction mechanism as well. The precursor complex formation is an exchange mechanism, with atrazine exchanging for a surface water molecule. At low pH values, this mechanism is a cation exchange mechanism, since both the oxide surface and atrazine are possibly protonated. Equation 5.4 illustrates this exchange (modified from Shin and Cheney 2005):

$$>Mn—OH_2^+ + {}^+HN\text{-atrazine} = >Mn—NH\text{-atrazine} + H_2O \quad (5.4)$$

In the equation, $^+$HN-atrazine is an atrazine molecule with a protonated ring N atom and >Mn—NH-atrazine is the surface precursor complex. The point of zero net charge (pH_{PZNC}) will play an important role here, because this determines the region of pH in which the mineral surface becomes protonated. The protonation of atrazine is also important. Therefore, the most suitable mineral surface for this complexation would be a surface with a pH_{PZNC} near the pK_a of atrazine (pH ~ 2). Quartz (pH_{PZNC} ~ 2), and then Mn-oxides (pH_{PZNC} ~ 3) (Laird and Koskinen 2008), are the most well-suited for the formation of this surface complex. However, since the quartz surface is redox inactive, no appreciable degradation of atrazine occurs. The adsorption is less pronounced on the Mn-oxide surface, but due to the greater redox potential, appreciable amounts of degradation occurs. The Fe-oxide surface is an intermediate case. Although the Fe-oxide surface has a redox potential (0.67 V) approximately half that of the Mn-oxide surface (1.23 V), the degree of atrazine degradation by goethite is only approximately a quarter of the degradation by birnessite. Ferrihydrite, a Fe-oxide usually noted for its reactivity and high surface area, appears to show almost no reactivity toward atrazine. This could be indicative of atrazine having a lower affinity for the Fe-oxide surfaces (pH_{PZNC} ~ 7; Laird and Koskinen 2008) than it has for the quartz and Mn-oxide surfaces. The electron transfer via the cation-N bridge in the precursor complex from N to the cation (oxidation) could facilitate hydroxyatrazine formation as it too draws electron density away from the ring, in the same way protonation does (Erickson et al. 1989). A catalytic hydroxylation mechanism is proposed in Figure 5.11.

A comparison between the moist and drying experiments reveals that atrazine degradation is dependent on moisture content. One possible reason for this, which has already been explored, is the effect drying appears to have on pH (e.g. Clarke et al. 2011), with increased drying leading to increased acidity. However, there exists the possibility that drying the mineral surface, and thereby decreasing the volume of water, simply has the effect of forcing contact between the mineral surface and atrazine, only because the atrazine has nowhere else to go. The results from the solvent-only drying experiments (Figure 5.9) further support the possibility that atrazine degradation could simply be a result of forced intimate contact between atrazine and the birnessite surface.

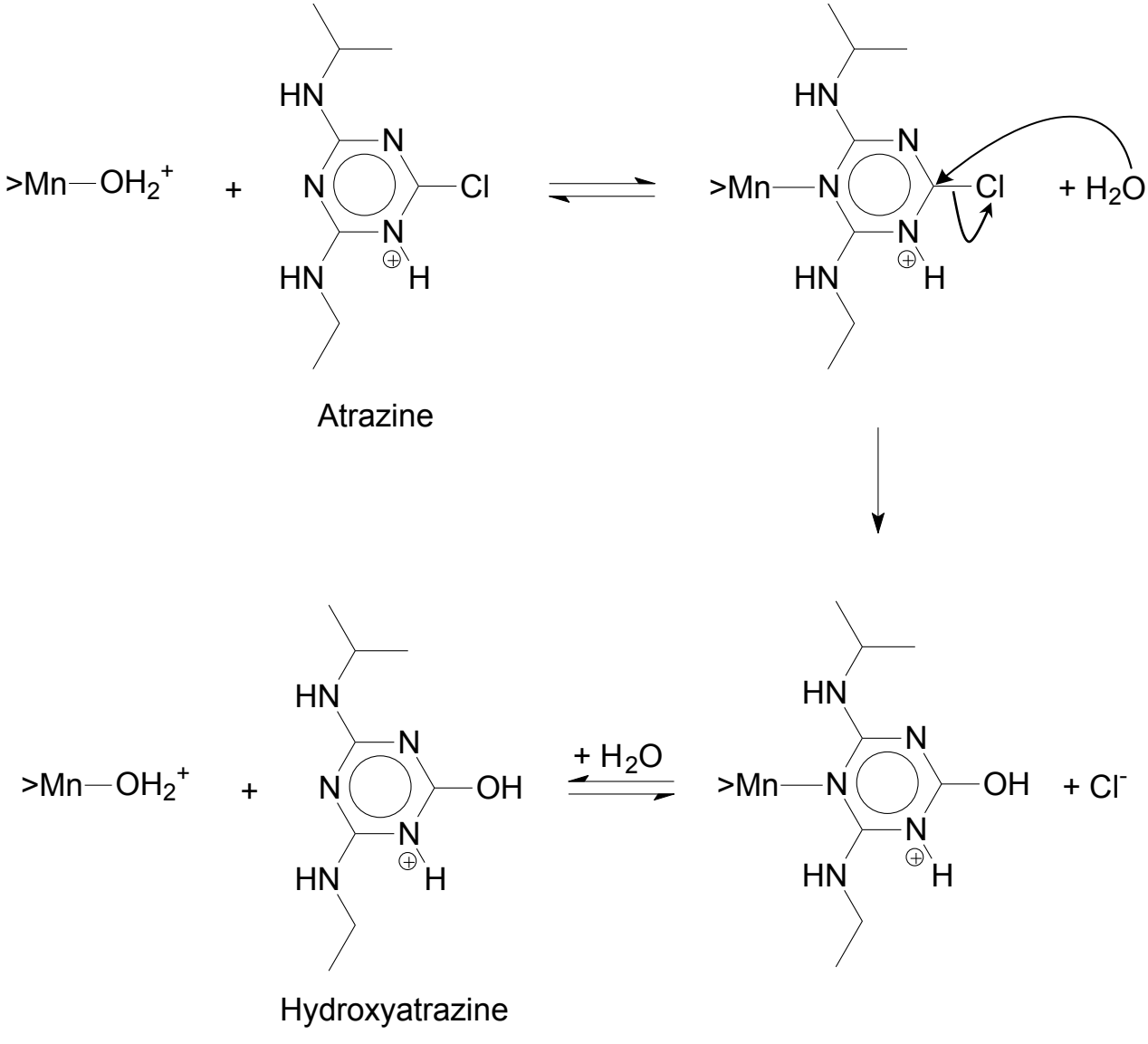

Figure 5.11 The catalytic hydroxylation of atrazine by a redox-active oxide surface via precursor surface complex formation, cation-N bridge formation and partial oxidation, using a Mn-oxide surface as example. Curved arrows indicate electron flow.

5.4.2 The dealkylation mechanism

Considering that both moisture content and liquid volume (inferred from the results of the water-absent solvent drying experiment) appear to be a limiting factors in the degradation of atrazine, it is likely that this implies intimate surface contact between atrazine and the birnessite surface is crucial for the reaction to initiate. This certainly supports the catalytic net non-oxidative degradation mechanism proposed before, as the formation of a surface atrazine complex with the birnessite surface appears to be a crucial first step in the reaction. The effect of drying appears to be twofold. As mentioned previously, the lowering of the pH as a result of drying possibly provides the optimal electrostatic conditions between the oxide surface and atrazine, favouring the formation of the surface complex. However, it also appears that water, at a residual gravimetric moisture content above 10%, prevents the atrazine molecules from reaching the birnessite surface, but drying (to below 10%) possibly has the effect of forcing atrazine to make intimate contact with the surface, as the molecule has no other place to go. Both processes are inter-dependent and are necessary for the degradation of atrazine.

Although the surface complexation mechanism for hydroxyatrazine formation is only proposed in this study, the work of Wang et al. (1999) and Shin and Cheney (2005) indicate that this surface complexation mechanism is highly applicable to the formation of deethylatrazine. The mechanism is outlined in Figure 5.12. It is apparent that intimate contact between atrazine and the birnessite surface is integral to the formation of deethylatrazine. However, if this surface catalysis mechanism controls the formation of deethylatrazine, then it is not clear why no other dealkylation products (deisopropylatrazine (DIA) and didealkylatrazine (DDA) as well as their hydroxy-analogues) have formed in this study, since they do in previous studies (e.g. Shin and Cheney 2005). The abiotic degradation of atrazine metabolites by birnessite have not been investigated yet, and this means that information about the kinetics of such a reaction is not available. It is possible that the degradation products of atrazine react much more slowly on the birnessite surface than atrazine, but this is not clear at this moment in time. It would appear, at least in this study, that deethylatrazine (and hydroxyatrazine) are the terminal products of the reaction of atrazine with birnessite under conditions of drying. The next section investigates possible degradation of these two atrazine metabolites by birnessite.

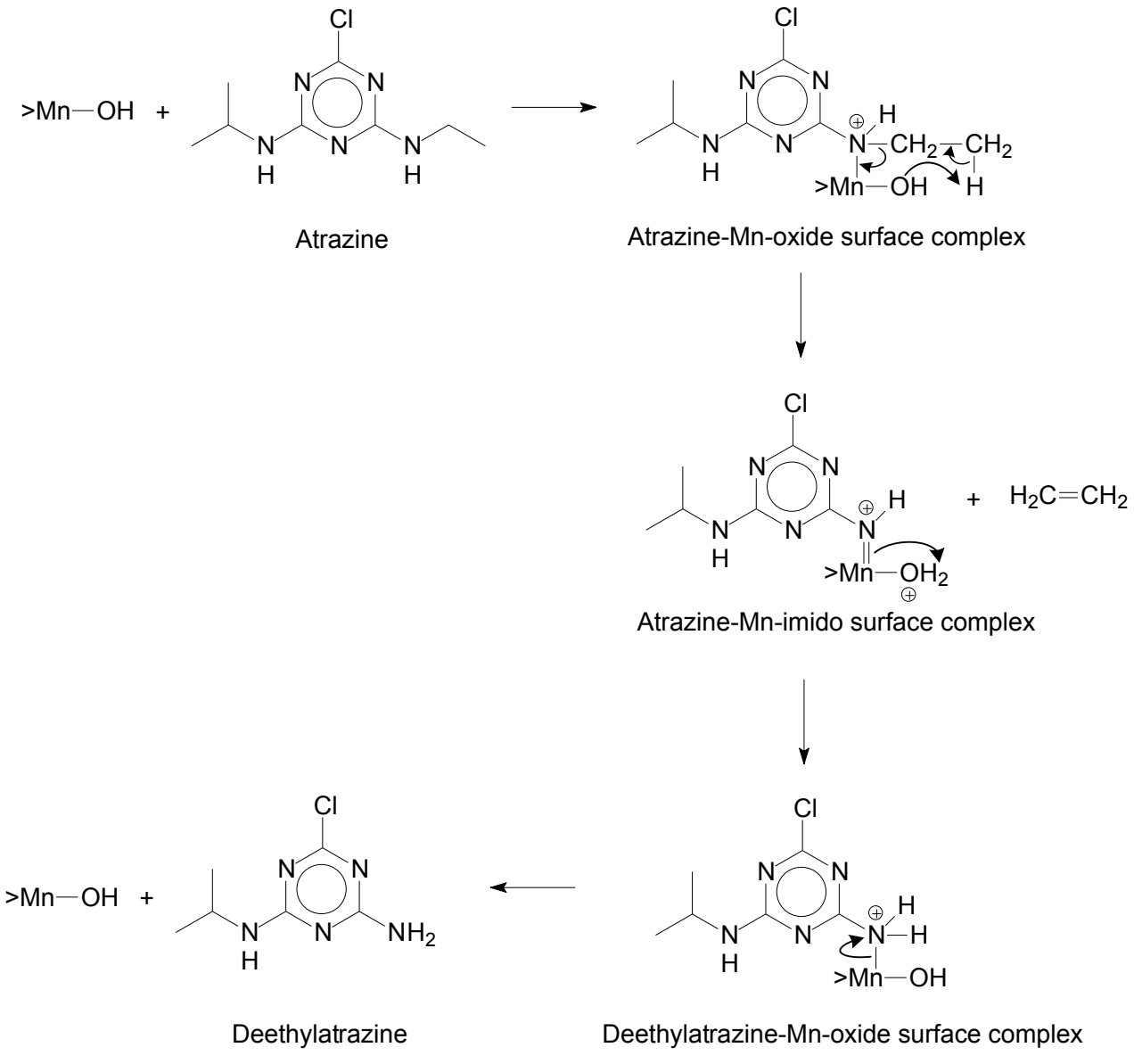

Figure 5.12 The formation mechanism of deethylatrazine using a Mn-oxide surface as example. Curved arrows indicate electron flow. Modified from Wang et al. (1999).

5.4.3 The degradation of atrazine metabolites by a drying birnessite surface

In order to establish if hydroxyatrazine and deethylatrazine are the terminal reaction products of the atrazine-birnessite reaction, these two compounds were individually reacted with birnessite, quartz and a non-mineral control. Due to the added acidity provided by acidified acetonitrile, required for hydroxyatrazine dissolution (see methods section 4.2.1.6), an acidified atrazine treatment was included for comparison. The results are shown in Figure 5.13.

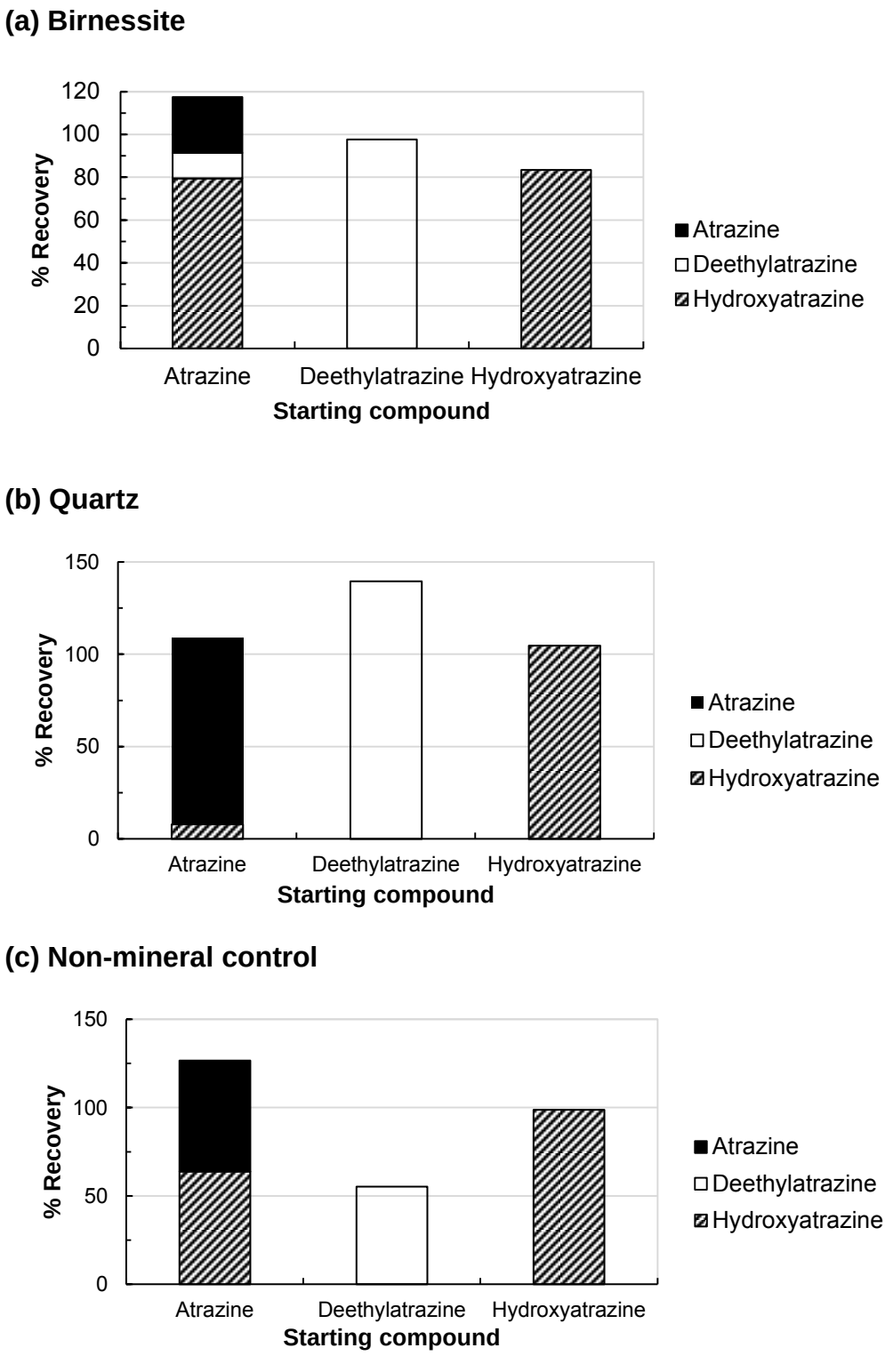

Figure 5.13 Results of the reaction of atrazine (solid black bar) as well as its metabolites deethylatrazine (white bar) and hydroxyatrazine (hatched bar) with a (a) drying birnessite surface and a (b) drying quartz surface, compared with a (c) non-mineral control. Experiments were conducted in a 9:1 acetonitrile: 0.1 mol L^{-1} drying solution as opposed to the usual solvent or aqueous drying.

The added acidity provided by the acidified acetonitrile solution did not appear to enhance degradation of atrazine on the birnessite surface over any previous results obtained. However, degradation by quartz appeared to increase slightly, from zero atrazine degradation, which was usually the case, to 7% atrazine degradation, forming only hydroxyatrazine as metabolite. The greatest increase in degradation was observed for the non-mineral control of atrazine, which increased from zero degradation previously to 50% degradation. In both mineral treatments further degradation of hydroxyatrazine and deethylatrazine was not observed. However, in the TIC chromatogram of the non-mineral control of deethylatrazine, deethylhydroxyatrazine (DEA-OH) (2-hydroxy-4-amino-6-isopropylamino-1,3,5-triazine) was detected. This explains the lower 55% recovery observed, given the absence of any mineral surface on which sorption could occur. The identity of the compound was confirmed by its mass spectrum, and both the TIC chromatogram and the mass spectrum of this compound are shown in Figure 5.14. The enhanced degradation observed in the non-mineral controls appear to be wholly hydrolytic in nature, due to the increased initial acidity from the acidic solution used in these experiments and the acidity caused by drying. This is confirmed by the presence of only hydroxy metabolites and no (further) dealkylated metabolites being present in the extract. It appears that the compounds in the non-mineral control were more prone to hydroxylation than they were on the mineral surfaces, which indicates a reduced acidity in the mineral samples as opposed to the non-mineral controls. This is probably a demonstration of the buffering capacity of mineral surfaces such as quartz and birnessite, compared to the non-mineral control samples which were completely unbuffered.

5.5 Effect of ultraviolet radiation

The results of the drying experiments exposed to ultraviolet (UV) radiation and their non-radiation drying reference (see methods section 4.2.1.4) are shown in Figure 5.15 and Tables A7 and A8 in Addendum A. It is useful to know the effect of UV-light on the degradation of atrazine during drying of a soil mineral surface, since it could provide possible insights into the exposure of the drying moist atrazine-mineral mixture to sunlight in the field. The effect of UV-radiation on the drying experiments was investigated by comparing the UV-exposed samples to a set of drying samples that were not exposed to UV-radiation (non-radiation, the three left-most bars of the bar charts in Figure 5.15). The wavelengths chosen, namely 365 nm and 254 nm, were based on several studies that conducted photo-degradation of atrazine with radiation at 254 nm (e.g. Hiskia et al. 2001; Azenha et al. 2003).

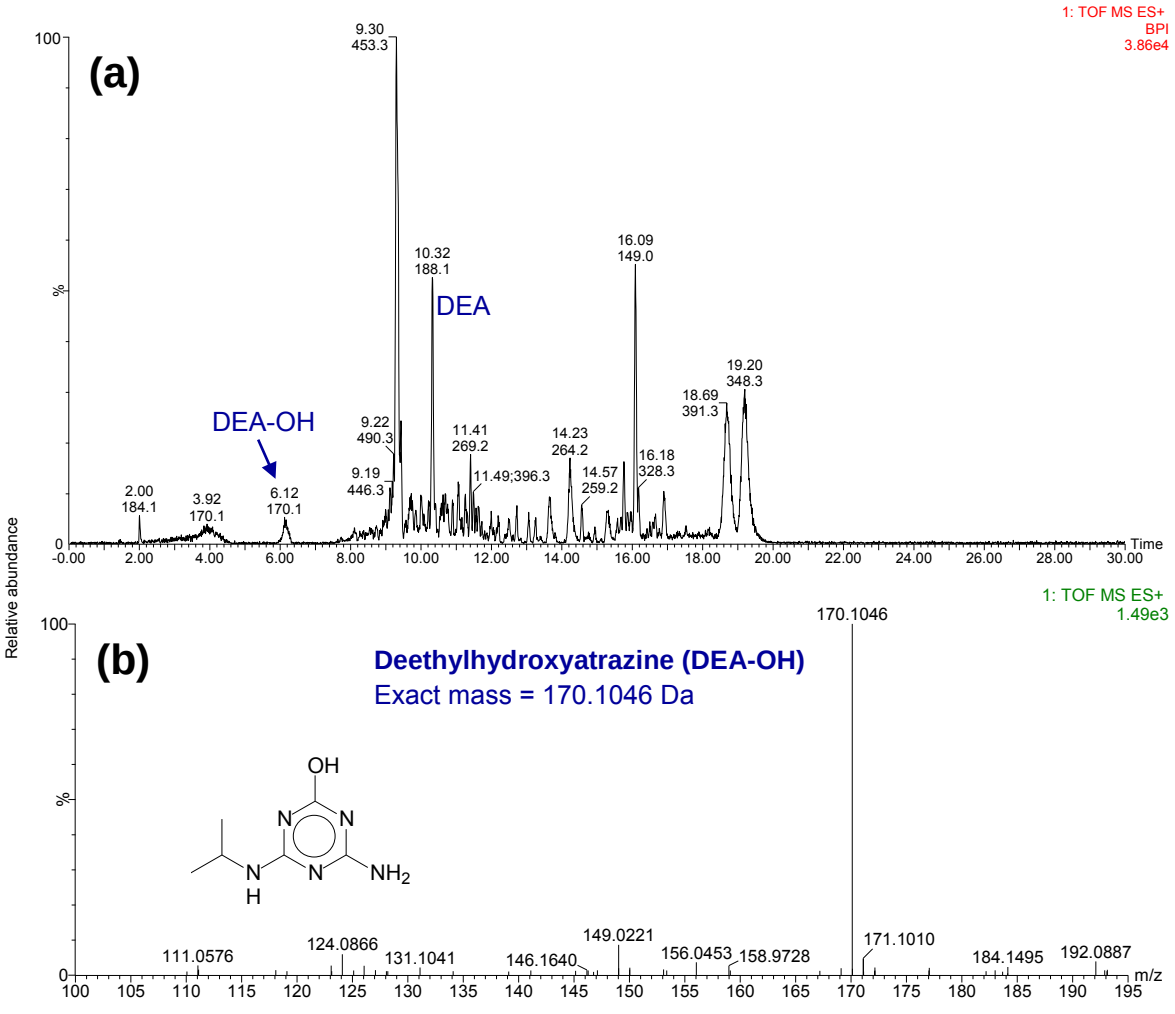

Figure 5.14 TIC chromatogram (a) and mass spectrum (b) showing the formation of deethyl-hydroxyatrazine (DEA-OH) in the non-mineral deethylatrazine drying control experiment. DEA = deethylatrazine.

The 365 nm radiation was chosen as it is prevalent in the solar radiation spectrum and is commonly used in the laboratory setting, providing a useful comparison for the wavelength at 254 nm.

The results for each mineral phase are from triplicate samples for each wavelength (and the non-radiation experiment) and the mean molar values of each compound are shown in the bar graphs in Figure 5.15. To compare the effects of each radiation wavelength on atrazine degradation, a significance, or *t*-test was conducted, comparing the means of the radiated samples to the non-radiated samples, for each compound.

(a) Birnessite

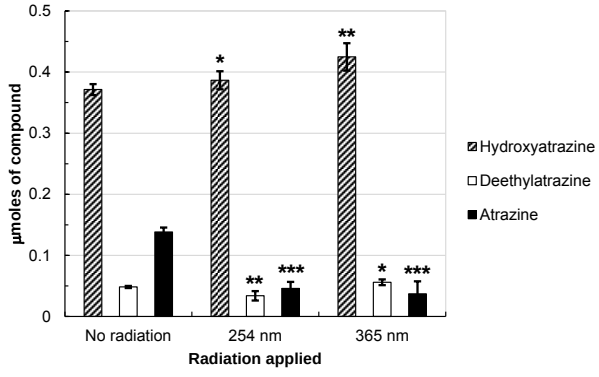

(b) Quartz

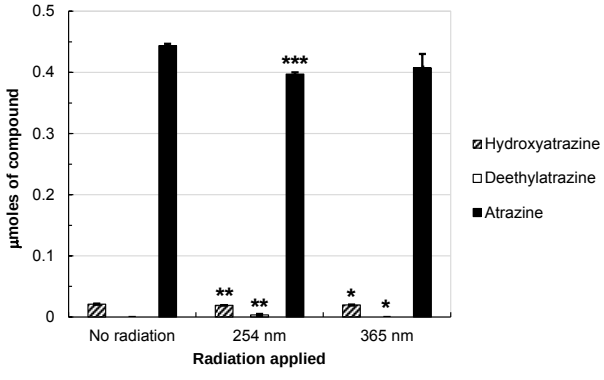

(c) Non-mineral control

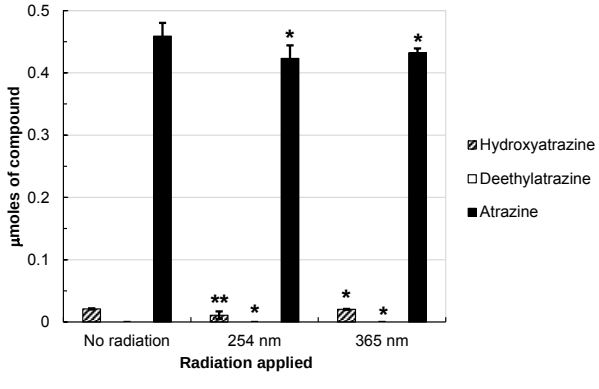

Figure 5.15 Results of the UV-radiation drying experiments using (a) birnessite, (b) quartz and (c) a non-mineral control, with no radiation, shortwave radiation at 254 nm and longwave radiation at 365 nm. Results from a signficance test are also shown, in which the mean mole value (three replicates, $n = 3$) of each compound extracted from the drying experiments subjected to radiation was compared to the corresponding mole values from the non-radiation experiments. Significant differences are denoted as: highly significant ($p < 0.01$) = ***, slightly significant ($0.01 \leq p < 0.05$) = ** and not significant ($p \geq 0.05$) = *. Bars depict the standard deviation of the three replicates.

Atrazine degradation on drying birnessite was significantly greater ($p < 0.01$) under UV-radiation of both wavelengths than the non-radiation experiments, whilst the formation of hydroxyatrazine was only slightly more significant ($0.01 \leq p < 0.05$) at 365 nm, compared to the non-radiation and 254 nm experiments. The formation of deethylatrazine was slightly lower ($0.01 \leq p < 0.05$) under 254 nm, but was insignificantly different between the non-radiation and 365 nm samples ($p \geq 0.05$). For the quartz-drying experiments, the application of radiation at 254 nm had the greatest effect on degradation, enhancing the degradation of atrazine ($p < 0.01$) and formation of both metabolites ($0.01 \leq p < 0.05$). For the non-mineral control samples, no significant enhancements or inhibitions were noted with the addition of UV-radiation, except for a slight decrease in the formation of hydroxyatrazine ($0.01 \leq p < 0.05$).

Ultraviolet (UV) radiation significantly enhances atrazine degradation on birnessite and quartz, but no corresponding significant increases in the amount of degradation products was observed. It is possible that UV-radiation is catalyzing the degradation reaction on the mineral surface (e.g. McMurray et al. 2006), but the lack of oxidation products (e.g. those in Tauber and von Sonntag 2000 and Tong et al. 2007) and an insignificant increase in hydroxyatrazine or deethylatrazine formation, is perhaps indicative of atrazine being lost by another process, such as volatilization. This is possible since the UV-radiation applied is capable of generating heat, which would in turn volatilize atrazine. However, atrazine volatilization was not covered in this study and is therefore a possible topic for future research.

5.6 Final insights into the degradation mechanism

Although the hydroxylation mechanism is well supported by the surface precursor complex – net non-oxidative mechanism proposed by Shin and Cheney (2005), the net non-oxidative mechanism proposed by Wang et al. (1999) for the dealkylation of atrazine on birnessite does not fully support some of the observations in this study. In all of the experiments where dealkylation occurred, no deisopropylatrazine (DIA) was observed in any of the experiments, despite its formation in all of the studies (Wang et al. 1999; Shin et al. 2000; Shin and Cheney 2004, 2005) where this mechanism was proposed for dealkylation. In all of the abiotic degradation studies conducted where this non-oxidative mechanism was proposed, equal proportions of deethylatrazine (DEA) and deisopropylatrazine (DIA) were formed. Differential formation of one dealkylation product over another are usually observed in the biodegradation of atrazine, where the removal of one of the alkyl chains is energetically favoured over the removal of another (Erickson et al. 1989). The formation of deethylatrazine in preference to deisopropylatrazine was

also observed in some hydroxyl radical ($^{\bullet}OH$) generating systems (e.g. Acero et al. 2000), and in these cases the formation of deethylatrazine was attributed to the reactivity of oxidation intermediates, such as 2-chloro-4-acetamido-6-isopropylamino-1,3,5-triazine (CDIT), which undergo further reaction to form deethylatrazine. Furthermore, the formation of deethylatrazine by oxidation mechanisms have peroxyl-radicals (C_3H_7-NH(C_3N_3Cl)NH-CH($^{\bullet}OO$)CH_3) as intermediates (Arnold et al. 1995a; Tauber and von Sonntag 2000). In this context, it is clear that steric hindrance could play a possible role, since molecular oxygen (O_2) would more than likely preferably attack the less bulky ethyl group on atrazine, as opposed to the more bulky isopropyl group. The reaction of these oxidation intermediates to form deethylatrazine is accompanied by the concomitant release of ethanal (acetaldehyde), which can be readily detected.

The authors who proposed the non-oxidative mechanism, namely Wang et al. (1999), Shin et al. (2000) and Shin and Cheney (2004, 2005), detected appreciable amounts of acetaldehyde and acetone, after the formation of deethylatrazine and deisopropylatrazine, respectively. Under a nitrogen (N_2) atmosphere, however, they only detected unoxidized ethylene and propylene, despite detecting very similar amounts of deethylatrazine and deisopropylatrazine as they did in the non-N_2 atmosphere experiments. The authors therefore concluded that oxygen was oxidizing these olefins after their release from atrazine, and their hypothesis was supported by the time lag that existed between dealkylation and formation of acetaldehyde and acetone.

Unfortunately, due to time and equipment constraints, these by-products were not analyzed for in this study. However, a comparison of the air-dried and N_2-dried data does reveal very similar rates of atrazine degradation (as well as hydroxyatrazine and deethylatrazine formation), which means that it is highly likely that the mechanism originally proposed by Wang et al. (1999) for dealkylation (see Figure 5.12 for a slightly modified version) does hold true in this study. However, this mechanism does not account at all for the apparently strong preference for the formation of deethylatrazine over deisopropylatrazine (DIA was not detected at all). In addition, further degradation to the didealkyl- (didealkylatrazine, DDA) and other hydroxy-metabolites (deethylhydroxyatrazine, DEA-OH; deisopropylhydroxyatrazine, DIA-OH; and ammeline, DDA-OH), which was observed for the reaction of atrazine with birnessite in a study by Shin and Cheney (2005), was not observed in this study. Once hydroxyatrazine and deethylatrazine had formed in this study, they only accumulated on the birnessite surface and did not degrade further to any other products. This was confirmed by the conservation of the total moles of *s*-triazines in the system, and by the lack of degradation observed when these metabolites were reacted with

birnessite (Figure 5.13). It is not clear at this point why only these two metabolites formed in the reaction, why there was a preference for deethylatrazine formation over deisopropylatrazine, and why no further degradation occurred. It could be possible that in the fully hydrated system investigated by Shin and Cheney (2005), the atrazine molecule has more freedom to move and reconfigure itself to align itself with the birnessite surface in the most efficient way for the reaction to occur. Furthermore, in these hydrated systems, it is also possible that the reaction products are free to move off of the birnessite surface and back into the aqueous solution once they have formed, especially since they are often much more polar than the original atrazine molecule, and perhaps are even repelled by the birnessite surface somewhat. In the drying system presented in this study, once all the moisture has evaporated, the atrazine molecule may be fixed in a certain position, well contained within a thin film of water molecules. In this configuration, the atrazine molecule may be configured in such a way that it is sterically aligned to the mineral surface, or aligned in a manner that is energetically most favourable, considering that it is a hydrophobic compound, and that it is generally repelled by charged mineral or sesquioxide surfaces. Since it is forced to make intimate contact with the mineral surface, as a result of the loss of water volume during drying, it would probably do so in the most favourable manner, which is not necessarily the most efficient for its reaction with birnessite, but is favourable for its forced contact with the mineral surface. In this manner, steric hindrance might be an important controlling factor for interaction between the mineral surface and the moieties on the atrazine molecule. In addition to this, once the metabolites have formed, they cannot leave the surface and return to solution in the manner they perhaps do in fully hydrated systems. They are forced to remain on the mineral surface, where they are possibly stabilized by various interactions, preventing further reactions to other metabolites. For example, hydroxyatrazine contains the OH group on position 2 of the triazine ring, rather than the more electron-withdrawing Cl group. Electron donation into the ring, and subsequent resonance rearrangements of electrons to the alkylamino moieties could stabilize the Mn-N bridge that is formed, not allowing sufficient electron transfer to occur, which could possibly explain the lack of products such as deethylhydroxyatrazine (DEA-OH), since the Mn-N bridge electron transfers are critical in dealkylation. With deethylatrazine (DEA), it is possible that since the molecule cannot leave the surface it might rearrange within the thin water film to have its amino (—NH_2) (polar) moiety directed more toward the birnessite surface, perhaps removing the isopropyl moiety out of reach of the birnessite surface and thus preventing the removal of the isopropyl group and subsequent formation of didealkylatrazine (DDA). It is thus possible that the drying surface is necessary for

rapid initial degradation of atrazine, but could be greatly inhibiting to further reactions of the metabolites with the mineral surface. The exact degradation mechanisms of atrazine on a drying birnessite (or soil mineral) surface is thus not fully elucidated in this study, but it is clear that drying certainly has an enhancing effect on atrazine degradation relative to moist systems, and that oxygen is most likely not the oxidant in these reactions. Water appears to have a critical role in the degradation of atrazine (compared with water-absent solvent systems) on drying mineral surfaces. It appears that surficial water probably plays a key role in the formation of a surface atrazine-birnessite complex, and that inherent water content within birnessite is not sufficient to initiate the reaction. Drying forces contact between the mineral surface and atrazine, where interaction most likely occurs between surficial waters and ring N atoms of atrazine, leading to ring-N protonation and subsequent hydroxylation. It is not clear why hydroxyatrazine forms as major product over deethylatrazine, but it could be related to possible preferences of the mineral surface waters and central cation interacting preferably with the ring N atoms over the N atoms within the alkylamino groups. It is also possible that the alkylamino chains are simply more hydrophobic than the triazine ring and thus interact less favourably with the mineral surface.

5.7 Practical applications

The fact that drying can enhance the rate of atrazine transformation, by the mineral surfaces of birnessite and goethite, means that where soils rich in these minerals occur, and where atrazine is applied to crops grown on these soils, simple and relatively inexpensive practices such as tilling or windrowing might greatly enhance the transformation of atrazine. Perhaps it may seem unnatural at first to apply experiments such as the rapid air drying experiments to natural settings, since it is often the case that natural, or even some agricultural soils would not attain the same degree of such extreme dryness over such a short period of time, as achieved in the laboratory. However, the practice of windrowing does have the potential to dry these soils to a much greater degree than they would normally, because of the manner in which it exposes the topsoils to wind and direct sunlight. It has been shown that exposure to UV radiation (also present in sunlight) has some enhancing effect on the degradation of atrazine on birnessite. Whether, the radiation causes more rapid drying, or whether it catalyzes the reaction, that much is not clear, but in a practical sense, it does not matter *how* the sunlight would enhance the degradation, what is important is that it simply *does*. Through windrowing and tilling it is possible for agricultural soils to experience this sort of rapid drying, and hence it is possible that this drying-induced degradation of atrazine might be more applicable than expected from natural soils, that do not experience this

sort of drying. Many studies do focus solely on pristine or natural soils and waters, because most concerns surrounding atrazine are based around its effects on natural ecosystems. The general consensus is that atrazine is highly persistent in these settings. However, atrazine is, per definition, a *xenobiotic* compound, and that its degradation or removal from the environment would most likely be most efficient in an unnatural setting. The practices of windrowing and tilling provide these extremes not seen in natural soils, taking these drying processes out of the laboratory making them a reality in the field. These drying processes could have many applications to atrazine degradation, and could be especially useful where there is atrazine phytotoxicity towards the crop being planted on that soil, where the intrinsic microbial population is largely inactive or unconditioned to atrazine, or where there has been an accidental atrazine spill. Windrowing appears to be an especially useful practice, since the accelerated drying of the soil, by wind for example, could lead to rapid transformation of atrazine, as demonstrated by the enhanced drying experiments under an air or N_2 stream. Since windrowing provides that extreme drying that is demonstrated in the accelerated drying experiments, these drying-induced and enhanced degradations of atrazine are very much applicable to agricultural settings.

The transformation of atrazine to its hydroxy metabolite, hydroxyatrazine cannot be deemed specifically as either advantageous or disadvantageous. Hydroxyatrazine is non-phytotoxic, unlike the atrazine parent molecule, or any of the chloro-metabolites of atrazine, including deethylatrazine. Since hydroxyatrazine is the major transformation product in all of the reactions in this study, the implication in the environment would be a detoxification of the atrazine applied to a field of maize for example. This might be advantageous for the ecology of the soil, since detoxification might prevent the destruction of sensitive flora in the soil system, but this same detoxification mechanism might render atrazine, *the herbicide*, less effective in managing weed plants, which could lead to losses in agricultural production. The production of deethylatrazine does not affect the phytotoxicity of atrazine, but deethylatrazine is more polar (and thus more water soluble) than atrazine, rendering it possibly more mobile in the soil system, and possibly a greater pollutant of water systems than the parent compound, atrazine. However, for the purposes of atrazine remediation, this possible enhancing effect of drying (given the right constituents) on the transformation of atrazine could be very advantageous. As a practice, tilling or windrowing of the soil simply to allow drying to occur is relatively inexpensive compared to specially-engineered systems involving advanced oxidation processes (AOPs), for example. A slight modification of current remediation strategies to involve a drying step could enhance the efficiency of atrazine removal greatly.

6 Conclusions and future work

6.1 Conclusions

6.1.1 The effects of mineral surface drying on atrazine transformation

In all of the experiments conducted in this study, degradation of atrazine only occurred in some of those experiments where the moist mineral-atrazine mixture was allowed to dry for a given period of time. For all of the moist analogues (where the mixtures were not allowed to dry), no appreciable atrazine degradation was observed in any of the cases. Under conditions of drying, not all of the mineral surfaces degraded atrazine, with four out of the six mineral surfaces investigated showing no real enhancement of atrazine degradation over its moist analogue. Only birnessite (Mn^{4+}-oxide) and goethite (Fe^{3+}-oxide) showed an appreciable amount of atrazine degradation, as well as the largest variety of degradation products formed. In terms of quantity of atrazine degraded per gram of mineral within 14 days, birnessite degraded 132 μg atrazine per g oxide, whilst goethite degraded 36 μg atrazine per g oxide. It was concluded that drying therefore has the capacity to enhance the degradation of atrazine, but only on a very limited number of mineral surfaces.

It is also apparent that only the oxidation-reduction (redox) active mineral surfaces (Mn^{4+}- and Fe^{3+}-oxides) have their reactivity enhanced by drying of the mineral surface. The relative reactivity of each mineral revealed a reactivity trend which follows the redox potential of the mineral surface, with Mn^{4+}-oxide as the most reactive, followed by Fe^{3+}-oxides. The non-reactive minerals under both drying and moist conditions are the non-redox active mineral phases, which include oxides of Al^{3+} and Si^{4+}, as well as the Al^{3+}-saturated smectite mineral. It is therefore envisaged that soils rich in Mn-oxide minerals have the greatest capacity to degrade atrazine relative to other soils. Soils rich in ferric oxyhydroxides, especially goethite (a common soil mineral), also have the capacity to degrade atrazine, albeit at a lower efficiency than soils rich in Mn^{4+}-oxides. Furthermore, drying of such a soil, as part of a drying-wetting cycle for example, is likely to increase the ability of that soil to transform atrazine. However, these model laboratory systems cannot be directly applied to the field setting, since numerous other factors, such as the soil microbial activity, organic carbon (OC) content and water content all affect the fate of atrazine. These model systems thus only provide a guideline as to which soil is more likely to degrade atrazine (abiotically) and all factors considered.

6.1.2 Critical moisture content

Using birnessite as a model mineral surface, investigations over the drying period revealed that atrazine degradation was initiated when the residual gravimetric moisture content reached a critical value of approximately 10% of the original gravimetric moisture content present at the beginning of the experiment. When expressed as gravimetric moisture content (%), this amount of moisture relates to a moisture content of 21%, three times greater than the inherent birnessite moisture content of 7%. Quartz was used as a reference mineral of low redox potential relative to birnessite, and no atrazine degradation was observed at any specific value of moisture content for this mineral. This confirms once again, that even under prolonged drying (30 days versus 14 days), the transformation of atrazine is only enhanced on redox-active soil mineral surfaces, the Mn-oxide birnessite in this case. It was also observed that once atrazine transformation had commenced on the near-dry to dry birnessite surface (< 10% residual gravimetric moisture content), atrazine continued to degrade on the dry birnessite surface until it was all virtually degraded, after 30 days.

Increasing the drying rate of the moist birnessite-atrazine mixture with the use of compressed air, enhanced atrazine transformation substantially, with virtually all of the atrazine applied being degraded within 4 days (compared to 30 days under gradual ambient drying). However, even with accelerated drying, quartz still showed no reactivity toward atrazine. Therefore, it appears that for birnessite, a redox-active mineral, the degree of transformation of atrazine is more a function of the moisture content on its surface than the contact time between it and atrazine. Furthermore, by manipulating the moisture content of the birnessite-atrazine mixture, the rate of atrazine transformation can be greatly varied.

At this point, moisture content, at least for birnessite, seems to be the major controlling factor in the transformation of atrazine on the birnessite surface. It appears that moisture content above the critical value of 10% has a general inhibitory effect on atrazine transformation, and transformation is simply a function of how rapidly that moisture can be removed. However, the solvent-only analogue of the gradual 30-day birnessite-atrazine drying experiment, conducted using no moisture only acetone, did not show enhanced degradation of atrazine relative to the aqueous drying experiment, as would be expected if moisture content was the major controlling factor of atrazine transformation on a drying birnessite surface. It is thus possible that any solvent could be an inhibitor of atrazine transformation by the birnessite surface, and that the initiation of the reaction of atrazine with the birnessite surface after a critical moisture content has been

reached is no more than the atrazine molecule being forced to make intimate contact with the birnessite surface, since it has no freedom of movement any longer (the liquid medium is gone).

6.1.3 Elucidation of the reaction mechanism

In this study, from the first set of drying versus moist experiments, the degradation of atrazine yielded two metabolites, namely hydroxyatrazine (major) and deethylatrazine (minor), which appeared only for the redox-active minerals birnessite and goethite. It is not completely clear why hydroxyatrazine is formed preferentially over deethylatrazine, but it is concluded that degradation is not driven by Lewis acidity of the cation in these minerals, since Al^{3+} and Si^{4+} (hard Lewis acids) showed no reactivity toward atrazine. Instead, degradation is controlled by redox potential, of which $Mn^{4+}O_2$ has the greatest, followed by $Fe^{3+}OOH$. However, since no atrazine oxidation products were detected, no appreciable reduction of Mn^{4+} to Mn^{2+} was observed during the degradation of atrazine on birnessite, and since degradation was equally efficient under drying with air or N_2, the following conclusions are drawn about the degradation mechanism:

- The overall degradation mechanism is a *net* non-redox mechanism, as postulated by previous authors investigating atrazine degradation on birnessite; however,

- Electron transfer is a crucial first step in the degradation reaction, and occurs via a bridge formed between the cation in the mineral surface (e.g. Mn^{4+}) and one of the N atoms on the atrazine molecule;

- In order to form this cation-N bridge, a surface precursor complex has to be formed between the mineral surface and the atrazine molecule, which can take the form of cation-exchange type sorption at low pH values, near the pK_a of atrazine and the point of zero net charge (pH_{PZNC}) of the mineral surface;

- The dealkylation of atrazine by the birnessite surface is oxygen (O_2)-independent, given the equally efficient deethylatrazine formation under air-drying and drying with N_2;

The reduction in moisture content has dual, yet seemingly opposing, effects on the atrazine transformation mechanism. By reducing the volume of water (or solvent for that matter) on the mineral surface, drying forces intimate contact between atrazine and the mineral surface, forcing the two components to interact. However, by removing the overlying solution through drying, any products such as hydroxyatrazine and deethylatrazine that form have no freedom of motion

as they would in a fully hydrated system for example. These molecules (that are fairly hydrophobic) have to conform in such a way that they interact with the mineral surface in the most energetically favourable manner. The lack of variety in the metabolites formed is perhaps the largest indicator of this. Furthermore, the lack of any further transformation occurring to both hydroxyatrazine and deethylatrazine when they were reacted with drying birnessite, in a manner analogous to the drying atrazine-birnessite mixtures, is perhaps further verification of this effect.

The exact mechanism of atrazine transformation, although partially elucidated, is still somewhat elusive, especially from the mineral surface's point of view. It is fairly well-known what changes the atrazine molecule undergoes during transformation, but the interaction between the atrazine molecule and the mineral surface prior to transformation, the oxidation states of the mineral surface cation during degradation, and even the existence of the surface atrazine precursor complex with the cation-N bridge is still largely speculation.

6.1.4 The effect of ultraviolet (UV) radiation on atrazine transformation

The effects of ultraviolet (UV)-radiation on these drying experiments appear to be somewhat significant, with increases in atrazine transformation on birnessite when UV-radiation was applied. However, the effect that UV-radiation has on the reaction mechanism is unknown, given that no additional transformation products were produced. At this point, it can only be concluded that radiation with UV-light has increased the transformation of atrazine on birnessite, relative to an analogue drying experiment with no radiation. Although it appears that UV-radiation has affected the transformation of atrazine in this laboratory study, the effects of real sunlight on atrazine transformation by a drying birnessite-containing soil, and of course the effects of sunlight on the drying rate, cannot be predicted by these results, given the vast range of radiation wavelengths present in direct sunlight and its heating effect on soil.

6.1.5 Environmental significance

At field scale, the formation of hydroxyatrazine as the major degradation product of atrazine degradation is considered to be the major pathway of detoxification of that field upon which atrazine was applied. This could possibly lead to an increase in soil health and biodiversity, but is not advantageous for the scenario where atrazine's phytotoxicity is a requirement (e.g. to eradicate weeds). Therefore, depending on the context, the detoxification of atrazine, which appears to be the major degradation pathway in this study, could be deemed either positive or negative. Furthermore, reduced efficiency of herbicides not only leads to losses in crop

production, but also encourages more regular use of practices such as conventional tillage to remove weeds. Tillage practices generally increase the degradation of soil organic carbon (SOC), leading to possible losses in the CO_2-sequestration ability of that soil. In terms of the mobility of atrazine, the formation of hydroxyatrazine as the major degradation product has the potential to retard the leaching of atrazine into water supplies, given the greater affinity that hydroxyatrazine (versus atrazine) displays for certain soil components, especially SOC. Therefore, the formation of hydroxyatrazine (the major degradation product in this study) is generally considered as a positive phenomenon, provided that it does not reduce the herbicidal efficiency of the atrazine originally applied.

6.2 Future work

Most of the future work on abiotic atrazine transformation on mineral surfaces is centred on the elucidation of the transformation mechanism. Although many metabolites and reaction intermediates have been identified, and the kinetics of atrazine transformation is established for mineral surfaces such as birnessite, the exact interactions between atrazine and the mineral surface, as well as the changes occurring within the mineral surface, still have to be investigated. It is very likely that this task will fall to spectroscopic methods, such as X-ray absorption spectroscopy (XAS), Fourier transform infrared (FTIR) spectroscopy and electron spin resonance (ESR) spectroscopy.

X-ray absorption spectroscopy (XAS), using a synchrotron light source, is a very powerful tool in elucidating oxidation states and interatomic distances within mineral lattices, such as those of birnessite. X-ray absorption near-edge structure (XANES) spectroscopy would be useful in determining the oxidation state of Mn during the reaction of atrazine with birnessite, confirming if indeed Mn^{2+} is temporarily formed in the solid state, or whether there might even be an intermediate step involving single electron transfer to form Mn^{3+} and then Mn^{2+}. This is all possible with XANES, which can probe the mineral surface directly. A softer technique, known as near edge X-ray absorption fine structure (NEXAFS) spectroscopy, is suitable for carbon-containing samples, and would be useful to probe the interaction of atrazine with the mineral surface.

A useful technique for investigating the interaction between a mineral surface and an organic compound is Fourier transform infrared (FTIR) spectroscopy. This technique would be useful especially in investigating the postulated cation-N bridge that is formed between the cation

in the mineral surface (e.g. Mn^{4+}) and the N atoms on atrazine. Furthermore, this technique can be applied in real-time with the use of attenuated total reflectance – Fourier transform infrared (ATR-FTIR) spectroscopy, which allows the observation of kinetically short-lived surface intermediates for example. This is especially useful if the cation-N bridge is only present for a short period of time during the reaction. A preliminary investigation was conducted in this study using ATR-FTIR to perhaps elucidate some of the surface interactions occurring between atrazine and the birnessite surface. The results of this investigation, along with a brief method description, are provided in Addendum B. The results of this investigation unfortunately yielded no clear evidence of bond formation or atrazine degradation, but adjustment of the techniques used could yield results in the future.

Possible oxidation steps within the atrazine degradation mechanism could have radicals or paramagnetic intermediates, which would be readily detected by electron spin resonance (ESR) spectroscopy. The detection of Mn^{2+} is a noteworthy example. This technique can be run in both the solid and liquid phase, which could provide the capability to track the formation of radical intermediates, allowing the elucidation of oxidation steps in the atrazine degradation mechanism. The peroxyl radical intermediate of atrazine found in the oxidation of atrazine by hydroxyl radicals ($^{\bullet}OH$), for example, is yet to be charac-terized by ESR spectroscopy. A preliminary investigation into ESR spectroscopy was also conducted in this study, and some of the spectra are shown in Figure B2 of Addendum B. In this preliminary study, it was found that Mn^{2+} could not be effectively detected in solid birnessite, but was detectable in solution, with a detection limit of 25 mg L^{-1}. This detection limit was greater than the concentrations of Mn^{2+} encountered in this study, but could be useful in studies where the concentrations are greater. However, the possibility still exists to characterize the production of peroxyl atrazine radicals using ESR, by possibly using a Fenton-reagent system. The advantage of this ESR technique is that it can also provide real-time data, since it would be possible to run an aqueous Fenton-oxidation experiment within the capillary analysis tube.

Another matter is also of possible future interest. As was shown in this study, it is also not clear why ultraviolet (UV) radiation had an enhancing effect on the transformation of atrazine on birnessite, relative to a drying birnessite-atrazine mixture that was not irradiated. No oxidation reactions are suspected, given the lack of any oxidation products. However, this is not conclusive, as it is not well-known how stable any intermediates might be in the presence of UV radiation, and even less is known about any possible catalytic role birnessite might be playing in the

reaction mechanism, when exposed to UV radiation. There is scope in this topic for various applications of methods such spectroscopy (visibly track the mechanisms over time) and chromatography, to find new possible transformation intermediates or end products.

It is apparent that detailed information about the atrazine degradation mechanism is possibly the most important consideration at present, but there is still scope for other studies. For example, the kinetics of atrazine degradation on mineral surfaces other than birnessite is still a subject that is not well-covered in the literature. The reaction of atrazine with Fe^{3+}-oxides is still not well understood, but is very important, given the prevalence, availability and ubiquity of Fe^{3+}-oxides in the environment relative to Mn^{4+}-oxides. Furthermore, with the vast array of mechanistic information that can be obtained with different techniques, there are bound to be new reaction intermediates and metabolites that need to be characterized, each requiring their own method of analysis and identification. This would almost certainly lead to new GC/MS/MS and LC/MS/MS methods being developed in order to study these new compounds, since these methods are still the most sensitive for the triazines.

7 References

Abate G, Masini JC. Adsorption of atrazine, hydroxyatrazine, deethylatrazine, and deisopropylatrazine onto Fe(III) polyhydroxy cations intercalated vermiculite and montmorillonite. J Agric Food Chem 2005a;53:1612–1619.

Abate G, Masini JC. Sorption of atrazine, propazine, deethylatrazine, deisopropylatrazine and hydroxyatrazine onto organovermiculite. J Braz Chem Soc 2005b;16:936–943.

Abián J, Durand G, Barceló D. Analysis of chlorotriazines and their degradation products in environmental samples by selecting various operating modes in thermospray HPLC/MS/MS. J Agric Food Chem 1993;41:1264–1273.

Abigail MEA, Lakshmi V, Das N. Biodegradation of atrazine by *Cryptococcus laurentii* isolated from contaminated agricultural soil. J Microbiol Biotech Res 2012;2:450–457.

Abigail EA, Salam JA, Das N. Atrazine degradation in liquid culture and soil by a novel yeast *Pichia kudriavzevii* strain Atz-EN-01 and its potential application for bioremediation. J Appl Pharm Sci 2013;3:035–043.

Acero JL, Stemmler K, von Gunten U. Degradation kinetics of atrazine and its degradation products with ozone and OH radicals: a predictive tool for drinking water treatment. Environ Sci Technol 2000;34:591–597.

Ackerman F. The economics of atrazine. Int J Occup Environ Health 2007;13:441–449.

Adams NH, Levi PE, Hodgson E. In vitro studies of the metabolism of atrazine, simazine, and terbutryn in several vertebrate species. J Agric Food Chem 1990;38:1411–1417.

Alekseeva T, Besse P, Binet F, Delort AM, Forano C, Josselin N, Sancelme M, Tixier C. Effect of earthworm activity (*Aporrectodea giardi*) on atrazine adsorption and biodegradation. Eur J Soil Sci 2006;57:295–307.

Alvey S, Crowley DE. Survival and activity of an atrazine-mineralizing bacterial consortium in rhizosphere soil. Environ Sci Technol 1996;30:1596–1603.

Arnold SM, Hickey WJ, Harris RF. Degradation of atrazine by Fenton's reagent: condition optimization and product quantification. Environ Sci Technol 1995a;29:2083–2089.

Arnold SM, Talaat RE, Hickey WJ, Harris RF. Identification of Fenton's reagent-generated atrazine degradation products by high-performance liquid chromatography and megaflow electrospray ionization tandem mass spectrometry. J Mass Spectrom 1995b;30:452–460.

Aslam M, Alam M, Rais S. Detection of atrazine and simazine in ground water of Delhi using high performance liquid chromatography with ultraviolet detector. Curr World Environ 2013;8:323–329.

Assaf NA, Turco RF. Accelerated biodegradation of atrazine by a microbial consortium is possible in culture and soil. Biodegradation 1994;5:29–35.

Azenha MEDG, Burrows HD, Canle M, Coimbra R, Fernández MI, García MV, Peiteado MA, Santaballa JA. Kinetic and mechanistic aspects of the direct photodegradation of atrazine, atraton, ametryn and 2-hydroxyatrazine by 254 nm light in aqueous solution. J Phys Org Chem 2003;16:498–503.

Bakke JE, Larson JD, Price CE. Metabolism of atrazine and 2-hydroxyatrazine by the rat. J Agric Food Chem 1972;20:602–607.

Baláž P, Achimovičová M, Baláž M, Billik P, Cherkezova-Zheleva Z, Criado JM, Delogu F, Dutková E, Gaffet E, Gotor FJ, Kumar R, Mitov I, Rojac T, Senna M, Streletskii A, Wieczorek-Ciurowa K. Hallmarks of mechanochemistry: from nanoparticles to technology. Chem Soc Rev 2013;42:7571–7637.

Balduini L, Matoga M, Cavalli E, Seilles E, Riethmuller D, Thomassin M, Guillaume YC. Triazinic herbicide determination by gas chromatography–mass spectrometry in breast milk. J Chromatogr B 2003;794:389–395.

Barrett KA, McBride MB. Oxidative degradation of glyphosate and aminomethylphosphonate by manganese oxide. Environ Sci Technol 2005;39:9223–9228.

Barriuso E, Baer U, Calvet R. Dissolved organic matter and adsorption-desorption of dimefuron, atrazine, and carbetamide by soils. J Environ Qual 1992;21:359–367.

Barriuso E, Koskinen WC, Sadowski MJ. Solvent extraction characterization of bioavailability of atrazine residues in soils. J Agric Food Chem 2004;52:6552–6556.

Bayless ER. Atrazine retention and degradation in the vadose zone at a till plain site in central Indiana. Ground Water 2001;39:169–180.

Beale DJ, Porter NA, Roddick FA. A fast screening method for the presence of atrazine and other triazines in water using flow injection with chemiluminescent detection. Talanta 2009;78:342–347.

Behki RM, Khan SU. Degradation of atrazine by *Pseudomonas*: N-dealkylation and dehalogenation of atrazine and its metabolites. J Agric Food Chem 1986;34:746–749.

Benotti MJ, Trenholm RA, Vanderford BJ, Holady JC, Stanford BD, Snyder SA. Pharmaceuticals and endocrine disrupting compounds in U.S. drinking water. Environ Sci Technol 2009;43:597–603.

Berg M, Müller SR, Schwarzenbach RP. Simultaneous determination of triazines including atrazine and their major metabolites hydroxyatrazine, desethylatrazine, and deisopropylatrazine in natural waters. Anal Chem 1995;67:1860–1865.

Beyer MK, Clausen-Schaumann H. Mechanochemistry: the mechanical activation of covalent bonds. Chem Rev 2005;105:2921–2948.

Bezbaruah AN, Thompson JM, Chisholm BJ. Remediation of alachlor and atrazine contaminated water with zero-valent iron nanoparticles. J Environ Sci Health B 2009;44:518–524.

Binet F, Kersanté A, Munier-Lamy C, Le Bayon R-C, Belgy M-J, Shipitalo MJ. Lumbricid Macrofauna alter atrazine mineralization and sorption in a silt loam soil. Soil Biol Biochem 2006;38:1255–1263.

Blume E, Bischoff M, Moorman TB, Turco RF. Degradation and binding of atrazine in surface and subsurface soils. J Agric Food Chem 2004;52:7382–7388.

Boffetta P, Adami HO, Berry SC, Mandel JS. Atrazine and cancer: a review of the epidemiologic evidence. Eur J Cancer Prev 2013;22:169–180.

Bosch DD, Truman CC. Agrichemical transport to groundwater through coastal plain soils. Trans ASAE 2002;45:1385–1396.

Boyd-Boland AA, Pawliszyn JB. Solid-phase microextraction of nitrogen-containing herbicides. J Chromatogr A 1995;704:163–172.

Burken JG, Schnoor JL. Uptake and metabolism of atrazine by poplar trees. Environ Sci Technol 1997;31:1399–1406.

Byer JD, Struger J, Sverko E, Klawunn P, Todd A. Spatial and seasonal variations in atrazine and metolachlor surface water concentrations in Ontario (Canada) using ELISA. Chemosphere 2011;82:1155–1160.

Castelo-Grande T, Augusto PA, Barbosa D. Removal of pesticides from soil by supercritical extraction—a preliminary study. Chem Eng J 2005;111:167–171.

Cavas T. In vivo genotoxicity evaluation of atrazine and atrazine–based herbicide on fish *Carassius auratus* using the micronucleus test and the comet assay. Food Chem Toxicol 2011;49:1431–1435.

Cea M, Cartes P, Palma G, Mora ML. Atrazine efficiency in an Andisol as affected by clays and nanoclays in ethylcellulose controlled release formulations. RC Suelo Nutr Veg 2010;10:62–77.

Ceccatti JS. Resisting insects: shifting strategies in chemical control. Endeavour 2004;28:14–19.

Celis R, Barriuso E, Houot S. Sorption and desorption of atrazine by sludge-amended soil: dissolved organic matter effects. J Environ Qual 1998;27:1348–1356.

Chang SW, Lee SJ, Je CH. Phytoremediation of atrazine by poplar trees: toxicity, uptake, and transformation. J Environ Sci Health B 2005;40:801–811.

Chappell MA, Laird DA, Thompson ML, Evangelou VP. Cosorption of atrazine and a lauryl polyoxyethylene oxide nonionic surfactant on smectite. J Agric Food Chem 2005;53:10127–10133.

Cheney MA, Shin JY, Crowley DE, Alvey S, Malengreau N, Sposito G. Atrazine dealkylation on a manganese oxide surface. Colloids Surf A 1998;137:267–273.

Clarke CE, Aguilar-Carrillo J, Roychoudhury AN. Quantification of drying induced acidity at the mineral–water interface using ATR-FTIR spectroscopy. Geochim Cosmochim Acta 2011;75:4846–4856.

Clarke C, Tourney J, Johnson K. Oxidation of anthracene using waste Mn oxide minerals: the importance of wetting and drying sequences. J Hazard Mater 2012;205–206:126–130.

Clay SA, Koskinen WC. Adsorption and desorption of atrazine, hydroxyatrazine, and S-glutathione atrazine on two soils. Weed Sci 1990;38:262–266.

Cook AM. Biodegradation of *s*-triazine xenobiotics. FEMS Microbiol Rev 1987;46:93–116.

Cook AM, Beilstein P, Grossenbacher H, Hütter R. Ring cleavage and degradative pathway of cyanuric acid in bacteria. Biochem J 1985;231:25–30.

Cook AM, Hütter R. *s*-Triazines as nitrogen sources for bacteria. J Agric Food Chem 1981;29:1135–1143.

Cook AM, Hütter R. Deethylsimazine: bacterial dechlorination, deamination, and complete degradation. J Agric Food Chem 1984;32:581–585.

Crawford JJ, Traina SJ, Tuovinen OH. Bacterial degradation of atrazine in redox potential gradients in fixed-film sand columns. Soil Sci Soc Am J 2000;64:624–634.

Dagnac T, Bristeau S, Jeannot R, Mouvet C, Baran N. Determination of chloroacetanilides, triazines and phenylureas and some of their metabolites in soils by pressurised liquid extraction, GC–MS/MS, LC–MS and LC–MS/MS. J Chromatogr A 2005;1067:225–233.

Dehghani M, Nasseri S, Hashemi H. Study of the bioremediation of atrazine under variable carbon and nitrogen sources by mixed bacterial consortium isolated from corn field soil in Fars Province of Iran. J Environ Public Health 2013;2013:1–7.

de la Casa-Resino I, Valdehita A, Soler F, Navas JM, Pérez-López M. Endocrine disruption caused by oral administration of atrazine in European quail (*Coturnix coturnix coturnix*). Comp Biochem Physiol, Part C: Toxicol Pharmacol 2012;156:159–165.

de Souza ML, Newcombe D, Alvey S, Crowley DE, Hay A, Sadowsky MJ, Wackett LP. Molecular basis of a bacterial consortium: interspecies catabolism of atrazine. Appl Environ Microbiol 1998;64:178–184.

DeSutter TM, Clay SA, Clay DE. Atrazine sorption and desorption as affected by aggregate size, particle size, and soil type. Weed Sci 2003;51:456–462.

Díaz JM, Farach HA, Poole CP. Electron-spin-resonance study of Mn^{2+} in natural wollastonite. Am Mineral 1990;75:262–266.

Dolan T, Howsam P, Parsons DJ, Whelan MJ. Is the EU drinking water directive standard for pesticides in drinking water consistent with the precautionary principle? Environ Sci Technol 2013;47:4999–5006.

Dombek T, Dolan E, Schultz J, Klarup D. Rapid reductive dechlorination of atrazine by zero-valent iron under acidic conditions. Environ Pollut 2001;111:21–27.

Dorado J, Tinoco P, Almendros G. Soil parameters related with the sorption of 2,4-D and atrazine. Comm Soil Sci Plant Anal 2003;34:1119–1133.

Doruk AY, Kolankaya N. Biodegradation of atrazine by a selected white-rot fungal strain in optimized conditions. Eur Int J Sci Technol 2012;1:1–10.

Dowding CE, Borda MJ, Fey MV, Sparks DL. A new method for gaining insight into the chemistry of drying mineral surfaces using ATR-FTIR. J Colloid Interface Sci 2005;292:148–151.

Du Preez C, Van Huyssteen C, Pearson M. Land use and soil organic matter in South Africa 1: a review on spatial variability and the influence of rangeland stock production. S Afr J Sci 2011. doi: 10.4102/sajs.v107i5/6.354.

Du Preez LH, Jansen van Rensburg PJ, Jooste AM, Carr JA, Giesy JP, Gross TS, Kendall RJ, Smith EE, Van Der Kraak G, Solomon KR. Seasonal exposures to triazine and other pesticides in surface waters in the western Highveld corn-production region in South Africa. Environ Pollut 2005;135:131–141.

Egaas E, Skaare JU, Svendsen NO, Sandvik M, Falls JG, Dauterman WC, Collier TK, Netland J. A comparative study of effects of atrazine on xenobiotic metabolizing enzymes in fish and insect, and of the in vitro phase II atrazine metabolism in some fish, insects, mammals and one plant species. Comp Biochem Physiol C Pharmacol Toxicol Endocrinol 1993;106:141–149.

Erickson LE, Lee KH, Sumner DD. Degradation of atrazine and related s-triazines. Crit Rev Env Contr 1989;19:1–14.

Erickson LE, Minkevich IG, Eroshin VK. Application of mass and energy balance regularities in fermentation. Biotechnol Bioeng 1978;20:1595–1621.

Eskilsson CS, Björklund E. Analytical-scale microwave-assisted extraction. J Chromatogr A 2000;902:227–250.

Espinoza J, Báez ME. Determination of atrazine in aqueous soil extracts by high-performance

thin–layer chromatography. J Chil Chem Soc 2003;48:19–23.

Esser HO, Dupuis G, Ebert E, Marco GJ, Vogel C. s-Triazines. In: Kearney PC, Kaufman DD, editors. Herbicides: Chemistry, Degradation, and Mode of Action, 2nd ed., vol. 1. New York, NY, USA: Marcel Dekker; 1975. pp. 129–208.

FAO. FAOSTAT. Rome, Italy: Food and Agriculture Organization of the United Nations 2010; Available: http://faostat.fao.org/site/424/DesktopDefault.aspx?PageID=424#ancor [Accessed 19 April 2013].

FAO. FAOSTAT. Rome, Italy: Food and Agriculture Organization of the United Nations 2011; Available: http://faostat.fao.org/site/339/default.aspx [Accessed 11 December 2013].

Farenhorst A, Topp E, Bowman BT, Tomlin AD. Earthworms and the dissipation and distribution of atrazine in the soil profile. Soil Biol Biochem 2000a;32:23–33.

Farenhorst A, Topp E, Bowman BT, Tomlin AD. Earthworm burrowing and feeding activity and the potential for atrazine transport by preferential flow. Soil Biol Biochem 2000b;32:479–488.

Francioso O, Bak E, Rossi N, Sequi P. Sorption of atrazine and trifluralin in relation to the physio-chemical characteristics of selected soils. Sci Total Environ 1992;123–124:503–512.

García-González V, Govantes F, Shaw LJ, Burns RG, Santero E. Nitrogen control of atrazine utilization in *Pseudomonas* sp. strain ADP. Appl Environ Microbiol 2003;69:6987–6993.

Gascón J, Oubiña A, Barceló D. Detection of endocrine-disrupting pesticides by enzyme-linked immunosorbent assay (ELISA): application to atrazine. Trend Anal Chem 1997;16:554–562.

Gerecke AC, Schärer M, Singer HP, Müller SR, Schwarzenbach RP, Sägesser M, Ochsenbein U, Popow G. Sources of pesticides in surface waters in Switzerland: pesticide load through waste water treatment plants—current situation and reduction potential. Chemosphere 2002;48:307–315.

Giardina MC, Giardi MT, Filacchioni G. 4-Amino-2-chloro-1,3,5-triazine: a new metabolite of atrazine by a soil bacterium. Agric Biol Chem 1980;44:2067–2072.

Giardina MC, Giardi MT, Filacchioni G. Atrazine metabolism by Nocardia: elucidation of initial pathway and synthesis of potential metabolites. Agric Biol Chem 1982;46:1439–1445.

Gilchrist TL. Heterocyclic Chemistry, 2nd ed. Harlow, England: Longman Scientific & Technical. 1992;396pp.

Guse D, Bruzek MJ, DeVos P, Brown JH. Electrochemical reduction of atrazine: NMR evidence for reduction of the triazine ring. J Electroanal Chem 2009;626:171–173.

Gustafson DI. Groundwater ubiquity score: a simple method for assessing pesticide leachability. Environ Toxicol Chem 1989;8:339–357.

Hance RJ. Effect of pH on the degradation of atrazine, dichlorprop, linuron and propyzamide in soil. Pest Manag Sci 1979;10:83–86.

Hang S, Barriuso E, Houot S. Behavior of ^{14}C-atrazine in Argentinean topsoils under different cropping managements. J Environ Qual 2003;32:2216–2222.

Hayes TB, Collins A, Lee M, Mendoza M, Noriega N, Stuart AA, Vonk A. Hermaphroditic, demasculinized frogs after exposure to the herbicide atrazine at low ecologically relevant doses. Proc Natl Acad Sci USA 2002;99:5476–5480.

Hill EA. On a system of indexing chemical literature; adopted by the classification division of the U. S. patent office. J Am Chem Soc 1900;22:478–494.

Hiskia A, Ecke M, Troupis A, Kokorakis A, Hennig H, Papaconstantinou E. Sonolytic, photolytic, and photocatalytic decomposition of atrazine in the presence of Polyoxometalates. Environ Sci Technol 2001;35:2358–2364.

Hogrefe W, Grossenbacher H, Cook AM, Hütter R. Biological treatment specific for an industrial wastewater containing *s*-triazines. Biotechnol Bioeng 1985;27:1291–1296.

Hu D, Henderson K, Coats J. Fate of transformation products of synthetic chemicals. In: Boxall ABA, editor. Transformation Products of Synthetic Chemicals in the Environment. In: Hutzinger O, Barceló D, Kostianoy A, editors. The Handbook of Environmental Chemistry, vol. 2, Part P. Berlin, Germany: Springer-Verlag; 2009. pp. 103–120.

Huang PM, Hardie AG. Role of abiotic catalysis in the transformation of organics, metals,

metalloids, and other inorganics. In: Huang PM, editor. Handbook of Soil Science, 2nd ed. Boca Raton, FL, USA: CRC Press; 2011. pp. 18-1–18-40.

Issa S, Wood M. Degradation of atrazine and isoproturon in surface and sub-surface soil materials undergoing different moisture and aeration conditions. Pest Manag Sci 2005;61:126–132.

Jayachandran K, Steinheimer TR, Somasundaram L, Moorman TB, Kanwar RS, Coats JR. Occurrence of atrazine and degradates as contaminants of subsurface drainage and shallow groundwater. J Environ Qual 1994;23:311–319.

Jeannot R, Sabik H, Sauvard E, Genin E. Application of liquid chromatography with mass spectrometry combined with photodiode array detection and tandem mass spectrometry for monitoring pesticides in surface waters. J Chromatogr A 2000;879:51–71.

Jenks BM, Roeth FW, Martin AR, McCallister DL. Influence of surface and subsurface soil properties on atrazine sorption and degradation. Weed Sci 1998;46:132–138.

Jessee JA, Benoit RE, Hendricks AC, Allen GC, Neal JL. Anaerobic degradation of cyanuric acid, cysteine, and atrazine by a facultative anaerobic bacterium. Appl Environ Microbiol 1983;45:97–102.

Jin R, Ke J. Atrazine and its degradation products in surface and ground waters in Zhangjiakou District, China. Chin Sci Bull 2002;47:1612–1616.

Johnson RM, Sims JT. Sorption of atrazine and dicamba in Delaware coastal plain soils: a comparison of soil thin layer and batch equilibrium results. Pest Manag Sci 1998;54:91–98.

Jowa L, Howd R. Should atrazine and related chlorotriazines be considered carcinogenic for human health risk assessment? J Environ Sci Health, Part C: Environ Carcinog Ecotoxicol Rev 2011;29:91–144.

Jutzi K, Cook AM, Hütter R. The degradative pathway of the *s*-triazine melamine. Biochem J 1982;208:679–684.

Kaupp G. Mechanochemistry: the varied applications of mechanical bond-breaking. Cryst Eng Comm 2009;11:388–403.

Kells JJ, Rieck CE, Blevins RL, Muir WM. Atrazine dissipation as affected by surface pH and tillage. Weed Sci 1980;28:101–104.

Kersanté A, Martin-Laurent F, Soulas G, Binet F. Interactions of earthworms with atrazine-degrading bacteria in an agricultural soil. FEMS Microbiol Ecol 2006;57:192–205.

Khromonygina VV, Saltykova AI, Vasil'chenko LG, Kozlov YuP, Rabinovich ML. Degradation of the herbicide atrazine by the soil mycelial fungus INBI 2-26 (–), a producer of cellobiose dehydrogenase. Appl Biochem Micro 2004;40:285–290.

Kim SH, Fan M, Prasher SO, Patel RM, Hussain SA. Fate and transport of atrazine in a sandy soil in the presence of antibiotics in poultry manures. Agric Water Manage 2011;98:653–660.

Koivunen ME, Dettmer K, Vermeulen R, Bakke B, Gee SJ, Hammock BD. Improved methods for urinary atrazine mercapturate analysis—assessment of an enzyme-linked immunosorbent assay (ELISA) and a novel liquid chromatography–mass spectrometry (LC–MS) method utilizing online solid phase extraction (SPE). Anal Chim Acta 2006;572:180–189.

Kokotou MG, Thomaidis NS. Behavior and retention models of melamine and its hydrolysis products. Chromatographia 2012;75:457–467.

Kovačić N, Prosen H, Zupančič-Kralj L. Determination of triazines and atrazine metabolites in soil by microwave-assisted solvent extraction and high-pressure liquid chromatography with photo-diode-array detection. Acta Chim Slov 2004;51:395–407.

Kovaios ID, Paraskeva CA, Koutsoukos PG, Payatakes AC. Adsorption of atrazine on soils: model study. J Colloid Interface Sci 2006;299:88–94.

Krutz LJ, Burke IC, Reddy KN, Zablotowicz RM, Price AJ. Enhanced atrazine degradation: evidence for reduced residual weed control and a method for identifying adapted soils and predicting herbicide persistence. Weed Sci 2009;57:427–434.

Krutz LJ, Shaner DL, Weaver MA, Webb RMT, Zablotowicz RM, Reddy KN, Huang Y, Thomson SJ. Agronomic and environmental implications of enhanced *s*-triazine degradation. Pest Manag Sci 2010;66:461–481.

Kyle JH, Posner AM, Quirk JP. Kinetics of isotopic exchange of phosphate adsorbed on gibbsite. J Soil Sci 1975;26:32–43.

Laird DA. Interactions between atrazine and smectite surfaces. In: Meyer MT, Thurman EM, editors. Herbicide Metabolites in Surface Water and Groundwater. ACS Symposium Series, vol. 630. Washington, DC, USA: American Chemical Society; 1996. pp. 86–100.

Laird DA, Barriuso E, Dowdy RH, Koskinen WC. Adsorption of atrazine on smectites. Soil Sci Soc Am J 1992;56:62–67.

Laird DA, Koskinen WC. Triazine soil interactions. In: LeBaron HM, McFarland JE, Burnside OC, editors. The Triazine Herbicides: 50 years Revolutionizing Agriculture. San Diego, CA, USA: Elsevier; 2008. pp. 275–299.

Laird DA, Yen PY, Koskinen WC, Steinheimer TR, Dowdy RH. Sorption of atrazine on soil clay components. Environ Sci Technol 1994;28:1054–1061.

Lamoureux GL, Stafford LE, Shimabukuro RH, Zaylskie RG. Atrazine metabolism in sorghum: catabolism of the glutathione conjugate of atrazine. J Agric Food Chem 1973;21:1020–1030.

LeBaron HM, McFarland JE, Burnside OC. The triazine herbicides: a milestone in the development of weed control technology. In: LeBaron HM, McFarland JE, Burnside OC, editors. The Triazine Herbicides: 50 years Revolutionizing Agriculture. San Diego, CA, USA: Elsevier; 2008. pp. 1–12.

Leo PD, Pizzigallo MDR, Ancona V, Benedetto FD, Mesto E, Schingaro E, Ventruti G. Mechanochemical transformation of an organic ligand on mineral surfaces: the efficiency of birnessite in catechol degradation. J Hazard Mater 2012;201–202:148–154.

Lerch RN, Donald WW. Analysis of hydroxylated atrazine degradation products in water using solid-phase extraction and high-performance liquid chromatography. J Agric Food Chem 1994;42:922–927.

Lin CH, Lerch RN, Garrett HE, George MF. Bioremediation of atrazine-contaminated soil by forage grasses: transformation, uptake, and detoxification. J Environ Qual 2008;37:196–206.

Loague K, Green RE. Statistical and graphical methods for evaluating solute transport models: overview and application. J Contam Hydrol 1991;7:51–73.

Loos R, Locoro G, Comero S, Contini S, Schwesig D, Werres F, Balsaa P, Gans O, Weiss S, Blaha L, Bolchi M, Gawlik BM. Pan-European survey on the occurrence of selected polar organic persistent pollutants in ground water. Water Res 2010;44:4115–4126.

Lopano CL, Heaney PJ, Post JE, Hanson J, Komarneni S. Time-resolved structural analysis of K- and Ba-exchange reactions with synthetic Na-birnessite using synchrotron X-ray diffraction. Am Mineral 2007;92:380–387.

Lucas AD, Schneider P, Harrison RO, Seiber JN, Hammock BD, Biggar JW, Rolston DE. Determination of atrazine and simazine in water and soil using polyclonal and monoclonal antibodies in enzyme-linked immunosorbent assays. Food Agric Immunol 1991;3:155–167.

Ma M, Bong D. Determinants of cyanuric acid and melamine assembly in water. Langmuir 2011;27:8841–8853.

Ma J, Graham NJD. Degradation of atrazine by manganese-catalysed ozonation: influence of humic substances. Wat Res 1999;33:785–193.

Ma J, Graham NJD. Degradation of atrazine by manganese-catalysed ozonation—influence of radical scavengers. Wat Res 2000;34:3822–3828.

Ma L, Southwick LM, Willis GH, Selim HM. Hysteretic characteristics of atrazine adsorption-desorption by a Sharkey soil. Weed Sci 1993;41:627–633.

Marco-Urrea E, Reddy CA. Degradation of chloro-organic pollutants by white rot fungi. In: Singh SN, editor. Microbial Degradation of Xenobiotics: Environmental Science and Engineering. Berlin, Germany: Springer-Verlag; 2012. pp. 31–66.

Matocha CJ, Sparks DL, Amonette JE, Kukkadapu RK. Kinetics and mechanism of birnessite reduction by catechol. Soil Sci Soc Am J 2001;65:58–66.

McBride MB. Environmental chemistry of soils. New York, NY, USA: Oxford University Press. 1994;416pp.

McCalley DV. Analysis of the *Cinchona* alkaloids by high-performance liquid chromatography

and other separation techniques. J Chromatogr A 2002;967:1–19.

McKenzie RM. The synthesis of birnessite, cryptomelane, and some other oxides and hydroxides of manganese. Mineral Mag 1971;38:493–502.

McKenzie RM. Manganese oxides and hydroxides. In: Dixon JB, Weed SB, editors. Minerals in Soil Environments, 2nd ed. Soil Science Society of America (SSSA) Book Series, no. 1. Madison, WI, USA: Soil Science Society of America; 1989. pp. 439–465.

McMaster MC. LC/MS: A Practical User's Guide. Hoboken, NJ, USA: John Wiley & Sons. 2005;184pp.

McMurray TA, Dunlop PSM, Byrne JA. The photocatalytic degradation of atrazine on nanoparticulate TiO_2 films. J Photochem Photobiol A 2006;182:43–51.

Menne H, Köcher H. HRAC classification of herbicides and resistance development. In: Jeschke P, Witschel M, Krämer W, Schirmer U, editors. Modern Crop Protection Compounds, 2nd ed., vol. 1. Weinheim, Germany: Wiley-VCH; 2007. pp. 5–28.

Mougin C, Laugero C, Asther M, Dubroca J, Frasse P, Asther M. Biotransformation of the herbicide atrazine by the white rot fungus *Phanerochaete chrysosporium*. Appl Environ Microbiol 1994;60:705–708.

Mudhoo A, Garg VK. Sorption, transport and transformation of atrazine in soils, minerals and composts: a review. Pedosphere 2011;21:11–25.

Mueller TC, Steckel LE, Radosevich M. Effect of soil pH and previous atrazine use history on atrazine degradation in a Tennessee field soil. Weed Sci 2010;58:478–483.

Mullet JE, Arntzen CJ. Identification of a 32–34-kilodalton polypeptide as a herbicide receptor protein in Photosystem II. Biochim Biophys Acta 1981;635:236–248.

Nash RG. Solid-phase extraction of carbofuran, atrazine, simazine, alachlor, and cyanazine from shallow well water. J Assoc Off Anal Chem 1990;73:438–442.

Ngigi A, Dörfler U, Scherb H, Getenga Z, Boga H, Schroll R. Effect of fluctuating soil humidity on *in situ* bioavailability and degradation of atrazine. Chemosphere 2011;84:369–375.

Oliveira RS, Koskinen WC, Ferreira FA. Sorption and leaching potential of herbicides on

Brazilian soils. Weed Res 2001;41: 97–110.

Ongley ED, Krishnappan BG, Droppo G, Rao SS, Maguire RJ. Cohesive sediment transport: emerging issues for toxic chemical management. Hydrobiologia 1992;235–236:177–187.

Pacáková V, Štulík K, Jiskra J. High-performance separations in the determination of triazine herbicides and their residues. J Chromatogr A 1996;754:17–31.

Panshin SY, Carter DS, Bayless ER. Analysis of atrazine and four degradation products in the pore water of the vadose zone, central Indiana. Environ Sci Technol 2000;34:2131–2137.

Panuwet P, Nguyen JV, Kuklenyik P, Udunka SO, Needham LL, Barr DB. Quantification of atrazine and its metabolites in urine by on-line solid-phase extraction–high-performance liquid chromatography–tandem mass spectrometry. Anal Bioanal Chem 2008;391:1931–1939.

Panuwet P, Restrepo PA, Magsumbol M, Jung KY, Montesano MA. An improved high-performance liquid chromatography–tandem mass spectrometric method to measure atrazine and its metabolites in human urine. J Chromatogr B 2010;878:957–962.

Pastoor T. Atrazine is safe. Environ Sci Technol 2007;41:6C.

Pichon V, Chen L, Guenu S, Hennion M-C. Comparison of sorbents for the solid-phase extraction of the highly polar degradation products of atrazine (including ammeline, ammelide and cyanuric acid). J Chromatogr A 1995;711:257–267.

Picó Y, Rodríguez R, Mañes J. Capillary electrophoresis for the determination of pesticide residues. Trend Anal Chem 2003;22:133–151.

Pospíšil L, Trsková R, Fuoco R, Colombini MP. Electrochemistry of *s*-triazine herbicides: reduction of atrazine and terbutylazine in aqueous solutions. J Electroanal Chem 1995;395:189–193.

Pozzebon JM, Vilegas W, Jardim ICSF. Determination of herbicides and a metabolite in human urine by liquid chromatography–electrospray ionization mass spectrometry. J Chromatogr A 2003;987:375–380.

Radosevich M, Traina SJ, Hao Y-L, Tuovinen OH. Degradation and mineralization of atrazine by

a soil bacterial isolate. Appl Environ Microbiol 1995;61:297–302.

Radosevich M, Traina SJ, Tuovinen OH. Biodegradation of atrazine in surface soils and subsurface sediments collected from an agricultural research farm. Biodegradation 1996;7:137–149.

Ralebitso-Senior TK, Senior E, van Verseveld HW. Microbial aspects of atrazine degradation in natural environments. Biodegradation 2002;13:11–19.

Raveton M, Ravanel P, Serre AM, Nurit F, Tissut M. Kinetics of uptake and metabolism of atrazine in model plant systems. Pestic Sci 1997;49:157−163.

Roeth FW, Lavy TL, Burnside OC. Atrazine degradation in two soil profiles. Weed Sci 1969;17:202–205.

Ross DS, Hales HC, Shea-McCarthy GC, Lanzirotti A. Sensitivity of soil manganese oxides. Soil Sci Soc Am J 2001;65:736–743.

Ross G. Atrazine ban premature. Environ Sci Technol 2007;41:6C.

Rusiecki JA, De Roos A, Lee WJ, Dosemeci M, Lubin JH, Hoppin JA, Blair A, Alavanja MCR. Cancer incidence among pesticide applicators exposed to atrazine in the Agricultural Health Study. J Natl Cancer Inst 2004;96:1375–1382.

Russell JD, Cruz M, White JL, Bailey GW, Payne WR, Pope JD, Teasley JI. Mode of chemical-degradation of *s*-triazines by montmorillonite. Science 1968;160:1340–1342.

Rustum AM, Ash S, Saxena A, Balu K. Reversed-phase high-performance liquid chromatographic method for the determination of soil-bound [^{14}C]atrazine and its radiolabeled metabolites in a soil metabolism study. J Chromatogr 1990;514:209–218.

Sanchez-Camazano M, Sanchez-Martin MJ, Rodriguez-Cruz MS. Sodium dodecyl sulphate-enhanced desorption of atrazine: effect of surfactant concentration and of organic matter content of soils. Chemosphere 2000;41:1301–1305.

Satapanajaru T, Anurakpongsatorn P, Pengthamkeerati P, Boparai H. Remediation of atrazine-contaminated soil and water by nano zerovalent iron. Water Air Soil Pollut 2008;192:349–359.

Sawhney BL, Singh SS. Sorption of atrazine by Al- and Ca-saturated smectite. Clays Clay Miner 1997;45:333–338.

Schwertmann U, Cornell RM. Iron Oxides in the Laboratory: Preparation and Characterization. 2nd edition. Weinheim, Germany: Wiley VCH. 2000;706pp.

Sene L, Converti A, Secchi GAR, Simão RdeCG. New aspects on atrazine biodegradation. Braz Arch Biol Technol 2010;53: 487–496.

Shaner DL, Henry WB, Krutz LJ, Hanson B. Rapid assay for detecting enhanced atrazine degradation in soil. Weed Sci 2007;55:528–535.

Shaner D, Stromberger M, Khosla R, Helm A, Bosley B, Hansen N. Spatial distribution of enhanced atrazine degradation across northeastern Colorado cropping systems. J Environ Qual 2011;40:46–56.

Shelton DR, Sadeghi AM, Karns JS, Hapeman CJ. Effect of wetting and drying of soil on sorption and biodegradation of atrazine. Weed Sci 1995;43:298–305.

Shimabukuro RH. Atrazine metabolism in resistant corn and sorghum. Plant Physiol 1968;43:1925–1930.

Shimabukuro RH, Swanson HR, Walsh WC. Glutathione conjugation. Atrazine detoxication mechanism in corn. Plant Physiol 1970;46:103–107.

Shimabukuro RH, Frear DS, Swanson HR, Walsh WC. Glutathione conjugation. An enzymatic basis for atrazine resistance in corn. Plant Physiol 1971;47:10–14.

Shimabukuro RH, Walsh WC, Lamoureux GL, Stafford LE. Atrazine metabolism in sorghum: chloroform-soluble intermediates in the N-dealkylation and glutathione conjugation pathways. J Agric Food Chem 1973;21:1031–1036.

Shin H-S, Lim D-M, Lee D-H, Kang K-H. Reaction kinetics and transformation products of 1-naphthol by Mn oxide-mediated oxidative-coupling reaction. J Hazard Mater 2009;165:540–547.

Shin JY, Buzgo CM, Cheney MA. Mechanochemical degradation of atrazine adsorbed on four synthetic manganese oxides. Colloids Surf A 2000;172:113–123.

Shin JY, Cheney MA. Abiotic transformation of atrazine in aqueous suspension of four synthetic manganese oxides. Colloids Surf A 2004;242:85–92.

Shin JY, Cheney MA. Abiotic dealkylation and hydrolysis of atrazine by birnessite. Environ Toxicol Chem 2005;24:1353–1360.

Sims GK, Cupples AM. Factors controlling degradation of pesticides in soil. Pestic Sci 1999;55:598–601.

Singh J, Shea PJ, Hundal LS, Comfort SD, Zhang TC, Hage DS. Iron-enhanced remediation of water and soil containing atrazine. Weed Sci 1998;46:381–388.

Solomon KR, Baker DB, Richards RP, Dixon KR, Klaine SJ, La Point TW, Kendall RJ, Weisskopf CP, Giddings JM, Giesy JP, Hall LW, Williams WM. Ecological risk assessment of atrazine in North American surface waters. Environ Toxicol Chem 1996;15:31–76.

Sorenson BA, Wyse DL, Koskinen WC, Buhler DD, Lueschen WE, Jorgenson MD. Formation and movement of ^{14}C-atrazine degradation products in a sandy loam soil under field conditions. Weed Sci 1993;41:239–245.

Sposito G, Martin-Neto L, Yang A. Atrazine complexation by soil humic acids. J Environ Qual 1996;25:1203–1209.

Sprague LA, Herman JS, Hornberger GM, Mills AL. Atrazine adsorption and colloid-facilitated transport through the unsaturated zone. J Environ Qual 2000;29:1632–1641.

Stearman GK. Enzyme immunoassay determination of atrazine degradation in soil: moisture, sterilization, and storage effects. J Soil Contam 1993;2:331–342.

Steinheimer TR. HPLC determination of atrazine and principle degradates in agricultural soils and associated surface and ground water. J Agric Food Chem 1993;41:588–595.

Stewart BW. Priorities for cancer prevention: lifestyle choices versus unavoidable exposures. Lancet Oncol 2012;13:e126–e133.

Stipičević S, Fingler S, Zupančič-Kralj L, Drevenkar V. Comparison of gas and high performance liquid chromatography with selective detection for determination of triazine

herbicides and their degradation products extracted ultrasonically from soil. J Sep Sci 2003;26:1237–1246.

Stone AT. Reductive dissolution of manganese(III/IV) oxides by substituted phenols. Environ Sci Technol 1987;21:979–988.

Stone AT, Morgan JJ. Reduction and dissolution of manganese(III) and manganese(IV) oxides by organics. 1. Reaction with hydroquinone. Environ Sci Technol 1984a;18:450–456.

Stone AT, Morgan JJ. Reduction and dissolution of manganese(III) and manganese(IV) oxides by organics: 2. Survey of the reactivity of organics. Environ Sci Technol 1984b;18:617–624.

Stutz H, Pittertschatscher K, Malissa H. Capillary zone electrophoretic determination of hydroxymetabolites of atrazine in potable water using solid-phase extraction with Amberchrom resins. Mikrochim Acta 1998;128:107–117.

Suzawa M, Ingraham HA. The herbicide atrazine activates endocrine gene networks via non-steroidal NR5A nuclear receptors in fish and mammalian cells. PLoS ONE 2008;3:1–11.

Swanton CJ, Gulden RH, Chandler K. A rationale for atrazine stewardship in corn. Weed Sci 2007;55:75–81.

Tao QH, Wang DS, Tang HX. Effect of surfactants at low concentrations on the sorption of atrazine by natural sediment. Water Environ Res 2006;78:653–660.

Tauber A, von Sonntag C. Products and kinetics of the OH-radical-induced dealkylation of atrazine. Acta Hydrochim Hydrobiol 2000;28:15–23.

Tong SP, Wang Z, Ma CA. Study on the mechanism of ozonation of organic combination with UV radiation [article in Chinese]. Huan Jing Ke Xue 2007;28:342–345.

Topp E, Gutzman DW, Millette J, Gamble DS, Bourgoin B. Rapid mineralization of the herbicide atrazine in alluvial sediments and enrichment cultures. Environ Toxicol Chem 1995;14:743–747.

Ulrich H-J, Stone AT. Oxidation of chlorophenols adsorbed to manganese oxide surfaces. Environ Sci Technol 1989;23:421–428.

USEPA. National Primary Drinking Water Regulations. Washington, DC, USA: United States

Environmental Protection Agency 2009; Available: http://water.epa.gov/drink/contaminants/upload/mcl-2.pdf [Accessed 19 April 2013].

Vermeulen NMJ, Apostolides Z, Potgieter DJJ, Nel PC, Smit NSH. Separation of atrazine and some of its degradation products by high-performance liquid chromatography. J Chromatogr 1982;240:247–253.

Waggoner JK, Kullman GJ, Henneberger PK, Umbach DM, Blair A, Alavanja MC, Kamel F, Lynch CF, Knott C, London SJ, Hines CJ, Thomas KW, Sandler DP, Lubin JH, Beane Freeman LE, Hoppin JA. Mortality in the agricultural health study, 1993-2007. Am J Epidemiol 2011;173:71–83.

Wang D, Shin JY, Cheney MA, Sposito G, Spiro TG. Manganese dioxide as a catalyst for oxygen independent atrazine dealkylation. Environ Sci Technol 1999;33:3160–3165.

Waria M, Comfort SD, Onanong S, Satapanajaru T, Boparai H, Harris C, Snow DD, Cassada DA. Field-scale cleanup of atrazine and cyanazine contaminated soil with a combined chemical-biological approach. J Environ Qual 2009;38:1803–1811.

Webb RMT, Wieczorek ME, Nolan BT, Hancock TC, Sandstrom MW, Barbash JE, Bayless ER, Healy RW, Linard J. Variations in pesticide leaching related to land use, pesticide properties, and unsaturated zone thickness. J Environ Qual 2008;37:1145–1157.

Weed Science Society of America. Herbicide Handbook, 7th ed. Champaign, IL, USA: Weed Science Society of America. 1994;352pp.

Weichenthal S, Moase C, Chan P. A review of pesticide exposure and cancer incidence in the Agricultural Health Study cohort. Environ Health Perspect 2010;118:1117–1125.

Welhouse GJ, Bleam WF. Atrazine hydrogen-bonding potentials. Environ Sci Technol 1993a;27:494–500.

Welhouse GJ, Bleam WF. Cooperative hydrogen bonding of atrazine. Environ Sci Technol 1993b;27:500–505.

White JL. Determination of susceptibility of *s*-triazine herbicides to protonation and hydrolysis by mineral surfaces. Arch Environ Con Tox 1975/1976;3:461–469.

Whittig LD, Allardice WR. X-ray diffraction techniques. In: Klute A, editor. Methods of Soil Analysis, Part 1. Physical and Mineralogical Methods. 2nd edition, number 9. Madison, WI, USA: American Society of Agronomy, Soil Science Society of America; 1986. pp. 331–362.

WHO. Guidelines for Drinking-water Quality, 4th ed. Geneva, Switzerland: World Health Organization 2011; Available: http://whqlibdoc.who.int/publications/2011/9789241548151_eng.pdf [Accessed 19 April 2013].

Xiong G, Tang B, He X, Zhao M, Zhang Z, Zhang Z. Comparison of microwave-assisted extraction of triazines from soils using water and organic solvents as the extractants. Talanta 1999;48:333–339.

Yanze-Kontchou C, Gschwind N. Mineralization of the herbicide atrazine as a carbon source by a *Pseudomonas* strain. Appl Environ Microbiol 1994;60:4297–4302.

Yassir A, Lagacherie B, Houot S, Soulas G. Microbial aspects of atrazine biodegradation in relation to history of soil treatment. Pest Manag Sci 1999;55:799–809.

Zhang H, Huang C-H. Oxidative transformation of triclosan and chlorophene by manganese oxides. Environ Sci Technol 2003;37:2421–2430.

Zhang H, Huang C-H. Oxidative transformation of fluoroquinolone antibacterial agents and structurally related amines by manganese oxide. Environ Sci Technol 2005;39:4474–4483.

Zhang Y, Li Y, Zheng X. Removal of atrazine by nanoscale zero valent iron supported on organobentonite. Sci Total Environ 2011;409:625–630.

Zhang Y, Ning Z, Zhao J, Xinran P, Shuyan M, Miao H. Isolation of two atrazine-degrading strains and their degradation characteristics. Int J Agric Biol Eng 2009;2:27–32.

Zhou Q, Pang L, Xie G, Xiao J, Bai H. Determination of atrazine and simazine in environmental water samples by dispersive liquid-liquid microextraction with high performance liquid chromatography. Anal Sci 2009;25:73–76.

Addendum A

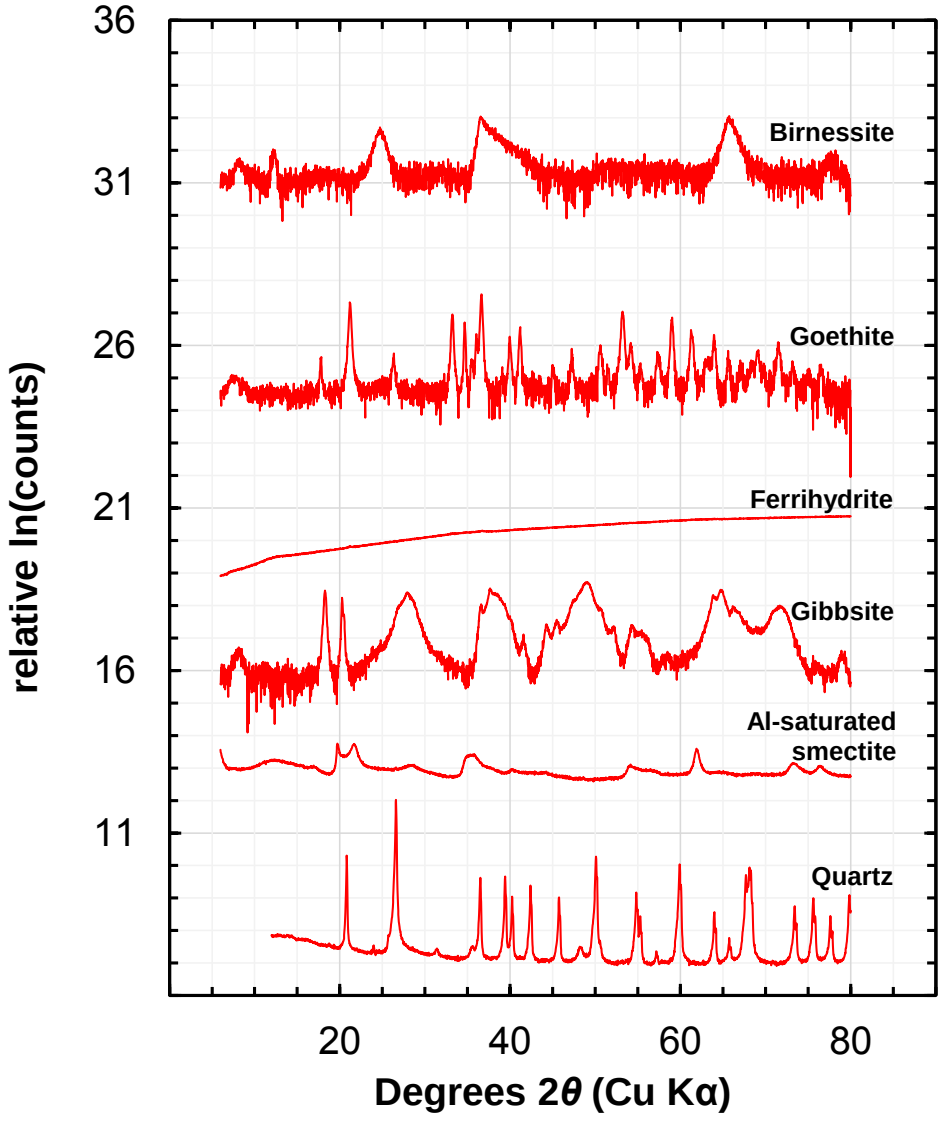

Figure A1 Powder X-ray diffractograms for the mineral phases used in this study.

Chromatograms from the mineral series drying experiments

- Birnessite-atrazine drying experiment (TD-br)

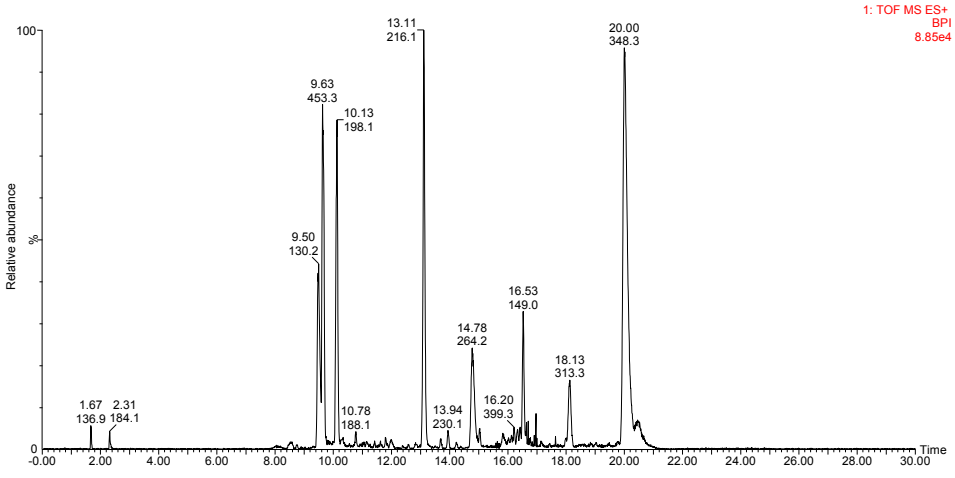

- Goethite-atrazine drying experiment (TD-gt)

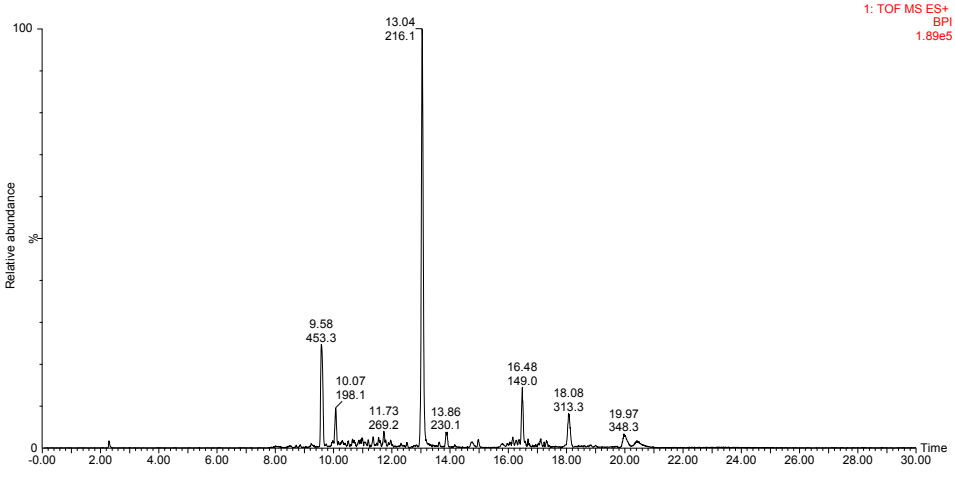

- Ferrihydrite-atrazine drying experiment (TD-fh)

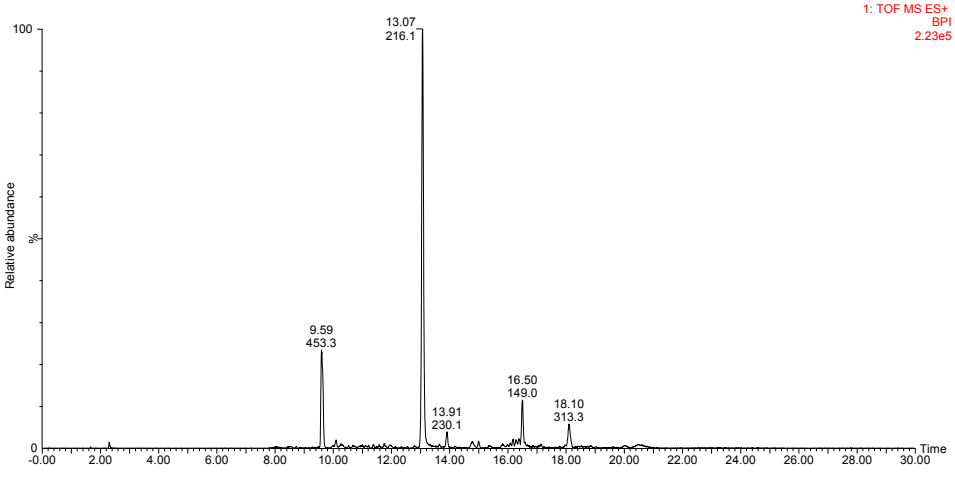

- Gibbsite-atrazine drying experiment (TD-gb)

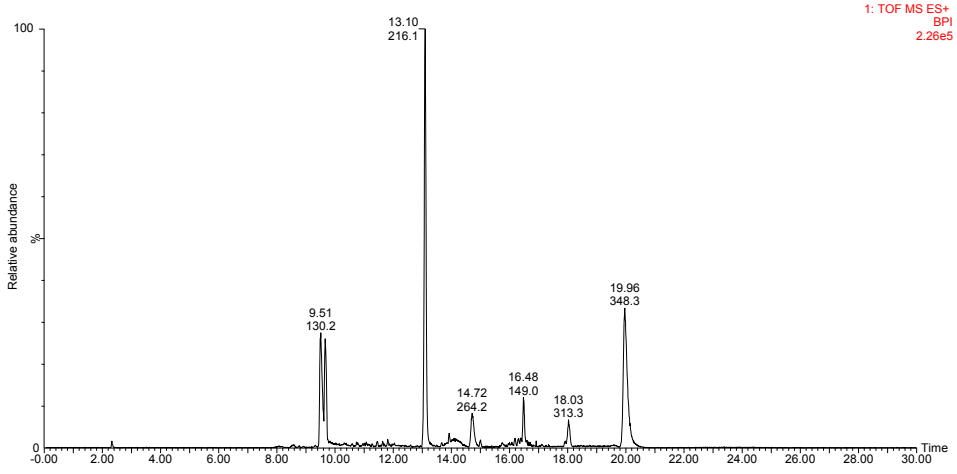

- Al-saturated smectite-atrazine drying experiment (TD-sm)

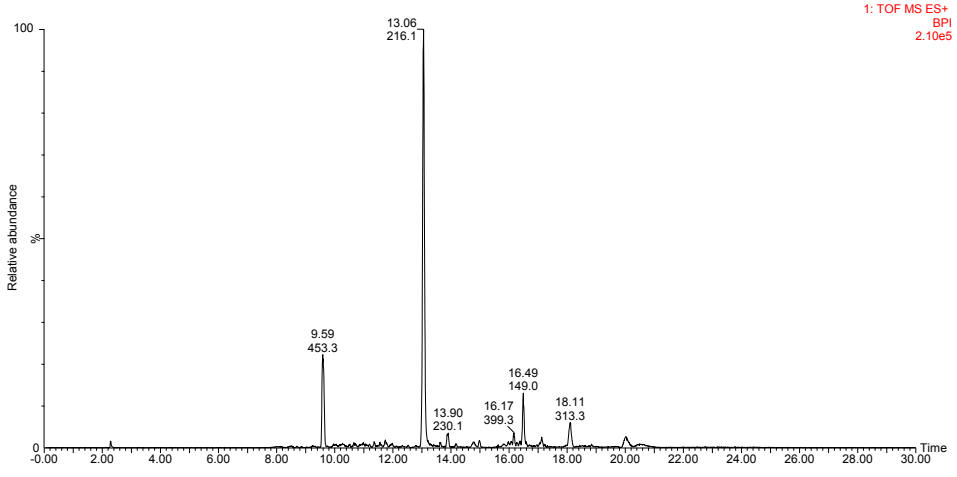

- Quartz-atrazine drying experiment (TD-qz)

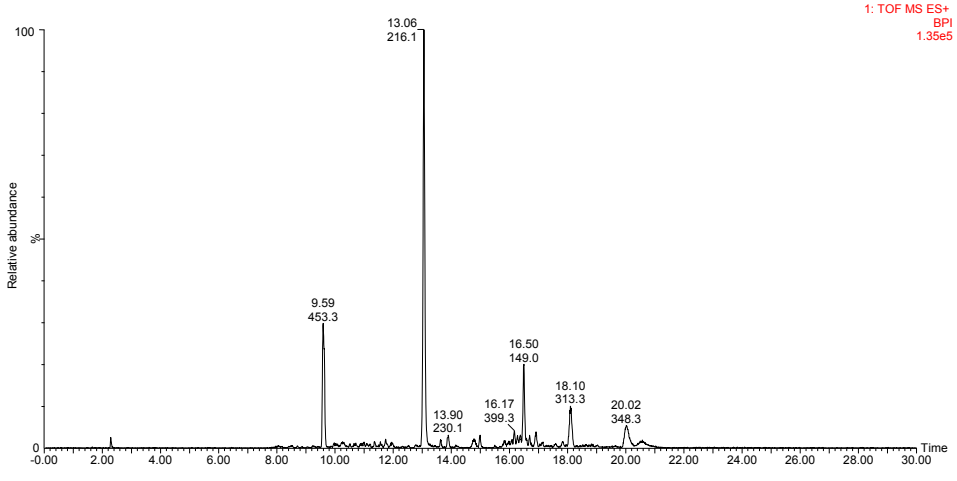

- Non-mineral atrazine control drying experiment (CD)

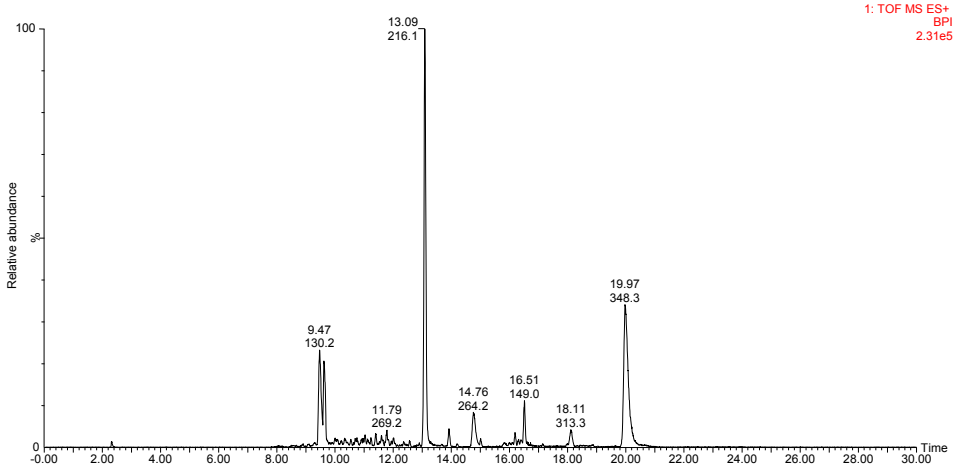

Chromatograms from the mineral series moist experiments

- Birnessite-atrazine moist experiment (TH-br)

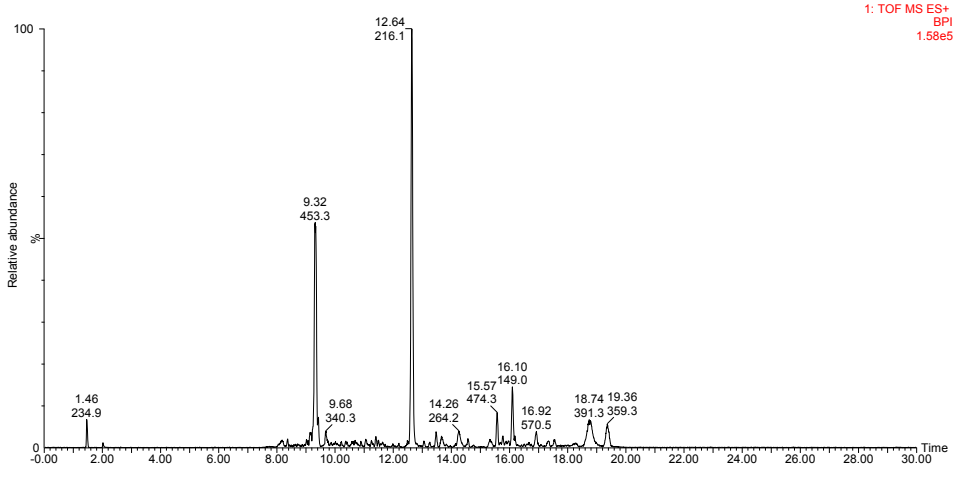

- Goethite-atrazine moist experiment (TH-gt)

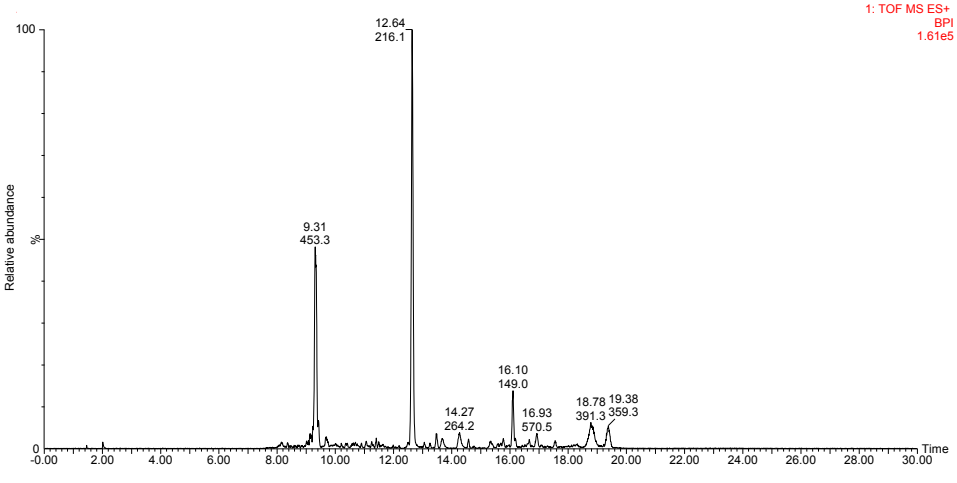

- Ferrihydrite-atrazine moist experiment (TH-fh)

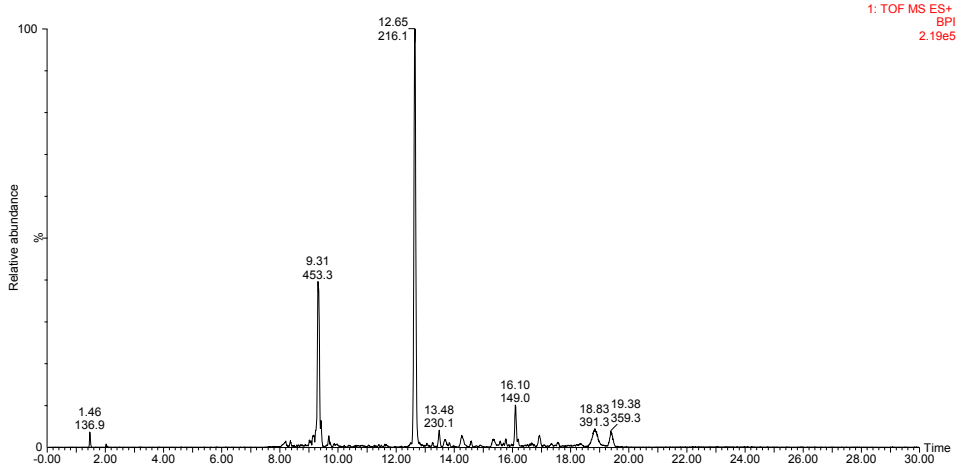

- Gibbsite-atrazine moist experiment (TH-gb)

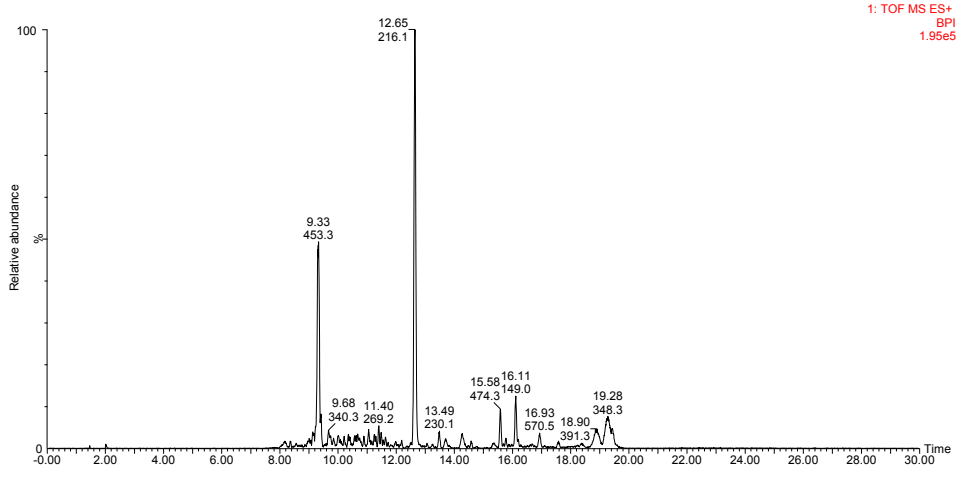

- Al-saturated smectite moist experiment (TH-sm)

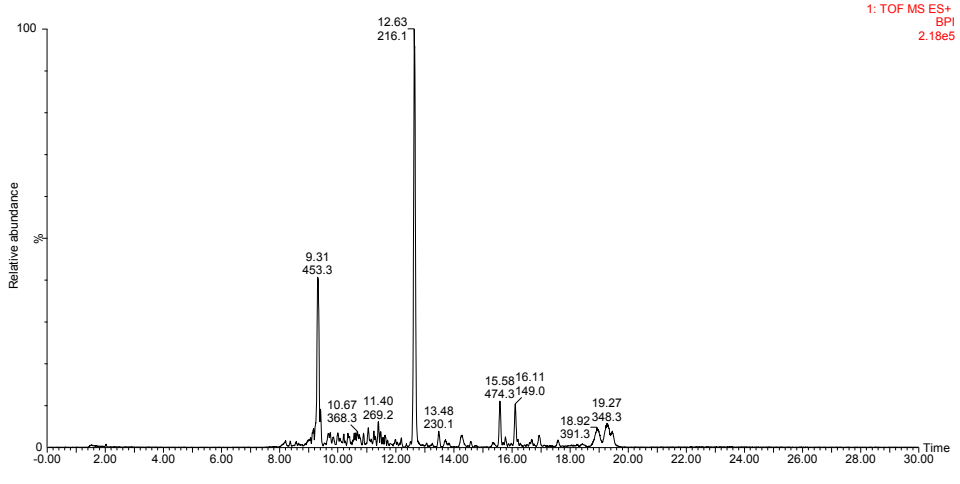

- Quartz-atrazine moist experiment (TH-qz)

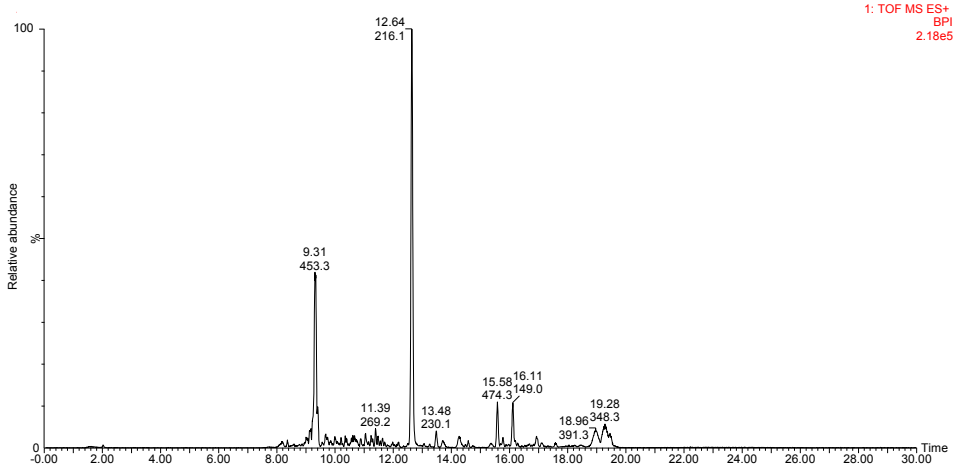

- Non-mineral atrazine control moist experiment (CH)

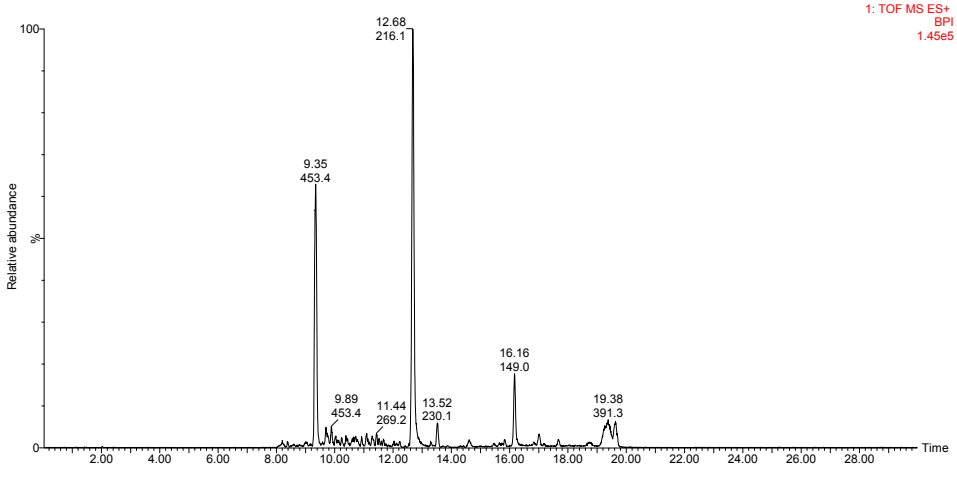

Chromatograms from the mineral series blank experiments

- Birnessite blank (B-br)

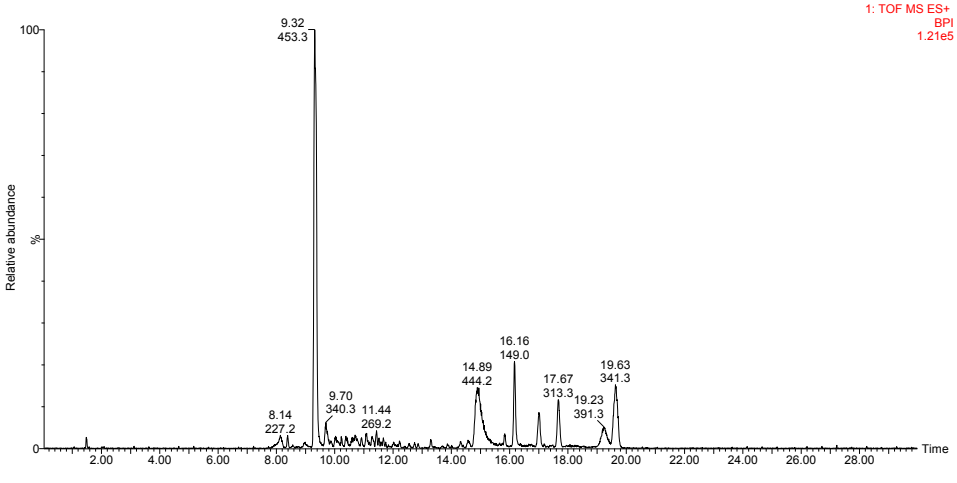

- Goethite blank (B-gt)

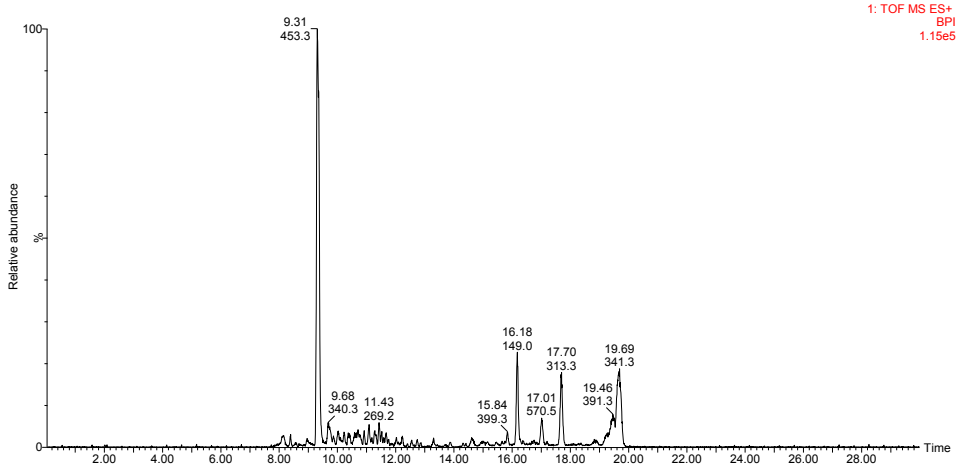

- Ferrihydrite blank (B-fh)

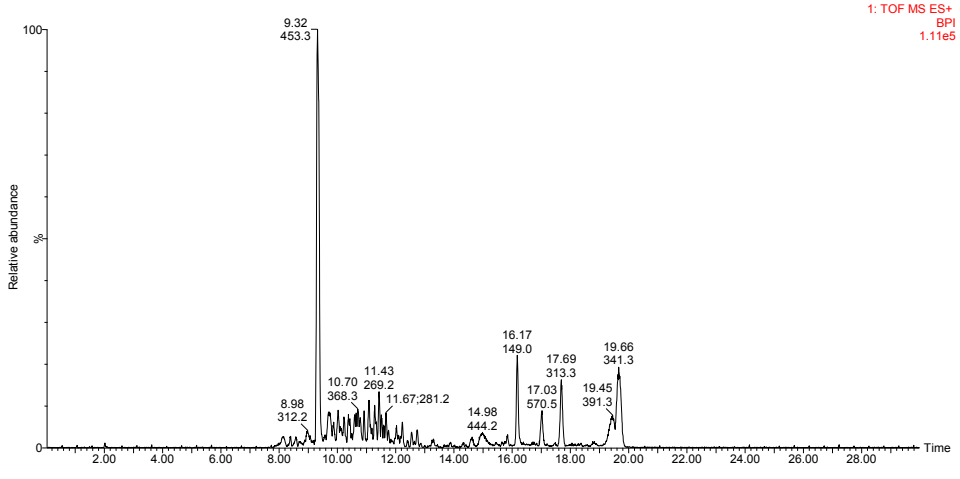

- Gibbsite blank (B-gb)

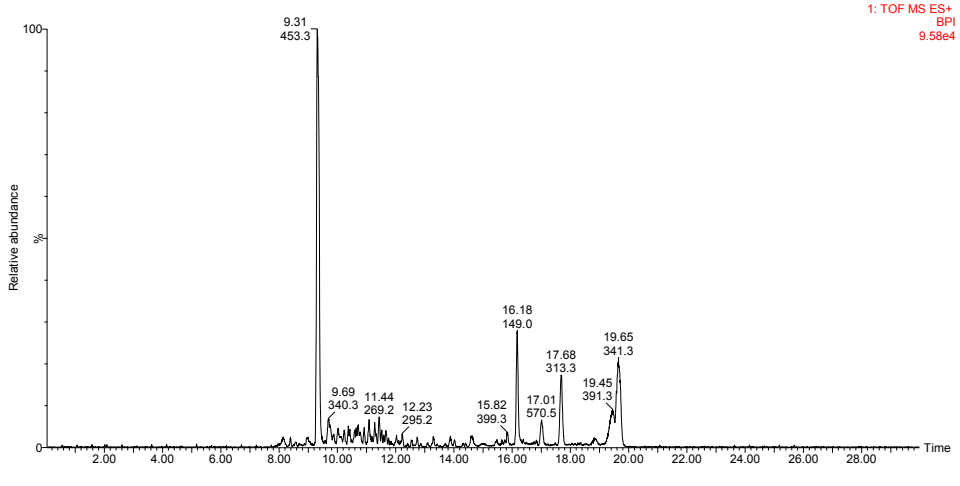

- Al-saturated smectite blank (B-sm)

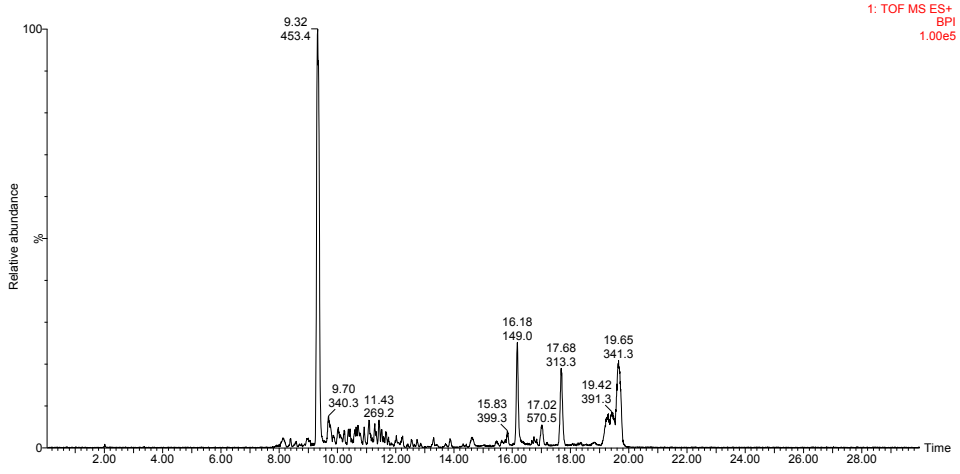

- Quartz blank (B-qz)

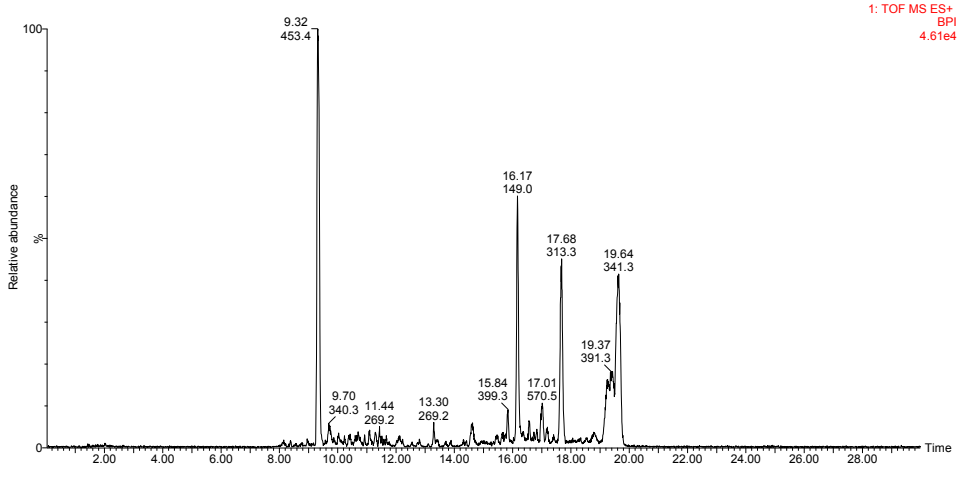

- Non-mineral control blank (CB)

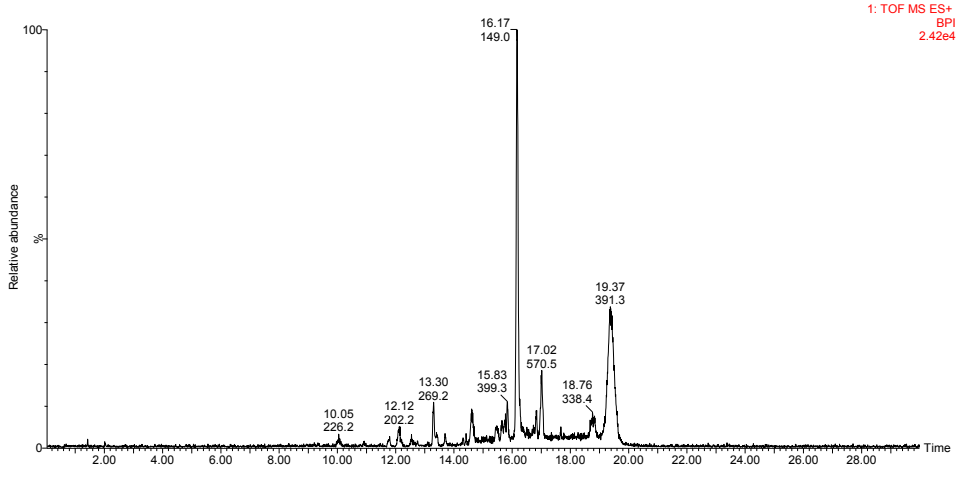

Table A1 Calibration of the LC/MS system for atrazine and its two metabolites, hydroxyatrazine and deethylatrazine.

Calibration parameter	Standard (mg/L)	Retention time peak area		
		10.08 (ATZ-OH)	10.73 (DEA)	13.06 (ATZ)
-	25	11572	3316	21452
-	10	6406	1576	10840
-	1	836	252	1774
-	0.1	68	36	232
-	0.01	-	-	11
Linear coefficient, a*	-	Set to zero	Set to zero	Set to zero
Angular coefficient, b*	-	487.88	136.25	890.48
Correlation coefficient, r^2*	-	0.967	0.990	0.985

*For the linear regression, y = a + bx, where y = peak area and x = concentration of the standard in mg/L

Table A2 Data from the mineral series experiments.

Sample	ATZ-OH (umol)	DEA (umol)	ATZ (umol)	Sum (ATZ-OH + DEA + ATZ) (umol)
TD-br	0.281	0.049	0.169	0.499
TD-gt	0.065	0.009	0.384	0.458
TD-fh	0.017	b.d.l	0.457	0.474
TD-gb	0.007	b.d.l	0.451	0.458
TD-sm	0.005	b.d.l	0.427	0.432
TD-qz	0.004	b.d.l	0.253	0.257
CD	b.d.l	b.d.l	0.467	0.467
TH-br	b.d.l	b.d.l	0.304	0.304
TH-gt	b.d.l	b.d.l	0.304	0.304
TH-fh	b.d.l	b.d.l	0.441	0.441
TH-gb	b.d.l	b.d.l	0.386	0.386
TH-sm	b.d.l	b.d.l	0.430	0.430
TH-qz	b.d.l	b.d.l	0.426	0.426
CH	b.d.l	b.d.l	0.448	0.448

b.d.l = below detection (and quantification) limit

Table A3 Calibration of the HPLC system for the short-term time series experiments.

Calibration parameter	Standard (mg/L)	Retention time peak area		
		10.08 (ATZ-OH)	10.73 (DEA)	13.06 (ATZ)
-	25	3282359	4946151	7353821
-	10	1257553	1920549	2892054
-	5	557137	871962	1336756
-	1	93617	175925	275500
-	0.1	3919	18260	32393
-	0.01	b.d.l	b.d.l	8320

linear coefficient, a*	_	Set to zero	Set to zero	Set to zero
angular coefficient, b*	-	129844	196265	292578
correlation coefficient, r^2*	-	0.998	0.999	1.000

*For the linear regression, y = a + bx, where y = retention time peak area and x = concentration (mg/L) , b.d.l = below detection limit

Table A4 Data from the short-term time series experiments.

Sample	Time (d)	Moisture content (g)*	ATZ-OH (umol)	DEA (umol)	ATZ (umol)	SUM (ATZ-OH + DEA + ATZ) (umol)
Birnessite drying						
TD-br-1	1	0.785	0.006	b.d.l	0.380	0.385
TD-br-2	2	0.606	0.019	b.d.l	0.417	0.436
TD-br-3	3	0.479	0.015	b.d.l	0.407	0.422
TD-br-4	4	0.334	0.005	b.d.l	0.402	0.407
TD-br-5	5	0.088	0.016	b.d.l	0.413	0.429
TD-br-6	6	0.026	0.055	0.007	0.411	0.473
TD-br-7	7	0.019	0.125	0.018	0.354	0.497
TD-br-8	8	0.012	0.088	0.013	0.379	0.479
TD-br-9	9	0.008	0.136	0.021	0.342	0.498
TD-br-10	10	0.014	0.195	0.030	0.273	0.497
Birnessite moist						
TH-br-2	2	0.977	0.012	b.d.l	0.373	0.386
TH-br-4	4	0.978	0.011	b.d.l	0.314	0.325
TH-br-6	6	0.980	0.028	b.d.l	0.377	0.405
TH-br-8	8	0.968	0.026	b.d.l	0.362	0.387
TH-br-10	10	0.993	0.017	b.d.l	0.353	0.371
Quartz drying						
TD-qz-1	1	0.823	0.003	b.d.l	0.355	0.358
TD-qz-2	2	0.653	0.003	b.d.l	0.402	0.405
TD-qz-3	3	0.544	0.012	b.d.l	0.418	0.430
TD-qz-4	4	0.408	0.003	b.d.l	0.389	0.392
TD-qz-5	5	0.187	0.004	b.d.l	0.429	0.433
TD-qz-6	6	0.071	0.007	b.d.l	0.452	0.459
TD-qz-7	7	0.033	0.012	b.d.l	0.438	0.450
TD-qz-8	8	0.010	0.011	b.d.l	0.447	0.458
TD-qz-9	9	0.009	0.011	b.d.l	0.436	0.447
TD-qz-10	10	0.049	0.011	b.d.l	0.427	0.438
Quartz moist						
TH-qz-2	2	0.990	0.002	b.d.l	0.371	0.373
TH-qz-4	4	0.989	0.004	b.d.l	0.317	0.320
TH-qz-6	6	0.989	0.013	b.d.l	0.399	0.413
TH-qz-8	8	0.996	0.012	b.d.l	0.345	0.358
TH-qz-10	10	1.000	0.012	b.d.l	0.362	0.374
Non-mineral control drying						

CD-2	2	0.612	b.d.l	b.d.l	0.399	0.399
CD-4	4	0.389	b.d.l	b.d.l	0.401	0.401
CD-6	6	0.105	0.012	b.d.l	0.442	0.454
CD-8	8	0.007	0.010	b.d.l	0.436	0.446
CD-10	10	0.039	0.010	b.d.l	0.485	0.495

*Moisture content is the mass of the vial and its contents at sampling time subtracted from the initial mass of the vial at the start of the experiment, b.d.l = below detection limit

Table A5 Calibration results for sessions 1, 2 and 3 (LC/MS calibration repeated here as session 3 for convenience).

Parameter	ATZ-OH	DEA	ATZ
Calibration 1			
Linear coefficient, a*	Set to zero	Set to zero	Set to zero
Angular coefficient, b*	101005	50992	77590
Correlation coefficient, r^2*	1.000	1.000	0.999
Calibration 2			
Linear coefficient, a*	Set to zero	Set to zero	Set to zero
Angular coefficient, b*	136092	60924	86393
Correlation coefficient, r^2*	1.000	0.999	0.999
Calibration 3 - LC/MS from table A1			
Linear coefficient, a*	Set to zero	Set to zero	Set to zero
Angular coefficient, b*	487.88	136.25	890.48
Correlation coefficient, r^2*	0.967	0.990	0.985

*For the linear regression, y = a + bx, where y = peak area and x = concentration (mg/L)

Table A6 Results of the long-term, nitrogen-dried and air-dried experiments.

Sample Pair	Cal*	Time (d)	Mean				Moist. dev. (g)	ATZ-OH dev. (umol)	DEA dev. (umol)	ATZ dev. (umol)	SUM (ATZ-OH + DEA + ATZ) (umol)
			Moisture content (g)	ATZ-OH (umol)	DEA (umol)	ATZ (umol)					
Birnessite drying											
TD-br-0A, B	1	0	0.923	0.034	-0.002	0.478	0.001	0.000	0.000	0.003	0.512
TD-br-5A, B	1	5	0.345	0.025	-0.001	0.465	0.033	0.001	0.000	0.000	0.490
TD-br-7A, B	1	7	0.105	0.029	-0.001	0.480	0.015	0.004	0.001	0.003	0.509
TD-br-9A, B	1	9	0.020	0.073	0.007	0.445	0.004	0.011	0.003	0.009	0.525
TD-br-11A, B	1	11	0.020	0.135	0.017	0.398	0.002	0.009	0.002	0.003	0.549
TD-br-13A, B	1	13	0.050	0.181	0.023	0.343	0.003	0.005	0.000	0.000	0.547
TD-br-16A, B	1	16	0.011	0.253	0.038	0.304	0.003	0.010	0.001	0.007	0.596
TD-br-20A, B	1	20	0.039	0.335	0.047	0.202	0.005	0.003	0.001	0.003	0.584
TD-br-25A, B	1	25	0.013	0.426	0.063	0.121	0.001	0.003	0.001	0.002	0.610
TD-br-30A, B	1	30	0.003	0.402	0.068	0.055	0.003	0.001	0.001	0.003	0.525
Quartz drying											
TD-qz-0A, B	1	0	0.949	0.035	-0.002	0.461	0.001	0.003	0.000	0.000	0.494
TD-qz-5A, B	1	5	0.447	0.028	-0.001	0.475	0.008	0.001	0.000	0.003	0.502
TD-qz-7A, B	1	7	0.128	0.029	-0.001	0.500	0.024	0.005	0.000	0.001	0.528
TD-qz-9A, B	1	9	0.008	0.022	-0.001	0.485	0.001	0.001	0.000	0.002	0.505
TD-qz-11A, B	1	11	0.006	0.020	-0.001	0.505	0.002	0.001	0.000	0.003	0.523
TD-qz-13A, B	1	13	0.029	0.023	-0.001	0.471	0.000	0.002	0.000	0.004	0.492

TD-qz-16A, B	1	16	0.004	0.021	-0.001	0.509	0.001	0.001	0.000	0.000	0.529
TD-qz-20A, B	1	20	0.035	0.022	-0.001	0.473	0.002	0.000	0.000	0.002	0.494
TD-qz-25A, B	1	25	0.005	0.021	-0.001	0.492	0.001	0.001	0.000	0.001	0.511
TD-qz-30A, B	1	30	0.002	0.016	-0.001	0.499	0.002	0.002	0.000	0.002	0.513
Non-mineral control drying											
CD-0A, B	1	0	0.956	0.029	-0.002	0.459	0.001	0.003	0.000	0.008	0.486
CD-5A, B	1	5	0.447	0.030	-0.001	0.468	0.015	0.001	0.000	0.002	0.496
CD-7A, B	1	7	0.162	0.029	-0.001	0.496	0.002	0.000	0.000	0.007	0.524
CD-9A, B	1	9	0.017	0.027	-0.001	0.502	0.009	0.001	0.000	0.005	0.528
CD-11A, B	1	11	0.004	0.023	-0.001	0.511	0.004	0.002	0.000	0.003	0.532
CD-13A, B	1	13	0.027	0.023	-0.001	0.479	0.002	0.000	0.000	0.003	0.501
CD-16A, B	1	16	0.008	0.024	-0.001	0.510	0.000	0.000	0.000	0.000	0.533
CD-20A, B	1	20	0.032	0.023	-0.001	0.474	0.001	0.000	0.000	0.001	0.496
CD-25A, B	1	25	0.007	0.021	-0.001	0.503	0.000	0.001	0.000	0.001	0.523
CD-30A, B	1	30	0.001	0.020	-0.001	0.503	0.001	0.001	0.000	0.004	0.521
N_2-dried birnessite experiment											
TD-br-N1, 2	2	1	0.002	0.123	0.034	0.168	0.003	0.006	0.000	0.026	0.325
TD-br-N3, 4	2	2	-0.028	0.202	0.065	0.025	0.015	0.016	0.003	0.002	0.292
TD-br-N5, 6	2	5	0.013	0.253	0.048	0.015	0.001	0.004	0.017	0.004	0.316
TD-br-N7	2	35	0.032	0.225	0.067	0.005	0.000	0.000	0.000	0.000	0.298
N_2-dried quartz experiment											
TD-qz-N1, 2	2	35	0.013	0.006	0.000	0.432	0.018	0.001	0.000	0.011	0.438
N_2-dried non-mineral control experiment											
CD-N1, 2	2	35	0.029	0.001	0.000	0.443	0.002	0.001	0.000	0.005	0.444
Air dried birnessite experiment											
TD-br-A1, 2	2	1	-0.071	0.163	0.044	0.140	0.061	0.056	0.021	0.001	0.348
TD-br-A3, 4	2	4	-0.116	0.245	0.058	0.038	0.001	0.036	0.012	0.001	0.341
TD-br-A5	2	35	0.000	0.347	0.045	0.012	0.000	0.000	0.000	0.000	0.404
Air dried quartz experiment											
TD-qz-A1	2	35	0.000	0.005	0.000	0.478	0.000	0.000	0.000	0.000	0.483
Air dried non-mineral control experiment											
CD-A1	2	35	0.000	0.000	0.000	0.487	0.000	0.000	0.000	0.000	0.487

*Refers to calibration sessions in table A5, moist. = moisture, dev. = deviation from mean

Table A7 Data from the UV-radiation experiments

	umol				umol standard deviation		
Sample	ATZ-OH	DEA	ATZ	Sample	ATZ-OH	DEA	ATZ
Birnessite							
No radiation	0.371	0.048	0.138	No radiation	0.009	0.002	0.007
254 nm	0.387	0.034	0.046	254 nm	0.015	0.008	0.011
365 nm	0.425	0.056	0.037	365 nm	0.023	0.005	0.020
Quartz							
No radiation	0.021	0.000	0.444	No radiation	0.001	0.000	0.003
254 nm	0.019	0.003	0.397	254 nm	0.000	0.002	0.003
365 nm	0.020	0.000	0.407	365 nm	0.001	0.000	0.023
Non-mineral control							

No radiation	0.021	0.000	0.459	No radiation	0.001	0.000	0.021
254 nm	0.011	0.000	0.423	254 nm	0.006	0.000	0.021
365 nm	0.020	0.000	0.432	365 nm	0.001	0.000	0.007

Table A8 Significance-test results (*p*-value) for the UV-radiation experiments

	umol				p-value		
Sample	ATZ-OH	DEA	ATZ	Sample	ATZ-OH	DEA	ATZ
Birnessite							
No radiation	0.371	0.048	0.138	No radiation	-	-	-
254 nm	0.387	0.034	0.046	254 nm	0.205	0.034	0.000
365 nm	0.425	0.056	0.037	365 nm	0.019	0.060	0.001
Quartz							
No radiation	0.021	0.000	0.444	No radiation	-	-	-
254 nm	0.019	0.003	0.397	254 nm	0.034	0.022	0.000
365 nm	0.020	0.000	0.407	365 nm	0.146	1.000	0.052
Non-mineral control							
No radiation	0.021	0.000	0.459	No radiation	-	-	-
254 nm	0.011	0.000	0.423	254 nm	0.046	1.000	0.105
365 nm	0.020	0.000	0.432	365 nm	0.361	1.000	0.106

Addendum B

Investigation of the interaction of atrazine with birnessite using attenuated total reflectance – Fourier transform infrared (ATR-FTIR) spectroscopy.

An investigation into the degradation mechanism of atrazine on a birnessite surface was investigated using attenuated total reflectance – Fourier transform infrared (ATR-FTIR) spectroscopy. A 200 µg sample of pure atrazine, hydroxyatrazine and deethylatrazine, each in a 1 mg mL^{-1} ethanol suspension, was deposited on a clean Ge internal reflectance element (IRE), and a spectrum was taken of each pure compound (ratioed against the Ge-IRE) and stored as reference spectra. Thereafter, an ethanol-based mixture of 10 mg birnessite and 50 µg atrazine was deposited onto a clean Ge-IRE, dried, and then allowed to react for one week. At the end of the week, a spectrum was taken (ratioed against the Ge-IRE) and was referenced against the spectra of the pure compounds. The spectra are shown in Figure B1.

Spectra were collected on a Nicolet® 6700 FTIR, with Omnic® 32 software, using a DTGS detector. Collections were performed in the mid-infrared range, from 4000–700 cm^{-1}, at a resolution of 4 cm^{-1}, with each spectrum consisting of 128 co-added scans.

The birnessite-atrazine spectrum shows no features attributable to either hydroxyatrazine or deethylatrazine, and virtually all of the peak assignments can be attributed to atrazine. The C-Cl vibration is present at 803–806 cm^{-1}, indicating no appreciable formation of hydroxyatrazine, whilst the C=N stretch at 1548 cm^{-1} correlates well with the C=N stretch of atrazine. The same holds true for the N-H vibrations at 3260 cm^{-1} and the C-H vibrations of the CH_3 group at 2975 cm^{-1}, which all correspond to those of atrazine.

Although no real bond formation and degradation was observed in these spectra after 1 week reaction time, a closer study of the Mn-O bonds at lower frequencies is perhaps the solution to determining the formation of a cation-N bridge, since one would be able to observe the changing of the Mn-O bond to a Mn-N bond. The stretching and vibrational bonds of the Mn-oxides are generally at lower frequencies (400–700 cm^{-1}), and it would therefore perhaps be more suitable to take transmission spectra using KBr pellets. However, this would not allow the real-time analysis of possible bond

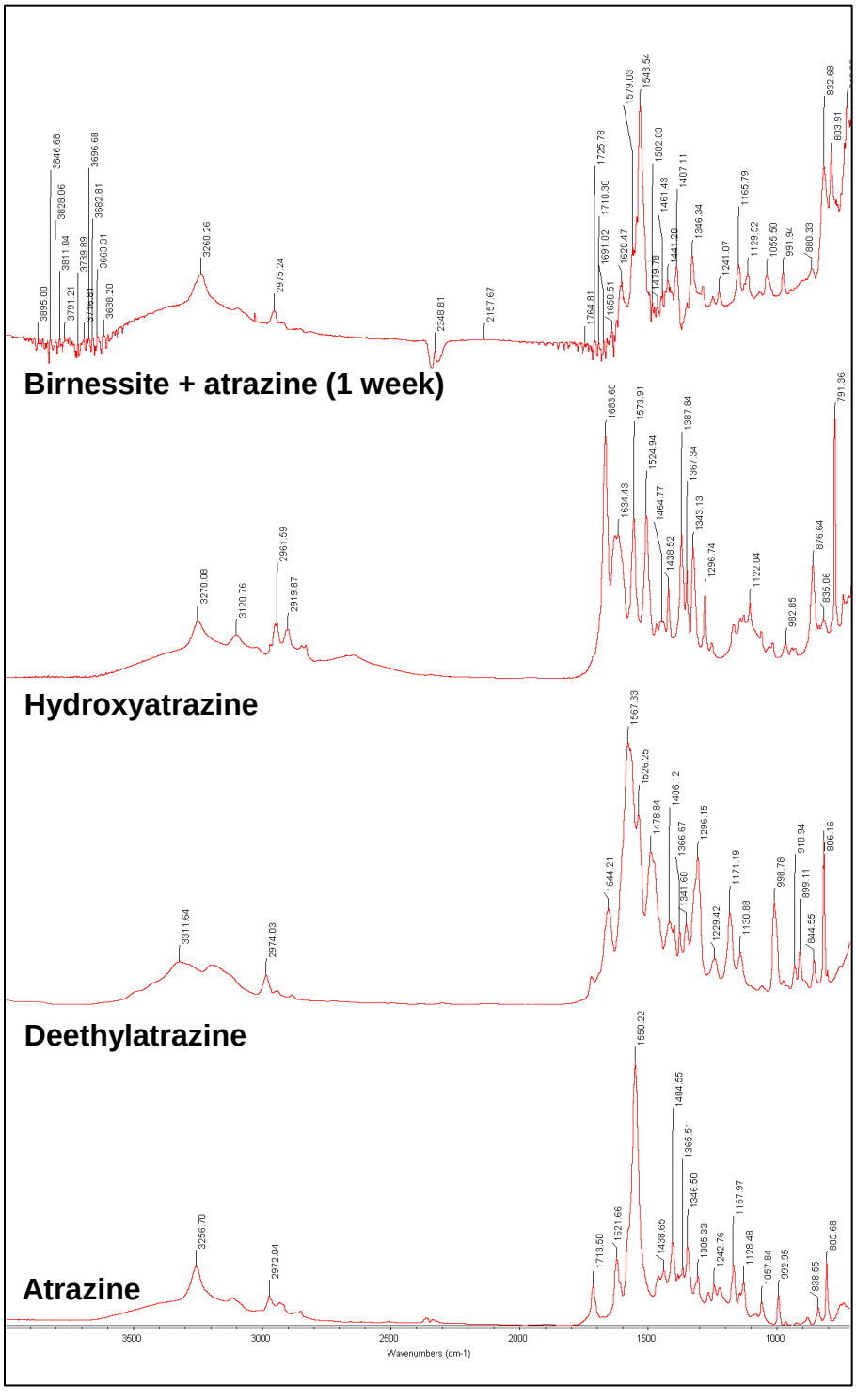

Figure B1 The ATR-FTIR spectra of atrazine, deethylatrazine, hydroxyatrazine and a mixture of atrazine and birnessite that was allowed to react for one week. Spectra were collected at a resolution of 4 cm^{-1}, and the number of co-added scans was 128.

formations and only water-absent analyses would be permissible. However, despite the lack of information obtained in this experiment, ATR-FTIR still seems viable for studying atrazine-birnessite interactions, at the mineral surface.

Spectra from the preliminary electron spin resonance (ESR) investigation of Mn^{2+} and birnessite

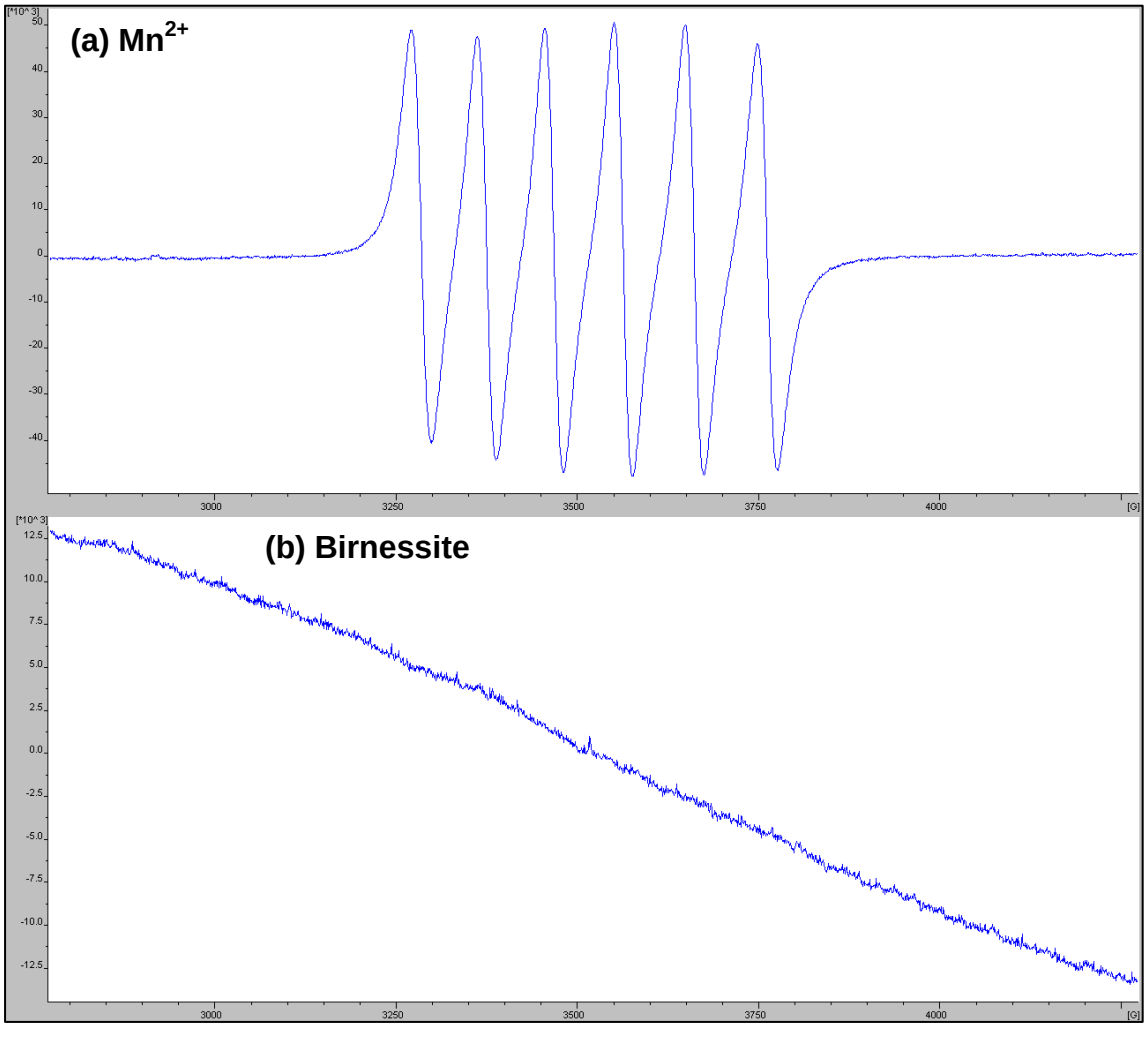

Figure B2 Electron spin resonance (ESR) spectra of (a) dissolved Mn^{2+} at 3 g L^{-1} and (b) neat birnessite. Spectra were collected at 9.168 GHz using a Bruker® Bio-spin EMXplus spectrometer.

Results from the simplified method validation of the HPLC method used in this study

- Biological error calibration – triplicates derived from three different standards:

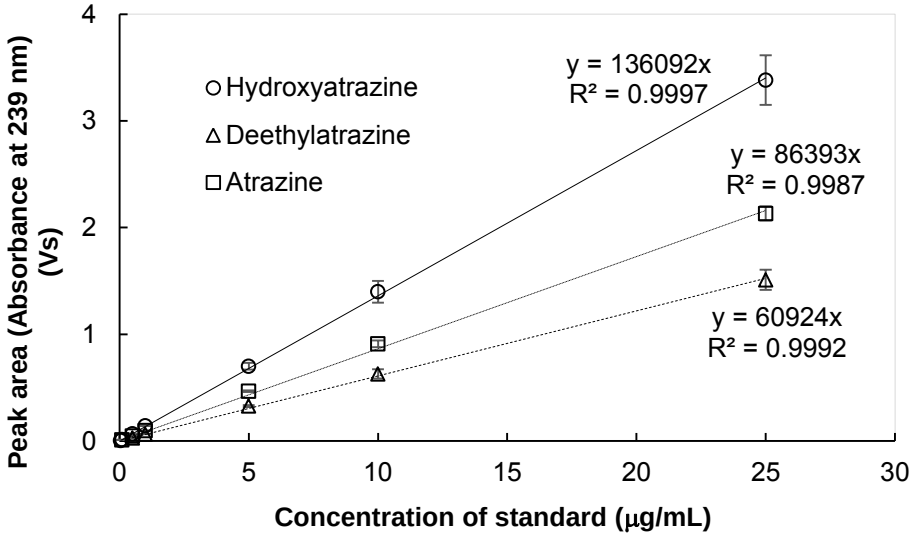

- Injection error calibration – triplicates derived from three injections of the same standard: